An Investigation into the Aerodynamic Performance of Future Commercial Vehicle Designs

J.P.Beatham

Department of Aeronautics and Astronautics,
Southampton University

A thesis submitted for the degree of
Master of Philosophy

April 1988

UNIVERSITY OF SOUTHAMPTON

ABSTRACT

FACULTY OF ENGINEERING AND APPLIED SCIENCE

DEPARTMENT OF AERONAUTICS AND ASTRONAUTICS

MASTER OF PHILOSOPHY

AN INVESTIGATION INTO THE AERODYNAMIC PERFORMANCE OF FUTURE COMMERCIAL VEHICLE DESIGNS

by Jeremy Peter Beatham

This thesis details the investigation into the aerodynamic performance of possible future commercial vehicle designs for the next decade. Previous testing within the Department has utilised the 2.1m * 1.7m low speed wind tunnel with a 2.0m * 1.1m moving belt to simulate ground effect. Testing of 1/6 scale trucks or 1/3 scale cars takes place at 25 m/s. As future road vehicles adopt more rounded shapes Reynolds number effects play a major part in the aerodynamic characteristics. This reason led to the construction of a 5.3m * 2.4m moving belt rig, to be installed in a newly acquired 3.5m * 2.6m tunnel. The greater scale of this moving ground and tunnel would allow much higher Reynolds numbers to be achieved and increased similarity to the full scale flow field would be achieved, this would also allow much greater detail to be included on the model. Initially this rig needed to be developed and commissioned. After this had been carried out through comparison tests of flow quality and operational parameters, it was used for testing of 1/4 scale commercial vehicle models. This moving ground facility is one of the largest in operation and its developement formed a large part of the initial work, described here. Balances also needed to be designed and developed, as the balance in the 3.5m * 2.6m tunnel was inadequate for these tests.

The main body of investigation then took place, starting from tests on a 1/4 scale model of a present day rigid box van. A design of cab was then initiated which could easily replace a modern cab without extreme modifications to the layout, size or basic chassis design of a present day vehicle. This design was tested in both 1/4 scale and 1/6 scale forms, the 1/6 scale model tested in both facilities, to assess performance of the cab and other drag reducing devices. An improved design was then built and again tested throughout a full range of yaw angles to assess crosswind performance. The flow field was measured and viewed to investigate the impact of the aerodynamic changes on the problem of spray. The final results were also related to practical economic benefits to the vehicle operator. This was done by calculating fuel economies to be made through low drag vehicles and the effect this has on operating costs.

Contents

LIST OF FIGURES

Fig.16 Schematic Plan View of Yawed 2.0m * 1.1m Moving Ground in the 3.5m * 2.6m Wind Tunnel.

Fig.17 Boundary Layer Plot over Yawed 2.0m * 1.1m Moving Ground in 3.5m * 2.6m Wind Tunnel (0 deg. Yaw).

Fig.18 Boundary Layer Plot over Yawed 2.0m * 1.1m Moving Ground in 3.5m * 2.6m Wind Tunnel (15 deg. Yaw).

Fig.19 2.1m * 1.7m Tunnel Overhead Weighbeam Balance Calibrations.
(a). Lift,
(b). Drag,
(c). Pitching Moment.

Fig.20 Typical 3.5m * 2.6m Tunnel Overhead Balance Calibration.

Fig.21 Load Cell Balance Calibrations.
(a). Drag
(b). Sideforce
(c). Yawing Moment

Fig.22 Strain Gauge Dynamometer Calibrations.
(a). Sideforce
(b). Rolling Moment
(c). Yawing Moment

Fig.23 Body Axis Co-ordinate System

Fig.24 1/4 Scale Model Variation of Drag Coefficient with Reynolds Number in 3.5m * 2.6m Wind Tunnel.

Fig.25 Variation And Repeatability of Drag Coefficient with Reynolds Number for 1/6 Scale Model in 2.1m * 1.7m Wind Tunnel.

Fig.26 Variation of Drag Coefficient with Reynolds Number for 1/6 Scale Model in 2.1m * 1.7m Wind Tunnel.

Fig.27 Variation of Lift Coefficient with Reynolds Number for 1/6 Scale Fast Front Mk.I in 2.1m * 1.7m Tunnel.

Fig.28 Variation of Wheel Lift Coefficient with Ground Clearance and Rotation.

Fig.29 Variation of Drag Coefficient with Reynolds Number for 1/6 Scale Model in 2.1m * 1.7m Wind Tunnel.

Fig.30 Variation of Lift Coefficient with Reynolds Number for 1/6 Scale Fast Front Mk.II in 2.1m * 1.7m Tunnel.

Fig.31 Variation of Coefficients with Yaw Angle for 1/6 Scale Fast Front Mk.II in 2.1m * 1.7m Tunnel.
(a). Drag Coefficient
(b). Lift Coefficient

Fig.32 Variation of Force Coefficients with Yaw Angle for 1/6 Scale Fast Front Mk.II in 2.1m * 1.7m Tunnel.
(a). Drag Coefficient
(b). Lift Coefficient
(c). Sideforce Coefficient
(d). Yawing Moment Coefficient

Fig.33 Surface Pressure Coefficients on 1/6 Scale Fast Front Mk.I in 2.1m * 1.7m Tunnel
(a). Position of Horizontal Ring (Side View)
(b). Plan View of Ring Showing Marking
(c). Baseline, 15 Degrees Yaw, 24.86 m/s
(d). Base plus Full Skirts, 15 Degrees Yaw, 24.86 m/s

Fig.34 Variation of Coefficients with Yaw Angle for 1/6 Scale Fast Front Mk.II in 2.1m * 1.7m Tunnel.
(a). Drag Coefficient
(b). Lift Coefficient
(c). Sideforce Coefficient
(d). Yawing Moment Coefficient

Fig.35 Variation of Coefficients with Yaw Angle for 1/6 Scale Fast Front Mk.II in 2.1m * 1.7m Tunnel.
(a). Drag Coefficient
(b). Lift Coefficient
(c). Sideforce Coefficient
(d). Yawing Moment Coefficient

Fig.36 Variation of Drag Coefficient with Reynolds Number for 1/4 Scale Model in the 3.5m * 2.6m Wind Tunnel.

Fig.37 Variation of Coefficients with Yaw Angle for 1/4 Scale Fast Front Mk.II in 3.5m * 2.6m Tunnel.
(a). Drag Coefficient
(b). Sideforce Coefficient
(c). Yawing Moment Coefficient

Fig.38 Variation of Coefficients with Yaw Angle for 1/4 Scale Fast Front Mk.II in 3.5m * 2.6m Tunnel.
(a). Drag Coefficient
(b). Sideforce Coefficient
(c). Yawing Moment Coefficient

Fig.39 Variation of Coefficients with Yaw Angle for 1/4 Scale Fast Front Mk.II in 3.5m * 2.6m Tunnel.
(a). Drag Coefficient
(b). Sideforce Coefficient
(c). Yawing Moment Coefficient

Fig.40 Variation of Coefficients for 1/6 Scale Fast Front Mk.II in the Two Tunnels.
(a). Drag Coefficient with Reynolds Number
(b). Drag Coefficient with Yaw Angle
(c). Sideforce Coefficient with Yaw Angle
(d). Yawing Moment Coefficient with Yaw Angle

Fig.41 Comparison of Coefficients for Various Models and Test Techniques.
(a). Drag Coefficient with Reynolds Number
(b). Drag Coefficient with Yaw Angle
(c). Sideforce Coeficient with Yaw Angle
(d). Yawing Moment Coefficient with Yaw Angle

Fig.42 Wake Contour Plot for 1/6 Scale Fast Front Mk.II in the 2.1m * 1.7m Tunnel at 185mm Behind Model.
(a). Baseline 0 Degrees Yaw Rotating Wheels
(b). Base plus Full Side Skirts, 0 Degrees Yaw, Rotating Wheels
(c). Base,Skirts and Undertray, 0 Degrees Yaw, Rotating Wheels
(d). Skirts, Undertray and Rear Boat-tails, 0 Degrees Yaw, Rotating Wheels.

Fig.43 Wake Contour Plot for 1/6 Scale Fast Front Mk.II in the 2.1m * 1.7m Tunnel at Rear Wheel Centreline, 1" off Body.
(a). Baseline, 0 Degrees Yaw, Rotating Wheels
(b). Base plus Full Side Skirts,0 Degrees Yaw, Rotating Wheels
(c). Skirts and Undertray, 0 Degrees Yaw, Rotating Wheels.

Fig.44 Wake Contour Plot for 1/6 Scale Fast Front Mk.II in the 2.1m * 1.7 Tunnel at 1000mm Behind the Model.
(a). Baseline, 0 Degrees Yaw, Rotating Wheels
(b). Base plus Full Side Skirts, 0 Degrees Yaw, Rotating Wheels
(c). Skirts and Undertray, 0 Degrees Yaw, Rotating Wheels
(d). Skirts, Undertray and Rear Boat-tails, 0 Degrees Yaw, Rotating Wheels.

Fig.45 Wake Contour Plot for 1/6 Scale Fast Front Mk.II in the 2.1m * 1.7m Tunnel at 1000mm Behind the Model.
(a). Baseline, 3 Degrees Yaw
(b). Base plus Skirts, 3 Degrees Yaw
(c). Skirts and Undertray, 3 Degrees Yaw
(d). Skirts, Undertray and Rear Boat-tails, 3 Degrees Yaw.

Fig.46 Wake Contour Plot for 1/6 Scale Fast Front Mk.II in the 2.1m * 1.7m Tunnel at 1000mm Behind the Model.
(a). Baseline, 15 Degrees Yaw
(b). Skirts, Undertray and Rear Boat-tails, 15 Degrees Yaw.

Fig.47 Overall Improvement of Drag Coefficient with Yaw Angle for 1/4 Scale Model in 3.5m * 2.6m Tunnel.

LIST OF PLATES

Plate 10. 1/6 Scale Fast Front MK.II in 2.1m * 1.7m Tunnel Lee-side Cab Flow with Wire Transition, 9 Degrees Yaw, 24.86 m/s.

Plate 11. 1/6 Scale Fast Front Mk.II in 2.1m * 1.7m Tunnel Lee-side Cab Flow without Transition, 9 Degrees Yaw, 24.86 m/s.

Plate 12(a). 1/4 Scale Fast Front Mk.II in 3.5m * 2.6m Tunnel Baseline, 0 Degrees Yaw.

Plate 12(b). as 12(a).

Plate 13(a). 1/4 Scale Fast Front Mk.II in 3.5m * 2.6m Tunnel Base plus Full Side Skirts, 0 Degrees Yaw.

Plate 13(b). as 13(a).

Plate 14(a). 1/4 Scale Fast Front Mk.II in 3.5m * 2.6m Tunnel Base, Full Skirts and Rear Boat-tails, 0 Degrees Yaw.

Plate 14(b). as 14(a).

Plate 15(a). 1/4 Scale Fast Front Mk.II in 3.5m * 2.6m Tunnel Baseline, 6 Degrees Yaw.

Plate 15(b). 1/4 Scale Fast Front Mk.II in 3.5m * 2.6m Tunnel Base plus Full Side Skirts, 6 Degrees Yaw.

Plate 16(a). 1/4 Scale Fast Front Mk.II in 3.5m * 2.6m Tunnel Baseline, 12 Degrees Yaw.

Plate 16(b). 1/4 Scale Fast Front Mk.II in 3.5m * 2.6m Tunnel Base plus Full Side Skirts, 12 Degrees Yaw.

Plate 17. Total Pressure Rake for Wake Studies (with Author).

List of Symbols

Cd	drag coefficient
Cd(55)	wind averaged drag coefficient for a vehicle velocity of 55 m.p.h.
Clf	front axle lift coefficient
Clr	rear axle lift coefficient
Cn	yawing moment coefficient
Cp	pressure coefficient
Cy	sideforce coefficient
dCd	change in drag coefficient (or any other with appropriate symbol) from that of the baseline configuration
d(mm)	boundary layer thickness
Re(l)	Reynolds number based on model length
Re(r)	Reynolds number based on leading edge radius
(u/V)5	boundary layer velocity deficit at 5mm above the ground
(u/V)10	as above at 10mm above the ground

Any other symbols used are not general and are defined in the relevant chapter when they are used.

Acknowledgements

Grateful thanks are expressed to the many people who supported this research program. Mr. K. Burgin for his patient, helpful and enthusiastic supervision of the project, thanks also to Prof. G.M. Lilley, Dr. D.W. Hurst and Mr. P.C. Adey for helpful discussion during the program. Mr. L. Gutteridge, of Leyland Vehicles Ltd., for the loan of the models involved.

The late Mr. L.J. Dykes is also owed a great many thanks for his considerable input to the wind tunnel facilities at Southampton University through his design and drawing work including the moving ground designs and balances. The cheerful support of the technicians involved is also acknowledged, the Electronics Dept. for electronics support, the workshop for their manufacture of the sometimes not fully explained designs given to them, and the wind tunnel operators. In particular Mr. M. Grinter, Mr. G.H. Moore, Mr. D. Odgers, Mr. I. Smart, Mr. D. Whitham and Mr. M. Wright for patient wind tunnel operation, and Mr. D.R. Browning, Mr. D.W. Davidson, and Mr. D.J. Goldsworthy for their excellent model preparation.

This research was funded by the Science and Engineering Research Council, S.E.R.C.

I would also like to thank all my family and friends for seeing me through thick and thin during my time in Southampton. The Charlie Nicholas Boys, League winners '83-'88, especially Pete, Barry, Mike, Cyril, Graham, Simon, Tony and Frank; "Keep it simple!". Martin Stephenson and the Daintees for optimism and Morrissey and the Comic Strip for lightening the load.

Finally this work is dedicated to Katharine whose understanding and support during this research never failed. Thanks.

Chapter 1. Introduction

Aerodynamics has over the last couple of decades become an increasingly important area of vehicle design. Spurred on by rapidly increasing fuel costs in the seventies the initial interest was placed in passenger car aerodynamics. Eventually though with the majority of goods being transported by road in commercial vehicles interest in the reduction in operating costs of these vehicles arose. As these vehicles were being operated on motorways at high speed the aerodynamic component of the power losses on these vehicles became important; at motorway speeds, the power loss due to aerodynamic drag can rise above 50%. Thus a vehicle operated mostly on motorways could have its fuel costs greatly reduced by aerodynamic improvements.

Initially, work was carried out on basic vehicles with simple add-on devices to control problem areas such as the large separation and interference area around the cab container region. Extensive tests on these devices were carried out both in this country and in America, see references, but most work was carried out at zero yaw angle. This angle is an idealised case and more recent work has shown the need to correctly asses the aerodynamic performance in crosswinds. This work has shown many of the simple devices initially developed and proved to reduce drag, to actually increase drag in crosswinds. Despite all this work aimed at improving the aerodynamics of commercial vehicles main improvements have been through add-on devices with the basic design of the vehicle remaining unchanged. Passenger car design has changed radically with the consideration of aerodynamics resulting in the smoothing of the general shape, front and rear, use of flush glass and the elimination of guttering and sharp edges. The same sort of developments appear not to have been considered in

relatively new commercial vehicle designs, with only light vans, based on car designs, benefiting from fundamental design changes.

As well as considering the aerodynamics a manufacturer also needs to consider production costs, maintenance problems and above all, the desires of the operators who will buy the vehicles. Resistance to fundamental design changes have probably arisen in these areas, since commercial vehicle manufacturing has been in decline recently. The aerodynamic drag of commercial vehicles is only one area of aerodynamic design of interest. Cooling of the engine and conditioning of the cab air flows for heating and cooling of the cab are also areas which need development in a new design. More importantly perhaps is the problem of spray generated by these vehicles at high speed on wet roads. As any regular motorway user knows the problem of visibility when travelling behind or alongside commercial vehicles is a major hazard, although often not a proven factor in accidents occurring on wet roads, it must be a contributory factor and in many cases the major cause of an accident. Previous work has again been carried out to investigate the main areas of spray generation and means of suppressing this but again moves to change designs or use known spray suppressants on commercial vehicles have been slow. It is only recently that it has become a requirement to fit spray reducing devices.

It therefore appears that there is great scope for improvements in commercial vehicle design to reduce both operating costs and spray emitted on wet roads. These factors could be mutually improved, with a lower drag design having a better flow field giving lower spray emmissions. The work carried out during the period reported

was along these two avenues of commercial vehicle design. The department had already been involved in commercial vehicle design in both areas mentioned and a large experience in wind tunnel testing had been built up.

Initially the work was carried out in accordance with the requirements of the sponsors S.E.R.C., grant referance GR/C/83432 which was a single year contract to develop unique facilities at the University for commercial vehicle wind tunnel testing. The work was to develop and commission the 5.3m * 2.4m moving ground for use in the 3.5m * 2.6m wind tunnel. Some preliminary work was carried out on basic vehicle aerodynamics to prove the facility. After this an additional two year contract was approved, grant referance GR/D/54873 which was titled 'Aerodynamic design of Large Road Vehicles for Drag and Spray Suppression in Crosswinds'. This work was intended as an investigation into the aerodynamics of commercial vehicles for the 1990's.

The work was carried out on scale models of rigid box vans in the two wind tunnels recording force measurements over a range of yaw angles, flow visualization studies, wake and surface pressure measurements. Thus a full picture of the behaviour of the vehicles tested could be built up as well as a picture of the facilities used and techniques employed. An introduction at the start of each chapter is given to fully explaining the work carried out in respect to the chapter itself and explaining the reasons behind it. Chapter 2 gives a wider background to the facilities used during the research. The main objectives were;

(i) To develop and commission the 5.3m * 2.4m moving ground to give good testing speed with excellent control,

no belt lift and to give high quality results.

(ii) To prove this facility by testing a 1/4 scale commercial vehicle model, comparing its performance to previous similar tests. Also to compare the two tunnels and the testing techniques used.

(iii) To produce data on the aerodynamic coefficients on a design of vehicle for the next decade and to develop this design from a present day vehicle.

(iv) To assess the performance of this design with regard to the suppression of spray and to maximise this suppression.

(v) to assess the impact of the aerodynamic improvements on the fuel economy and to further assess this impact on operating costs and charges.

(vi) To carry out all this testing both at zero yaw and non zero yaw to assess the affects of crosswinds on the forces, spray suppression and operating costs.

Chapter 2. Wind Tunnel Facilities

2.1. Wind Tunnels

2.1.1. 2.1m*1.7m Wind Tunnel

The main facility used for ground vehicle aerodynamic assessment is a 2.1m * 1.7m working section, closed return wind tunnel. This has been used for fourteen years in conjunction with a moving ground. The requirement to simulate the correct ground motion in wind tunnel tests was recognised and met with the installation of the 2.0m * 1.1m moving ground in 1973. This has since been used with great success,a full description of the moving belt rig can be found in ref. 7.

The top speed of the tunnel is 50 m/s although testing with the moving ground is limited to 25 m/s to improve the accuracy and repeatability of results taken. Models used in this tunnel are of a scale limiting blockage to below 5%, usual scales are 1/3 or 1/4 scale car models and 1/6 or 1/8 scale commercial vehicles. The Reynolds number obtained for a 1/6 scale rigid box van, as tested in this investigation is 1,960,000 based on model length.

The models are mounted using an adjustable strut passing through the roof of both the model and the tunnel, then connecting to an overhead balance on the tunnel roof. The balance is a fixed axis, three component, weigh beam balance which is fully electronically controlled. The three components measured are lift, drag and pitching moment. Results are sampled by a microcomputer and then processed to give print outs of all relevant

information.

The strut used to mount the models had a friction collet to provide both ride height and yaw angle adjustment. When the model was yawed an internally mounted strain gauge dynamometer was placed in the model to measure sideforce, rolling and yawing moments. These used together with the results taken on the overhead balance, corrected for yaw, then give the full details of forces on the model.

2.1.2. 3.5m*2.6m Wind Tunnel

This wind tunnel was a recent addition to the facilities at the University having been moved here from R.A.E. Farnborough in 1979. The tunnel is of conventional closed return design with a working section cross sectional area of 3.5m * 2.6m. A large scale moving ground was designed and built to be installed in this tunnel; a schematic representation of this moving belt rig is shown in fig. 4. Initial development work was commenced in the summer of 1984 on this rig (see Chapter 3).

The maximum speed in the working section is 55 m/s but this is restricted to a maximum, at the time of writing,of 35 m/s when using the moving ground. This speed is limited due to servere vibrations from the rollers on the moving ground and to give accurate and repeatable results a test speed of 28 m/s was used. At this speed no vibrations were transmitted to the model. In this tunnel as in the smaller tunnel the scale of models used was chosen so as to limit blockage to 5% maximum. The desirable scales are thus 1/2 scale car models and 1/4 scale models for commercial vehicles. The resulting Reynolds number for the 1/4 scale rigid box van used for this investigation is 3,650,000 based on model length.

The models are mounted as in the smaller tunnel using a strut passing through both model roof and tunnel roof attaching to the overhead balance on the tunnel roof. The balance in this tunnel was converted on its arrival to a load cell balance, its previous operation had been electromagnetic, it measured six components of force. This conversion was found to give accuracy and repeatability which was totally unsuitable for the road vehicle work. Two new load cell balances were then designed to measure the three components of force considered to be of primary importance, drag, sideforce and yawing moment. These are described in Chapter 4 and shown in fig. 1. The overhead balance was retained for mounting as it sat on a turntable and provided a more convenient yaw angle adjustment although the friction collet on the strut was retained for ride height adjustment. Once set, the strut was pinned to prevent any slippage.

The voltages from the load cells were sampled by a microcomputer which processed them and printed out a fully detailed results sheet.

Additional research carried out in the 3.5m * 2.6m wind tunnel was to mount the smaller, 2.0m * 1.1m, moving ground on a turn table to more fully represent the road conditions in cross winds. A full account of this investigation appears in ref. 1. Tests conducted on a 1/6 scale rigid box van measuring forces and surface pressures showed that the results obtained were not significantly changed. This suggests that the actual effect of ground motion is more significant with regard to boundary layer removal than actual direction of ground motion in the case of a commercial vehicle with large ground clearance.

2.2. Models

2.2.1. 1/6 Scale Rigid Box Van

This model is the model originally used in ref. 2. and was loaned to the University by Leyland Vehicles Ltd.. Originally an all wood model it was extensively modified for the work carried out here. Firstly a steel chassis, of ladder construction, was made with the cab mounted at one end and the box container mounted aft of this on top of the chassis. As detailed as possible an underbody was fixed underneath including air and diesel tanks, an exhaust pipe, an engine block and gearbox and drive train.

The major consideration in building a steel chassis was to provide a rigid 'backbone' from which to mount the rotating wheels. Solid wheels turned from nylon had bearings mounted in their centres and were suspended from swinging arms suspended from the steel chassis. These were attached through bearings to make the arms freely pivoting vertically,in this way only drag would be transfered to the balance and minor disturbances from the wheels running on the moving belt would be ignored. Yaw testing was carried out using fixed wooden wheels adjusted to the same position as the rotating wheels but with flats to give a running height of 5mm above the belt.

The model is shown in plates 1(a) & (b), and devices were made to test to investigate possible drag reductions with this configuration. Such devices consisted of various cab roof deflectors, gap seals, cab-container fairings, air dams and side skirts.

2.2.2. 1/4 Scale Rigid Box Van

This model was chosen as the preferable research tool due to its scale. Reynolds numbers would be higher reducing any scale effects; also the model could be made including greater detail. Leyland Vehicles Ltd. again provided the model which arrived as a display model and therefore had to be extensively modified for suitability to wind tunnel test. The only parts retained were the cab, a prototype T45 road train cab and the detail underbody parts which were fixed to a steel chassis, of ladder construction, designed to closely model the true chassis. A new box container was also made to the same dimensions as the one supplied which unfortunately was not to the same scale dimensions as the 1/6 scale example. This leads to difficulties in later data analysis but was not a serious problem.

Solid machined nylon wheels were again suspended on freely pivoting swinging arms more closely representing the leaf suspension on a typical modern truck. Greater detail than on the 1/6 scale model was built into the underbody,see plates 2(a) & (b), with the air and diesel tanks, engine block, drive train, exhaust pipe, light fittings and rear under rider. Cooling flow was also considered and a wire mesh radiator with some ducting was included in the cab modelling.

Devices were also made to test drag reduction devices presently popular on this Leyland T45 type vehicle, as a first step in the investigation. This test programme demonstrated that significant drag reduction could only be obtained by a redesign of the cab, see section 2.2.3 .

2.2.3. Fast Front Cab Design

After the initial experimentation had been carried out to assess the 'state of the art' in commercial vehicle aerodynamic design it was decided to redesign the cab as the main area of study. It has been suggested in other reports (ref. 3, 4, & 5) that something like 60%-70% of the overall wind averaged drag of trucks and buses is caused by the forebody pressure. Base pressure adding some 15%-25%. Results obtained on the baseline models here also suggest this, the best configuration arrived at when the cab was faired into the container this modification actually giving an 18% drag reduction. A faired cab/container front end was designed and made, see fig. 2 which was a wedge type front with two flat, angled nose sections radiused into each other, the sides, top and bottom.

The radii were increased following the initial wind tunnel tests and calculations using criteria suggested in ref. 4. The final Fast Front Design is shown in fig. 3 with dimensions for both the 1/6 and 1/4 scale models. The Mk.I cab ended with square sides along the top of the container although the Mk.II ended with a minimum radius continued from the cab sides along the top sides of the container.This was the minimum radius calculated in Ch.7.1. using the expression given in ref. 4 for full scale attached flow and was intended to improve the yaw performance of the model. The containers were otherwise unmodified so as to maintain the present load carrying capacity of the model class. A change in this would be a more long term and problematic change for manufacturers and operators to solve.

As far as possible both cabs were to be scale

replicas of each other, however as already mentioned, see Ch.2.2.2., the container of the 1/6 scale was relatively higher than on the 1/4 scale. This was unavoidable and was dealt with by keeping the radii on the cab and the angles of the flat panels equivalent but adjusting the length of these panels to provide the extra height. There was also some width difference on the models but this was negligible in comparison to the height.

The design parameters used to design the models were discussed with Leyland Vehicles Ltd. to give the required operating tolerances on such things as ground clearance for operation over rough terrain or to deal with curbs whilst manouvering. These parameters were (see fig. 3):

(i) a minimum approach angle of 15 deg.
(ii) a minimum ground clearance of:
200mm(full scale) at axles
300mm(full scale) mid wheelbase

These parameters were adhered to except the minimum mid wheelbase ground clearance which was taken as equal to that at the axle. This eased the manufacture and fitting of the flat undertray which needed to cover such parts as the engine block, propshaft and rear axle. These were fitted to their respective ground clearances, the rear axle and engine block, being at the axles, had clearances of approximately 200mm full scale. The flat undertray could therfore cover all underbody parts without exception if the smallest clearance was chosen. This then eased the problems of wind tunnel tests and was not considered a major problem as the vehicle was not primarily designed with the rough terrain operation for which these minimums are relevant. Modifications could easily be incorporated to suit a

vehicle with these considerations in mind.

Devices were also made to further increase the aerodynamic efficiency of the front cab, these included side skirts, a full and a partial flat bottom, rear panels, rear deflectors and rear boat-tails.

Other details included were a model radiator of scale dimensions on the 1/4 scale and a radiator inlet on both models. The radiator inlet was of an appropriate area whilst the radiator was modelled as blockage in this inlet, consisting of fine wire mesh and honeycomb. Although this is recognised as only part of the full model the results of open duct and closed duct revealed no change and the modelling was considered sufficient.

This then gave the required models with the greatest detail in order to test in the two wind tunnels for the successful completion of the work undertaken.

Chapter 3. Moving Ground Development

3.1. Introduction

Initial wind tunnel tests on road vehicle models at Southampton in the 1970's investigated the need to correctly simulate ground conditions. This was achieved by designing and building a moving belt rig which was placed in the tunnel and was operated at a speed synchronous with the air speed. This then correctly models a vehicle moving across the ground in stationary air. Experiments demonstrated the need to correctly simulate the ground condition,see refs. 6 & 7. The moving ground was developed and has been successfully used in ground vehicle work for fourteen years.

The success of this moving ground was such that it was chosen as the bench mark to assess the progress being achieved with the larger 5.3m * 2.4m moving belt rig which was developed for use in the larger 3.5m * 2.6m tunnel. All aspects of the belts performance were taken into account for the comparison,these were;

(i) flow quality over the belt
(ii) speed capability
(iii) controlability of speed,tracking and belt surface flatness
(iv) belt longevity.

Measurements of flow quality were taken as vertical total pressure traverses over the belt in the empty test section of the wind tunnel to assess the boundary layer present. These measurements being taken at various spanwise and chordwise positions over the belt, the main position being that directly under the centre of the

balance, ie. the mounting point for all models. A rake of total probes was designed, see plate 5, to measure total pressures in a vertical line of 21 pressures spaced at 5mm in proximity to the belt and 20 further pressures spaced at 10mm above those. The lowest probe was usually run at a clearance of 5mm to the belt surface. The probes were then connected to a multitube manometer and values of air velocity at the measurement point divided by tunnel velocity, (ie. velocity deficit (u/V)), deduced. This set up also gave a useful, immediate, visual picture of the boundary layer present. Levels of freestream turbulence were not measured as wind tunnel testing is an ideal situation and simulation of full scale turbulence is not considered. This would depend on climatic and traffic conditions at the particular time. The wind tunnel solution is to produce a relatively low turbulence stream of air to give reliable conditions for aerodynamic tests.

The other parameters are measured mostly qualitatively from experience of using the facility. Speed is assessed as a combination of keeping optimum flow quality and vibrations from the rotation of the mechanical components to a minimum. Control of speed and tracking of the belt is limited by the control systems of both whilst maintaining a flat, consistent belt surface is limited by the ability of the suction fans to reduce the pressure in the suction boxes below the belt to counter the low pressure wake of the model in the tunnel. Belt longevity is a result mainly of choosing the correct belt material. Interestingly temperature rise due to friction under the belt is not a problem at these speeds and cooling is not required.

3.2. 2.0m*1.1m Moving Ground in the 2.1m*1.7m Wind Tunnel

This moving ground is the original, which was to be made the standard for comparison with the larger ground which was to be developed. It consists of a continuous belt passing over rollers each end (uniquely one driving, one tracking) a flat solid surface is provided between the rollers by the suction boxes, shown schematically fig. 4.The endless belt is supplied already joined, the join being made so as not to create a region of thicker material which could cause the wheels to kick. Presently the belt material used is made up of a fabric base with a poly-urethane or P.V.C. upper surface, the lower surface has a low friction backing to reduce friction as it runs over the top surface of the suction boxes. The top surface of the suction boxes is made from steel, drilled with a grid of holes and anodised,also to reduce friction. The full moving ground rig set up is described in ref. 7.

The majority of the parameters were known from studying the testing history of the ground. Extensive use of the facility with a few belt failures with use of a number of differing belt materials and constructions has lead to a criteria where the belt is replaced after 6 months running. The retention of speed and tracking of the belt is excellent and the maintenance of the belt flatness was excellent at the testing speed of 25 m/s. This testing speed was largely deduced from 'feel' as this appeared to be the point at which the ground ran smoothly and repeatably, giving the best quality results. After measurements of the flow quality were taken a reason for this was established and the optimum speed for best flow quality for the set up proved to be 25 m/s.

3.2.1. Effect of Configuration Change

L.E Suction	Ground	d(mm)	(u/V)5
on	on	20	0.961
off	on	90	0.862
off	off	115	0.697
on	off	27	0.767

The figures above show the difference in the boundary layer present at the centre of balance position over the moving ground; the full data is plotted in fig. 5.

Clearly the main reason for reduction of the boundary layer is the effect of the suction box. It can be seen from fig. 5, that there are two distinct boundary layers present. A normal turbulent boundary layer curve in the ground stopped cases and the modified version of the turbulent layer with the region of air close to the belt returning to (u/V)=1 at the belt surface. This layer of air close to the belt accelerates through friction and viscosity effects due to the belt motion. The modification of the boundary layer causes the fold back in the velocity curve. The excellent, thin boundary layer present in the usual testing configuration of the 'all on' case has a boundary layer thickness of just 20mm and the minimum velocity being just 4% below the freestream condition. The edge of the boundary layer is taken as the point when the velocity has risen to 98% of the freestream velocity value to allow for loses in the tubing to the manometer and errors in the reading of the values of the manometer tubes.

Shutting off the l.e.suction increases the boundary layer by 70mm which is a 350% increase,the velocity at 5mm being reduced to 86% of freestream, a

decrease of 10%. Similarly for the ground stopped case the boundary layer thickness is increased by 88mm, (326%), when the l.e.suction is stopped. In this case the velocity is just 79% of freestream velocity. The effect of the leading edge suction box is thus seen to be very large which was surprising as the design was such that the major part of the tunnel boundary layer should have been fed through the slot left between the tunnel floor and the suction box. The suction box was then intended to remove the slight residue which then flowed over the upper surface. After flow visualization tests on the box it was found that the upper surface flow was separating and reattaching towards the rear of the perforate when the box was shut off. The effect of suction was to minimise the separation bubble, almost eliminating it, and then to remove a small amount of the residue boundary layer.

The effect of ground motion however was less although still significant, with l.e.suction on, stopping the ground led to an increase in boundary layer thickness of 7mm which is some 35%. Also the velocity at 5mm is decreased by a further 20% from freestream. The effect without l.e.suction is to increase thickness by 25mm, 28%, and decrease the velocity at 5mm a further 16% from freestream. The mechanism involved is that the air close to the belt surface is accelerated by the viscous effects of the belts motion, the velocity at the belts surface being freestream. When the belt is stopped this no longer happens and the air must become stationary at the belt surface leading to the classic turbulent boundary layer velocity profiles in fig. 5. The turbulent boundary layer starts at the leading edge of the suction box and grows along the box and the belt up to the centre of balance position.

3.2.2. Effect of Speed

The effect was assessed by comparing the usual testing speed of 24.86 m/s to measurements at a higher speed of 30.18 m/s. In both cases the belt was run synchronous with the air speed and l.e.suction was used, see fig. 6.

	d(mm)	(u/V)5
24.86 m/s	20	0.961
30.18 m/s	35	0.948

Clearly the effect of increasing the speed of both air and ground is to increase boundary layer thickness and reduce the velocity at 5mm. Simply the reason for this is that the fan evacuating the l.e.suction box is at maximum efficiency around 25 m/s and cannot remove the boundary layer air at the higher speed. The increased flow over the preforate is too much for the fan to remove and the increase in boundary layer thickness occurs.

3.2.3. Effect of Downstream Position

The effect of downstream position was assessed by taking a set of measurements down the centreline of the belt at positions 508mm (20") and 254mm (10") ahead of the balance centreline, at the balance centre and 254mm (10") rearward of the balance centre. These measurements are shown below, see fig. 7;

Height/mm	508mm fwd	254mm fwd	c/bal.	254mm rwd
0	1.000	1.000	1.000	1.000
5	0.953	0.956	0.956	0.961
10	0.988	0.985	0.983	0.981
15	1.000	0.997	0.995	0.992
20	1.000	1.000	1.000	1.000

These results confirm the initial description of the existance of the modified turbulent boundary layer over the ground. The lower layer being a region of air accelerated through friction and viscous effects by the belt surface. As can be seen in the table above the velocity of this region increases with downstream position as it is accelerated along the belt through viscosity. The velocity at 5mm increasing from 95% to 96% of freestream.

The conventional boundary layer exists on top of this accelerated region and is seen to grow with downstream position as expected. At 10mm height the initial velocity is 99% which falls to 98% of freestream at the rearward position.

These changes are very small and are not of great importance except that they give the detail of the mechanisms involved in the formation of the boundary layer on the belt.

3.2.4. Effect of Transverse Position

The full picture of the boundary layer as seen across the full width of the belt was assessed by taking a set of measurements from a traverse across the belt at the centre of balance position. This then built up information on the effectiveness of the leading edge suction box across

its full width. The results are plotted as a contour plot, looking upstream, shown in fig. 8.

This plot shows the effectiveness of the leading edge suction box in the centre of the tunnel where the model is positioned. Two regions either side of this central region also show up clearly, at 178mm (7") either side from the centre. These regions of relatively poorly removed boundary layer occur at the same width measurement as stringers incorporated in the suction box. These run longitudinaly and rise to the steel perforate cover to give structural stiffness to the box and help support the perforate. As a result of rising to the surface the suction experienced here is weakened resulting in the larger boundary layer at these positions.

A comparison of the central plot to that at 178mm (7") offset from centre is shown in fig. 9. This demonstrates the thickening of the boundary layer which is small but not negligible. A lowering or reshaping of these stringers to give a continuous uninterupted suction trough under the perforate would cure this problem.

3.3. 5.3m*2.4m Moving Ground in the 3.5m*2.6m Wind Tunnel

This moving ground was designed as a scaled up version of the highly successful 2.0m * 1.1m design, to be installed in the 3.5m * 2.6m wind tunnel. The design is shown schematically in fig. 4. During development, however, fundamental design changes have taken place, such as repositioning of the tracking roller. The details of development are given below in 3.3.1.

The main features of the ground are as on the smaller version. A continuous poly-urethane or P.V.C. belt

is fed around an arrangement of rollers which drive, track and tension it. The upper surface is fed over suction boxes between the two larger rollers to give the 5.3m long and 2.4m wide flat ground simulation which is positioned in the tunnel. The upper surface of the belt suction boxes is anodised steel, the belt having a low friction inner backing. Thus together running of the belt over these suction boxes does not cause any friction associated problems.

The belt suction boxes have holes in the upper surface and are evacuated using a number of fans so as to counter the low wake and underbody pressures which tend to lift the belt. A flat ground surface is thus maintained giving constant ride height which is of great importance in road vehicle testing. The rig is positioned higher than the original floor so as a slot exists between the old floor and the underside of the leading edge suction box to remove the tunnel boundary layer. Any residue boundary layer which is not removed is removed by the leading edge suction box by low pressure produced in the box under the perforate upper surface. This low pressure is produced by evacuating the box using a fan connected to it.

3.3.1. Development of the 5.3m * 2.4m Moving Ground

A major section of the initial work carried out in the research program was involved with development and commissioning of the large moving ground rig. Discussion of boundary layer development is given in this chapter in sections 3.3.2, 3.3.3, 3.3.4 and 3.3.5. Below is given the details an the mechanical development of the ground, the associated boundary layers measured as the ground progressed are shown in fig. 10.

August 1984

Initial tests of the moving ground were restricted due to servere vibration problems. Drive was by hydraulic motor on the upper rear 46 cm diameter roller, tracking was achieved by moving one end of the upper forward 46 cm roller vertically so the belt would run up or down it as required. This is identical to the system used on the smaller ground. Tensioning was provided by a 15 cm diameter roller mounted on vertical slides under the belt suction boxes. The belt suction was provided by a small vacuum pump and the boundary layer suction came from the fan used on the smaller ground.

The vibration problems were far too great to allow proper running and originated from the 15cm diameter tensioning roller which was out of balance and distorting in the centre so that it was 'wipping' against the belt. This 'wipping' motion being rotation around the centre of the tied ends with the roller between being a bowed cylinder, instead of rotating in the centre around the centre point it rotates about some offset point. Thus the centre point at the middle of the roller length rotates through an arc.

March 1985

Extensive modification of the tensioning system had been carried out, now a 23 cm diameter roller was used, mounted on swinging arms attached to the upper framework of the moving ground. The roller had been manufactured and balanced outside the University. Unfortunately during initial running of the rig a hydraulic line split close to the motor and covered the belt in hydraulic fluid. After extensive cleaning of the belt, rollers and suction boxes

the drive roller was found to be slipping badly. This limited the speed and since further cleaning was impossible a solution was reached by attaching 3M grit tape over the roller surface.

Further running revealed some limitations in the tracking mechanism which imposed a speed limitation. The problem was that the belt naturally tracked in one direction and there was insufficient movement on the front roller to bring it back. Various solutions were tried including addition of weight differentially to the tensioning roller, slewing the roller and use of springs to increase tension and provide easy adjustment of tension. None of these modifications resulted in an improvement, some made the problem worse. The set up was thus put back to the optimum for this time and boundary layer measurements taken at 23 m/s. These are shown in fig. 10 and discussed in 3.3.2.

May 1985

Work was carried out on the installation and running of the 2.0m * 1.1m moving ground as a yawed moving ground. The rig from the smaller tunnel was transferred and mounted on a turntable in the 3.5m*2.6m wind tunnel. A schematic plan of the installation is shown in fig. 16. More information on this installation is given at the end of this chapter, however,boundary layer measurements were taken over this ground which used the main leading edge suction box from the 5.3m * 2.4m ground.

During flow visualization tests separation was seen to occur off the leading radius of the box, in this case with the suction applied. This was prevented by adding a drooped nose section to the front of the box. Boundary

layer measurements then taken with various areas of the upper surface taped and this led to an optimised surface area on which to apply suction. This area was a a 15cm wide slot running the full width of the suction box, 15cm behind the leading edge of the box.

September 1985

The leading edge modifications to the suction box were incorporated and a new fan installed, rated at 5 m3/min at 1.02m W.G. Pressure. Swinging arm modifications were also incorporated consisting of adjustable spring loading and motor cycle dampers to to dampen the motion of the arms.

Heavy vibrations were again encountered at around 27 m/s and investigations were carried out with a strobe light to see were the vibrations were most evident. These revealed large movements in the frame and 'wipping' of the tensioning roller. The 'wipping' could not be cured but the frame was strengthened in key areas. The rig could then run at 30 m/s,wind off. Wind on running resulted in lifting of the belt from the suction boxes at these high speeds so the boundary layer measurements were taken at 24 m/s.

March 1986

A new 46 cm diameter roller was purchased to replace the 23 cm diameter tensioning roller, this had been dynamically balanced to 2000 R.P.M., a full speed of 50 m/s for the belt. Tracking was also altered, the large front roller now being fixed. Instead the smaller idling roller which feeds the belt onto the front roller was used, this being vertically adjusted using a jacking motor. Thus tension along the width of the belt is made differential

and the belt then moves right or left as this tension is altered.

All these modifications worked well and with increased frame rigidity, through extra ties and struts, wind off tests were able to reach 47.5 m/s, although vibrations were too great to test at this speed. A test speed of 35 m/s would, however, be possible. Belt lift at this speed was avoided by the use of four new suction fans connected to the belt suction. These fans rated at 28.3 m3/min at 0.15 W.G. Pressure. As 35 m/s was a maximum, testing was carried out at 28.55 m/s for all configurations and yaw angles with no problems.

May 1986

These tests involved the ground in its final specification for this research project. Belt suction had been improved by the addition of holes in the rear suction box and the connecting of two fans to it. This was done as belt lift always occured first at the rear of the ground, then moving forward as speed increases. The next box had a single fan connected to it whereas the front two boxes were interconnected to the remaining fan.

Boundary layer measurements were then taken and model tests performed at speeds up to 35m/s for all configurtions with no belt lift. Vibrations still limited speed to 35m/s as above this vibrations were transmitted to the model and interfered with the results. The speed however was considered to be more than sufficient with the larger scale of model to give good Reynolds numbers. At 28.55m/s, the standard test speed, this was 3,960,000 based on model length.

August/September 1987

In this period of final testing no extensive development was carried out until after the tests. The only modification was the repositioning of the leading edge suction fan which improved boundary layers as the delivery length was shorter between the fan and the suction box, thus reducing losses. These boundary layer measurements are discussed after this section as the final configuration used for the extensive final tests.

Further modifications have been incorporated in the leading edge suction, since August, to improve the boundary layers to those shown in figs. 10, 11, 12, 13 & 14. Results for the new configuration are shown in fig. 15 and described in Ch.3.3.5.

3.3.2. Boundary Layer Reduction

Throughout the ground development detailed in 3.3.1. measurements were taken using the boundary layer rake. Thus modifications to the boundary layer removal system could be judged and a knowledge of the empty test section flow over the belt attained. The major figures obtained from these tests are given below and are taken under the balance centreline, but offset 279mm (11") to the right. This was as a result of traverses across the width of the belt revealing the flow in the centre to be poor when compared with the rest of the traverse. This is fully explained in 3.3.5.

	d(mm)	(u/V)10
March 1985	210	0.842
September 1985	73	0.931
March 1986	45	0.945
May 1986	45	0.954
August 1987	22	0.971

The figures demonstrate the continuous development of the installation to its present state. The major achievements were obtained when a new suction fan was bought between March and September 1985. Also the flow visualization studies in May 1985 had revealed the leading edge separation which had been cured with a drooped leading edge. Even with the new fan poorly installed with a long connecting pipe between it and the suction box involving great losses, the thickness of the boundary layer was reduced by 66%. The velocity at 10mm was brought to 93% of freestream.

Subsequent testing consisted of attempting to improve belt suction and reducing vibrations to increase testing speed. This concentrated on the belt suction boxes and the tensioning roller, the boundary layer removal system was however subtly changed to achieve some improvement. Between September 1985 and March 1986 a large diameter hard walled tube was used to connect between the fan and the suction box to reduce losses. This improved the boundary layer greatly, reducing thickness by 50% but only increasing the velocity at 10mm by an extra 1.5%.

Modifications to reduce the blockage in the removal slot under the leading edge suction box lead to more efficient removal of the boundary layer by this method. This resulted in a layer of the same overall

thickness but of greater velocity at 10mm, now more than 95% of freestream.

The final improvement was also a major one, achieved by repositioning the fan closer to the suction box. This resulted in reducing the length of connecting tube by around 66% thus increasing efficiency. The boundary layer thickness was again reduced by 50%, resulting in a thickness of just 22mm, 2mm more than in the smaller tunnel. Allowing for the increased model scale in the larger tunnel means the boundary layer is relatively much better. The lowest velocity, at 10mm, was just 0.9% below the edge of the boundary layer condition (98% freestream velocity), also better than in the smaller tunnel and resulting in an almost negligable boundary layer. Thus the large ground matched the criteria layed down for it by the 'state of the art' smaller ground.

3.3.3. Effect of Configuration Change

Measurements were again taken, again on the balance centreline, 11" offset to the right, of the effect of leading edge suction and ground motion on the boundary layer,see fig. 11.

L.E.Suction	Ground	d(mm)	(u/V)10
on	on	22	0.971
on	off	38	0.794
off	off	76	0.776

The three plots again demonstrate the existance of a normal turbulent boundary layer coming away from from the leading edge suction box. In the case of the ground stopped this then continues back leaving a large boundary

layer, close to the ground. This layer is twice as thick with the leading edge suction off. The ground moving case, as in the smaller tunnel, shows that this boundary layer is modified as the air close to the belt surface is accelerated through friction and viscous effects. This greatly increases the velocities close to the belt, 97% of freestream at 10mm an increase of 20%. This being 0.9% from the 98% criteria giving an almost negligible boundary layer condition.

3.3.4. Effect of Downstream Position

The results taken by measurements taken 279mm (11") offset to the right at the balance centreline, 1092mm (43") forward and 1143mm (45") rearward of this centreline give the results plotted in figs. 12 & 13. One plot is for the leading edge suction on, ground on case the other being for the leading edge suction on, ground stopped case.

Most important is the ground moving case which shows little change with downstream position except for an increase in the velocity at 10mm as the air closest to the ground is accelerated through viscous effects and the ground motion.

	d(mm)	(u/V)10
1092mm Fwd.	40	0.948
C/Balance	22	0.971
1143mm Rwd	40	0.969

In the case of ground stopped the usual growth of boundary layer with downstream position is witnessed. The majority of growth occuring before the balance centreline.

3.3.5. Effect of Traverse Position Across Belt

These measurements a spanwise series of vertical traverses across the belt at the centreline of the balance.These were taken at a spacing of 140mm (5.5"). The plot, fig. 14 are the plots showing the major changes. The results proved symetric of the centreline so only one side is considered;

	d(mm)	(u/V)10
Centre of belt	51	0.950
140mm offset	40	0.965
280mm offset	22	0.971
420mm offset	30	0.965
560mm offset	40	0.965
700mm offset	40	0.970

Those at the centre, 280mm (11") offset and 560mm (22") offset are plotted in fig. 14. These results show that in the centre and at 560mm (22") offset the boundary layer is more than 200% thicker than that found 280mm (11") offset. The actual velocities at 10mm height are not very different, the centre case is 2% down but still 95% of freestream. The reason for these differences is the construction of the suction box.

The box is made in two halves and joined in the centre. At the end of each half and at 560mm (22") interval across them are longitudinal stringers dividing the box up. These stringers extend up to the perforate steel surface and are 19mm (3/4") wide. This results in an area of reduced suction at these points, a decrease in the centre of twice as much. This results in thicker boundary layers and lower velocities aft of these regions which are

seen in the traverse measurements.

Although these results show an imperfect situation the boundary layer present is of comparible state to that present in the 2.1m * 1.7m wind tunnel and as such was acceptable for the research carried out. Further improvements have been carried out on the leading edge suction box which have resulted in a uniform boundary layer over the width of the belt, shown in fig. 15. This is as a result of removing the strengthening stringers and making a continuous trough under the perforate which gives an even depression along its length thus giving even boundary layer removal. Other modifications are planned, highlighted during this research, which should also improve the speed limitation resulting in a very powerful facility for future work.

3.4. Yawed 2.0m*1.1m Ground in the 3.5m*2.6m Wind Tunnel

In order to obtain a better simulation of crosswinds in the wind tunnel the moving ground should be yawed to the oncoming air along with the model. In this way the motion of the ground is correct to the axis of the model and rotating wheels can be used on the model and run on the belt. If the wheels are suspended from the model full force measurements cannot be taken as sideforce and yawing moment would be reacted by the wheels on the belt. A full set of results would require that the wheels be in position but suspended on arms from the side of the ground and not attached to the model. The aerodynamic force on the wheel itself is then measured separately to the measurements on the model. This set up is ideal for pressure measurements where wheel rotation effects the flow and wheels can be mounted from the model so no outside mountings effect the flow. This simulation was achieved by

mounting the 2.0m * 1.1m moving ground on a turntable in the 3.5m * 2.6m wind tunnel, shown in schematic plan in fig. 16. As this was the configuration used in the smaller tunnel no problems were experienced in terms of tracking, belt tracking or speed control. Boundary layers however proved a different matter. The set up was initally used fitted flush with the existing floor and used both the leading edge suction boxes from both ground rigs. The boundary layers obtained were unacceptably high so the ground was raised to allow a slot at the leading edge to help remove the boundary layer. This together with a drooped leading edge as described earlier and a suction fan bought especially for the boundary layer removal gave improvements resulting in the boundary layers shown in fig. 17. This shows the excellent results obtained except for the central position which again was affected by the leading edge suction box design as described in 3.3.5.

Measurements taken at yaw were affected by the central partition and a loss of suction in the area where the front and side suction boxes joined and as yaw increased this played a bigger part in the boundary layers present.See fig. 18.

To summarise the best measurements show d=0mm and (u/V)10=0.985, the worst case, at the centreline,give d>60mm and (u/v)10=0.948. This configuration was considered acceptable for the work carried out using it as the velocities are within 5% of freestream. Greater detail of the testing configuration is given in ref. 8, with greater detail of work carried out, reported in ref. 1.

Chapter 4. Balance Assessment

4.1. Introduction

Since at the commencement of research a new wind tunnel was being used, its suitability for the work needed to be assessed. The size, speed and state of the ground, as previously described, are all part of this suitability. Another aspect, and possibly the main aspect, is the level of performance achievable by the force measuring equipment. Parallel studies of the various force balances in use were undertaken at the time of the ground development work. This would lead to a thorough knowledge of the various ways of obtaining force measurements from model tests over a moving ground.

All the original balances were assessed along with new balances designed specifically for this research when the old balances were found to be inadequate or limited for this work. The measurements used were various, from statically loaded calibration tests to dynamic repeatability tests on a model configuration. The static calibrations were carried out over a range of forces similar to those expected in the scale model tests. In this way the balances could be judged for accuracy and repeatability. Accuracy is the minimum quantity which can be confidently measured. Assessment of accuracy was made from static weight calibration tests together with a knowledge of data logging system used to take the readings. Repeatability is the ability of the balance to give the same result for a number of separate identical test runs. This was assessed by viewing both the repeatability of the static weight calibration tests and the repeatability of model tests of identical configuration. Sensitivity is also assessed by consideration of the minimum measurement

possible with the equipment used.

The descriptions of the balances are given first followed by the assessment of the statically loaded calibration tests. The discussion of the dynamic performance of all the balances is given in Ch.4.6. so that comparison of all the balances can be made in their major role, taking results from wind tunnel tests. Comparison is then made with other balances used for road vehicle work in other establishments.

4.2.1. 2.1m * 1.7m Wind Tunnel Balance

The balance used in this tunnel is of overhead weigh beam type which is fully automatic in operation. It is mounted on the working section roof, is fixed, co-ordinated to the tunnel axis and measures lift, drag and pitching moment. A vertical strut passes through the tunnel roof attaching to the model having passed through the model roof and via a pivot to leave the model free in pitch. Force is transmitted to the beams on which the balance of the beam is sensed. The electronics then drive stepper motors to move a sliding weights along the beams until each beam is balanced. The number of steps taken to balance each beam is displayed on a console and is read by a microcomputer.

4.2.2. Calibrations

These results were taken by applying static loads to the balance in whichever direction was of interest, any cross-coupling was also investigated. Typical results can be seen plotted in figs. 19(a), (b) and (c). In all cases the calibrations were linear with excellent repeatability. Throughout the calibration exercise the accuracy and

repeatability of the balance proved excellent giving the following results:

Lift	0.00418 N/step	+/- 0.05%
Drag	0.01668 N/step	+/- 0.05%
Pitch	-0.00254 N/step	+/- 0.05%

These were all within the shown margin of the calibrations quoted by the manufacturers, Elven, when the balance was installed in 1981. These results meant that the least sensitive channel, drag, could read 0.017 N static load, being 1 step, to 0.05%. In practice, however, this accuracy could not be achieved as due to the unsteady forces acting on the model in testing the final figure on the step readout was unsteady. Thus the computer is used and twenty samples are taken and averaged. The deviation on drag readings usually being 0.1%. The worst deviation found being for lift which was usually no more than 0.5%, the least accurate reading being to 1.3%. This poor reading was due to poor mounting of the underbody being tested and with more careful set up variations in the lift reading fell back to 0.5%. For a full assessment of the dynamic performance of the balance see Ch.4.6.

4.3.1. 3.5m * 2.6m Wind Tunnel Balance

The balance installed in this tunnel is the modified overhead balance used with the tunnel at R.A.E. before being moved to Southampton University. At R.A.E. it used electromagnets to to measure all six components of force, each being measured individually with the other five sections being locked. This was an old system and clearly inappropriate to the requirement of the tunnel here, measurements must also have been very time consuming to record. On installation here the balance was modified so

that measurements were taken from load cells attached to the relevant force beam on the balance. Initially only lift, drag and pitching moment were of interest, all three being unlocked and measured simultaneously. All other components being left locked.

The load cells are all connected to a common, stabilised voltage supply of 10 V, the cables are screened to maintain a 'clean' signal. Readings of the voltage output are then taken on a digital voltmeter, D.V.M., and minate system connected to a microcomputer.

4.3.2. Calibration

As previously described in 4.2.1. static weight calibrations were obtained on the various channels by loading them with weights over ranges as expected during model testing. This was done to assess repeatability of the calibrations and to investigate cross-coupling. The calibrations obtained showed both poor linearity and repeatability. There was a great deal of hysterysis present in the set up, as shown in an example plot for drag in fig. 20. The calibration figures found were:

Lift	137.03	N/mV	+/- 2.0%
Drag(222 N cell)	29.11	N/mV	+/- 7.0%
(111 N cell)	11.32	N/mV	+/- 6.0%
Pitch	11.17	N/mV	+/- 5.0%

All the load cells initially installed had maximum loads of 222 N (50 lbs). The poor accuracy and repeatability of the drag system led to the trial of a load cell with maximum loading of 111 N (25 lbs) to improve sensitivity.

The maximum reading sensitivity of the D.V.M.-minate system is one micro volt although this figure was never constant even for the static load cases described here. Thus the effect is to result in a lower accuracy than stated here. It can be seen that all the sensitivities for the static load calibrations are much less than for the smaller tunnel's balance, with the exception of the drag channel using the 111 N (25 lb) load cell. Using the smaller load cell the sensitivity is of the same order as for the weigh beam balance but its accuracy is to +/- 6%, more than a hundred times that of the weigh beam balance. Also the drag channel of the weigh beam balance is the least sensitive channel. Lift, although being comparibly repeatable, to +/- 2%, is thirty times less sensitive than the weigh beam balance.

These results together with the dynamic repeatabilities described in Ch.4.6. clearly show the ineffectivness of the balance for the commercial vehicle reseach. The balance had been designed for aeronautical work and the modifications to it had deteriorated its performance rendering it unsuitable for the research reported here. The repeat runs for various test configurations detailed in Ch.4.6. demonstrated the variations in the results obtained to be greater than the differences resulting from aerodynamic modifications. Thus new balances were then designed for the commercial vehicle work see Ch.4.4.

4.4.1. Internal Load Cell Balances

Due to the poor performance of the overhead balance in the 3.5m * 2.6m tunnel new balances were required in order to carry out the 1/4 scale model testing. In order to cut down on the complexity of the balances

required it was decided that a drag balance should first be designed and tested to prove its functioning. This was carried out sucessfully and an additional sideforce/yawing moment balance was designed using the same philosophy. The three components were chosen as those being of most concern to commercial vehicle aerodynamics as a full six component balance could not be developed. These balances are shown in fig. 1(a) and (b).

The balances are load cell balances with flexures used between the upper and lower plate. These flexures are used to tie the balance,allowing only forces in the direction of interest to be transmitted to the load cell. The load cell on the drag balance is mounted from the upper plate and a bearing assembly fixed to the lower plate. The bearings are brought into contact with a tongue attached to the load cell, thus allowing loads to be transmitted to it. In the sideforce/yawing moment balance two load cells are used, one forward and one rearward on the centreline. The outputs from these two load cells taken additionally will give sideforce and differentially to give yawing moment.

Initially the means of transfering loads to the sideforce/yawing moment balance utilised wasted down ties on just one side of each cell. These were fine in tension but as they were also required to take compressive loads needed to be changed and the bearing system used on the drag balance was used. A bearing race either side of a smooth tongue was attached to the load cell.

These balances were fixed inside the model, in the container of the box van, the strut mounting from the overhead balance then attaching to these balances. The overhead balance was locked in all components for these tests. Yawing of the model was simple as the overhead

balance was turntable mounted so all yaw angles could be easily set on the turntable, the balances always remaining body axis co-ordinated.

4.4.2. Calibration

The balances were mounted on a calibration stand and static loads could then be applied, over the ranges expected during model tests. Readings were taken to calibrate the balances and investigate any cross coupling effects. The results showed the calibrations to be linear, see figs. 21(a), (b) and (c), but some problems were encountered.

The bearings needed very careful setting up as this greatly affected both the linearity and the repeatability of the calibration. What occurred was that during loading, if some negative preload had been applied to the load cell through the bearing assembly, a position was reached when, although loaded, the balance was in its zero state. This meant a gap appeared between one or both of the bearings and the load cell tongue. Thus a step would appear in the plot of load against output voltage. This was, however, easily identified and overcome. In the case of the drag balance the bearings were set up so that slight positive preload was present on the load cell thus ensuring no 'zero point' was passed through.

The sideforce /yawing moment balance was a little harder to remedy. In this case no obvious preload could be placed on the load cells as the sideforce and yawing moment system acting on the model could result in forces acting on the load cells in either sense. An acceptable solution was achieved by extremely careful setting up resulting in either a minimum gap being left between each bearing and

the tongue using a feeler gauge, or more practically, each bearing being minutely adjusted to result in the load cell reading zero volts at zero load. Thus no other zero point exists and no step occurs at zero or small loads. This solution proved to work well.

Another problem encountered with the sideforce/yawing moment balance was that the sideforce calibrations, although linear and repeatable, were slightly different for positve or negative sideforces. Checking of the mounting and loading systems on the calibration stand revealed no misallignments. The problem is probably due to slight misallignments in the flexures or load cells in the balance. These would be unavoidable in the construction but as the calibrations are linear and repeatable the problem was overcome in the programming of the microcomputer sampling the D.V.M.. A relevant calibration being applied dependant on whether the sideforce witnessed was positive or negative. The calibrations found were:

Drag	24.817 N/mV	+/- 1.0%
Sideforce (+ve)	27.174 N/mV	+/- 3.0%
(-ve)	28.011 N/mV	+/- 3.0%
Yawing Moment	10.444 N/mV	+/- 1.0%

Repeatabilities were very dependant on the set up of the balance as described but if care was taken excellent repeatability was obtained. As with the overhead load cell balance the microcomputer D.V.M. system was used measuring to one microvolt. This time though during the static calibrations the final figure read was steady, again being at least a factor of ten less steady during dynamic tests. Thus for drag the sensitivity is of the same order as for the weigh beam balance in the 2.1m * 1.7m tunnel. The repeatability is less as a consequence of using load cells,

the load cell has a constant and instantaneous response to any load change on it, as found in model tests. The weigh beam balance, on the other hand, being automatic has a control loop in which some delay can be incoporated giving some damping to unsteady forces. This then gives rise to better repeatability through the smoothing of unsteady readings.

No cross coupling was found, the flexures working well, allowing only deflections in the desired direction. The dynamic performance of the balances is given in Ch.4.6..

4.5.1. Internal Strain Gauge Dynamometer

In order to test models at yaw in the 2.1m * 1.7m wind tunnel an internal strain gauge balance, measuring sideforce, yawing and rolling moments, needs to be used with the overhead balance. The design and full description of this balance is given in ref. 9. The overhead balance is fixed with its axis orientated to the tunnel working section, thus at yaw the model is yawed relative to the balance. Drag as measured by the balance is therefore a combination of drag and sideforce. The internal strain gauge balance stays orientated to the models body axis so by calculation from the six components measured, the full six components of the body orientated force and moment can be found.

4.5.2. Calibration

Calibrations of all forces and moments were carried out to give both calibrations for each channel and to check for any cross- coupling present. The calibrations proved linear and repeatable and although some

cross-coupling was evident it was both nonlinear and negligable compared to the outputs from forces on the correct channels. The results from the calibrations, see fig. 22(a),(b) and (c) are:

Sideforce	90.349 N/mV	+/- 0.2%
Yawing Moment	-10.996 Nm/mV	+/- 1.6%
Rolling Moment	41.445 Nm/mV	+/- 1.2%

During testing, rolling moment had to be disregarded as readings taken from it showed great scatter. This was later traced to a bad connection in the rolling moment circuit. It was not possible to deal with at the time and as sideforce and yawing moment were of primary interest testing was carried out without rolling moment measurements.

The calibrations show excellent linearity and repeatability. The D.V.M. and minate system used in the 2.1m * 1.7m tunnel is of the same type as used in the 3.5m * 2.6m tunnel, and reads to one microvolt. This is then sampled by a microcomputer which takes and averages a number of readings during a run. During the static load tests the final one microvolt figure was reasonably steady though for dynamic tests averages needed to be taken as the readings varied by tens of microvolts. The sensitivity of sideforce was not very high but since this would be measuring high forces at the high yaw angles this was not a problem. The sensitivity of the yawing moment channel was as for the load cell balance described in Ch.4.4. The dynamic performance is assessed in Ch.4.6.

4.6. Dynamic Performance

The assessment of the dynamic performance of the

balances was carried out by repeat runs of identical configurations to see how well the results repeated. Thus an accuracy could be placed on the coefficients calculated from the readings taken. The figures quoted here represent the variation of coefficients found ,on repeat test runs on the same and different days, from the average coefficient calculated for that particular configuration. These are then compared to results found for other wind tunnels carrying out similar work. Firstly ref. 10. gives the variation in coefficients from the average, for four North American wind tunnels as:

Cl	+/-0.011
Cd	+/-0.002
Cm	+/-0.004
Cy	+/-0.005
Cn	+/-0.003
Cr	+/-0.005

The lift coefficient repeatability was reported as being poor due to the particularly poor repeatability of one tunnel. The average repeatability in lift coefficient for the remaining three tunnels is +/-0.006.

Data is also given in ref. 11, on the repeatability of drag coefficients about the mean for a given configuration. The variations are given as:

N.R.C.,Canada	+/-0.001
N.M.I.,Britain	+/-0.005
Fachhofschule,Germany	+/-0.004
Cranfield,Britain	+/-0.005
M.I.R.A.,Britain	+/-0.002

Results of this kind were found here, for the

various balances, and used to compare with the results listed above. Some of these results from truck work carried out at the start of this research and during other research are given in ref. 1. These results are given here together with more recent figures:

2.1m * 1.7m Tunnel Overhead Balance

Date	Configurations	Repeats	Cl	Cd	Cm
8/84	20	48	.003	.006	.002
9/84	11	22	.005	.006	-
4/85	1	23	.004	.007	.004
8/85	2	38	.005	.006	.003
8/85	9	18	.001	.002	.001
9/85	34	68	.002	.001	.001
1/86	11	22	.002	.001	.001
7/86	5	25	.005	.007	.004
9/86	5	40	.002	.004	.002
10/86	10	34	.003	.002	.002
4/87	9	18	.002	.002	.002

3.5m * 2.6m Tunnel Overhead Balance

Date	Configurations	Repeats	Cl	Cd	Cm
11/84	5	12	.012	.078	.027
3/85	2	12	.008	.034	.018
7/85	1	3	.014	.017	.014
	(111 N) 1	3	-	.050	-
9/85	4	16	.005	.011	-
	(111 N) 2	6	-	.014	-

Load Cell Balances

Date	Configurations	Repeats	Cd	Cy	Cn
9/85	6	22	.005	-	-
10/85	76	152	.005	-	-
7/87	25	73	.002	.003	.001
9/87	5	26	.003	.005	.004

Strain Gauge Dynamometer

Date	Configurations	Repeats	Cy	Cn	Cr
9/84	11	22	.021	.004	.009
11/84	5	12	.005	.003	.016
10/85	76	152	.007	.008	.006
4/87	6	43	.005	.002	-

These results are all the average variations, positive and negative, about the mean coefficient. The results for the 2.1m * 1.7m tunnel show excellent repeatability throughout all the testing. The slight trend noticeable is of improving repeatability with familiarization and the more precise model set up that good testing requires. A problem that did show up, however, was an occasional step change in the coefficient was obtained. Modification to the model still gave the same change in result but the baseline figure had changed. This step change would always be in the range +/-0.005 in the coefficient and as it had no effect on the trends and changes due to modifications on the model it was not considered a major problem. It was accounted for by taking an average result from a number of repeat runs taken over a number of days on the baseline configuration of the model. The trends in the aerodynamic characteristics then relate to this average.

The reason for the step change is due to changes in the day to day performance of the leading edge suction box. The box was found to have separation from its leading radius which just reattached when suction was applied to the box. The fan was therefore operating at its limit and small condition changes to the air in the tunnel could affect the amount of reattachment. Thus the boundary layer would be affected which would alter the underbody

performance of the model leading to slight step changes in the baseline coefficients. As the more major changes to the model are carried out above the boundary layer zone, the performance of these modifications would be unalterred. This futher demonstrates the great effect the ground simulation can have on results on ground vehicles. Overall the 2.1m * 1.7m tunnel weigh beam balance is accurate and highly repeatable being better than that obtained with the balances used in refs. 10 & 11.

The poor performance of the 3.5m * 2.6m tunnel overhead balance is again demonstrated. Even the use of the 111 N (25 lb) load cell does not improve matters and the balance was clearly unsuitable for the work to be undertaken. All the repeats obtained were a factor of ten greater than required, although lift showed promising repeatability. Generally the scatter in the results was greater than the effect of some of the changes to the model. As a result the load cell balances were designed and built so that satisfactory results could be obtained for the 1/4 scale model in the 3.5m * 2.6m tunnel.

Repeatability of the load cell balances was dependant on the careful setting up of the bearings transfering the forces, as described in Ch.4.4.2. When care was taken the repeatabilities proved excellent,+/-0.003 for drag coefficient and at worst +/-0.005 for sideforce coefficient. During the 1/4 scale tests the variation in the drag readout was better than 2%.These excellent figures for the 1/4 scale where also reiterated when the 1/6 scale model was tested with its corresponding lower forces. The sideforce and yawing moment coefficients repeatability was also excellent although for some readings the variation in the load cells output was over 100%. This was due to measurements when the force system acting on the model was

such that one load cell was varying around its zero point giving large percentage deviations. When this was combined with the output from the other load cell the variations were more of the order +/-5%.

These results demonstrate that the balances designed were of equal capabilities as the balances descibed in refs. 10 & 11. Also, around this time, smaller scale automotive models were being tested and a new six component load cell balance was purchased for this purpose. This was unsuitable for the 1/4 scale work but has proved reliable in the limited use it has experienced so far.

The strain gauge dynamometer also shows excellent dynamic behaviour, up to the standard of the balances used in the North American tunnels. This was both surprising and pleasing as initially the balance had been designed as a third year undergraduate project and between the tests detailed during 10/85 and 4/87 the balance had been redesigned and rebuilt. No deterioration in performance was evident, in fact a slight improvement occured. The balance had been modified to lower its overall height as this limited its use in some scale car models. The poor sideforce repeatability during 9/84 had been due to play in the mounting system between the dynamometer and the strut and was overcome by a redesign of the pivot assembly.

The balances used here in Southampton University tunnels are of excellent standard, comparing as favourably if not more so than others detailed from other establishments carrying out road vehicle research. The results from this chapter demonstrate the accuracy and reliability of the measurements taken here. All results quoted in this report are given to three decimal places, as is the common practice, but confidence can be placed in

them due to the results reported in this chapter.

Chapter 5. Present Day Commercial Vehicles

5.1. Introduction

Initially the work undertaken was to develop the 3.5m * 2.6m wind tunnel into a viable moving ground test facility. It was felt that this would be best done by proving it using a model representing a typical modern day rigid box van. Results could then be compared to similar studies in the 2.1m * 1.7m tunnel and with a bank of similar data found in refs. 1-5, 8, 10, 11, 13, 16-21, and in the bibliography. Although anomalies do occur in this published data the overall picture of the aerodynamic behaviour is well established. The main reason for differences in results being scale, ground representation, model detail, set up detail, blockage and other test facility differences. The forces measured throughout this work are in the senses shown in fig. 23, as given for general use in the S.A.E. recommended practice, ref, 12.

5.2. 1/4 Scale Model

A 1/4 scale model was loaned by Leyland Vehicles Ltd., the scale being chosen as the most suitable for the 3.5m * 2.6m tunnel to give good Reynolds numbers and to keep blockage below 5%, as given in the S.A.E. Test Procedure for Trucks and Buses, ref. 12. The model supplied was a rigid box van, of 10-30 ton type, with a T45 prototype cab and rectangular box container, see plate 2.

The model was very detailed with engine and cooling fan, exhaust manifold and silencers, gearbox and drive train, axles, suspension and all exterior tanks well modelled. The chassis was made from thin sheet steel and was originally a display model and therefore lacked the

rigidity required of a wind tunnel model. Also as the model had fixed wooden wheels it required suspension from which to mount rotating wheels to upgrade it for use over the moving ground.

In fact all that was kept from the original model was the fibre glass cab and detailed underbody parts. A new rigid steel chassis was built, the cab and underbody parts being fitted to this chassis. A new box container was built in wood, to the same overall dimensions as the original corrigated version. This was done to ease access into the container and for fixing of add-ons to the container. The suspension was made from solid steel bars and fashioned to mimic the leaf suspension of the original model. Each swinging arm was attached to the chassis via bearings in blocks screwed to the chassis. The arm was then able to freely pivot up and down thus allowing only the drag of the rolling wheel to be transmitted to the balance. Rolling resistance was eliminated from the results by first zeroing the balance with the belt moving with no wind blowing. After this the wind speed was increased allowing the aerodynamic forces to be measured.

Cooling was also modelled using a metal frame over which a fine gauze was stretched. This simulated radiator was then placed in position with a small under bumper scoop to feed air to it. The devices made for these tests were similar to those used as add-ons on vehicles today. Three flat plate deflectors of varying size, a 3-d, Leyland style deflector, four sizes of air dam and rear mounted spoilers to minimise the wake were constructed to test.

Force measurements and some flow visualizations were then carried out on the model in various

configurations at zero yaw angle and then at steps of 5 degrees up to 15 degrees of yaw. The velocity in the plane of the model was measured by four pitot-static tubes placed around the working section. These were averaged and this speed then set to match the moving belt. This was also taken as the test speed to calculate the coefficients and thus no blockage correction applied. Freestream velocity was also noted and area blockage corrected results recorded for comparison, these always gave lower values and for the purpose of this report coefficients relating to the working section velocity are used unless indicated. All coefficients are calculated referenced to a standard baseline frontal area. Thus although addition of an airdam increases the frontal area, if the result is referenced to a standard area its true effect on the aerodynamic forces is witnessed in the coefficient. This avoids complicating area related effects.

5.3. Discussion

The forces acting on the model arise from differences in the pressures acting on opposing faces of the model. Drag arises from a build up of pressure on the front face and low pressures in the wake acting on the base. Pressure differences between upper and lower surfaces result in lift and between the sides result in sideforce. The distibution of these pressures on the surface alters the effective centre of these forces resulting in moments. Due to its bluff nature the majority of drag arises from the high frontal pressures built up on cab and container faces. Separations from any sharp edges increase drag through increasing the wake size of the vehicle.

The vehicle tested here was equipped with a modern cab, a T45 prototype, so was equipped with radiused

leading edges. Flow visualization revealed that no separation occurred over the cab roof, unlike the case of a square edged cab. This has two converse effects, the drag component of the cab is reduced but the drag component of the container is increased as the flow incident on its front face is now of greater velocity. Thus although the cab is improved overall the performance is poor due to containers contribution.

The drag distribution has been estimated as about 60-70% from the forward faces and 15-25% from the base faces. Therefore the best savings are to be made from modifications to the front of the vehicle, to relieve pressure and prevent separations from any leading edges. This philosophy has resulted in some of the add-ons in use today as these were the simplest most easily applied solutions to a present day vehicle.

Readings obtained for sideforce and yawing moment were not as reliable as hoped due to the means of transmission used in the load cell balance, see Ch.4.4.1.. An idea of trends can, however, be deduced and thus most of this chapter refers to drag readings but with some description of the other components.

5.3.1. Reynolds Number Effects at Zero Yaw

The variation of the drag coefficient with Reynolds number is shown in fig. 24. A classic effect is shown with with an initial constant value suddenly falling between 26 and 28 m/s then becoming constant again. This is the effect of the separations on the side of the cab. Flow visualization showed the flow on the upper cab radius to be attached, and the flow from the sides and upper edge of the container to be separated as expected. The flow around the

side radii, being smaller than the upper radius, is detatched becoming attached as the Reynolds number is increased. Then with fully attached flow developed on the cab the drag again becomes constant, with separations from the square container edges. Testing at 28.55 m/s, Re(l)=3,650,000, is justified for this scale in this tunnel. See also Ch. 6.3.1.

5.3.2. Cab Roof Deflectors

The most obvious way to ease the flow around the forebody of a cab-container configuration is to use a deflector matching the flow over the cab to the flow over the container. Thus the container front face pressures are relieved, as are separations, and the flow down between the gap is reduced and with it the lift induced drag from the underbody flow. Initially flat plate deflectors were used but now 3-d deflectors have evolved. All these types were tested, including three flat plates of different size and a Leyland type 3-d deflector. Each was built to a specification to optimise flow matching over the cab roof.

At zero yaw the the flat plate deflectors reduced drag progressively from the smallest to the largest. The 3-d deflector was slightly less effective than the largest flat plate, this being as a result of the shielding effect of the 3-d defector being less. It did not span as much width as the flat plate deflector and thus some build up of pressure on the container upper front corners will occur. This slight decline in the effectiveness of the 3-d deflector is small and unimportant in comparison to its performance at yaw, as described later. The savings on the drag coefficient at zero yaw are given over the page;

Flat plate no.1	-0.010
Flat plate no.2	-0.044
Flat plate no.3	-0.069
Leyland style	-0.064

It is seen that the matching achieved by the flat plate no.3 and the 'Leyland' style deflector is the same and was confirmed by flow visualization showing fully attached flow over the top of the container. Flat plates 1 and 2 still resulted in separation from the container leading edge as fully matched flow was not achieved. Their drag reducing performance was from shielding a portion of the container front face, thus the greater the shielding the greater the drag reduction.

When yawed the effectiveness of the deflectors changes, the reductions in drag coefficient for the various yaw angles are given below;

	5 deg.	10 deg.	15 deg.
Flat Plate no.1	-0.049	-0.009	-
Flat plate no.2	-0.047	-0.009	-
Flat plate no.3	-0.075	-0.013	+0.006
Leyland style	-0.096	-0.071	-0.067

As these results clearly demonstrate as yaw increases the effectiveness of the flat plate deflectors diminishes rapidly, at 15 degrees the largest deflector gives a drag increase. The two smaller deflectors giving maximum performance at 5 degrees yaw then having little effect at 10 degrees. One reason for this is that as the model is yawed their shielding effect is only that from the area which projects onto the container front face. As yaw increases some of the deflectors area now lies outside the container front face and is simply producing extra drag.

Also since the deflector sides are sharp there is a sharp edge effect of the windward edge of the deflector on the crosswind. The air either is fed over the deflector or it is allowed to continue to build up the pressure on the now exposed portion of the container front face. The 3-d deflector, however, is designed so that at yaw the solid side part of the deflector helps flow deflect down the windward side of the container, still resulting in the relief of the container fore-pressure. Its design is also such that little, if any, of its projected area falls outside the container area until very high angles of yaw are reached. Thus no additional drag results via this mechanism.

The 3-d deflector is then the ideal choice of deflector as it works as well in crosswinds as it does at zero yaw. This is also demonstrated in the wind averaged drag coefficients. These are calculated using the formulae given in refs. 4, 5, 12, and given in Appendix 1. In order to ease comparison the S.A.E. practice, using an average wind of 7 m.p.h. and a vehicle speed of 55 m.p.h. is used here. The resulting values are;

	Cd(55)
Baseline	0.786
Flat plate no.1	0.749
Flat plate no.2	0.742
Flat plate no.3	0.718
Leyland style	0.705

These results again demonstrate the effect of the devices at yaw. The two smaller plate deflectors have similar results and the third plate deflector works well but the 3-d deflector is clearly better. The calculation relies heavily on the vehicle speed chosen,the faster the

speed the lower the statistical yaw angles resulting become. Thus for a speed of 55 m.p.h. the maximum yaw angle used is 7.2 degrees, for a lower speed a higher maximum yaw angle would result. This would show an even greater benifit from the 3-d deflector.

Comparing these results to those in ref. 4, the results published are of remarkably similar order. The results published are for a basic straight truck, (a rigid box van), the baseline wind averaged drag factor was Cd(55)=0.775 and with a slightly curved plate deflector this fell to Cd(55)=0.695. These results agree closely with those obtained here, the differences in wind averaged drag factor due to a flat plate plate here and a slightly curved plate in ref. 4, were -0.069 flat plate and -0.078 curved plate. The better result due to curving of the plate helping its yaw performance.

The effects of the deflectors on sideforce was to lower the value; although the change was small. This is as a result of the shielding effect on the container front face. The change is small since, although shielding and hence reduction takes place, an extra component due to the deflector itself is introduced. This component also results in the yawing moment becoming negative as the shielding effect causes the loss of sideforce from the front face of the container. Thus the centre of sideforce is shifted rearwards changing the sign of the yawing moment. The magnitude of the yawing moment appears to be the same order but of different sign. Again the 3-d deflector is the optimum, minimising the yawing moment, even though the sideforce is nearly identical for all deflectors.

5.3.3. Fairing

A fairing was made to fill the gap between the cab with the 3-d deflector fitted and the container. It was designed to make the smoothest possible blend between the two. Continuity was obtained along both sides and the upper surface. In addition the upper surface of the 3-d deflector matched to the container upper surface and the sides of the 3-d deflector matched to the upper sides of the container. The drag coefficient reductions, from the baseline and from the baseline plus 3-d deflector, were found to be;

	0 deg.	5 deg.	10 deg.	15 deg.
Deflector + Fairing	-0.116	-0.201	-0.209	-0.190
Fairing	-0.052	-0.105	-0.138	-0.123

These results show the effectiveness of completely avoiding the build up of pressure on the container face, fully matching the flow from cab to container and avoiding flow through the gap to interfere with underbody or side flows. It also demonstrates that the interference which exists between cab and container is at its greatest at yaw and thus the fairing is most useful at yaw. The wind averaged drag factor for this configuration is Cd(55)=0.608, a reduction of 0.107, 15%, from the deflector only case. This is a very useful saving since it is greater than the saving for a 3-d deflector over the baseline configuration. Thus simple matching of the flow between cab and container is not an ideal solution and the interference caused by the gap is of equal importance and needs dealing with, especially when considering operation in crosswinds.

As would be expected though both sideforce and yawing moment are increased with this configuration. The

gap when completely sealed obviously causes a greater build up of pressure on the windward side and stops some relief of the leeward side wake which would occur from flow filling this wake flowing between cab and container. Thus sideforce is increased and the point of action moved forward increasing the yawing moment. Here the shielding of the container front face which resulted in the centre of sideforce moving rearward is more than equalled by the shift forward caused by blocking the gap. The yawing moment results are unreliable but at least the general effect can be seen.

5.3.4. Gap Seals

As demonstrated in Ch.5.3.3., the flow between cab and container has a major influence on the overall performance of the vehicle at yaw. As well as the complete fairing, simple vertical plates were tested as a means of sealing the gap, preventing any through flow. Two plates were tested, one sealing from the chassis to the cab roof and the other sealing the full height of the container. They were tested both individually and in conjunction with the 3-d deflector. As there was negligable difference between the two only the larger is described below. There was no benefit from the gap seal at zero yaw, the reductions of drag coefficient at yaw are given below;

	5 deg.	10 deg.	15 deg.
Gap Seal	-0.010	-0.034	-0.004
Deflector +Gap Seal	-	-0.105	-0.112

It is clear that in both these cases use of a gap seal creates a drag reduction at low yaw angles, however at 15 degrees the saving is just -0.004 in drag coefficient. In comparison to the reductions achieved using a full

fairing to seal the gap, a vertical plate seal is an inefficient means of controlling the gap flow.

The effect on sideforce and yawing moment is similar to the full fairing, sideforce is increased and its centre shifted forward. The amount of increase is as for the fairing thus since less drag saving is achieved a vertical plate seal must be seen as an ineffective device for this class of vehicle. However, some drag reduction is achieved with it and since this would be a much simpler device to attach to an articulated vehicle may still be of benefit.

5.3.5. Airdams

Airdams have become a typical feature on modern vehicle to reduce drag and aid stability in crosswinds by restricting underbody flow which on encountering obstructions would give rise to drag and lift. Four airdams were tested; they were made of flat plates which fitted to the shape of the cab bumper and ran full width to just ahead of the front wheels. They were of depths of 20mm, 40mm, 60mm and 80mm, and all had cut- outs to allow cooling simulation. The effect on drag coefficient is shown below, all are referenced to the 3-d deflector and fairing configuration as the base;

	0 deg.	5 deg.	10 deg.	15 deg.
20mm	-0.015	+0.005	-0.007	+0.006
40mm	-0.017	+0.006	+0.010	+0.008
60mm	-0.018	0	+0.026	+0.045
80mm	-0.019	+0.021	+0.050	+0.089

Clearly the optimum performance is achieved at zero yaw and at yaw the use of an airdam on this configuration is detrimental. This may at first appear to

be an anomaly but on closer inspection is as would be expected. In this configuration a deflector and fairing are used so that the normal flow component flowing down the cab-container gap and under the vehicle is absent. Thus the only underbody flow is that arising from flow passing under the front bumper and any flowing in down the sides. At zero yaw air passing under the vehicle encounters obstructions and a build up in pressure occurs raising drag and lift. Also, as a result of this, air then escapes between the front and rear wheels and interferes with the side flow of the vehicle causing a degradation of this flow, increasing the wake and raising the drag. When an airdam is fitted flow under the vehicle is restricted by various degrees depending on the depth of the airdam. Thus less air passes into the same underbody space resulting in lower underbody pressures and so reducing the drag component from that obtained from the previous pressure build up. Outflow from the underbody is also reduced, if not eliminated, so that the wake is not added to in the same way also reducing this component of the drag.

At yaw the position changes, now the oncoming air, at an angle to the vehicle, passes under the vehicle from both the front and the windward side. Also the main obstructions to the underbody flow are the rear wheels, axle and differential, which will all tend to block the flow passing under the vehicle from side inflow. Thus giving the associated pressure rise and increase in lift and drag. As yaw increases the airdam provides less and less shielding of the underbody components and simply becomes extra drag producing area on the front face of the cab. This may be more the case with the simple flat airdams tested here and this drag increasing tendancy may not occur with an optimised, shaped airdam.

The effect of airdams on sideforce and yawing moment was insignificant, sideforce being slightly reduced. It was felt, however, that more effect on lift and pitch would be seen.

5.3.6. Skirts

The effect of skirts down the entire length of the model was tested. They extended from just behind the front wheel wells to the rear of the container, with a cut out round the rear wheels so the whole wheel was visible. They had an unrepresentative ground clearance of 20mm which would have been too low for practical operation full scale but for the purpose of these tests was acceptable. The results gave the reductions of drag coefficient shown below;

	0 deg.	5 deg.	10 deg.	15 deg.
Skirts	-0.032	-0.070	-0.119	-0.153

As would be expected the effectiveness of the skirts increases with increasing yaw angle. The configuration they were tested on was with 3-d deflector, fairing and 80mm airdam. In this configuration the skirts smooth the flow down the sides of the container, preventing any outflow or disturbance from any underbody flow and containing the rear wheel disturbed flow. As at yaw most of the underbody drag arises from side flow passing under the vehicle and hitting obstructions the skirts prevent this. As yaw increases this effect would increase and hence the increasing effectiveness of the skirts. The smoothing of the flow down the side of the vehicle also results in a less disturbed wake resulting in lower drag. The wind averaged drag coefficient for this configuration is Cd(55)=0.560, the reduction due the skirts is -0.066, 11%,

a reduction similar to that achieved from use of an optimised 3-d deflector.

Skirts do have a detrimental effect on the sideforce, as by blocking underbody flow and deflecting flow down the sides of the container a pressure build up results which increases the sideforce. Also this restricted underbody flow prevents some of the leeside pressure relief which would otherwise occur and this increases sideforce. Yawing moment results look less reliable although little effect is in evidence. The increased sideforce appears close to the wheelbase centre thus minimising its effect on yawing moment.

5.3.7. Rear Turning Vanes

Previous reports have suggested various means of reducing the wake size and giving drag reductions. One means suggested was to use turning vanes on the rear corners of the container to increase the wake pressures by turning the flow inwards. The devices tested here were aerofoil sections mounted on the rear corners of the container such that varying angles could be applied to them. The aerofoils outer surface was curved whilst its inner surface was flat, they were mounted to upper and both side corners. Although these were not of the most efficient shape, their purpose was to indicate possible savings to be made from this area. Firstly the aerofoils were optimised at zero yaw, tested through a range of angles to give the best result. This result was for an angle of 7.5 degrees and gave a drag coefficient change of -0.033.

This was a favourable result and a good drag reduction, however, at yaw this same saving was not found and drag was actually increased for all angles tested. As

from a practical stand point the side mounted aerofoils would be unsafe, the use would be limited to the upper rear corner only. This together with the view that even an optimised aerofoil/vane would not be effective at yaw and their use would not be recommended. In future work other means of wake reducing devices would be tested, ie. boat-tailing.

5.3.8. Blocked Cooling

The cooling, modelled by a fine mesh grill as the radiator with a ducted flow to it, was tested open and blocked to test its effect. The cooling flow modelling used was the best option since although not strictly accurate to present practice any modifications to the cab for through flow would have been difficult to achieve. The effect of blocking the cooling on the drag coefficient was;

	0 deg.	5 deg.	10 deg.	15 deg.
Blocked Cooling	-0.004	-0.005	-0.011	-0.015

The results show the effect of blocking the cooling duct, at zero and low yaw angles this is small, but still reduces the drag. The use of a duct under the front bumper means that blocking of it results in its becoming a small airdam. Its shielding at low yaw is good as it is positioned on the centreline as is the propshaft and rear differential. Thus its shielding effect is beneficial. Its inceasing effectiveness with yaw must mean it is closer to the optimum set up than the full width airdams as it only spans a third of the vehicle width.

The effect it has on sideforce and yawing moment is small, sideforce is reduced due to the blocking creating a wedge from the scoop instead of the two sideforce

generating walls the scoop would have provided. The effect on yawing moment was negligible.

5.3.9. Mirrors

A pair of mirrors of plane vertical plate design were attached to the cab to test their effect on the overall flow. These were mounted on the cab in typical fashion from an upper and lower arm. As expected the effect was to increase drag at zero yaw, due to the mirrors contribution. As yaw was increased this increase fell away until no increase was seen at 15 degrees yaw. The reason is that when the vehicle is yawed the mirror on the leeside becomes shielded by the cab and the windward mirror actually partially shields the cab. The effects were small and as expected, so further testing of mirrors was not carried out.

5.4. Conclusions

The major reasons for these tests was to prove the viability of the newly developed facility and to give a platform from which to carry out the future commercial vehicle testing. On both counts the tests were a great success. The operation of the moving ground together with a 1/4 scale model with rotating wheels was carried out without problem. The drag balance worked well although the sideforce/yawing moment balance required extra work.

The results obtained compared very favourably with those described in refs, 1, 2, 3, 4, 13, etc. and although small differences did occur these could arise from a number of factors. These include Reynolds number for smaller scale tests, model detail, moving ground and wheels and model dimensions. Overall the results compare very well

when all these differences are taken into account, especially as the major effect on results is from the overall vehicle dimensions and configuration. Ref. 13, states that in tests on two models of different design the effects of identical devices vary due to the effective flow field from the vehicle tested. Thus the facility must be judged a success for moving ground road vehicle testing.

The major reducers of drag were modifications to the cab-container area, deflectors and fairings. Also at yaw shielding of the underbody by the use skirts is of great benefit. There also appears to be savings to be made from attempts to reduce wake size on the base of the vehicle.

Chapter 6. Fast Front Mk.I Cab Design

6.1. Introduction

This chapter gives the initial results taken in both wind tunnels on 1/4 scale and 1/6 scale models of the Fast Front Mk.I cab design. This initial testing was carried out at zero yaw. The cabs were tested for Reynolds number effects and various devices were tested on the 1/6 scale model to establish their drag reducing potential at zero yaw. Also viewed were the effects of wheel rotation on the results. Most configurations were tested with fixed wheels, with flats to give clearance to the moving belt. In these cases the axles were fixed in a position so the wheels were in identical positions to the rotating wheels and a 5mm gap left between belt and wheel flat. Firstly the cab design is described and then the various results are given under their respective headings.

6.2. Mk.I Cab Design

After proving the tunnel and testing of the basic add on devices to present day commercial vehicles, a more fundamental modification to the aerodynamics was needed. The initial testing had confirmed the drag distribution as being 60-70% forebody pressure and 15-25% base pressure, see refs. 3 & 5. This fact together with the initial findings on the add-ons suggested that the major design change should be a cab-container change. Extending the idea of the best add-on device, that being a 3-d deflector with cab-container fairing, it was decided that a wedge shaped cab completely faired to the container was best, making a fully integrated cab-container design. This cab was designed to stay within the original overall length of the present day configuration. Also left unchanged was the

container dimensions as this was felt to be too major a change and the aerodynamics for this load capacity carrying vehicle was to be investigated. Any change in the container would be of much greater effect to the operation of the vehicle so the limits imposed by present day capacities and operation were kept.

Other restrictive design parameters imposed were as suggested by Leyland Vehicles Ltd, see Ch.2.2.3. These were suggested operational constraints such as ground clearance which would restrict the surfaces over which the vehicle could be run, see Ch.2.2.3. Shown in fig. 2 & 3, are these dimensions for 1/6 scale and 1/4 scale models, the approach angle being the same for both models. This angle is the angle made to the ground by a line from the front of the contact area of the front wheel to the lowest point of the vehicle forward of this. This angle was to be a minimum of 15 degrees. The minimum ground clearances for the 1/4 scale were 50mm at axle centres and 75mm at mid wheelbase. The corresponding 1/6 scale values were to be 33mm at axle centres and 50mm at mid wheelbase.

The cabs were made to fit the original chassis and containers so that with the baseline configuration the only change to the model was the fitting of this cab. The first model made was the 1/4 scale model, see fig. 2. This had side radii on the leading sides of the cab, two flat inclined surfaces for the front surfaces, one from the radiused nose had a length of 440mm. A radius then faired this to the second flat surface⊗. This then led up to the container upper surface with a radius between the two. The larger surface was inclined at 59 degrees to the horizontal the second surface at 37 degrees to the horizontal. The radius of the nose was 82mm the radii of the joins between the plane surfaces were maximums, approximately 85mm. The

⊗ of 270 mm length

side radii tapered from an initial 40mm at the nose to a radius of 25mm at the join between the plane surfaces. This then tapered to a square edge where the cab joins the container. This was the original cab design but due to time and financial constraints after the first tests of this cab, the development had to be moved to the 2.1m * 1.7m wind tunnel using the 1/6 scale model.

The 1/6 scale model was made as close as possible to the 1/4 scale using 'scaled' radii. The radius of the nose was 42mm, the sides tapering from 25mm at the nose to 15mm at the join between the two front flat surfaces, then tapering further to square edges at the container. Unfortunately the container of the 1/6 scale was found to be relatively higher than the 1/4 scale container. To account for this the lengths of the two inclined front surfaces were extended. The section from the nose to the 'roof line', inclined at 59 degrees, rose for a length of 350mm. The upper section was lengthened 150mm, the slope was still 37 degrees. This resulted in both a slightly stretched version of the 1/4 scale cab and an overall increase in the model length. This must be remembered when comparing the results from the two models, they are similar but not identical. As with the 1/4 scale model chassis, underbody detail and container where left as tested previously, see ref. 1.

A number of devices were made up to add to the baseline configuration so as to arrive at a minimum drag configuration. These devices consisted of side skirts, both fully enclosing and open around the rear wheel, a flat undertray to smooth underbody flow, a base-board to add to the rear 'under rider' and rear boat-tail modifications.

6.3. Reynolds Number Effects at Zero Degrees Yaw Angle

Initially a 'first look' test was carried out on the 1/4 scale model in the 3.5m * 2.6m tunnel but restrictions then moved the testing into the 2.1m * 1.7m tunnel using the 1/6 scale model. The development of the devices was done on the smaller scale. Firstly Reynolds number investigations were carried out on both scales to see if any effects were evident.

6.3.1. 1/4 Scale Mk.I Cab

The original T45 prototype cab had shown Reynolds number dependancy, see fig. 24. The initial drag coefficient measured was steady over the lower Reynolds number range, then a drop was seen and at higher still Reynolds numbers the drag again is seen to be constant. The drop occurs in the range 3,260,000 to 3,520,000 . As the cabs leading edges are radiused this drag reduction could be due to separations around these edges. Original flow visualization had shown the roof radius to prevent separation but due to roughness, caused by the 'A' pillars, there was separation from the cab side radii. Also Reynolds effects could be effecting the flow around the wheels causing this drag drop. As the Reynolds number for the tests on the devices was 3,650,000 and this was in the region of steady coefficient after this fall region the tests were considered acceptable.

The Fast Front Mk.I cab does not demonstrate this same drag drop, see fig. 24. A slight steady fall in the value of drag coefficient is seen, this drop being -0.021 over the full range tested. The majority of this fall occurs above the 28.55 m/s test speed, after which the fall is just -0.002. This again demonstrates that the testing at

these Reynolds numbers, being considerably higher than recommended by S.A.E. practice, ref. 12, are ideal for this testing.

What is possibly occurring on the front radii and causing this small fall in the drag coefficient is slight changes in the boundary layer flowing around the smallest radii close to the container square edges. As speed is increased small separations from the smaller radii are suppressed giving an increasingly smaller separated region, resulting in the small drag loss. Flow visualization showed fully attached flow although this was not caried out in such fine detail as to see the effect close to the square edges, see plate 4.

6.3.2. 1/6 Scale Mk.I Cab

Allowing for the radiused forward edges of the Fast Front design a great dependance on Reynolds number might be expected as described in ref. 4, where varying the radius on the leading edges of a bluff body was investigated. Over the range of Reynolds numbers tested in this case, no such large drop in drag was seen only a slight decline in the coefficient, see fig. 5. This decline is not the same as the drop described by Cooper, ref. 4, but is due to similar effects. In his case, the model was made up with all leading edges of equal radius. When the critical Reynolds number was reached intermittent attachment and separation occurred in the critical region developing to fully attached flow above this region. This attachment would occur to all the radii at nearly the same instant giving a greater change in the flow and hence the drag. This occurs even more rapidly for smaller radii where the change from separated to attached flow is more sudden. These same mechanisms apply to the Fast Front design though

their effect is less dramatic.

Flow visualization using wool tufts reveals that separation is occurring part way up the sides of the cab, the lower flow and flow over the front and upper cab onto the container roof is fully attached. Therefore at these Reynolds numbers the radii above the separation point are too sharp to maintain attached flow. This separation is shown in plates 3(a)&(b), (a) is at Re(l)=1,960,000 and (b) is at Re(l)=2,365,000. These demonstrate the differing separation due to the movement of the separation point upwards to a smaller radius on the taper with the increased Reynolds number. Although the difference is small it is significant and gives rise to the dropping drag coefficient seen. Looking at the third row of tufts back from the nose, the upper four tufts are all showing upward flow indicating separation. The fifth tuft down is unsteady in (a) and steady in (b) demonstrating attached flow is now at this level at the higher Reynolds number. In both cases where separation is apparent the length of the separation bubble grows as the radius from which it originates decreases. The length of the separation bubble is seen to decrease for each radius with higher Reynolds number, this effect also described by Cooper, ref. 4.

It would appear that at still higher Reynolds numbers that all the separation would disappear, as seen on the similar 1/4 scale cab. The drag cofficient would then stabilise at a plateau value. The speed limitation of the tunnel is such that this could not be verified but since fully attached flow as observed over the 1/4 scale cab resulted in only marginally lower drag coefficients, the testing of the devices is still acceptable although consideration of the Reynolds number performance would need to be assessed to finalise any design configuration.

Another effect, discussed in Ch.3.2.2, was the performance of the leading edge suction box on the smaller ground at high speed. It is seen that the performance is reduced with increasing the speed as the suction fan is overworked. This effect on any drag figures at high speed would need to be accounted for and has a major effect on the results in the ground simulation and with a boundary layer present. It is more important to test the configurations under optimum tunnel conditions. Thus the testing was carried out at 24.86 m/s, Re(l)=1,960,000.

The effect of rotating or stopped wheels was also investigated during this testing. The drag coefficient change is negligible until the higher Reynolds numbers are reached, see fig. 26. At higher Reynolds numbers the drag of the rotating wheel configuration is seen to fall more quickly than the stopped wheel case giving a lower drag. This is as a result of effects on the flow caused by the wheel rotation and how these effects are Reynolds number dependent. The effects are those described in refs. 14 & 15. The separation point on the wheel circumference is seen to move forward in the rotating wheel case and instead of the resulting larger wake giving larger drag the converse was found. The wake pressures were seen to increase and the drag decrease. This was found for an exposed, isolated wheel and for a vehicle the effect would be smaller, as seen here, since the wheel is shielded from the flow thus reducing the effects.

The effect of Reynolds number on the front and rear lift coefficients is also very small, see fig. 27. Clearly there is very little change in either coefficient with increasing Reynolds number for either wheel condition. This is not surprising as for all conditions the flow over the cab onto the container was observed to be fully

attached from the nose to the base, all the separations occurring down the sides of the model. Large variations in the absolute coefficients were found, however, between tests. This change could be as great as to change the sign of the pitching moment. This was thought to be as a result of the wedge cab having sensitivity to the model set up in pitch and yaw. Subsequent tests on the Mk.II cab proved this to be the case. The lift coefficients became excellently repeatable when the model was set up for each test with extreme care.

The effect of stopped wheels is also demonstrated in fig. 26, with little effect on frontal lift but greater effect evident on the rear lift. This difference is simply accounted for by the front wheels being fully enclosed and hence shielded mostly from the flow. The rear wheels are exposed to the side and underbody flows, also, being twice as wide as the front wheels this doubles any effects. As seen in fig. 28, the lift generated by a wheel is highly dependant on both rotation and the gap between the wheel and the ground. When no gap is used the rotating wheel has no lift whereas the stopped wheel has a coefficient approaching one. As a gap is created the rotating wheel develops a downforce due to the Magnus effect and also due to a venturi being set up under the wheel which is enhanced by the wheel and ground motion. The stopped wheel still develops its lift although this is reduced by a venturi effect under the wheel but in this case it is less strong. Thus the increase in rear lift of the model is due the stopped wheel developing a lift, especially on the larger, exposed rear wheels.

6.4. Aerodynamic Devices at Zero Yaw

This section discusses the results found in conjunction with devices added to the Mk.I cab configuration. The model is the 1/6 scale model tested in the 2.1m * 1.7m tunnel at a Reynolds number of 1,960,000 based on model length.

6.4.1. Baseline Configuration

This configuration is cab-container only, all other aspects of the model are as for a modern day vehicle, the sides, rear and underbody are all open to the flow. The baseline coefficients for the rotating wheel and fixed wheel cases were found for the Mk.I cab configuration with no devices added. These were;

	Rotating	Fixed
Cd	0.498	0.500
Clf	-0.080	-0.076
Clr	-0.172	-0.107

The effect of wheel motion is evident as described in Ch.6.3.2. and as in ref. 14. The simple modification of the cab has resulted in a drag reduction of near 35% from the previous baseline configuration of the 1/6 scale model. The equivalent coefficients for the typical present day model, 1/6 scale with no devices added were;

	Rotating	Fixed
Cd	0.765	0.769
Cl(total)	0.036	0.097
Cm	0.423	0.404

These figures show the drag reduction for the cab only, also the change from lift to downforce which helps the stability of the vehicle and the reduction in pitching moment for the Fast Front cab. That is the downforce centre is closer to the wheelbase centre again helping stability. Once again the effect of stopped wheels is shown, slightly raising drag, increasing lift, especially on the large exposed rear wheels, thus decreasing pitching moment. All the results now described relate to the Fast Front baseline figures.

6.3.2. Skirts

Four skirt configurations were tested on the model to find the best configuration. Small and large open wheel skirts with an opening around the rear wheel were used with ground clearances of 60mm for the small and 35mm for the large skirts. Also tested was a fully enclosing skirt running from the rear of the cab front wheel valance to the rear of the container. This skirt had a ground clearance of 30mm and was tested flat to the container sides and with tapering aft of the rear wheels to minimise the wake and produce a lower drag. The major effect of the skirts on the flow at zero yaw is to prevent turbulence from air mixing with the underbody flow between the wheels and prevent the turbulence created around the rear wheels flowing out and producing a larger more turbulent wake. The effect on the model coefficients, with rotating wheels, was found to be;

	dCd	dClf	dClr
Small open wheel	-0.035	-0.034	-0.010
Large open wheel	-0.036	-0.033	-0.012
Full side	-0.041	-0.030	-0.019
Full tapered side	-0.045	-0.031	-0.008

Clearly the best skirts are the tapered full side skirts, the tapering reducing the drag slightl y from the straight case. The performance of the two open wheel types of skirt is identical and leads to the conclusion that no gain is to be made at zero yaw, with an open underbody, by reducing the ground clearance of the skirts. The Fast Front design is such that no underbody parts protrude below the line of the cab underbody, which is a flat undertray between the nose and the front axle line. In this way the underbody flow is restricted and the underbody parts shielded. The volume aft of the nose is greater and no underbody pressure rise should occur, so little out flow should occur. The small skirts therefore seem sufficient in depth to prevent this flow and create smooth side flow, the larger open wheel skirts would not have any extra benefit.

A small decrease in drag coefficient is then seen by employing the fully enclosing side skirts. This arises from the benefits of smoothing the flow around the rear wheels. The open skirts do not prevent interaction between the sideflow, the flow around the wheel and the wheel itself. This complex region will create some effects on the flow down the side of the model effecting the drag as seen. The possibility is that turbulence in this region causes some degradation of the wake and the drag rise observed. Enclosing the wheels prevents any sideflow encountering the wheel so eliminating this drag producing problem. Tapering of the sides aft of the rear wheels as a form of boat-tailing helps minimise the wake by bringing the sideflow in and gives the further drag reduction shown above.

The baseline configuration produces negative lift, this arises from underbody pressures and from the

wedge front with angled surfaces creating a downwards component from the high pressures acting on these surfaces. The split is near 30% at the front axle and 70% at the rear axle and this mostly arises from the drag force component from the bluff body producing a nose up pitching moment. The effect of the skirts is to increase downforce slightly moving the centre forward giving a more balanced distribution. The reason for this probably lies with the effect of the nose. The skirts producing better channelling of the air under the model create better conditions at the nose, giving a greater flow there. This increase in flow rate would result in lower pressure under the nose, giving the downforce measured. The rear axle lift increase found with tapering, results from the slight pressure increase in the wake caused by the tapering reducing the flow at the rear end causing a slight pressure increase in this area resulting in less downforce. This change is small and therefore does not effect the conditions upstream at the nose and no change is seen there.

When the wheels are stopped the corresponding coefficient changes due to the skirts are;

	dCd	dClf	dClr
Small open skirts	-0.030	-0.026	-0.031
Large open skirts	-0.030	-0.034	-0.039
Full side	-0.033	-0.031	-0.056
Full tapered side	-0.046	-0.039	-0.039

These results show slight variation from those taken with rotating wheels. The trends are the same but drag reductions are reduced except for the tapered side skirts. The front axle lift changes are close to those for rotating wheels but there is a large difference between the small and large open skirts. The rear axle lift change is

more negative.

The drag is showing the same trend of lower drag with rotating wheels as previously discussed although here they must be seeing more limited flow.The rear lift is more negative, as now greater flow under the rear wheel due to the channelling of the underbody flow creates a better venturi through the wheel/ground gap, generating downforce. This effect is enhanced by the fully enclosed skirts as no air is able to escape around the wheel so the flow is increased. The tapering of the sides produces the same effect as before of increasing the presure in this rear area and thus reducing the downforce.

The results again show the tapered fully enclosing skirts to be the optimum for reduced drag at zero yaw. The effect of increasing downforce and moving the centre of action forward towards the wheelbase centre is also beneficial as this would have a stabilising effect.

6.4.3. Undertray (Underbody Masking)

The effect of totally smoothing the underbody flow was investigated using a flat undertray which fully masked the underbody. It was used in conjunction with the two types of full side skirts and was mounted at a ground clearance of 30mm, the same as the skirts. The cooling flow through the nose opening was allowed to pass between the underbody and the undertray and into the wake through the open rear. As well as being tested completely flat it was also tested for three diffuser angles aft of the rear axle. The effect on the coefficients by the flat undertray were;

	dCd	dClf	dClr
Full Side and Undertray	-0.056	+0.116	-0.012
Tapered side and Undertray	-0.057	+0.124	-0.029

The effect of the undertray on drag is to further reduce the coefficient by -0.015 from that of the configuration with skirts fitted. This saving is achieved by preventing any underbody flow encountering the underbody obstructions. As the nose on the Fast Front design has a flat undertray to the front axle line under which no underbody part protrudes these parts are already shielded. Thus the effectiveness of the undertray is less than could be expected if total shielding was needed. This drag reduction is useful and mainly arises from prevention of the underbody flow encountering the rear axle and wheels.

The use of this undertray creates lift at the front and a slight increase in the downforce at the rear axle. The change at the rear axle is small compared to the change at the front axle. This change arises from the masking of the underbody. Unmasked the volume under the container is greater than that under the nose creating a low pressure region helping flow under the nose creating downforce. This would be lost using the undertray as the underbody volume is now constant and this extra force due to flow under the nose is no longer present. The air which was drawn under the nose now passes over the body which gives higher speeds over the truck. The associated lower pressures give greater lift especially over the front radii. Thus the extra lift acts on the front of the model giving the distribution shown.

The use of stopped wheels causes the drag to reduce, to lower the lift increase at the front axle and increase downforce at the rear axle. These effects are all

caused by the introduction of the gap between wheel and belt. The flow is now almost totally distributed over the top, sides and below the undertray, very little flow occurs between container and undertray. Therefore the flow seen by the wheels is limited to that under the undertray. As this encounters less wheel area the drag is reduced. Also as the air encounters the curved part of the wheel and the flat a venturi is set up under the wheel. This then causes the front and rear downforces which effect the coefficients as shown.

The effects on the coefficients of the flat undertray configuration are given below, the diffuser angles were measured approximately to give a guide;

	dCd	dClf	dClr
2 deg.	+0.003	+0.007	-0.037
3 deg.	+0.006	+0.014	-0.068
5 deg.	+0.012	+0.024	-0.104

These effects are on the tapered full side skirts configuration with rotating wheels, and the effects on the full flat skirts are of the same order. The effect of stopped wheels is as already discussed. The diffuser is clearly working and creating a pressure drop below itself. The drag is raised as some of this low pressure has a component in the drag direction. Its effect is changed by the pressure drop caused and the angle of the diffuser, as the angle grows the drag component grows. The pressure drop created also creates downforce at the diffuser which shifts the overall downforce centre rearwards giving the slight lift increase seen at the front axle. These effects all serve to degrade the performance of the model and use of the flat undertray is the optimum shielding device, the use of a diffuser is unnecessary.

6.4.4. Blocked Cooling

The cooling flow was either left fully open or fully blocked. The configuration on which this was tested was with full side skirts. The effect of blocking the cooling on this configuration was;

	dCd	dClf	dClr
Rotating wheels	+0.004	-0.016	-0.008
Stopped wheels	+0.012	-0.017	-0.014

Little blockage actually ex isted as simulation of the radiator for the 1/6 scale so the effects are basically for an open duct or a blocked duct, which should amplify any effects blocking the duct may create. As expected the blocking of this duct gives a drag rise since where flow could pass unhindered it is now blocked giving drag. However, considering the duct is close to the stagnation point of the front and the open duct could be considered fully open, the drag increase is small. It is therefore clear that addition of radiator blockage would not give as great a drag rise as might have been expected and does not present problems. Both these configurations give extra downforce, equal at the front axle but greater for stopped wheels at the rear axle. Greater flow under the nose due to the cooling flow now flowing under and over the nose gives a lower pressure under the nose giving the front downforce, (see also Ch.6.4.2.). This flow then continues back and encountering the rear wheels, stopped with gaps, improves the venturi effect through the gap giving greater downforce at the rear.

6.4.5. Back Board

A flat back board was added to the configurations using full side skirts only and full side skirts and blocked cooling. The effect of the back board on these configurations was found to be;

	dCd	dClf	dClr
Full Side	+0.054	+0.092	+0.201
Full Side +Blocked Cooling	+0.039	+0.093	+0.198

As can clearly be seen the use of a back board is of very detrimental effect. Its presence blocks the underbody flow out into the wake at the rear of the container causing a build up of pressure under the container. This leads to increased drag and the configuration almost looses nearly all its downforce. The major effect on lift is at the rear axle where the blocking and pressure rise occurs although this feeds upstream causing the lift at the front axle. Blocking the cooling flow means some of this flow now passes over the model and less flow is fed under the model. Thus the build up of pressure on the back board is not as great and so the drag rise is less. Although this also means that the lift from the underbody is lowered this is cancelled by the extra flow over the model creating lower pressures on the upper surface giving the same lift increase as with open cooling. As no benefits of this back board could be conceived and as its effect would probably be to cause outflow under the model degrading the wake, its use even as a spray suppresion device must be in doubt.

6.4.6. Rear Boat-tailing

Extensions were added to the rear face of the

container along the top and side edges. These were of almost square 1" section in clay running from the bottom of the container right round the container periphery to the bottom of the other side following the container edges. Clay was used so that progressive angles could be tested on these boat-tails so that an optimum angle could be approached, at which drag would be a minimum. Their purpose is to allow the base region wake to be relieved by greater flow turning the rear corners, filling the wake. The results found by their addition to to the configuration using tapered full side skirts and a flat undertray, the model using rotating wheels, were found to be;

	dCd	dClf	dClr
4 deg. slope	-0.012	-0.005	+0.028
5.8 deg. slope	-0.021	-0.016	+0.057
9 deg. slope	-0.029	-0.026	+0.086

These slope angles were approximately measured, being the average values that the boat-tails made to the container surface. Variation in the clay could not be avoided and the side tails could only be approximately measured. The main effects can clearly be seen. Firstly the wake is relieved by the turning of more flow into it and hence the drag is reduced. This reduction increases with slope suggesting an optimum has not yet been reached. In each case, the flow must be attached and the greater the angle the greater the filling of the wake. This would be expected to reach a maximum and then any increase in slope would reverse this falling drag trend until the addition would be of no effect on the drag without the boat-tails.

The effect on lift is such that flow flowing over the horizontal upper boat-tail accelerates as it follows the contour giving rise to a negative pressure. This

produces a lift which gives a nose down pitch. This then accounts for the increased downforce at the front and decreased downforce at the rear. This is not of detrimental effect, infact it is of benefit in that the centre of the overall downforce created by the aerodynamics is moved forward towards the wheelbase centre. This is a stabilising effect as the configuration added to has a nose up pitch with lift at the front and downforce at the rear. The boat-tails reduce this in strength which would improve the handling of the vehicle.

The effectiveness of these boat-tails is encouraging and probably is helped by the state of the flow arriving at them from the aerodynamics of the front. The better the flow over the container, that is to say the more attached the flow, the better the boat-tails will perform. This is the case described in ref. 16, which shows the performance of identical boat-tails on configurations with bad and good frontal characteristics.

6.4.7. Rear Turning Aerofoil

The aerofoils mounted on the rear edges of the container as described in Ch.5.3.7. were used here on the upper surface only to test their effect on the boat-tails. The configuration used was with full tapering side skirts, flat undertray and the 9 degree slope boat- tails. The angle of the aerofoil was optimised and its effect on the models coefficients was;

	dCd	dClf	dClr
Optimum Aerofoil	-0.004	-0.024	-0.075

This shows that the drag saving to be made at optimum set up is negligible. The effect on lift is as

described in Ch.6.4.6. with the boat-tails only with the aerofoil generating the rear lift the effect is increased. As previously described this would be a stabilising influence and hence desirable. It may be considered desirable to use aerofoils for this trimming of lift as there is no drag penalty, although at yaw this would not be the case, see Ch.5.3.7. Therefore their use would not be considered an attribute.

6.5. Conclusions

These results show the Fast Front Mk.I cab design to be a good step forward from modern conventional cab design. The drag reductions achieved with the cab could be further improved with additions to the configuration to smooth side and underbody flow and increase the pressures in the wake by use of boat-tails.

The cab has shown in 1/6 scale form to develop separations from the upper side radii. This effect was Reynolds number dependent but also since the radii tapered to square edges at the join to the container this was considered not to be the optimum design for the cab particularly when considering crosswind performance. A much better design would appear to be to taper the sides to a minimum radius and then continue this along the top edges of the container. Reports were read, particularly ref. 4, and investigations carried out to determine the Reynolds number performance of leading edges, ref. 1. The Mk.II was then conceived, see next chapter.

Chapter 7. Fast Front Mk.II Cab Design

7.1. Introduction

After extensive 1/6 scale tests,and flow visualization comparisons with the 1/4 scale, it was evident that due to the small radii on the upper sides of the Mk.I cab that Reynolds effects were occurring. It was then decided to modify both cabs, similarly, to overcome these effects. Instead of the side radii tapering to square edges where they meet the container, they would taper to a minimum radius. This radius would be continued from its initial point of occurrence back along the top side edges of the container to the rear of the container. This would not lead to much cargo space loss and should benefit the cross wind performance of the models.

In improving the leading edge radii a number of factors needed to be considered. The reports, ref. 4, 17, 18, 19, 20 & 21, show studies of Reynolds number effects and edge radii on simple bluff bodies give similar findings. Square and small radiused edges produce separations which effect the flow field of the model. This usually results in a drag increase but with a tandem cab container type model a drag reduction can be achieved from matching the cab roof separation to the container height. In this way shielding of the container front face is achieved with a drag loss. Increasing the radius of these edges reduces the size of the separations and by increasing the radius further fully attached flow results. The most comprehensive study, by Cooper, ref. 4, shows the data collapsing to a relationship where the critical Reynolds number for attached flow is constant based on the radius, the number being:

$Re(r)=130,000$

Using this expression a radius for the 1/4 scale model of 57mm was calculated using the 3.5m * 2.6m tunnel speed of 28.55 m/s, the 1/6 scale radius was found to be 76mm.The full scale interpretation of this expression resulted in a radius of 91mm, 23mm for the 1/4 scale and 15mm for the 1/6 scale, based on this figure. Cooper continued his expression since at yaw this optimum radius increased or the critical Reynolds number for a given radius was increased with yaw. Taking this into account leads to the radii for the scale models, from full scale calculations, of 35mm for the 1/4 scale and 27mm for the 1/6 scale. Consideration of the flow visualization of the 1/6 scale Mk.I cab, see plates 3(a) & (b), shows separation at around half way up the first side radius, at a point where the radius is approximately 18mm. The 1/4 scale, however, showed no signs of separation, see plate 4. This behaviour is possibly due to the higher Reynolds numbers on the 1/4 scale model also the fact that the models are not bluff simple blocks as used by Cooper. The expression used does not take account of the boundary layer state arriving at the corner which for this wedge front end is considerably different from that of a bluff front at 90 degrees to the flow.

It was therefore decided a convenient solution to the question of what size to make the radii, after examination of the radii on the Mk.I cab, that the lower corner would be kept as the Mk.I. The radius at the point where the two sloping flat front faces join was an ideal size and this was then continued back over the container to the rear. These radii were 25mm for the 1/4 scale and 15mm for the 1/6 scale model. These correspond well to those initially calculated from the relationship developed by

Cooper for the full scale vehicle. It would be expected that fully attached flow would be seen on the 1/4 scale but separations would still occur on the 1/6 scale. Investigations on the Reynolds effects on the 1/6 scale model could then be carried out including tripping of the boundary layer before the corners. The 1/4 scale would have a much more representative flow to the full scale vehicle.

Aside from this modification to the cab the other devices remained the same as for the Mk.I, although boat-tailing was further investigated. Forces were measured at both zero yaw and at yaw angles, flow visualization and wake total pressure surveys carried out. Initially this work was carried out in the 2.1m * 1.7m tunnel 1/6 scale but was finally verified and compared in the 3.5m * 2.6m tunnel with both models. Comparison of the tunnels and measuring techniques was also possible.

7.2. Reynolds Number and Transition on 1/6 Scale Model

The effects of Reynolds number were measured to assess their effect on the performance of the 1/6 scale model with greater radiusing. The effect of tripping the boundary layer and the variation of this with Reynolds number was also investigated. The results are plotted in fig. 29 , for the effect on drag and fig. 30, for the effect on lift.

The effect of Reynolds number on the drag coefficient of the baseline configuration can be seen to be small. A similar situation to that found on the Mk.I cab, with rising Reynolds number causing a fall in drag. The overall change in drag coefficient over the range of numbers tested was 0.022. Plates 6(a) & (b) show the flow around the front corners at 24.86 m/s and 30 m/s

respectively. It is clear that separation is occurring and comparison with plates 3(a) & (b) shows that the difference between the Mk.I and the Mk.II is small. The separation occurring in both cases is probably less for the Mk.II giving the lower drag results.The separation point is still around the 18mm radius point the lengths of the separations from each point on the corner appearing equal resulting in a diagonal flow pattern up the side of the container. The separation from the upper corner being strong and reattachment is not observed on the area seen. Plate 6(b) shows the difference between the flows at the two speeds to be little different, the initial separation point moving slightly upwards resulting in the lowering of drag coefficient with speed seen in fig. 29. The critical point of initial separation moves up as radius reduces for attached flow as Reynolds number increases. It would be expected that as the speed increased further a more dramatic drag drop would be seen as the flow from the upper edge of 15mm radius would attach as the critical Reynolds number was reached. As this would effect the full side at once, a greater drag loss would be seen. The effect on the surface flow is seen in plates 7 and 8 where tripping has been used to help prevent separation.The effect of Reynolds number on this tripped flow is seen in fig. 29.

The major effect on the drag coefficient has been through the use of devices on the baseline configuration although the tripping of the boundary layer has been effective in further reducing the drag. The reduction at 24.86m/s from the 60 grade grit was -0.010 and from the 22 gauge wire the reduction was -0.030, no difference in the lift or its distribution was evident. The carborandum grit was of 0.30 mm diameter the wire of 0.70 mm diameter. Information relating to the choice of transition size for various Reynolds numbers gives an ideal size of 0.40 mm

diameter falling between the two sizes tested, see ref. 22. The figures and the visualization show the wire to be much more effective than would be expected. The grit being of smaller diameter than recommended is not of sufficient size to trip the boundary layer and hence does not prevent separation. The wire does trip the boundary layer sufficiently to almost create fully attached flow. The effect of increasing the speed is to help tripping of the flow, as can be seen in plate 7(b), the flow is close to fully attached. This large flow change gives the greater dependancy on Reynolds Number seen in fig. 29, for the configurations using trips.

The lines for the two configurations tripped are tending to converge, the flows are tending to fully attached flow. The difference between plates 7(b) and 8(b) shows the flows in both cases being almost indistinguishable as the flow is very close to being fully attached. In this case the drag readings will be tending to the same figure. The trips are then seen to perform in their expected manner and the effect of Reynolds number on the flow round the sides is demonstrated as in Ch.6.3.2. It would also be expected that as the lines in fig. 29, are converging and are very close at the high speed and the flow visualization shows nearly fully attached flow,that the 1/4 scale tests at higher Reynolds number should prove to demonstrate no Reynolds dependancy with fully attached flow.

There is no effect on lift or its distribution as can be seen in fig. 30. As seen previously on the Mk.I cab the only separations are down the sides of the cab with fully attached flow over the upper surfaces. The control of these separations therefore has no effect on lift and tripping the boundary layer is of no effect. The major

change in lift being caused by the devices on the baseline, the actual distribution being the same but the overall downforce being less. The lines appear to show slight increase in front axle downforce with Reynolds number and slight increase in lift for the rear axle, the changes being insignificant. The main point to note is the pitch of both baseline and fully developed designs is nose down, a stabilising characteristic which would help handling characteristics.

7.3. The Effect of Devices on the 1/6 Scale Mk.II Cab Design

The effectiveness of various devices, skirts, undertrays and boat-tails was tested on the 1/6 scale Mk.II design at zero yaw and over a range of yaw angles to assess their cross wind performance. These devices were the same as tested on the Mk.I design so the better performing devices were chosen, the fully enclosing skirts for example, and boat-tailing was further investigated and optimised. The results are discussed under their relevant headings, both yawed and unyawed results being discussed in the same section. Measurements of drag, lift, sideforce yawing moment and rolling moment were taken to give the full range of measurements. Rolling moment was unreliable although some trends could be seen and in most cases is only discussed in qualitative terms. The primary interest lies with drag, sideforce and yawing moment.

7.3.1. Transition

The effect of placing 22 gauge transition wire in front of the front corners to trip the boundary layer and prevent separation is shown in figs. 31(a) & (b). The main effect being on drag coefficient with little effect on

frontal downforce. No effect on sideforce or yawing moment with yaw angle was seen. The major effect is the promotion of more attached flow round the corners of the cab, described in Ch.7.2., continuing throughout the yaw range. This effect can be seen in plates 9 & 10 showing the leeside flow at 3 degrees and 9 degrees yaw with transition. The previous separation was much greater as demonstrated in plate 11, the Mk.I cab with no transition at 9 deg yaw. The radii at the upper sides is also decreased for the Mk.II but the separation in plate 11 is occuring on unchanged radii to those showing attached flow for the Mk.II in plate 10. Thus the wire is tripping the flow to promote attachment to the corners and the drag is subsequently lower.

Lift is unchanged at the rear but a slight loss in downforce is seen at the front. This is due to the tripping of the boundary layer over the upper radius onto the container roof. Although previously attached without the wire the flow over the upper radius increases its pressure slightly,the low pressure previously is increased and a loss in lift experienced.

7.3.2. Skirts

As the results on the Mk.I cab proved the fully enclosing skirts to be of more benefit to drag reduction at zero yaw these were chosen as the most fitting modification. It was felt that having studied refs, 24-28, on the areas of spray generation that fully enclosing the underbody and wheels would be of great benefit to suppress the carrying of spray into the side flows and wake. Initial tests also demonstrated the improved drag reduction with the full skirts diffused to the rear aft of the rear wheels, so the open wheeled skirts and the straight full

skirts were dropped from the program.The changes in the force coefficients measured over the yaw range are plotted in figs. 32(a), (b), (c) & (d).

Firstly it can be seen that using the full diffused skirts lowers the drag for the range of yaw angles. As explained in Ch.6.3.2. the reason for the reduced drag at zero yaw is to prevent underbody flow flowing out and degrading the side flow and also side flow encountering the rear wheels. These are both mechanisms giving rise to drag and if the side flow can be kept smooth the wake will be improved lowering the drag. As the model is yawed the drag reduction varies slightly, although it is always of the order of a drag coefficient reduction of -0.040. As the model is yawed and the side is presented to the oncoming air stream, the prevention of underbody flow from the side, flowing between the front and rear wheels and under the model becomes more important. If this flow was allowed, a build up of pressure due to the large volume of air trying to flow under the model, thus hitting the underbody obstructions, would occur. This would give rise to drag and lift as in the case at zero yaw. The skirts being of greater area than the underbody obstructions do give rise to some extra drag due to this area but the streamlining of the side flow into the wake creates a far less turbulent wake with the results that the overall drag is reduced.

The reduction of the drag coefficient throughout the range of yaw angles tested gives a large reduction in the wind averaged drag coefficient for this configuration.The wind averaged drag coefficients, again calculated for the 55 m.p.h. speed, for the baseline configuration and for the skirted configuration are;

	Cd(55)
Baseline	0.527
Full Tapered Side Skirt	0.494

These figures compare favourably with those found for the original 1/4 scale model of a typical modern vehicle. A rigid box van of today was found to have a wind averaged drag factor of 0.797 and the best add-on devices reduced this to 0.560. Using skirts lowered the figure by -0.066 and for the Mk.II Fast Front the corresponding reduction was -0.033. In this way it can be seen that the standard of flow from the front of the vehicle affects the performance of devices on the subsequent flow. This was also stated by Gilhaus, ref. 23. If the flow down the sides of the vehicle is relatively uniform then the skirts have less 'tidying up' to do, if the flow is turbulent then the skirts control this and stop further degredation in the flow. In all cases the skirts can still be seen to be of great benefit especially to cross wind performance.

The effect of the skirts on lift is more variable with yaw angle. At zero yaw, as with the Mk.I cab, they create a downforce since the channelling of the underbody flow together with the low nose of the cab developes low underbody pressures resulting in this downforce. In this case, the distribution front and rear is unaffected, with the low pressures developed from increasing the flow speed under the nose for frontal downforce and the channelling of this flow into a larger volume under the model causes a depression rearwards to balance the downforce. As the model is yawed the general trends of front and rear lift are the same although compared to the baseline configuration there is a difference with frontal lift. Frontal lift increases with yaw angle and this increase is greater when skirts are

fitted. Thus initially, the downforce is increased with skirts but at high yaw angles downforce is lost at the front. Rear lift, positive for the baseline, decreased but still positive with the skirts, decreases and becomes negative with yaw.

The effect with skirts is of similar form to the baseline only a greater decrease is seen at small angles of yaw. Overall this gives rise to a rearwards shift in the centre of action of the downforce with pitch becoming less nose down but a downforce still remains at the nose. The main reason for these effects is that as the model is yawed less air flows directly under the nose between the front wheels. As a result the venturi effect on the flat under nose surface is diminished and downforce is lost in this region. As yaw increases less air is channelled this way and the loss of downforce here is compounded. Since less air is flowing under the model the overall underbody pressure is reduced so a gain towards the rear of the underbody arises from these decreased pressures producing downforce. The overall effect then is for the fully enclosing tapering skirts to produce downforce the centre of action of which moves rearwards with yaw.

Sideforce and yawing moment coefficients are effected in an expected fashion, both are raised by the skirts this rise increasing as the yaw angle increases, see figs. 32(c) & (d). Since the side area presented to the oncoming flow is increased with the skirts fitted the sideforce, based on simple pressure build up on the added area, is increased accordingly. The growth of sideforce with yaw is the normal, linear, relationship as described in other vehicle work. The build up of extra pressure on the windward side due to the skirts can be seen in the fig. 33(c) 6 (d), showing the surface pressure coefficients in a

ring round the model at a height of 150mm. Figs. 33(a) & (b) show the location and marking of the ring of surface pressure tappings. The pressures on the windward side all become positive except at the rear as the flow accelerates round the base corner into the wake. It is also clear that the centre of action of this pressure is ahead of the mid wheelbase position resulting in the increased yawing moment. Negative pressures on the front leeside corner and over the whole leeside also contribute to the sideforce. Their centre of action is also forward mostly arising from the flow accelerating around the front edge. The pressures are so low here that separation occurs as seen from flow visualization studies. The skirts also tend to even out the pressure down the side of the model eliminating underbody and rear wheel effects. The leeside pressures are not seen to be changed only smoothed by the skirts thus the only effect of the skirts is the build up of pressures on the windward side.

The largest increase in sideforce coefficient, at 15 degrees yaw, was 0.340. In comparison with data taken on the 1/6 scale model in present day configuration shows the sideforce of the baseline and skirted versions to be, see ref. 1;

	Cy	Cn
Baseline	1.15	-0.05
Base + Skirts	1.38	-0.05

These results demonstrate the performance of the Fast Front Mk.II cab to be of similar levels to a present day vehicle, the sideforce coefficients being slightly higher, the yawing moment is higher and positive. This arising from the low pressures around the leeside front corner and the prevention of relief of leeside pressure

from flow between the cab-container gap on a present day configuration. The sideforce build up in this respect is not considered detrimental to the performance of the overall configuration the yawing moment being regarded in the same way. The rolling moment was seen to rise although was still small and thought to be of similar size to that for a present day vehicle and of no large, destabilising magnitude.

7.3.3. Undertray

The effect of masking the rough underbody using a flat undertray was investigated as with the Mk.I cab. Again the flow through the cooling duct was allowed to pass above this undertray and into the wake. The ground clearance was again 30mm, although below the recommended mid axle minimum, it was to the level of the skirts. This was not considered a problem as today many methods of controlling the ride height of a vehicle and for the purposes of this aerodynamic study the minimum clearance at the axles was used. The configuration on which the undertray was tested included the tapered full skirts, the effect of the undertray is shown in figs. 34(a), (b), (c) & (d).

Drag coefficient, as at zero yaw with the Mk.I cab, is reduced but this reduction is effected by yaw. The drag reduction achieved at small yaw angles diminishes as yaw increases to a minimum reduction of just -0.012 for the coefficient at 7.7 degrees of yaw. At higher yaw angles the drag reduction again grows. The method of assessing wind averaged drag factor includes only the converging sector of Fig.34 (a)$^{\circledast}$ is taken into account. Quite why the drag saving becomes a minimum at 7.7 degrees is not clear. Possibly a situation arises when the oncoming air close to the ground being affected by the ground motion reaches a choking point

$^{\circledast}$ to 7.2°

as it flows under the model as it is yawed. This point arises as the model to ground geometry reaches a point where this choking affects the drag to a maximum. Above this yaw angle the effect is seen decreasingly for drag giving the converging then diverging lines in fig. 34(a).

The major drag reducing mechanism is as described before that shielding the underbody prevents a build up in pressure under the model around obstructions. This then gives both a smoother flow under the body but also into the wake giving higher base pressures. The resulting wind averaged drag for this configuration is;

	Cd(55)
Tapered skirts + Undertray	0.463

This result is a difference of -0.031 in the averaged coefficient from the skirted configuration and represents a useful saving. As mentioned before when discussing the Mk.I cab, the effect is possibly lower than would be expected when considering the rough nature of a commercial vehicle underbody. The reason for this being the low ground clearance of the nose with flat undersection to the front axle. This is lower than any of the underbody parts so a large shielding effect is already in play.

The effect on lift is to halve the downforce at small angles of yaw and as yaw increases the overall effect diminishes. In fact the undertray causes the overall lift to return to the level of the baseline configuration. The main reason for this is the loss in downforce at the front axle previous arising from a venturi set up under the nose. As described in Ch.6.4.3. the skirts help retain suction in the larger underbody volume which pulls extra air through the smaller nose volume thus creating extra low pressure

and downforce. When the undertray is fitted the extra pull is lost and the volume under the model is constant. This results in loss of the venturi effect and loss of lift. This is shown in fig. 34(b), showing loss in frontal downforce and an increase in rear downforce with the centre of force now moving rearward but the pitch always remains nose down. The main reason for these trends is that as the model is yawed less flow is channelled between the front wheels since less opening is presented to the flow. As previously explained flow accelerates to pass under the nose giving lower pressures and now this effect is reduced and downforce is lost in this region. At the rear the situation is different. Here, as the model is yawed,a larger entry gap is presented to the flow and the effect of ground motion is to help pull air under the model. Thus, as it is yawed, a greater flow rate is experienced under the model at the rear. As the air must speed up to achieve this, lower associated pressures are found giving the increasing downforce with yaw seen at the rear.

The effect on sideforce and yawing moment is small, a slight increase in each is seen in figs. 34 (c) & (d). This increase is a little unexpected as it would seem that better underbody flow would give lower coefficients. The increase probably arises from a small extra build up in windward side pressures due to the fixed volume under the model through which any flow must pass. At yaw the flow encountering the skirts increasingly trying to flow under the body is restricted by the gap. This would lead to a build up of pressure on the windward side giving higher sideforces which must be centred just forward of mid wheelbase giving the higher yawing moments. This small increase in sideforce would be expected to slightly increase rolling moment but the measured value was only half the expected value and was unreliable. This must be

due to the distribution of the low pressures under the model with the elimination of underbody obstructions. this must counteract the increased sideforce giving much lower rolling moment.

Overall there is little change in the characteristics other than drag. The use of underbody fairings is therefore beneficial with no handling or stability degradations.

7.3.4. Boat-tail Extensions

Rear boat-tails were tested as on the Mk.I cab described in Ch.6.4.6. Initially these were again fashioned from clay so that the angle they made to the container upper surface could be optimised. The optimised boat-tails were then made up in wood so they could be reliably placed on the model during yaw angle testing. The results from the first optimising tests, at zero yaw, showing the changes to the coefficients of;

	dCd	dClf	dClr
Flat Extensions	-0.007	-0.004	+0.013
5.5 deg slope	-0.016	-0.015	+0.042
7.5 deg slope	-0.034	-0.024	+0.087
10 deg slope	-0.033	-0.030	+0.094
12.5 deg slope	-0.043	-0.042	+0.117

These results show the effect of the various extensions on the lift and drag coefficients when they were added to the baseline configuration. When added to the 'low drag' configuration with tapered full skirts and flat undertray the following trends were seen;

	dCd	dClf	dClr
7.5 deg slope	-0.034	-0.024	+0.087
10 deg slope	-0.037	-0.025	+0.118
12.5 deg slope	-0.035	-0.019	+0.147

These results demonstrate that the savings possible from devices depends upon the configuration on which they are tested and the general flow field changes. The baseline configuration results show the optimum tested to be 12.5 degrees slope on the boat-tails whereas the second set of result show it to be a 10 degree slope. The general trends of the coefficients are obvious that as the slope is increased the flow turns the corner filling the wake and increasing its pressure. In this way drag is reduced, the flow in the first set of results showing increasing turning in each case. The flow must therefore be attached on the boat-tails in each case. This also shows in the lift coefficient trends. As the flow accelerates round on the boat-tails a pressure drop results on this section of the model. This drop on the upper boat-tail gives extra rear lift and as a result of pitching nose down a corresponding front downforce is seen. As the flow is attached in each case the extent and effect of this pressure drop on the boat-tails is increased with increasing angle.

Similar trends are seen in the second set of results although here the flow appears to have become slightly detached from the 12.5 degree sloping boat-tail. Here the increasing drag reduction with increasing slope is lost and a small loss of drag reduction is seen. Also the effect on front lift is slightly lost although the rear lift is greatly increased. The optimum angle therefore appears to be between 10 and 12.5 degrees, with intermittent separation on the larger angle. This result is

confirmed from result given in ref. 4, which shows rear boat-tailing to be optimised at the same angles found here. As the separation was intermittent and would not be a problem when testing 1/4 scale the 12.5 degree slopping boat-tails were chosen and made in wood to test throughout the yaw range. It was also decided to test them on the 'low drag' configuration, with tapered full skirts and flat undertray. The boat-tails were also continued down to the level of the skirts so as the full base region was modified. The results on the coefficients over the yaw range are shown in figs. 35(a), (b), (c) & (d).

The effect on drag coefficient is to reduce it by around the same amount over the complete yaw range. The upper flow on the container roof being attached has the same effect over the yaw range. The side extension on the windward side is also always effective as until higher yaw angles are reached it still angles away from the flow into the wake. A small decrease in the drag reduction is seen above 12.5 degrees when the side is no longer 'filling in' the wake, ie. it now makes a small yaw angle to the oncoming flow. The wind averaged drag factor calculated for this configuration is;

	Cd(55)
Tapered Skirts, Undertray + Extensions	0.421

This represents a change in this coefficient of -0.042 resulting from the use of these rear extensions. This is an excellent drag saving from a rear modification altering the wake, their good performance enhanced by the state of the flow arriving at the base.

The effect on lift coefficients is as described above and this does not change significantly with yaw. The

flow accelerating over the upper boat-tail causes a reduction in pressure thus creating lift on the rear of the container and the boat-tail. This gives a nose down pitch with rear lift and front downforce as seen in fig. 35(b). Over the range of yaw angles the increased downforce at the front is again lost, the lift at the rear falling away as less flow is seen by the upper extension. Overall a downforce increase is seen from the small lift generated at zero yaw, the centre of action of this downforce moving rearward as the rear lift falls away.

The effect on sideforce and yawing moment coefficients is small and generated in the same way as the effect on lift. The flow down the windward side accelerates as it flows round the rear boat-tail causing the associated fall in pressure. The leeside does not see this same effect as the flow is not as strong down that side with separations. The resulting effect is a negative sideforce being developed on the rear windward side which lowers the sideforce of the model. As this acts at the rear of the container it adds to the yawing moment of the model, this increase rising as yaw rises. The effect on sideforce is negligible although the effect on yawing moment is worthy of consideration to its effects on the handling of the vehicle.

Also seen was the effect of transition using 22 gauge wire on this final configuration which was the same as the effect on the baseline configuration. The effects on all the coefficients is as described for the baseline configuration in Ch. 7.3.1. Drag is reduced, frontal downforce is lost with no effect on rear lift, little effect is seen for sideforce and only a small drop in yawing moment is seen at intermediate yaw angles. The reasons for these changes is as previously described. The

major effect is again on drag coefficient and the resulting wind averaged drag coefficient for this configuration becomes;

	dCd(55)
Tapered full skirts,undertray,12.5 deg rear +wire	0.389

This is a change of -0.032 due to the wire so it would be expected that at higher Reynolds numbers the drag would drop to this level. The 1/4 scale should have a drag of around this level as experience with the Mk.I cab revealed fully attached flow without extra radiusing. The same saving of -0.033 in wind averaged drag factor was found for the wire using the baseline configuration. Changes to the frontal flow are then seen to dominate the drag reduction picture as the savings tripping the boundary layer to promote attached flow give the same result regardless of the configuration. The devices tested in addition to the cab have shown the dependance on the history of the flow incident to them, the state of the flow, attached,separated and the degree of turbulence effects the way in which the devices affect the flow field.

7.4. Reynolds Number on 1/4 Scale Model

The Mk.II cab made up 1/4 scale was tested in the 3.5m * 2.6m wind tunnel, a full range of tests including force measurements and flow visualization were performed. In this section the effect of Reynolds number will be assessed on the model at zero degrees yaw. The results for drag coefficient are shown in fig. 36. A similar trend to that observed on both the Mk.I cab and with the 1/6 scale model of the Mk.II cab is seen, the drag coefficient falls nearly linearly with increasing Reynolds number. The flow visualization taken on the 1/4 scale Mk.I cab showed

attached flow, although at the very upper parts of the side corners separation must be occurring, see plate 4. The report by Cooper ,ref. 4, suggests that the radii now on the 1/4 scale should not provide fully attached flow, see Ch.7.1. Thus small separation bubbles possibly exist on the upper side radii which reattach before the tufts placed on the sides. These bubbles would reduce in size as the Reynolds number increases giving a corresponding decrease in drag. This would explain the steady fall in drag coefficient. It also shows the majority of the drag reduction occurs below the normal testing speed of 28.55 m/s, above this speed the reduction is small. At normal testing speed the flow must be approaching fully attached flow as the reattachment point moves forward. The small nature of the change above 28.55 m/s, as also witnessed for the 1/4 scale Mk.I cab demonstrates the validity of the greater scale, more realistic Reynolds number testing for which the 3.5m * 2.6 m tunnel was developed.

The other two lines on the plot show the low drag configuration, full tapered side skirts, flat undertray and rear boat-tails, over the range of Reynolds numbers and the baseline configuration at 3 degrees yaw over the range Reynolds numbers. Both these cases further confirm the description of the flow with Reynolds number given above. The low drag case showing less effect on the drag with Reynolds number again all the drag reduction occurs before the usual testing speed of 28.55 m/s. The yawed baseline model demonstrates a change to this trend in that the drag fall with Reynolds number is much more pronounced. This is as a result of the flow round the leeside front corner which as the model is yawed gives greater separations. The flow, in effect, must flow further round the radius so when separation occurs the bubble to reattachment is larger. In this way as Reynolds number increases the effect is similar

to the unyawed model with smaller radii and larger separation bubbles. The higher Reynolds numbers give smaller separations until attached flow is established and the drag 'plateaus' with increasing Reynolds number. As the separations are larger for the yawed case the region on the figure over which drag loss is seen with increasing Reynolds number is in effect shifted to the right and as described by Cooper, ref. 4, the critical Reynolds number is increased.

7.5.The Effect of Devices on the 1/4 Scale Mk.II Cab Design

As in Ch.7.3. various devices to further reduce the drag of the 1/4 scale Mk.II cab model were made and tested over the range of yaw angles to assess their full yaw dependant performance. These devices were the 1/4 scaled versions of the devices optimised from the 1/6 scale testing. Fully enclosing tapering side skirts were tested, these having a ground clearance of 50mm. Again this is less than the minimum mid axle ground clearance and represents the clearance at the axle, this clearance given to the front wheel skirt then continued back on the detachable side skirt. This is not restrictive in the terms of this aerodynamic study as already described in Ch.2.2.3. A flat undertray was also tested covering the full ground plan of the model, also it was made in three sections being divided lengthways. This could then be attached to fully cover the underside or leave the central drive section,into which the cooling flow fed, open. Rear boat-tail extensions of 12.5 degrees slope to the container were also made up. Fixed wheels and stopped ground cases were also cosidered. Measurements of drag, sideforce and yawing moment were taken with some flow visualization using smoke was also performed to help explain the results.

7.5.1. Skirts

The effect on the coefficients measured with yaw angle is shown in figs. 37(a), (b) & (c), the only configuration tested was with the tapered full skirts.

As expected the effect on drag coefficient is to reduce it in the same way it was reduced on the 1/6 scale model. Two different aspects are clear in comparison with the results previously taken on the 1/6 scale model . Firstly the skirts are reducing the drag increasingly well with increasing yaw angle and secondly that above 12 degrees yaw the rising drag then falls with increasing yaw angle. The performance of the skirts is again of great benefit and the increasing performance with yaw is a return to the situation with the 1/4 scale present day model performance. This suggests that the blockage of the yawed 1/6 scale in the 2.1m * 1.7m tunnel is effecting the results at high yaw angles. This blockage being less and the width of the yawed model to tunnel width ratio being lower in the 3.5m * 2.6 m tunnel with the 1/4 scale model result in more reliable measurements at the higher yaw angles. It would be expected as the model is yawed for the drag reduction to increase since the reduction arises mostly from the prevention of flow under the container and striking obstructions resulting in drag. As this flow would increase with yaw the savings from its prevention increase.

The drag fall at high yaw angles results from the relief of the high frontal pressures as the incident flow sees less of the frontal area and the major pressures act towards sideforce rather than drag. The resulting wind averaged drag factor for this configuration and the baseline Mk.II cab are;

	Cd(55)
Baseline	0.488
Tapered Full Skirts	0.447

This is a difference of -0.042 due to the skirts again demonstrating that the savings possible from modifications to the model configuration depend on the flow arriving. The state of the flow down the sides is important, if it is turbulent the skirts reduce drag to a greater extent than if the flow is smooth as in this case.

The effect on sideforce and yawing moment is as expected to increase both. The sideforce is increased due to incident flow encountering a greater side area than the under body obstruction, the pressure on the windward side builds up increasing the sideforce. The distribution of this pressure gives a rise in the yawing moment as the increased sideforce acts towards the front of the model adding to the yawing moment. These findings are in agreement to the results found for the 1/6 scale model.

7.5.2. Undertray

The addition of a flat undertray to the configuration using skirts was tested. Two configurations were tested. The undertray was divided into three, lengthways, with two outer panels and an inner pannel. the inner panel was as wide as the ladder chassis, roughly a third of the overall width of the model. Tests were then performed with only the sides masked by the undertray and with the complete underside masked by the full undertray. This was tested to see the difference obtained by leaving the central passage open to allow the flow to mix with the cooling flow and to provide extra flow to cool the drive train. Having the underside fully covered may lead to

cooling problems in these areas and a feel of how productive it is to cover the central region would be an asset. The results are shown in figs. 38(a), (b) & (c).

The drag is reduced for both undertray cases; the fully covered underside expectedly being the lower drag configuration over the full yaw range. More surprisingly is that the difference between the two configurations is greatest at small yaw, thus flow in the central section is greatest at small yaw angles. As the vehicle is yawed lower rates of flow are fed down the body axis from under the nose and since the flow passing under from the sides is restricted by the skirts and side undertrays less flow exists in the central cavity. This flow encountering the rear axle and other obstructions causing increases in pressure around them give the greater drag with the central region open. As the yaw increases and this flow reduces the drag arising from this region is reduced as are the possible savings from covering this area. The resulting wind averaged drag coefficients for the two configurations, with tapered full skirts, are;

	Cd(55)
Side Undertrays	0.418
Full Undertray	0.380

These figures show a difference of -0.038 is achieved by covering the central section; this arises from the calculation of the figure to be found from small yaw angles where the difference between the cases is largest. The saving made by use of the full undertray is -0.085, a large saving showing the greater detail of the underbody of the 1/4 scale model to have a much more pronounced effect on the flow than the 1/6 scale tests would suggest.

The sideforce and yawing moment plots again show little affect for the undertrays. Sideforce is slightly reduced as the shielding of the underbody is increased, the full undertray being the better configuration. The yawing moment is very slighty increased with both types of undertray. These results disagree slightly with the results found for the 1/6 scale model in the 2.1m * 1.7m tunnel which was probably affected by blockage at high yaw, see Ch.7.6.1. The effects are small and possibly affected by repeatability. The main shielding of the underbody appears to be from the skirts the undertray doing little to further improved underbody flow.

7.5.3. 12.5 Degree Rear Extensions

The rear boat-tail extensions optimised for the 1/6 scale model were made up to scale dimensions for the 1/4 scale, they extended 50mm from the base of the container. They were identical to the 1/6 scale versions extending below the container to the ground level of the skirts, extending the skirts back at a rate of 12.5 degrees to the container sides. The results obtained, for the use of the extensions on the 'low drag' configuration, with skirts and full undertray, are shown in figs. 39(a), (b) & (c).

As previously measured, drag is reduced across the full range of yaw angles and the reduction achieved is almost constant for the full range. This is achieved by the 'filling in' of the wake, the effective reduction in base area reducing the component of drag from the low wake pressures acting on the base. The reduction achieved is again considerable when regarding the low percentage of drag estimated to arise from this region, although the percentage distribution for the drag producing areas for

this low drag producing cab will be considerably altered. As the front becomes more efficient the wake contribution to drag will grow. The wind averaged drag factor calculated for this configuration is;

	Cd(55)
Full Tapered Skirts,Underbody+Extensions	0.340

This is a change in this coefficient of -0.040, a large saving, due to the addition of the rear extensions. This configuration has given the lowest drag of all so far and represents a change from a present day rigid box van of -0.457 in the wind averaged drag coefficient, a drop of 57%. This figure is also now around the figures achieved for modern saloon cars showing that when the aerodynamics of commercial vehicles are improved along similar lines to how passenger cars have been improved in the last decade then considerable drag reductions can be achieved without compromising the load size or layout.

The effect of the extensions on sideforce and yawing moment are the same as found before. The flow on the windward side flowing around the extension accelerates producing a low pressure region around the extension. This low pressure gives rise to a negative sideforce applied at the rear of the container. Resulting from this is the fall in sideforce but rise in yawing moment associated with such an applied sideforce. The effect on sideforce being beneficial although the rise in yawing moment would effect the handling characteristics of the vehicle in crosswinds. The rise is, however, small and the effect on handling minimum.

7.6 Comparison of Tunnels/Techniques

In this section the results taken from tests of two scales of models, in two tunnels using two measurement techniques are discussed. Comparisons of scale and technique can then be made along with assessment of the tunnels suitabilities for this type of testing. All data was taken to S.A.E. recommended practice, ref. 12. The comparison of the testing carried out to recommended practice is shown below;

S.A.E Practice	2.1m*1.7m Tunnel	3.5m*2.6m Tunnel
max 5% blockage	5.8% blockage	3.6% blockage
max Ht=0.3 tunnel Ht	0.24 tunnel Ht.	0.16 tunnel Ht.
max w =0.3 tunnel w	0.22 tunnel w	0.26 tunnel w
Re(min)=700000	Re(A)=750000	Re(A)=1080000
	Re(w)=650000	Re(w)=1282000

The other stipulations about modelling, mounting and testing procedures were all carried out as standard practice at Southampton University and met with the recommended practices. Testing was carried out in the 3.5m * 2.6m tunnel with both 1/4 and 1/6 scale models using the load cell balances and in the 2.1m * 1.7m tunnel the 1/6 scale was tested using both overhead and internal strain gauge balances and load cell balances only. In this way a full set of results was built up testing for both Reynolds number effects and assessing yawed performance.

7.6.1. Comparison of Tunnels

This comparison is best carried out from the results taken using the 1/6 scale model in both tunnels, taking the results from the load cell balances. The results are shown in figs. 40 (a), (b), (c) & (d). The first two plots shown the drag in the larger tunnel to be significantly lower. The decrease is mainly at lower yaw

angles and as yaw increases the drag values converge. The wind averaged drag coefficients work out to be quite different, Cd(55)=0.464 for the 2.1m * 1.7m tunnel and Cd(55)=0.437 for the 3.5m * 2.6m tunnel. The reasons for this fall are two fold, firstly the blockage of the 1/6 scale in the larger tunnel is negligible whilst in the smaller tunnel it is just larger than the minimum 5% recommended. This may cause a slight increased build up of pressure on the front of the model giving increased drag. This would however be accounted for by applying a blockage correction which when applied to the two sets of results still reveals the same drag relation. A more feasable explaination is that the turbulence level in the 3.5m * 2.6m tunnel is above that in the 2.1m * 1.7m tunnel. This would then lead expectedly to the lower drags seen in the larger tunnel. A turbulence grid was tested in the smaller tunnel which did bring the level of drag down below that found in the larger tunnel. As no figure on the level of turbulence produced was available and since this would be much higher than for the larger tunnel this result is inconclusive but a useful guide.

The sideforce and yawing moment coefficients compare very well, again for the reasons used to explain the drag loss in the larger tunnel there is a sideforce loss also. The yawing moments compare well until at high yaw the rate of increase of yawing moment with yaw angle in the larger tunnel drops but stays relatively the same for the smaller tunnel. This must be a blockage effect as at these yaw angles the blockage of the model in the smaller tunnel is approaching 17%. As this occurs the flow is restricted thus building up pressure along the windward side and creating reduced wake pressures; the distribution of these pressures leading to increased yawing moment. This sideforce in the larger tunnel must act more rearward with

less blocked flow giving the reduced yawing moment measured. This would be as expected as more side area is presented to the incident flow and the sideforce increasingly must act more centrally on the side.

7.6.2. Comparison of Models

Comparing the results taken in each tunnel on the respective models and the results taken in the same tunnel with the two model scales should give a comparison of the relative merits of each set of tests. Straight comparisons cannot be used, however, as the models are similar and not identical, as previously described. The results obtained for the models are shown in figs. 41 (a), (b), (c), & (d), showing the Reynolds number and yawing characteristics.

The drag with Reynolds number plot shows two trends which relate to the results for each model. The 1/6 scale Mk.I and Mk.II cabs are initially different in drag levels but tend to the same drag coefficient at higher numbers. This is seen in the flow visualization in plates 3 & 6, showing the flows, despite extra radiusing on the Mk.II, to be the same. Thus the drag mechanism for both cabs is the same. The two cabs show distinct differences for all Reynolds numbers for the 1/4 scale model as fully attached flow was seen for both cabs. The Mk.II with greater frontal rounding will have relieved frontal pressure and hence a lower drag. The 1/4 scale has a lower drag than the 1/6 scale both as a result of the fully attached flow at the higher Reynolds numbers and since it is relatively smaller in frontal area due to the container height. The major effect is however the fully attached flow.

Sideforces are seen to be in close agreement for

both models over the full range of yaw angles and for all configurations. In each scale the baseline is lowest and adding skirts raises this to the highest value. Addition of a flat undertray and rear extensions lowers the raised sideforce but it remains higher than for the baseline configuration. The actual values are the same for the configurations 1/4 or 1/6 scale. The yawing moments do show differences with them being lower for the 1/6 scale model. The only reason for this appears to be that for this set up the pitch wire is mounted off the model centre line for yaw angles this offset increasing with yaw. The effect on this is to cause some cross coupling since the pivot between strut and model still acts along the model centre line. As a result of this interaction with pitch the yawing moment is mostly effected because of the moment arm between strut and pitch wire, the interaction is negligible on the other components due to their size. Yawing moment is less sensitive as a result of this interaction and as shown in the results a lower yawing moment is measured. This is also shown in the results shown in Ch.7.6.1. where no diffenence in yawing moment was seen using the load cell balances, which are unaffected by this pitch wire interaction.

Analysis of the results obtained with the 1/6 scale model in the 2.1m * 1.7m tunnel the effect of Reynolds number is in evidence, as previously described. The results and flow visualization both help demonstrate this point. The test Reynolds number is only just the S.A.E. recommended minimum which in work described in refs. 4 & 10, is shown as a low estimate for a minimum. Thus comparisons of the results must take this into account and the 1/4 scale results taken as most representative. Still the smaller tunnel is a useful facility were work can be carried out quickly and efficiently to build up a set of data which can then be analysed and full scale or at least

larger scale tests carried out to finalise modifications.

7.6.3. Comparison of Techniques

In comparing the techniques from the results shown above the main point seems to be that using the overhead balance gives larger drag figures than the use of internal balances. The reason for this lies in the recording of tare values for the forces on the exposed strut which are sensed by the overhead balance and not for the internal balances. The method used to record the values was to set the strut for its position and height when mounting the model. Then the tunnel was run up to a speed calculated as the speed for the model testing plus an area blockage correction for the missing model. The speed being measured in the plane of the model. This however gives tare values which are too high since the increased speed due to the model pres ence is only seen by the lower part of the strut where the flow is accelerated by the area effect of the model. When the tunnel speed is increased to make up for the removal of the model the complete strut is now effected and the strut away from the model is of larger area than close to the model resulting in larger forces. A way around this problem would be to take tare readings with the model in place to account for any model/strut interferences on the section of strut closest to the body.

Little difference is then seen on the other measurements taken although as described above care must be taken with tares and interactions which cause incompatibility of results. Otherwise the results from the two tunnels with the two models taking into account Reynolds numbers seem to compare and agree and show the two tunnels to be good for the testing of these types of vehicles.

7.7 Conclusions

(i) The Mk.II cab is an improvement over the Mk.I with better yawing performance although for the smaller scale at the Reynolds numbers tested the radii are inadequate for attached flow.

(ii) A low drag configuration was found, as for the Mk.I cab, using skirts, undertray and rear extensions which gave a wind averaged drag coefficient of 0.340, 1/4 scale, a reduction of -0.457 from a present day standard configuration.

(iii) Cross wind performance was not seriously compromised by these modifications although yawing moments were increased substantially.

(iv) The two tunnels compared well giving similar results although comparison of absolute figures needs care.

(v) Both techniques for measuring forces worked well but better corrections for tares and interactions are needed for the overhead balance with internal stain gauge balance, the load cell balances worked extremely well within their design parameters.

(vi) Within Reynolds number ranges use of the two scale models caused no problems although Reynolds number effects were found and future testing where critical radiusing is to be used should be carried out at highest possible Reynolds numbers to avoid effects. This can be achieved by higher speeds or greater scale equally well.

Chapter 8. Fuel Economy and Operating Costs

8.1. Introduction

One of the problems when assessing the aerodynamics of a road vehicle is to estimate the impact on the fuel economy of the improved aerodynamics. The problems occur since the effects are speed related, the higher the speed of the vehicle the larger the proportion of resistance is aerodynamic. The power requirements from the engine are related to the forces acting multiplied by the velocity. The rolling resistance power requirement increases in proportion to velocity whereas the aerodynamic power requirement increases with the cube of velocity. Other power requirements are also accountable due to the road gradient and other equipment losses such as for air compressor, power steering and cab ventilation systems. All these requirements have an effect on the fuel economy and hence the operating costs of a vehicle. The main interest from an operators point of view is the impact of any aerodynamic changes on operating costs and the benefits to the profit levels from these changes. This chapter attempts to put some quantitative data relating to the effects on fuel economy and the associated effects on operating costs and profit levels.

8.2. Effects on Fuel Economy

The effect of the aerodynamics on fuel economy can be estimated using the formulae and assumptions given by Drollinger, ref. 5. From the various power requirements an expression can be deduced for the total power required at a fixed velocity;

$$Pt=((Fa+Fg+Fr).V)/Mef + Pe$$

where;

Pt = total power required
Fa = aerodynamic force
Fg = road gradient force (assumed zero for a level road)
Fr = rolling resistance
V = velocity
Mef= mechanical efficiancy (assumed 90%)
Pe = equipment power requirement

The various forces can be found, for a level road the road gradient term is zero, and the total power required of the engine calculated for a velocty of V. The equipment power requirement is assumed to be 8 h.p. (5966 W), for the vehicle running without the cooling fan, as could be assumed for a high constant velocity case. A vehicle in good condition can be assumed to have a mechanical efficiency of 90%. The aerodynamic force is calculated in the usual way, however since a given velocity is used in the equation the corresponding wind averaged drag factor can be used to take account of crosswinds to give the wind averaged aerodynamic drag expected. An expression for the rolling resistance of a commercial vehicle is given in ref. 5, which states;

$$Fr=(0.0041+0.000041.V).GVW$$

where;

V = velocity in m.p.h. (the constants in the equation make this dimensionless)
GVW = gross vehicle weight

The velocity is rendered dimensionless so the equation becomes a fraction of the gross vehicle weight. The maximum gross vehicle weight for a rigid box van is

30,490 kg. The effect of speed has a bearing on the fuel economy of a vehicle, the quicker the speed the lower the fuel economy and the better the aerodynamics the quicker the possible speed can be. Thus there is a conflict in improving the aerodynamic drag that trades fuel economy against possible speed. It is therefore necessary to estimate the savings at two speeds, those chosen being 55 m.p.h. and 60 m.p.h. The wind averaged drag factors for the four main configurations are;

	Cd(55)	Cd(60)
Present Day Base	0.797	0.787
Best Present Day	0.560	0.551
Fast Front II	0.488	0.481
F/F II + devices	0.340	0.332

Thus using these values the aerodynamic force can be found and added to that of rolling resistance. Then substituting into the first expression to give the total power requirement at 55 or 60 m.p.h. The percentage of total power required of the aerodynamic drag is;

	55 m.p.h.	60 m.p.h.
Present Day Base	42 %	45 %
Best Present Day	33 %	37 %
Fast Front II	30 %	33 %
F/F II + devices	23 %	26 %

Thus it is seen that improvement of the aerodynamics reduces its contribution to power requirement to a great extent also that a speed increase gives an increase in the aerodynamic power requirement as expected. The values for total power requirement can then be used in an expression for fuel economy;

$$m.p.g. = K.V.Tef.Et/Pt$$

where;

m.p.g. = miles per gallon
K = 1/1609 miles/m to convert from metres to miles
V = velocity (m/s)
Tef = thermal efficiency of the engine
Et = calorific value of diesel oil (172.522 MJ/gal)
Pt = total power required

Ref. 5 suggests using a thermal efficiency of 0.37 but it was considered more appropriate to cal culate a figure using the value of 9 m.p.g. quoted in ref. 29 for a 30 ton present day rigid box van. This figure can then be used for our present day baseline configuration at a constant speed of 55 m.p.h. and all the fuel economies and costings related to this. Thus a thermal efficiency of 0.34 was calculated. The miles per gallon figures were then calculated for the four cases;

	55 m.p.h.	60 m.p.h.
Present Day Base	9.0 m.p.g	8.7 m.p.g
Best Present Day	10.3 m.p.g.	10.1 m.p.g.
Fast Front II	10.8 m.p.g.	10.6 m.p.g.
F/F II + devices	11.9 m.p.g.	11.8 m.p.g.

These figures show the savings to be made by improving the aerodynamic drag of a commercial vehicle keeping all else constant. Two main points appear, firstly improved aerodynamics improve fuel economy and secondly the loss of fuel economy due to high speed operation is greatly reduced with an aerodynamically efficient vehicle. The loss was 3.3% for a present day type vehicle and just 0.8% for the fully developed Fast Front II design. These savings

could then be translated into operating cost savings, and although the improvements appear small, given the large mileages travelled by these vehicles the savings would add up showing much better returns for high mileages. The figures do show that reducing aerodynamic drag is an effective way of improving fuel economy and minimising the effects that speed has on this. Although these figures are deduced for constant high speed cases savings would also be made at lower speeds, these figures are representative of motorway driving, a condition for which a high proportion of time is spent with todays commercial vehicles.

8.3. Operating Costs

Operators of commercial vehicles want to see their operating costs minimised to increase profit margins or make their charges more competitive in todays market place. Thus the m.p.g. figures given above need to be translated into cost savings and profit increases. Tables of operating costs are obtainable for various classes of vehicle, see ref. 29 , these tables giving a break down of all costings. Two types of cost are detailled each having a number of contributary sections. Firstly standing costs, those of licences, wages, rent and rates, insurances and interest, these are estimated and averaged and given as a cost per week. The figure for a 30 ton rigid box van is £ 494.22 per week. This figure is assumed to remain constant for the four configurations under consideration.

The second cost is running costs under which fuel is listed, other cost items are lubricants, tyres, maintainence and depriciation. Again these have been averaged and listed as a cost per mile. The fuel cost per mile is calculated from the m.p.g. figure and an estimated average fuel cost of £ 1.30 a gallon, this is an averaged

bulk stored fuel price not pump price. Thus applying the m.p.g. figures calculated new running costs can be found, these are worked out for the two extreme cases given in the tables for mileages of 500 or 2,500 per week. The present day baseline case is again considered as the case given in the tables and the m.p.g. figure assuming constant speed operation as a necessary simplification. The total operating cost in € per week is given below, the first figure is for 55 m.p.h. and the second for 60 m.p.h.;

	500 miles	2,500 miles
Present Day Base	729.17 / 731.67	1668.97 / 1681.47
Best Present Day	720.07 / 721.32	1623.47 / 1629.72
Fast Front II	717.17 / 718.27	1608.97 / 1614.47
F/F II + devics	711.57 / 712.07	1580.97 / 1583.47

When these figures are then compared, adding 30 % to give a minimum charge per week, with the minimun charge for the present day baseline configuration the possible increase in profit (or decrease in charge) can be seen. These percentages are given below again the first figure is for 55 m.p.h. and the second for 60 m.p.h.;

	500 miles	2,500 miles
Best Present Day	4.2% / 4.8%	9.1% / 10.6%
Fast Front II	5.5% / 6.2%	12.0% / 13.7%
F/F II + devices	8.0% / 9.1%	17.6% / 20.1%

The effect on the profit by the increase in average speed, a 9% increase, is;

	500 miles	2,500 miles
Present Day Base	-1.1%	-2.5%
Best Present Day	-0.5%	-1.1%
Fast Front II	-0.5%	-1.0%
F/F II + devices	-0.2%	-0.4%

These figures show the large impact the improvement of aerodynamics can have on the operation of a commecial vehicle even at low mileages. A present day vehicle with all the modifications could return a increase in profits of around 5% for low milage and 9-10% for high mileage. This compares to the Fast Front design with all the devices which would return 8-9% for the low mileage and 17-20% for high mileage. This shows that great savings can be made from reduction of the aerodynamic drag and that work is needed to alter the basic design of commercial vehicles to produce these savings. The effect of driving faster is also shown that by a small increase in speed a relatively large fall in the profit increase is seen. This effect is greatest for the less efficient configuration and is greatly reduced for the Fast Front with all devices configuration. Overall a desirable effect on operating costs is seen with improved aerodynamics, and even if this effect is decreased, from the aerodynamic effect only to the effect on operating costs due to the other factors, it is still seen to be worthwhile.

8.4. Conclusions

Although some simple assumptions have been made in the workings of this chapter improved aerodynamics are seen to have a great effect on fuel economy and this reflects in the operating costs of the vehicle. This reduced costing could be used in a number of ways, as a selling point to operators whose primary concern with these

vehicles is to provide as cost effective a service as possible. The operator can use the savings to either reduce charges to the customer or to increase profits or a combination of both. These savings were calculated from constant speed figures and although the vehicles do not operate at constant speed the majority of their operational time is spent on high speed roads to maximise their operational value. Speed is seen to have an effect on costs although a favourable reduction in this effect is seen for a more aerodynamic vehicle. Overall a number of factors apply to operating costs and aerodynamics is just one but obviously an important one. In providing a better vehicle for the next decade other factors such as maintainance charges and engine efficiencies would also need improving to give a complete vehicle package.

Chapter 9. Wake and Spray Studies

9.1. Introduction

The majority of aerodynamic studies on commercial vehicles, as with this investigation, centre around the reduction of drag in an effort to improve the fuel economy of these vehicles. This is of primary interest as the marketing and operational costs of commercial vehicles are of most interest to both manufacturers and operators. The operational costs of these vehicles is also reflected in the cost of goods which need to be distributed from factories or warehouses to retail outlets. In this way costs must be kept down both for an operator to be competitive and to for the cost increase of goods due to transportation not to be excessive.

There is, however, another extremely important area in which the aerodynamics of the vehicle plays a vital role. This area is the problem of spray generated by these vehicles in wet conditions which can in certain situations be a major hazard to other road users. The vision of drivers, following or overtaking, is impaired by the spray and is a contributory factor in some accidents in wet weather. Any driver has experience of these problems, which are particularly in evidence on motorways and other roads were vehicle speed is high. This chapter gives details of tests carried out during this program of work aimed at ways of relieving this problem through improved aerodynamics.

9.2. Spray Generation and Suppression

A number of previous studies have been carried out with relative success aimed at both prevention of spray generation and the entrainment of any spray into the flow

field. In these two areas the must successful work has dealt with minimising the generation of spray, see refs. 24, 25, 26, 27 & 28. In these reports the work carried out is detailed which is summarised in this section, it deals with the mechanisms of spray generation and its subsequent dispersal and methods of minimising it.

There are two problems to consider, splash and spray, spray is a result of splash striking obstructions and breaking down into fine droplets. The major areas of spray production are from the water sheet ejected from the tyre treads,this then breaking up on hitting underbody obstructions and capillary adhesion spray when water held in the tread is forced out by pressure in the surrounding air. The tread throw problem occurs just aft of the tyre contact patch, the water sheet/droplets breaking up to fine spray when they encounter the mudguards, container surfaces, etc. This was found to be best contained by use of materials such as plastic grass which caught the droplets without them breaking up into spray.

The spray was not totally prevented from forming by the plastic grass as not all the water ejected was captured and spray was still generated. Capillary adhesion spray still existed and as this was generated from the tyre the spray was not controlled by plastic grass. Thus spray was not going to be eliminated due to the working of a tyre tread, its generation could be minimised but not stopped. Some other details on the workings of spray were found. The generation of spray was equally as strong from the front wheels as the rear wheels. This is a result of the front wheels encountering an undisturbed water layer on the road surface. Since the drying effect of the front wheels on the road is seen by the rear wheel this lowers the spray generated at the rear wheels. Flow at the sides

of the vehicle was only seen to flow outwards around the rear wheels. Other ways of reducing the generation of spray could be taken up, ie. the use of porous road surfaces to minimise the depth of standing water on the surface, but it was clear the distribution of spray in the flow field needed to be controlled.

Allen,Burgin & Lilley, ref. 26, carried out comprehensive tests in the wind tunnel and on the test track to establish both the mechanisms of spray generation and the subsequent effect of the aerodynamics on the distribution. Firstly pressure data was taken on small scale models with flow visualization to establish the flow field. A wheel assembly was tested in the tunnel to establish the local flow field around the wheel, this gave two main points. The pressure distribution around the wheel was unaffected by the presence of a mudguard. Secondly the suctions developed on the upper surface of the wheel, as also described in refs. 14 & 15, were reduced with side valencing of the mudguard. Full scale tests on various devices were then carried out also detailed in refs. 19, 25 & 27.

The findings of these tests showed the methods of reducing the generation of spray that were most effective. The valencing of mudguards over the upper section of the wheel were seen to be effective though not a complete solution. Collection of the ejected water and channelling by gutters to avoid catchment by the rear wheels was also effective. The modifications to the aerodynamics, with a cab roof deflector, airdam and back board were shown to be of little effect. The theory of producing a low pressure region under the vehicle to pull in the sideflow and contain any spray proved of little effect. The cab roof deflector preventing down flow between cab and container

was seen to be highly cross wind dependant, the spray problem increased with yaw angle. More effective means of generating these low underbody pressures should prove more useful. Results taken by Weir, ref. 28, also agree with those above the best devices reduced the generation of spray.

The overall picture obtained by all tests demonstrated the spray problem to be highly speed dependent. This is probably the most crucial area in the control of spray. The density of spray is shown to increase with the cube of velocity, that is spray would be greatly reduced if in bad weather speed restrictions were to be observed. The areas of study for this program would deal with the changes in the flow field of the modified models which would effect the distribution of the spray into the side and wake regions. This was decided after consideration of present devices, which work well at minimising the spray generation. It was felt that removal of separation regions and reductions in turbulence levels in the flow field would have great benefits to suppressing the spray that would still be generated. The tests performed were mostly attempts to visualize the flow field using smoke injected around the wheels to simulate spray, use of smoke to assess the general flow field and measuring the total pressures in the wake to view the wake structure.

9.3 Flow Visualization Studies

The initial studies carried out involved injection of smoke at a number of points around the wheels of the 1/4 scale model. This it was hoped would simulate the generated spray around the wheels and the entrainment into the flow could be observed. This was carried out on the model using the T45 prototype cab and was of limited success. The general flow patterns could be seen although

the volume of smoke possible was insufficient to photograph well. Observations were still recorded and a picture of the spray distribution was around this model was possible.

The flow from the front wheel moves outward from infront of the wheel. The flow above the wheel wraps around the top of the wheel arch and then down the back of the rear section of the arch, caused by the strong downflow between the cab and container, eventually mixing with the frontal outflow. Also the flow at the rear of the wheel flows out, all these streams mix and continue down the side of the vehicle. The flow being tubulent soon breaks up the smoke and just general haze can be seen, this must represent poor regions of spray suppression. Little difference was observed when the wheels were stopped, only a slight increase in the out flow from the upper section over the top of the arch. Valencing of the upper arch to cover the upper part of the wheel stopped this wrap around flow. The overall outflow did not appear to reduce if anything the flow from the front and rear of the wheels was stronger. The overall height of the smoke plume then fell so although the smoke passing into the sideflow is of similar density its reduction in height would be of benefit.

The rear wheel was tested both with and without a mudguard, without the guard the smoke showed the flow around the wheel separating close to the top point. This lifted but was held by the container lower surface before being broken down by the turbulent wake. Thus no sideflow was in evidence and the problem here would be in the wake, the large wake soon distributing the smoke as would occur to the spray. Stopping the wheels resulted in a larger smoke filled wheel wake, flow staying attached further around the wheel. This gave a greater break up of the plume

which would increase the spray distribution. The flow with the mudguard was similar to that observed for the front wheel strong outflow into the sideflow of the model with some wrap of the smoke over the top of the guard. Again this wrap increased when the wheels were stopped and was eliminated with valencing; the density of the overall plume increased with valencing. Thus the same effects were observed for front and rear wheels. The strong outflow for the rear wheels, with mudguards, creates an increased side spray problem whilst reducing the wake problem.

The flow outward from both sets of wheels creates the bad spray problem for this configuration. The sideflow is turbulent due to the separated frontal flow, the mixing with the outflow ahead of the rear wheels caused by blockage to the underbody flow and the effect of the rear wheels. This outward flow is strongest from the front of the wheel where larger pressures are seen. Above the wheel the pressure is slightly negative so the outflow here must be caused by the low pressures in the turbulent sideflow pulling the smoke outward. As the sideflow is turbulent the smoke or spray is distributed over a larger area which causes increased problems. As previous successful valencing tests suggest, the best means to suppress this would be to reduce the amount of outflow by covering as much of the wheel as possible, leading to fully enclosed wheels. This would appear the best solution as attempts at preventing outflow from under the vehicle had no effect. Also to reduce the turbulence in the sideflow would result in less break down of any spray close to the sides of the vehicle reducing the spray further out. This would naturally lead to the fully enclosed skirts developed for low drag. Any spray entering the wake is going to be distributed by the turbulent flow and lifted by the low pressures causing bad spray conditions. If the wake can be minimised and the flow

smoothed as much as possible this will result in less spray density in the wake. Thus the fully attached flow with better filling in of the wake using the rear boat-tails should help to suppress the spray in this region.

The next flow visulization took place on the Mk.II 1/4 scale model in the 3.5m * 2.6 m tunnel where a smoke probe was used to test the overall flow field and its effects on any spray distribution deduced. The tests were carried out on three basic configurations, the baseline, fully skirted with or without undertray and the skirted with undertray and rear boat-tails configuration. Early tests showed that no difference was visible to the outer flow by addition of the undertray. The three configurations were then tested over a range of yaw angles to see any flow change.

The flow for the baseline configuration shows that the flow follows generally along the side of the vehicle, see plate 12 (a) & (b) . No evidence of inward or outward flow from the underbody interference is apparant. The smoke plume is not consistent and is seen to break up due to the turbulence present. This arises from the flow from the exposed rear wheels interfering and mixing with the sideflow causing this turbulence. This would have a bad effect on spray as it would cause it to be caught up and distributed into the sideflow as for a present day truck. The flow around the front of the model is smooth showing no separations and no interference from the front wheel on the flow. Aft of the model the large turbulent wake formed is seen to break up the smoke further with a possible vortex being seen. This large wake tended to lift spray into it thus reducing visibility behind the model. The solutions to these problems would appear to be to reduce the affect of the rear wheels on the sideflow and reduce the size of the

wake and attempt to smooth the flow into the wake.

The effect of the skirts is shown in plates 13 (a) & (b). Here the flow is seen to be much more consistent, the plume of smoke staying together until it reaches the wake. Thus the flow has been greatly improved by the full skirts which as well as decreasing the amount of spray generated and passed into the flow would also result in that generated being contained by the strong sideflow and not distributed out into the rest of the sideflow. Also the flow into the wake is shown to be greatly smoothed and 'fills in' to a greater extent which would result in higher pressures and less spray lifting. This configuration with much improved side and wake flow would result in little spray down the sides of the vehicle and reduced spray in the wake. The strong sideflow would probably keep any spray generated at the lower part of the wheels from rising and propagating into the flow.

The effect of the rear boat-tails is shown in plates 14 (a) & (b). Again the flow down the sides of the model is still consistent and smooth with no break up in the flow. The change to the flow is an increased flow back into the wake of the model, the flow bending back into the wake region around the rear boat-tails. This should lead to less spray lifting in the wake as the pressure in the wake is raised. Also the flow appears to be less turbulent as the flow turns back into the wake. Thus any small amount of spray down the sides of the vehicle would not be broken up and distributed over as large a region as before and thus the overall problem would be reduced.

At yaw the flow changes are more distinguishable. The baseline flow is greatly disturbed even at small yaw angles, see plate 15 (a) at 6 degrees yaw. This shows large

break up of the flow down the side due to turbulence in the flow. This would be bad for spray which would be pulled into the flow and distributed into the side and wake flows causing visibility problems. The addition of skirts greatly reduces this break up of the flow, see plate 15 (b). The turbulence is reduced and the smoke plume is seen to flow down the sides of the skirts with no separation then into the wake. There is a greater break up of flow in the wake than at zero yaw for the same configuration though this is expected due to the larger wakes exsisting at yaw. The skirted version is seen again to improve the sideflow which would aid spray suppression preventing the spray spreading into the side and wake flows. Also a better 'pull back' into the wake is seen from the tapering of the skirts again this would was improved by the rear boat-tails lessening the wake and reducing turbulence.

At higher yaw angles again the flow down the leeside is seen to deteriorate, plates 16 (a) & (b). The plume of smoke in plate 16 (a) is shown to break up to a much greater extent, aft of the rear wheels the flow back into the wake shows a large level of turbulence. This shows the region would not help contain spray which would be pulled into the side and wake flows and be distributed well into the flow. Using the skirts again helps the flow stay attached and flow smoothly down the side, see plate 16 (b). The plume is slightly more disturbed than for the lower yaw case showing that in the sideflow little spray dispersal would result. Again a degradation in the wake is seen though overall the flow is less turbulent and the wake smaller than for the baseline. This was again aided by the rear boat-tails which would result in less spray lifting into the wake.

Overall then the flow is seen to be greatly

improved by the aerodynamic improvements to the basic model. The flow, particularly at yaw, is reduced in turbulence and helped pass straight down the sides of the model by the skirts. The rear boat-tails help fill the wake which would result in a higher pressure, reduced turbulence wake which would prevent lifting of the spray in this area. The undertray which would increase the velocities and make the flow at the ground less turbulent would also help stop lifting of the spray into the wake. It is important to reduce wake size to leave the area between the undertray and the container open. This allows flow from the cooling to pass out into the wake which also helps raise its pressure. This was seen in drag measurements and would be seen in spray patterns in the wake.

The only problems with these devices are from an operational point of view, both for access to the wheels and for cooling of brakes and tyres. These problems could readily be solved with consideration to 'tuning' of these devices and creating adequate cooling flow to the brakes, the flow to the tyres would need to be considered carfully in view of spray suppression, use of higher temerature rubber compounds could be a solution. The construction of the skirts could easily allow access to the wheels. This was not however the purpose of this study and attention is just drawn to possible problems that would need consideration if the results found were to be used further in the design process for a possible vehicle.

9.4. Total Pressure Wake Surveys

In order to further assess the effectiveness of the devices on the flow of the model it was decided to carry out a study of the total pressures in the wake. This was also a back up to the flow visualization carried out

into spray suppression. A rake of hypodermic tubing was made up into a grid of ten by ten tubes. The spacing of the tubes was 25mm and they were all tied to give the rake rigidity and so no movement in the positioning of the tubes would take place due to the air pressure. A picture of the rake in the 2.1m * 1.7m tunnel with the 1/6 scale model is shown in plate 17.

Initially it was thought the bunching of tubing at the centre upper portion of the rake would interfere with the pressure readings. The rake was then initially tested tunnel empty and no effects were seen, the rake performing well. The tubes in the rake were connected to a scani-valve pressure sensing transducer, the tubes being fine bore had to be allowed to settle and provision was made for this. The results being recorded on a microcomputer were then reduced and a linear interpretation used to plot the Cp points used for the constant pressure lines plotted. Three positions were tested at zero yaw, 185mm behind the model at the most rearward position on the moving ground, at the rear wheel position 25mm off the container side and 1m behind the model. This last position was the position chosen for the yaw tests as more useful results were achieved. Unfortunately this position was over the stationary tunnel floor behind the model. This did not appear a problem though some small boundary layer would exsist.

9.4.1. 185mm Rearwards of the Model

The plots for the four configurations are shown in figs. 42 (a), (b), (c) & (d). The initial plot for the baseline immediately shows the region of pressure lower than Cp=0.0 to show the general outline of the base of the model. The container is seen together with the chassis

underneath it. Also shown on each plot is a region either side of the model which relates to the boundary layer formed on the stationary tunnel floor each side of the moving ground. It is clear these regions do not interfere with the model flow and are not caused by it. The major area of interest is the flow from the rear wheels which appears to be causing an increasing broadening of the wake towards the ground. in these regions there is large pressure changes which would lead to turbulence in the flow around these regions. These areas are in effect regions of unclean flow which are both drag producing and detrimental to the suppression of spray. Another area shown is under the model, little flow occurs here a few points of Cp=0.1 were found but not enough to determine the contour, it was felt best to leave out the points for clarity. Thus the blockage by underbody parts causes little flow to arrive at the rear, the rest of which must flow outwards to some extent increasing the spray problem.

The addition of the full tapering skirts eliminates these regions and the freestream velocity flow is pulled in close to the sides right down to the ground. The flow at the skirts is actually seen to be pulled further in by the action of the tapering. This elimination of these areas of changing pressure result in a smoother flow which is very beneficial to drag and spray suppression as seen by the visualization. The strong sideflows would prevent great outflows of spray into the sides of the model. The region of lower than Cp=0.0 is larger, interestingly, which would lead to greater base drag but this is not reflected in the overall drag figures. This leads to the conclusion that the skirts, restricting the flow to the rear wheels and axle, results in a larger drag reduction than first realised. The turbulence caused by the rear wheels, without skirts, must also have such an affect

as to cause wheel base drag which is eliminated with skirts. There is also a slight in flow close to the ground caused by the containment of the underbody flow and greater velocities in the flow under the model. Overall the wake is much more tidy and narrower with stronger, smoother flows at the sides which would give a greatly reduced spray pattern both at the sides and in the wake of the model.

Adding the flat undertray to this, fig. 42 (c), has little effect but small detremental patterns can be seen. The small inflow close to the ground is lost and a slight outflow seen, shown by the curving outwards of the constant Cp lines close to the ground. This is now a result of the high velocity flow under the nose now continuing down the full length of the body and not being able to diffuse into the underbody section. Then encountering the rear wheels pressure builds up and small outflow close to the ground results. This is detremental to the spray pattern though not the drag. Drag must be more greatly affected by the low pressures set up under the container and any turbulences set up in this flow. Again the lower than Cp=0.0 area is seen to be enlarged as now the only flow between the undertray and the container is from the restricted cooling flow, also this increased size is not witnessed as a drag increase. This is further explained by the results taken further to the rear were different wake patterns are seen.

The rear boat-tails when added to the above configuration show little effect, the outflow close to the ground is a little more apparent but this is more likely to be repeatability. The only real effect and the expected one, is a small decrease in the overall width of the wake as the flow is pulled in by the boat-tails. The effect is small so close to the base of the model although it is

still apparent and detectable. This reduction of the wake size corresponds with the drag reduction found and would suppress the lifting of spray in the wake of the model.

9.4.2. 25mm Off the Container Side at the Rear Wheel Centre

These tests were to view the total pressures along side the model at the rear wheel position to see any local flow disturbances which would affect the spray control. There was little difference in the results for all, The best, least disturbed flow was with the skirts only which showed just freestream flow down the sides. The baseline showed some low speed flow close to the ground which must have been caused by outflow due to the presence of the exposed wheels. When the undertray was added again this outflow was seen and appeared stronger than for the baseline. This must again result from the prescence of the wheels to the underbody flow which is now faster as it does not reduce due to flow into the underbody cavity. Thus this local outflow is stronger and would carry spray causing a detrimental effect. These plots are shown figs. 43 (a), (b) & (c). These effects, particularly with the exposed rear wheels, are smaller than expected and must result from the quality of the sideflow arriving at the rear wheels. The attached flow round the front corners and the subsequent skirting of the front wheel means undisturbed air flows down the sides with little cause to move in. As a result little of the flow is affected by the rear wheels and the effects do not propagate out far from wheel. This demonstrates why the history of the flow has a great effect on the possible benefits achievable by modifications downstream.

9.4.3. 1000mm Rearwards of the Model

(i) Zero Yaw

The results taken at zero yaw for the four configurations are shown in figs. 44 (a), (b), (c) & (d). The model was also tested with fixed wheels with a 5mm gap in all configurations at zero yaw. As a result of the lowest measurements being at 25mm ground clearance no differences moving to stopped wheels were found. The plots discussed here are for the rotating wheel case. No time was available to assess the difference moving or stopped ground and this was thought unnecessary as the more realistic flow is moving ground. Previous reports have demonstrated the need for moving ground and its use in this is not in question. The region of boundary layer flow to the side of the wake is again due to the boundary layer formed on the stationary sides to the moving ground and is not an affect of the model flow. The two flows are just apart and not interfering at this position though at yaw and further back they will be mixing. This must be remembered when looking at the yawed wakes.

The baseline configuration again shows the main features discovered previously, namely the outflow towards the ground causing the outward sweep of the constant Cp lines. The overall wake size is seen to be large, mostly due to this out sweep, no regions lower than Cp=0.3 are seen in any of the plots. This region for the baseline model is a small region close to the ground not being of great effect though there is a large region above before the Cp=0.5 lines. Overall the flow seems dominated by the out flow causing the enlarging of the wake, with turbulence also in these regions, which would result in poor spray suppression in the wake.

The skirts again cause the pulling in of the out sweep of constant Cp lines close to the ground as seen previously. The lines continuing inward as straight lines following the sides of the model until the enlarged lower than Cp=0.3 region in the centre. The flow down the sides of the model are thus seen to be smooth and turbulence free for the full height of measurements. Also the slight pull in of the Cp lines close to the ground is seen, a result of the skirt tapering and a help to spray suppression. The smaller overall wake size and the tidy up of the turbulent flow from the rear wheels give the drag reductions found for the skirts.

As found from the measurements closer to the model the effect of the undertray is to recreate the outflow prevented by the skirts. The size of the outflow is small compared to the baseline model and although it would be detrimental to spray suppression other drag reduction considerations may outway this small deterioration. The size of the lowest pressure and velocity region, $Cp<0.3$, is much reduced as is the region above it til $Cp=0.5$. Thus the drag reductions are produced by the higher velocity flow flowing from under the model into the wake increasing the wake pressures. This effect was not seen close to the model but is seen well in these measurements further from the model.

Adding the rear boat-tails futher enhances this wake filling with the low pressure regions all reducing in size with a pulling in of all lines towards each other. The lowest pressure region is lost and the region of $0.3<Cp<0.5$ closes up towards the upper measurements. The outward flow and sweep of Cp lines due to the undertray are still as strong and this would cause degredation in the spray

pattern. Overall, however, the wake pattern is smaller and the spray lifting into the wake of the vehicle would be reduced although some spray would be passed outwards around the rear wheels this would be a reduced effect to the baseline configuration and would need to be compromised with drag reductions.

(ii) Yawed Wake

The important point to remember when viewing the plots of constant Cp for the yawed model is that the 'slice' of the wake is not perpendicular to the model axis. Thus as the model is yawed a growth in the width of the wake will be seen since the measurements are taken at an angle across it. It is therefore easier to compare wakes of differing configurations with the same yaw angle to those of the same configuration at different yaw angles. Some changes in the wake outline are decernable as the model is yawed changing the general flow pattern.

The first change seen for the baseline and other configurations at 3 degrees yaw is shown in figs. 45 (a), (b), (c) & (d). This change is a sweeping out of the Cp lines close to the ground on the leeside of the model, and a straightening of the lines on the windward side. This results from the pressure build up on the windward side helping straighten the flow down the side and into the wake. The sweeping out of the flow on the leeside is as a result of some of the windward sideflow flowing under the model and slowing down due to the wheels and underbody obstructions. This slowing of the flow causes the low Cp's and this sweeping out of the lines. The baseline configuration again shows the out-sweep and turbulence due to the exposed wheels on the windward side although the size is smaller due to the stronger sideflow. The overall

size of the wake is little changed by the yaw angle, with just added slow flow on the leeside.

Adding the skirts again straightens the flow down to the ground on both sides. The wake is again reduced in width close to the ground as a result of the better inwards flow caused by the tapering of the skirts. This causes an inwards sweep of the constant Cp lines on the windward side and a large reduction in the out-sweeep of the lines on the leeside. Some flow still passes under the skirts from the windward side and slows down due to obstructions causing this slow outflow on the leeside. The effect of these two sweeps of the Cp lines is to cause the wake to appear to be leaning towards the windward side. The overall width of the wake again seems to be reduced although the region lower than Cp=0.3 is larger than for the baseline configuration. The outflow and turbulence cause by the exposed wheels giving a larger wake close to the ground must give the higher drag found for the baseline.

The flat undertray giving much higher velocities under the model almost causes this region of lowest pressures to disappear. Only a small region close to the ground is seen, thus the pressure in the wake is increased which would reduce the lift of spray into the wake. This would also give the lower drag found. There is not such a large increase in the outflow and sweep of the Cp lines close to the ground as found for this configuration at zero yaw. In fact little change in the wake other than the reduction in the size of the lowest pressure region is evident thus for the yaw case only benefits are seen and not the possible spray increasing problems seen at zero yaw.

The rear boat-tails this time cause a degradation

in the wake causing similar problems as the undertray at zero yaw. The wake size in the upper region is closed up due to more in flow due to the boat-tails although as the flow approaches the ground outsweeping of the Cp lines is seen. Separations must be occuring from the rear boat-tails at this yaw angle where the flow has already followed the tapering of the skirts. The extra tapering due to the boat-tails must cause an adverse pressure gradient resulting in separations. As a result the overall wake is enlarged near the ground and the region of $Cp<0.3$ is increased. These separations do not occur off the container sides or top so the extensions pull in the flow reducing the wake above skirt level. Thus, overall, the wake size is reduced, reducing drag although the increased low pressure region close to the ground could be detremental to controlling the lifting of spray in the wake.

These effects are all evident with the same changes in wake with configuration across the yaw range. As yaw increases the 'leaning' of the wake to the windward side increases showing much slower moving air down the leeside close to the ground whereas the flow appears to increase in speed close to the ground on the windward side. The baseline and baseline with all devices configurations at 15 degrees yaw are shown in figs. 46 (a) & (b). These plots show a major difference in the wakes at this high yaw which demonstrate the more efficient aerodynamics of the final configuration.

The baseline configuration again shows the large out- sweep on the leeside due to the slow, obstructed, turbulent flow under the model. This large area would lead to spray lifting and flowing into the sideflow in large amounts. The increasing inward sweep towards the ground on the windward side arises from the flow turning in just aft

of the rear wheel below skirt level whereas this does not occur til the base of the container above the skirt height. This then gives rise to the slant in the wakes at yaw. When using the skirts the tapering gives a similar effect. There is still a large Cp<0.3 region in the centre of the wake giving rise to larger drags and which would lift spray into the wake. This region has in fact grown for this configuration as it was yawed, at the lower yaw angles the this region fell to a minimum at 9 degrees then enlarged at higher yaw as the base area enlarged.

The add-ons cause this region to disappear which it had done at lower yaw for the skirts and undertray configuration at 6 degrees yaw. It was not until 9 degrees that it was lost for this configuration. The wake size is roughly of equivalent extreme dimensions although the flow within the wake is of higher pressure and thus higher velocity. Overall then the wake is greatly reduced for this configuration at this yaw angle this would give good spray suppression and lower drag as found previously. There would be less spray in the leeside flow as there is less Cp contours in the region and the spread is therefore less. The lifting of spray into the leeside flow region would thus be much reduced.

9.5. Conclusions

These results demonstrate the minimised effect on the side and wake flows brought about by the much improved aerodynamics. This improvement is brought about both by the cab design and the devices fitted subsequently. Together all the devices bring about an improvement in a certain area, this is always beneficial to the reduction of drag. The effect on possible spray suppression appears more complex with some aerodynamic improvements causing possible

spray problems in certain conditions. The overall effect of the devices is shown to reduce turbulence and low pressures in the sideflows and to decrease the size of the wake and increase the pressures in it. These changes can only be of benefit, reducing the lifting of spray into the sideflow and wake. All the changes together over the yaw range are effective in reducing the aerodynamic areas of spray problems.

Chapter 10. Conclusions

This chapter briefly states the conclusions drawn in the preceding chapters from the work carried out.

10.1 Facilities

(i) Moving ground test facilities now exist for large scale models in the 3.5m * 2.6m wind tunnel, the moving ground plan dimensions being 5.3m * 2.4m. The ground runs synchronous to the air stream at 30 m/s with excellent control. Boundary layer thickness is negligible and uniform across the width of the belt.

(ii) The 2.0m * 1.1m moving ground can be installed in the 3.5m * 2.6m wind tunnel to allow yawed belt and model testing to better simulate the crosswind case.This is unneccessary for commercial vehicle testing though may be valid for lower ground clearance vehicles where the interaction between underbody flow and ground motion is much more critical.

(iii) The moving ground facility in the 2.1m * 1.7m wind tunnel remains an excellent facility for moving ground testing. The facility has been in use for some fourteen years giving an excellent broad base from which to commence aerodynamic investigations. Improvements could be incorporated to update the facility;

(a) a new variable rate boundary layer suction box with a constant trough as now used in the 3.5m * 2.6m tunnel to give uniform boundary layer removal at varying speeds.

(b) improved, controllable belt suction to allow

testing at speeds to 35-40 m/s to better simulate Reynolds number at small scale.

(iv) Measurements can be taken accurately and repeatably in both tunnels. Since the overhead balance in the 3.5m * 2.6m tunnel proved inaccurate and unrepeatable, balances needed to be designed and developed for the 1/4 scale testing giving the main three components of interest for crosswind testing. The overhead balance in the 2.1m * 1.7m tunnel proved an excellent tool being extremely sensitive and repeatable; also it proved easy to use, a great advantage. The strain gauge balance for use at yaw in this tunnel performed well, perhaps its age was shown by its inability to measure rolling moment although this was not a serious problem. It is time to a new dynamometer should be designed/built.

(v) A 1/4 scale rigid box van of present day configuration was successfully tested over the 5.3m * 2.4m ground in the 3.5m * 2.6m tunnel. The results showed excellent compatability to other similar configured models tested here and at other establishments. The techniques, facility and model were all proven and the ground commissioned for wind tunnel work.

10.2 Present Day Commercial Vehicles

(i) The basic present day vehicle with a wind averaged drag coefficient of Cd(55)=0.797 could with a number of devices available today be reduced to 0.667. Fairing the gap between cab and container further reduced this to 0.560, around the lowest drag achievable with a present day design, see fig. 47.

(ii) These improvements could increase fuel

economy to 10.3 m.p.g. from a base of 9 m.p.g. at a constant 55 m.p.h. although an increase of speed to 60 m.p.h. would give a 2-3% decrease in these figures. These savings can be related to costs and hence profits, the best configuration tested could give increases in profits of 4.2-4.8% for a weekly mileage of 500 miles and 9.1-10.6% for a 2,500 miles weekly average. These savings could also translate to lower charges as well as increased profits.

10.3 Future Commercial Vehicle Designs

(i) A Fast Front cab design was tested and developed through Mk.I to Mk.II stages, both 1/4 scale and 1/6 scale models being used, the results of which compared well. The wind averaged drag factor of the final Mk.II cab baseline configuration was 0.488 (1/4 scale), already showing an improvement over the best present day configuration. Use of additional devices further reduced this figure to 0.340 (1/4 scale). Fig. 48, shows the improvements achieved over the yaw range for the various configurations mentioned in (vi) and (viii).

(ii) As the model was yawed no large increases in the other components were found, thus the devices could be used without extreme loss of stability or handling characteristics.

(iii) As with the present day configurations these drag reductions can be seen to affect the m.p.g. figures for a vehicle. The Fast Front II cab only configuration would return 10.8 m.p.g. at 55 m.p.h. whereas the final configuration could return 11.9 m.p.g. at 55 m.p.h. An increase in the average speed reduces these figures, though less than for the present day configurations; for the final configuration the figure

becomes 11.8 m.p.g. at 60 m.p.h., a reduction of less than 1%. Reflecting these figures on operating costs and profits shows that for the cab only a 5.5-6.2% increase in profits for a mileage of 500 miles weekly and 12.0-13.7% increase for 2,500 miles weekly. The corresponding figures for the final configuration are 8.0-9.1% for 500 miles and 17.6-20.1% for 2,500 miles. The effect of the higher average speed is again reduced for this configuration, falling below a 1% reduction of the increased profit.

10.4 Model Testing Techniques

(i) The results from both the scale tests from the two tunnels compare well, the differences occurring due to modelling dissimilarities and different tunnel turbulence levels.

(ii) The two tunnels as testing facilties compare well, using an identical model in both shows differences arising from both the differing turbulence levels and to a lesser extent to the boundary layer differences at the time of testing.

(iii) Reynolds number effects were found and require greater consideration in smaller scale testing as progress to more radiused shapes is made. Higher Reynolds numbers need to be aquired either by increasing the testing speed for smaller models or by use of larger scale models, as here, to fully represent the Reynolds effects.

10.5 Wakes and Spray

(i) Facilities including a wake total pressure rake were developed to attempt to investigate spray problems.Tests in wind tunnels were found to useful to

discover the general flow field but limited to studies of the wake region in dealing with spray.

(ii) Wake studies of pressure and flow visualization proved useful to assess the effects of improving the aerodynamics of the vehicle on spray. The improved flow down the sides of the vehicle for all Fast Front cab configurations would suppress the distribution of spray.

10.6 Overall Conclusions

(i) Overall an extremely low drag commercial vehicle shape was developed, using exsisting container dimensions and chassis type and layout. No great degradation in the other components affecting stability were found. The improved flow field would suppress spray although present methods to suppress the generation of spray would still need to be used.

(ii) The facilities exsist for all wind tunnel testing of road vehicles up to a maximum scale of 1/4 scale for commercial vehicles and 1/2 scale for passenger and other cars over a moving ground with excellent Reynolds number representation. Using these facilities a low drag future commercial vehicle design was developed which would also have a reduced spray problem due to its aerodynamic design.

Chapter 11. Future Work

The main area for improvement for future aerodynamic work on road vehicles is to better simulate full scale conditions in the wind tunnel. The moving ground with no boundary layer above it is the correct simulation of road motion to the model under test. As car aerodynamics dictates car designs with more rounded shapes the problems of separation become a major part of any aerodynamic investigation. In order to correctly assess these problems the scale test Reynolds number needs to be pushed closer to the full scale value. The two ways to achieve this are to increase model scale, as here in this research, or to increase the test speed of smaller scale tests.

It is felt that the maximum test scale has been reached with 1/4 scale models of commercial vehicles and 1/3 or 1/2 scale cars. These models can be tested at high Reynolds number in the large tunnel. However it is often easier to start with small scale models of basic shapes and for this reason it would be of great value to increase the test speed in the smaller tunnel. This would involve improved belt and boundary layer suction. The two tunnels could then be used to full effect as both have their respective merits for aerodynamic design. The smaller scale tunnel is simpler to use and a series of tests can be carried out quickly and with confidence, allowing fundamental basic shapes to be assessed. The larger scale tunnel then allows a more finalised model with much greater detail to the true vehicle to be tested at realistic Reynolds numbers. Surface detail is important when looking at the flow for separations and boundary layer transition. These studies would then give confidence towards final full scale testing of a developed design.

Other improvements would concern tunnel equipment such as improved flow visualization equipment and techniques, and automatic wake surveying. These facilities would give much more power to the aerodynamist in any investigation. Computation facilities would need strengthening to support these developments and this is currently in hand. Thus almost instant surface Cp plots or contours could be produced greatly helping the understanding of flow mechanisms at work during a test. The computer is also particularly useful for quick access to previously recorded data to plot or compare with new data.

Although futher testing of models using smoke or a laser technique ⊛ to investigate the spray problem of commercial vehicles it is clear that full representation of real conditions is required. This calls for a programme of full scale testing in correct climatic conditions in order to fully understand the influence of aerodynamics on the distribution of spray into the flow field.

A full investigation of Reynolds number effects would be a very useful program of work, to assess the effects of rounding, sloping these radii to the flow, and the surfaces for and aft of these radii. This information could then lead to the development of a computer code to model frontal flows and accurately predict separations and laminar or turbulent surface flow. This would be a powerful tool in the initial design of vehicles with regard to frontal aerodynamics.

⊛ is needed

References

1. ADEY P.C. 'The aerodynamic characteristics of commercial vehicles using two wind tunnel models over a moving ground.' M.Phil Thesis, Department of Aeronautics and Astronautics, University of Southampton. 1986.

2. GUTTERIDGE L. 'Tunnel to tunnel correlation with 1/12 and 1/6 scale truck models.' Leyland Vehicles, Preston, England. 1984.

3. COOPER K.R. 'A wind tunnel investigation into the fuel savings available from the aerodynamic drag reduction of trucks.' Natl. Res. Counc. (Canada), Dept. Mech. Eng., Natl. Aero. Est., Quaterly Bulletin, 1976/3.

4. COOPER K.R. 'The effect of front edge rounding and rear edge shaping on the aerodynamic drag of bluff vehicles in ground proximity.' S.A.E. Paper No. 850288. 1985

5. DROLLINGER R.A. 'Heavy duty truck aerodynamics.' S.A.E. Special Publication No. SP-688, 1987.

6. GEORGE A.R. 'Aerodynamics of simple bluff bodies including effects of body shape, ground proximity and pitch.' Aerodynamics of Transportation. ASME Niagra Falls 1979.

7. HURST D.W. 'Some aspects of the aerodynamics of bluff bodies in proximity of the ground.' Ph.D Thesis, Department of Aeronautics and Astronautics, University of Southampton. 1982.

8. BURGIN K., ADEY P.C. & BEATHAM J.P. 'Wind tunnel tests on road vehicles using a moving belt simulation of ground effect.' Proc. 6th Colloquium on Industrial Aerodynamics (Aachen) 1985.

9. NEWELL P.G. 'An experimental investigation into the aerodynamics of a racing sports car, involving the design, construction and calibration of a three component strain gauge dynamometer.' B.Sc. Hons. Project, Dept. of Aero and Astro, University of Southampton. 1983.

10. COOPER K.R., MASON W.T.Jr. & BETTES W.H. 'Correlation experience with the S.A.E. wind tunnel test procedure for trucks and buses.' S.A.E. Paper No. 820375, 1982.

11.COOPER K.R., GERHARDT H.J., WHITBREAD R., GARRY K.P. & CARR G.W. 'A comparison of aerodynamic drag measurements on model trucks in closed jet and open jet wind tunnels.' Proc. 6th Colloquium on Industrial Aerodynamics (Aachen). 1985.

12.S.A.E. Wind Tunnel Test Procedure for Trucks and Buses. S.A.E. Publication No. J1252. 1979.

13.GARRY K.P. 'A summary of the scale model wind tunnel measurements and pressure tests on Leyland T45 and DAF3300 vehicles used for the TRRL spray dispersal programme.' College of Aeronautics, Cranfield. Report No. 8707. 1987.

14.FACKRELL J.E. & HARVEY J.K. ' The flow field and pressure distribution of an isolated road wheel.' Advances in Road Vehicle Aerodynamics, B.H.R.A. Fluid Engineering, Paper No. 10. 1973.

15.STAPLEFORD & CARR G.W. 'Aerodynamic Characteristics of exposed rotating wheels.' M.I.R.A. Report No. 1970/2. 1970

16.GILHAUS A. 'Aerodynamics of heavy commercial vehicles.' Notes for Short Course in Vehicle Aerodynamics, von Karman Institute for Fluid Mechanics, Belgium. 1986.

17.CARR G.W. ' The aerodynamics of basic shapes for road vehicles, part 1 (simple rectangular bodies).' M.I.R.A. Report No. 1968/2, 1968.

18.STOLLERY J. & GARRY K.P. 'Techniques for reducing commercial vehicle drag.' Int. J. of Vehicle Design, Special Publication SP3, 1983.

19.ALLEN J.W. ' Aerodynamic drag and pressure measurements on a simplified tractor-trailer model.' Proc. 4th Colloquium on Industrial Aerodynamics (Aachen). 1980.

20.COWPERTHWAITE N.A. ' An investigation of the effect of rear body pitch on the aerodynamic characteristics of a simplified tractor-trailer model.' Proc. 6th Colloquium on Industrial Aerodynamics (Aachen). 1985.

21.GILHAUS A. 'The influence of cab shape on air drag of trucks.' Proc. 4th Colloquium on Industrial Aerodynamics (Aachen). 1980.

22.PANKHURST R.C. & HOLDER D.W. 'Wind Tunnel Technique: an account of experimental methods in low- and high-speed wind tunnels.' Pittman Press, London. 1952. (x-55-434557-8).

23.GILHAUS A. 'Aerodynamics of a design study for a modern long haul truck.' Int. J. of Vehicle Design, Special Publication SP3, 1983.

24.MAYCOCK G. 'The problem of water thrown up by vehicles on wet roads.' T.R.R.L., Ministry of Transport, TRRL Report No. 4. 1966.

25.CHATFIELD A.G., REYNOLDS A.K. & FOOT D.J. 'Water spray from heavy goods vehicles: an assessment of some vehicle modifications.' Vehicle Standards and Engineering Div., Ministry of Transport. Report No. VSE 513. 1979.

26.ALLEN J.W., BURGIN K. & LILLEY G.M. 'On water spray generation by road vehicles and methods for its control.' AASU Memo No. 77/2, Dept. of Aeronautics and Astronautics, University of Southampton. 1977. also contract report to TRRL, Ministry of Transport. 1977.

27.ALLEN J.W. & LILLEY G.M. 'The reduction of water spray from heavy road vehicles.' Int. J. of Vehicle Design, Special Publication No. SP3. 1983.

28.WEIR D.H. 'Truck splash and spray-some recent results.' S.A.E. Paper No. 800529. 1980.

29.Tables of Operating Costs, Commercial Motor in association with Mercedes Benz (UK) Ltd., Commercial Motor, Qaudrant House, Sutton, Surrey. 1987/88.

Bibliography

Idealised Trucks

BERTA C. & BONIS B. 'Experimental shape research of ideal aerodynamic characteristics for industrial vehicles.' S.A.E. Paper No. 801402. 1980.

CARR G.W. 'The aerodynamics of basic shapes for road vehicles (part 3 streamlined bodies.' M.I.R.A. Report No. 1970/4, 1974

HOWELL J.P. 'Force and wake characteristics of simple bluff bodies in ground proximity.' Dept. of Engineering, University of Warwick.

KANGAS T. 'The use of small scale wind tunnel data in the design of cab over engine tractor trailer combinations.' S.A.E. Paper No. 790767, 1979.

KRAMER C., GERHARDT H.J. & HELLING J. 'Wind tunnel tests on bluff bodies regarding truck aerodynamics.' Fluid Mechanics Laboratory, F.H. Aachen.

MARKS C. & BUCKLEY F.T.Jnr. 'The effect of tractor trailer interaction on the drag and distribution of drag on tractor trailer trucks.' S.A.E. Paper No. 801403, 1980.

Trucks and Devices for Aerodynamic Drag Reduction

BUCKLEY F.T.Jnr. 'Comparisons of Effectiveness of commercially available devices for the reduction of aerodynamic drag on tractor trailers.' S.A.E. Paper No. 750704. 1975

CARR G.W. 'Reduction of aerodynamic drag of road vehicles by means of add-on devices.' M.I.R.A.

DUNCAN L.T. 'Aerodynamic evaluations of the 1980 F-series of medium trucks and the 1978 CL-9000 heavy truck.' S.A.E. Paper No. 801405, 1980.

GARRY K.P. 'A review of commercial vehicle aerodynamic drag reduction techniques.' Proc. Instn Mech. Engrs. Vol. 199 No. D3, 1985

GREGG W.W. 'GMC Aero Astro body panels.' S.A.E. Paper No. 831003, 1983.

GUTTERIDGE L. & STAPLEFORD W.R. 'Drag reduction techniques

applied to a range of truck configurations using 1/8 scale models.' Leyland Vehicles Ltd, Preston, England. (internal report).

HOLMES H.R. 'Practical economic aspects of tractor trailer aerodynamics.' S.A.E. Paper No. 760103, 1976.

LISSAMAN P.P.S. 'Development of devices to reduce the aerodynamic resistance of trucks.' S.A.E. Paper No. 750702, 1975.

MARKS C.H., BUCKLEY F.T.Jnr. & WALSTON W.H. 'An evaluation of the aerodynamic drag reductions produced by various cab roof fairings and a gap seal on tractor trailer trucks.' S.A.E. Paper No. 760105, 1976.

MASON W.T. 'Wind tunnel development of the dragfoiler- a system for reducing tractor trailer aerodynamic drag.' S.A.E. Paper No. 750705, 1975.

McDONALD A.T. & PALMER G.M. 'Aerodynamic drag reduction of intercity buses.' S.A.E. Paper No. 8014004, 1980.

MUIRHEAD V.U. & SALTZMAN E.J. 'Reduction of aerodynamic drag and fuel consumption for tractor trailer vehicles.' J. Energy Vol. 3 No. 5, 1979.

STEERS L.L., MONTOYA L.C. & SALTZMAN E.J. 'Aerodynamic drag reduction tests on a full scale tractor trailer combination and a representative box shaped ground vehicle.' S.A.E. Paper No. 750703, 1975.

STOLLERY J.L. & GARRY K.P. 'Keep on trucking- but please change the shape.' Aerogram Vol. 2 No. 2, College of Aeronautics, Cranfield. 1980.

WONG H.Y. & RAJAN A.A. 'Aerodynamic devices for reducing drag on tractor trailer vehicles.' Report No. 8002, Dept. of Aero and Fluid Mech., University of Glasgow, 1980.

General Road Vehicle Aerodynamics

AHMED S.R., RAMM G. & FALTIN G. 'Some salient features of the time averaged ground vehicle wake.' S.A.E. Paper No. 840300, 1984.

BEARMAN P.W. 'Some observations on road vehicle wakes.' S.A.E. Paper No. 840301, 1984.

BEARMAN P.W., DAVIS J.P. & HARVEY J.K. 'Measurements of the structure of road vehicle wakes.' Int. J. of Vehicle Design, Special Publication SP3, 1983

COGOTTI A. 'Wake surveys of different car body shapes with coloured isopressure maps.' S.A.E. Paper No. 840229, 1984.

DAVIES P.O.A.L. 'The new 7 by 5.5 ft. and 15 by 12 ft. low speed wind tunnel at the University of Southampton.' AASU Report No. 202, Dept. of Aero. and Astro., University of Southampton. 1961.

FANGER-VEXLER S., KATZ J. & FOUX A. 'Full scale, on the road study of the effect of automobile shape on its aerodynamic charateristics and comparison with small scale wind tunnel results.' S.A.E. Paper No. 850287, 1985.

HURST D.W., ALLEN J.W. & BURGIN K. 'Pressure measurements on a full scale tractor trailer combination and comparison with data from wind tunnel tests.' Int. J. of Vehicle Design, Special Publication SP3, 1983.

INGRAM K.C. 'The wind averaged drag coefficient applied to heavy goods vehicles.' TRRL Supplementary Report No. 392, 1978.

Collections/Books

Int. J. of Vehicle Design, Special Publication SP3, 1983.

Journal of Wind Engineering and Industrial Aerodynamics. Vol 22. 1986

Aerodynamics: Recent Developments. S.A.E. Special Publication No. SP-656, 1986.

Automotive Aerodynamics: An Update. S.A.E. Special Publication No. SP-706, 1987

Lecture Notes to Accompany 'Vehicle Aerodynamics' Lecture Series. V.K.I. Inst. of Fluid Mech., Brussels, Belgium. 1986.

APPENDIX 1

Wind Averaged Drag Factor

A vehicle driving along a road experiences, in still wind conditions, a force equivalent to a stream of air hitting the stationary vehicle square on. This is the ideal case and in reality a crosswind exsists which acts on the vehicle at a certain angle. Taking the resultant of the vehicle velocity and the crosswind velocity gives the single velocity of the effective stream of air. In order to give a feel for the general effect of crosswinds the wind averaged drag factor was developed, see ref. 12, which with the aid of some assumptions gives a figure which can be used to compare the crosswind performance of different vehicles. The main assumption used is that the crosswind is equally likely to act at any angle, which would seem justified given that roads lie in all directions and the variation of winds throughout the year. It is also assumed that the wind speed is the national average; 7 m.p.h. The wind averaged drag factor is then the average of a weighting multiplied by the drag coefficient for the particular yaw angle;

$$Cd(Vt) = \frac{1}{6} \cdot \sum_{1}^{6} M(j).Cd(j)$$

where Cd(Vt) = the wind averaged drag factor at vehicle speed Vt
M(j) = the weighting given by the formula below
Cd(j) = the drag coefficient at yaw angle

$$M(j) = 1 + \left(\frac{Vw}{Vt}\right)^2 + 2.\ \frac{Vw}{Vt}\ .\cos\varnothing(j)$$

$$\varnothing(j) = (j.30) - 15$$

$$Cd(j) = Cd(\psi(j))$$

$$\psi(j) = \tan^{-1}\left(\frac{(Vw/Vt).\sin\varnothing(j)}{1+(Vw/Vt).\cos\varnothing(j)}\right)$$

where Vw = wind speed relative to the ground
Vt = vehicle speed
$\varnothing$ = wind angle relative to the vehicle
ψ = resultant yaw angle of vehicle

These equations then allow tables to be drawn up of M(j) and (j) for a particular vehicle speed from which the wind averaged drag factor can be calculated. The speed chosen for this report to allow comparisons with similar data from America is 55 m.p.h. The figures for this are therefore;

j	M(j)	(j)
1	1.262	1.6
2	1.196	4.7
3	1.082	6.8
4	0.950	7.2
5	0.836	5.6
6	0.770	2.2

Similar figures were also caculated for 60 m.p.h. which is more representative of this country and were used in the fuel economy workings in Ch.8.

j	M(j)	(j)
1	1.239	1.6
2	1.179	4.4
3	1.074	6.2
4	0.953	6.6
5	0.849	5.1
6	0.788	1.9

Obviously these figures give a lower value as the effect of the crosswind on the vehicle is reduced by the higher velocity of the vehicle, ie. the resultant yaw angles are smaller. Thus this factor is velocity dependant but comparisons of figures for a single speed are valid and a useful way of assessing crosswind performance.

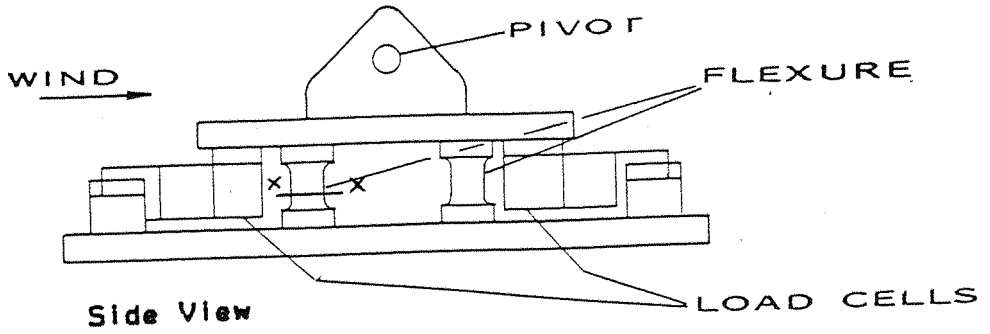

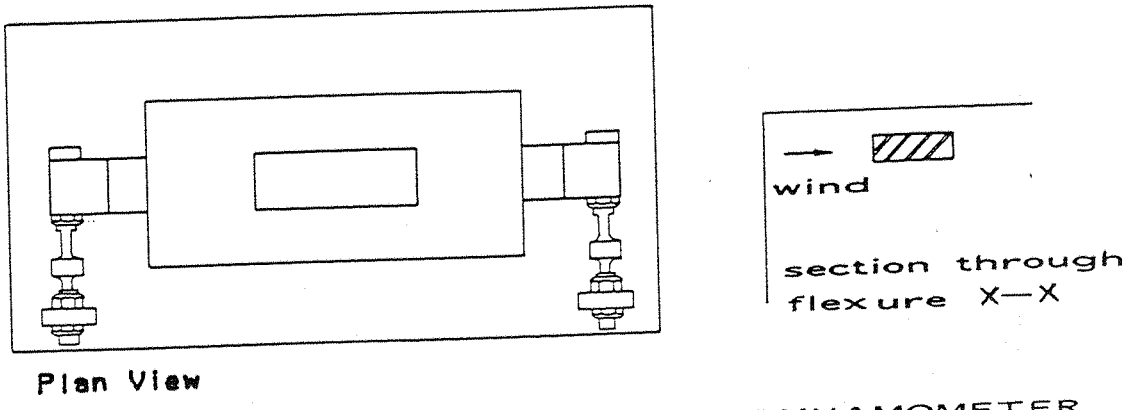

a) SIDE FORCE AND YAWING MOMENT DYNAMOMETER

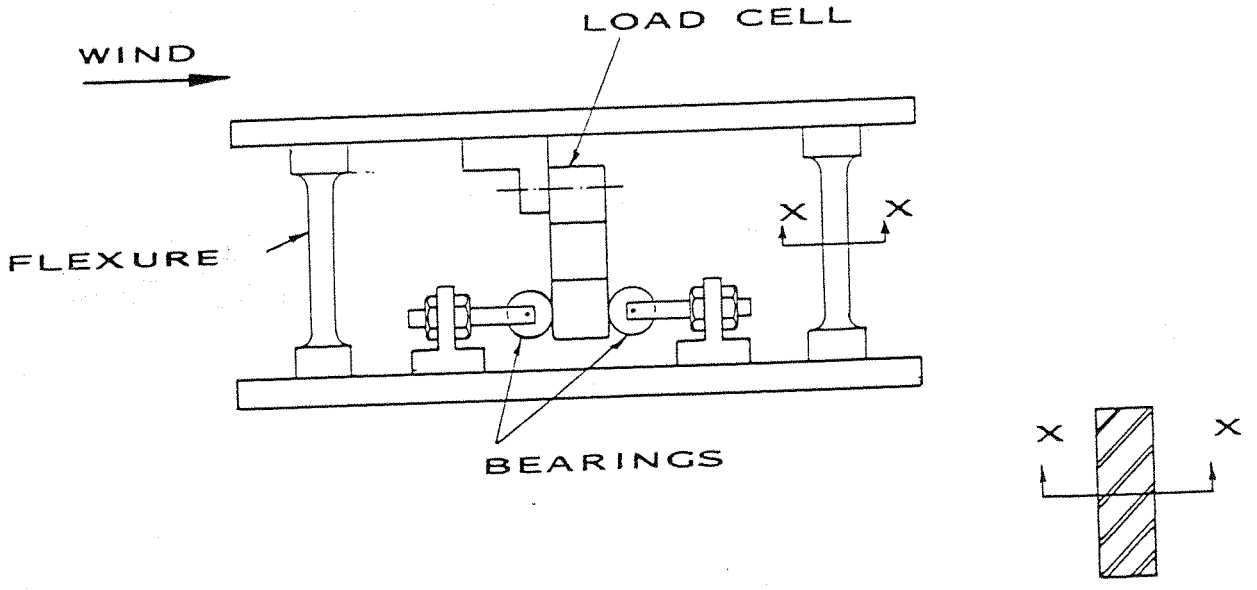

b) DRAG DYNAMOMETER: SIDE ELEVATION

Fig.1 Internal Load Cell Dynamometers

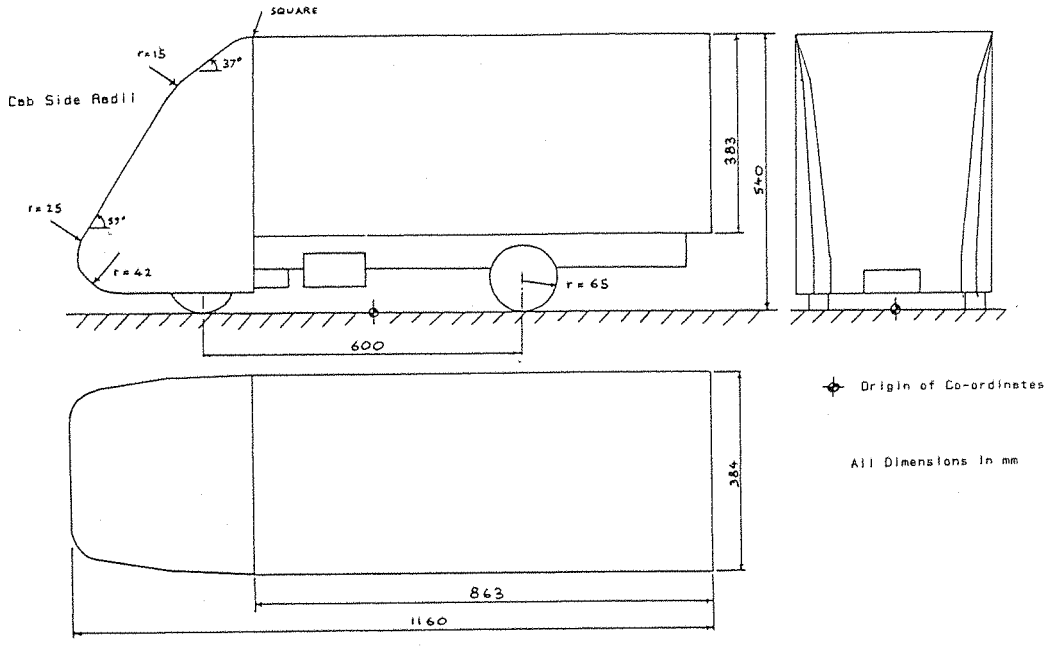

Fig.2 Fast Front Mk.I with Major 1/6 Scale Dimensions

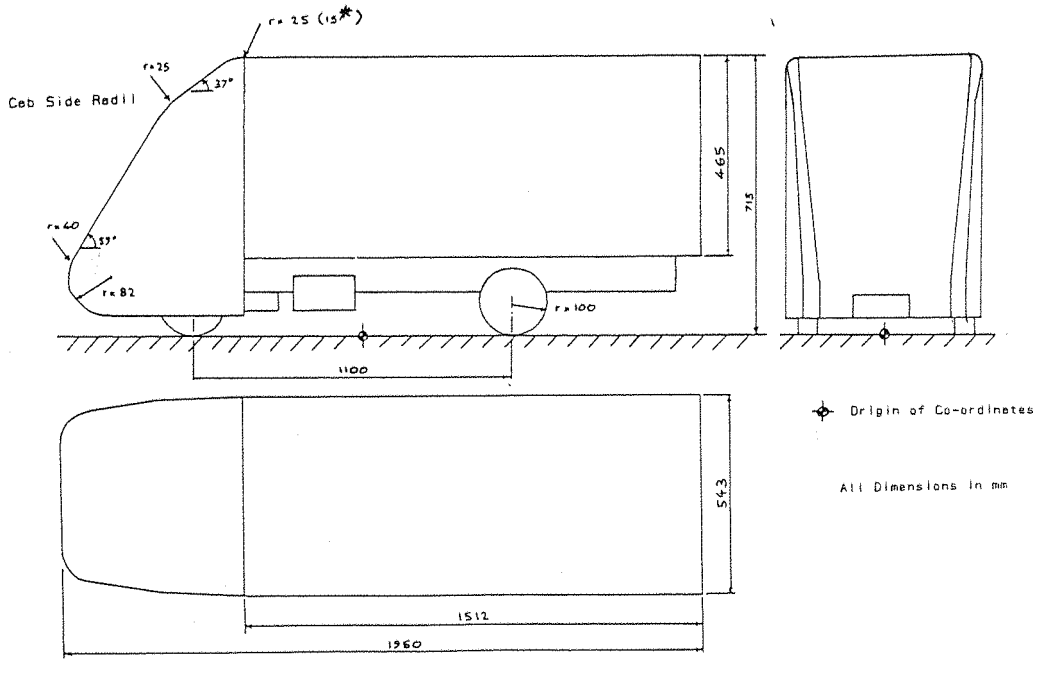

Fig.3 Fast Front Mk.II with Major 1/4 Scale Dimensions

* 1/6 Scale Minimum Cab-Container Radius

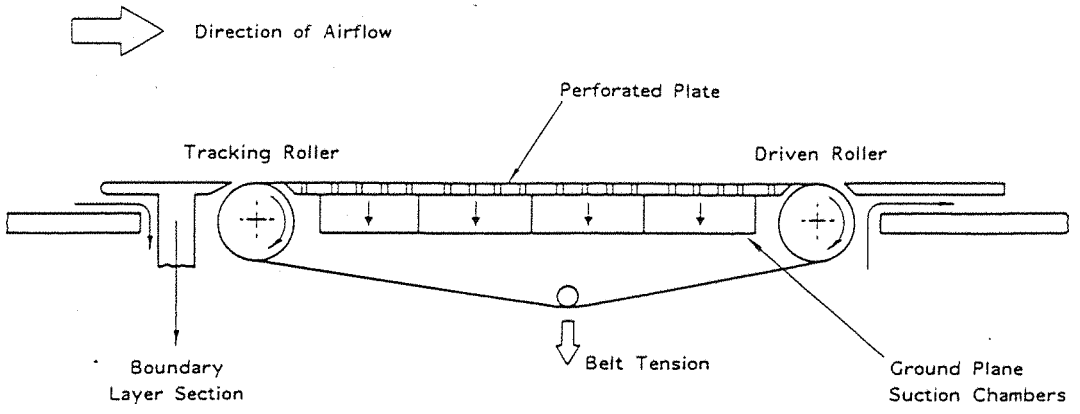

2.1m x 1.7m Wind Tunnel, Moving Ground Length = 2m and Width = 1.1m
3.5m x 2.6m Wind Tunnel, Moving Ground Length = 5.3m and Width = 2.4m

Fig.4 SCHEMATIC LAYOUT OF MOVING GROUND PLANE, SOUTHAMPTON UNIVERSITY

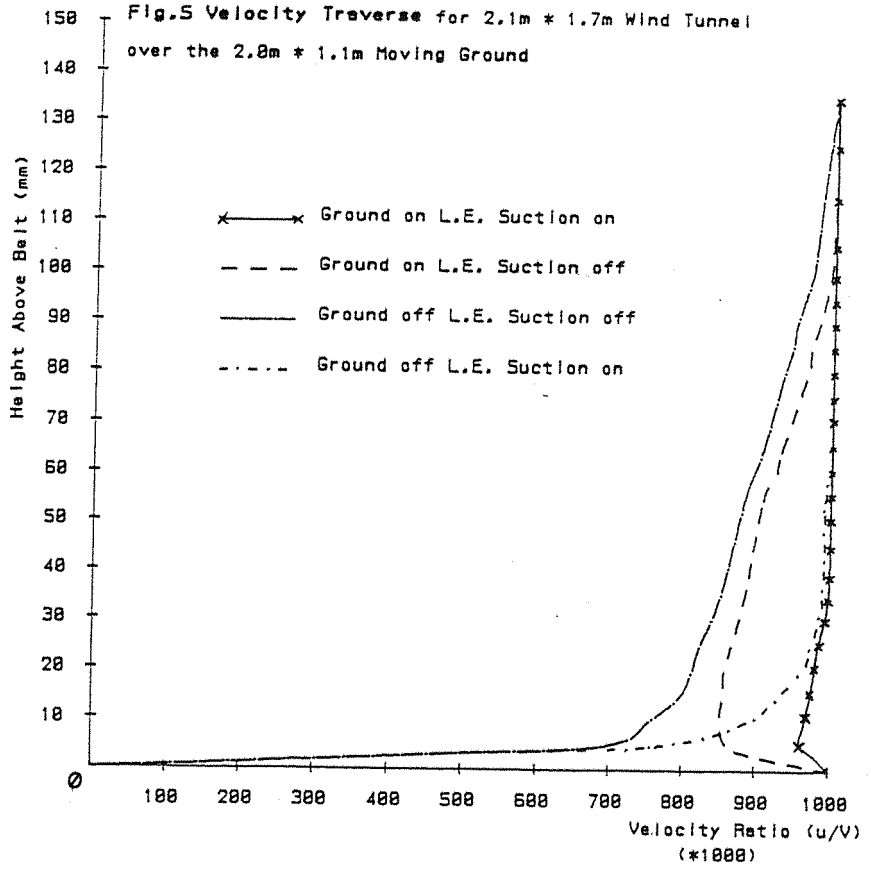

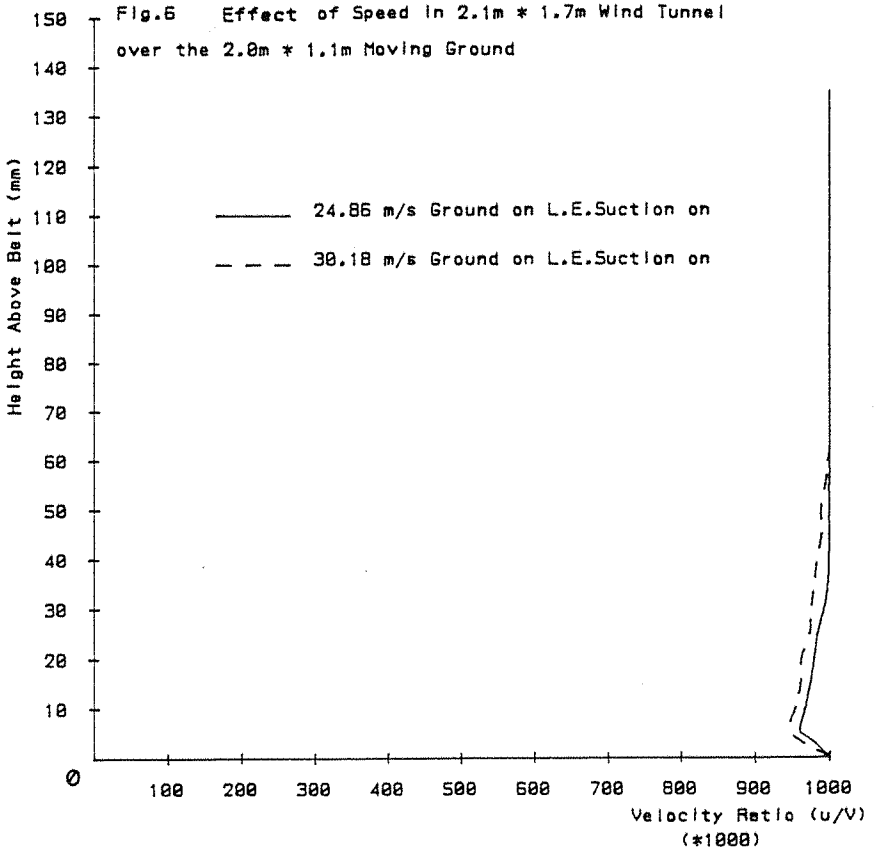
Fig.6 Effect of Speed in 2.1m * 1.7m Wind Tunnel
over the 2.0m * 1.1m Moving Ground
24.86 m/s Ground on L.E.Suction on
30.18 m/s Ground on L.E.Suction on
Height Above Belt (mm)
150
140
130
120
110
100
90
80
70
60
50
40
30
20
10
0
100
200
300
400
500
600
700
800
900
1000
Velocity Ratio (u/V)
(*1000)

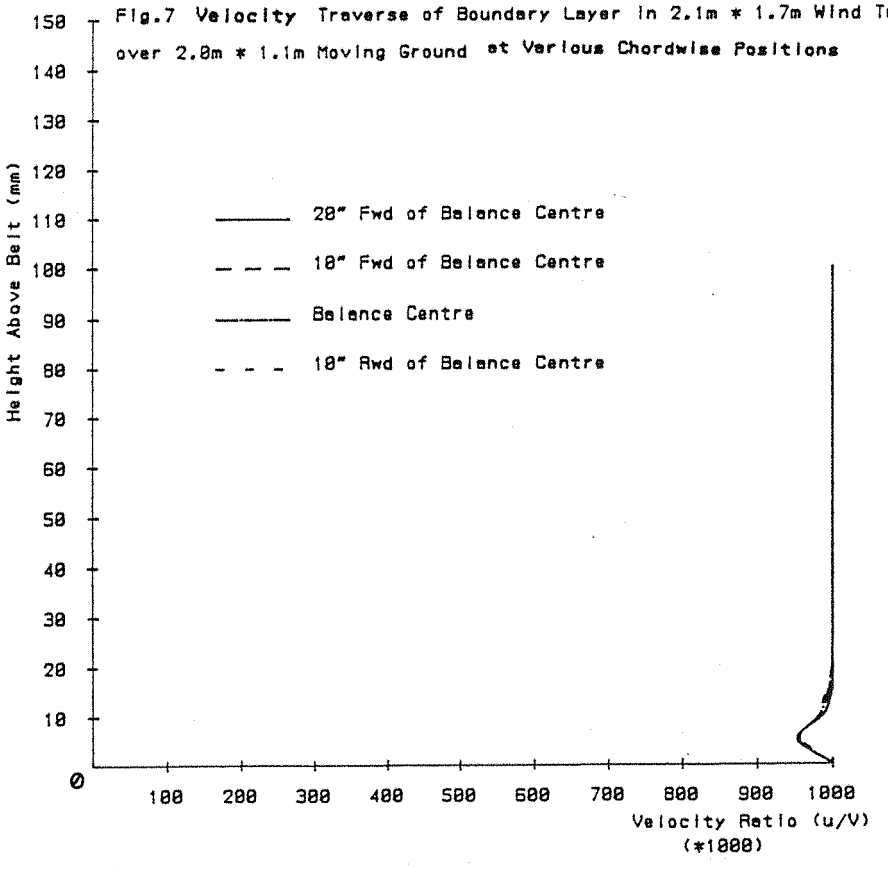
Fig.7 Velocity Traverse of Boundary Layer in 2.1m * 1.7m Wind Tunnel
over 2.0m * 1.1m Moving Ground at Various Chordwise Positions
20" Fwd of Balance Centre
10" Fwd of Balance Centre
Balance Centre
10" Rwd of Balance Centre
Height Above Belt (mm)
150
140
130
120
110
100
90
80
70
60
50
40
30
20
10
0
100
200
300
400
500
600
700
800
900
1000
Velocity Ratio (u/V)
(*1000)

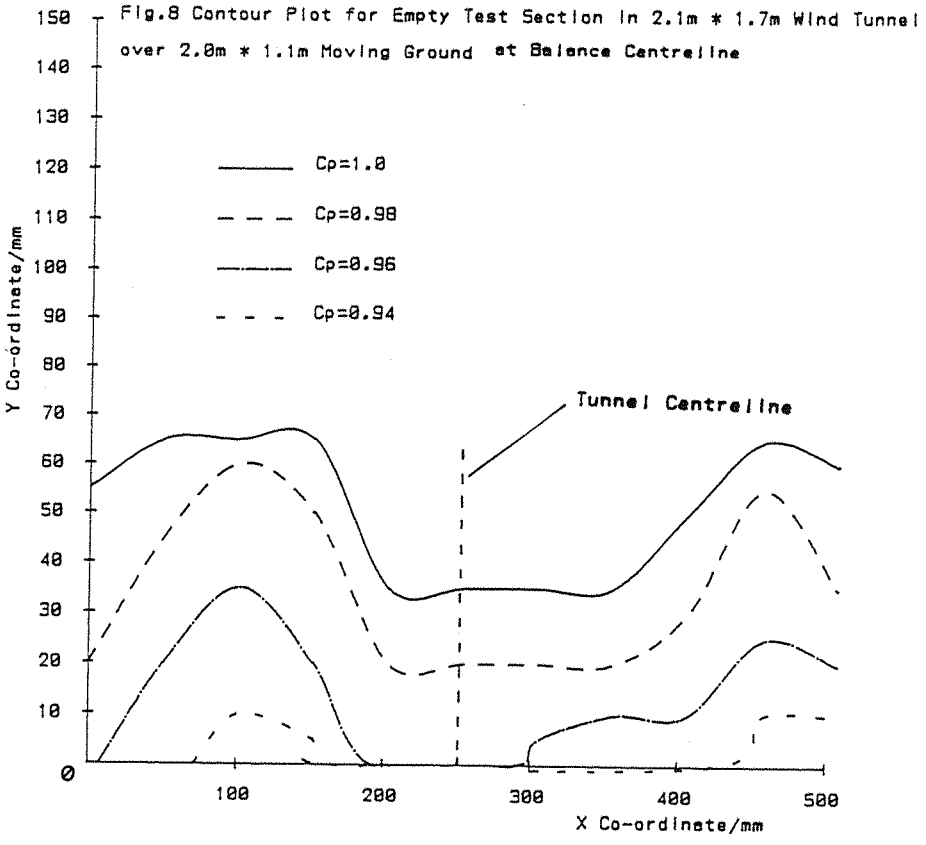
Fig.8 Contour Plot for Empty Test Section in 2.1m * 1.7m Wind Tunnel over 2.0m * 1.1m Moving Ground at Balance Centreline
Cp=1.0
Cp=0.98
Cp=0.96
Cp=0.94
Tunnel Centreline
Y Co-ordinate/mm
X Co-ordinate/mm
150
140
130
120
110
100
90
80
70
60
50
40
30
20
10
0
100
200
300
400
500

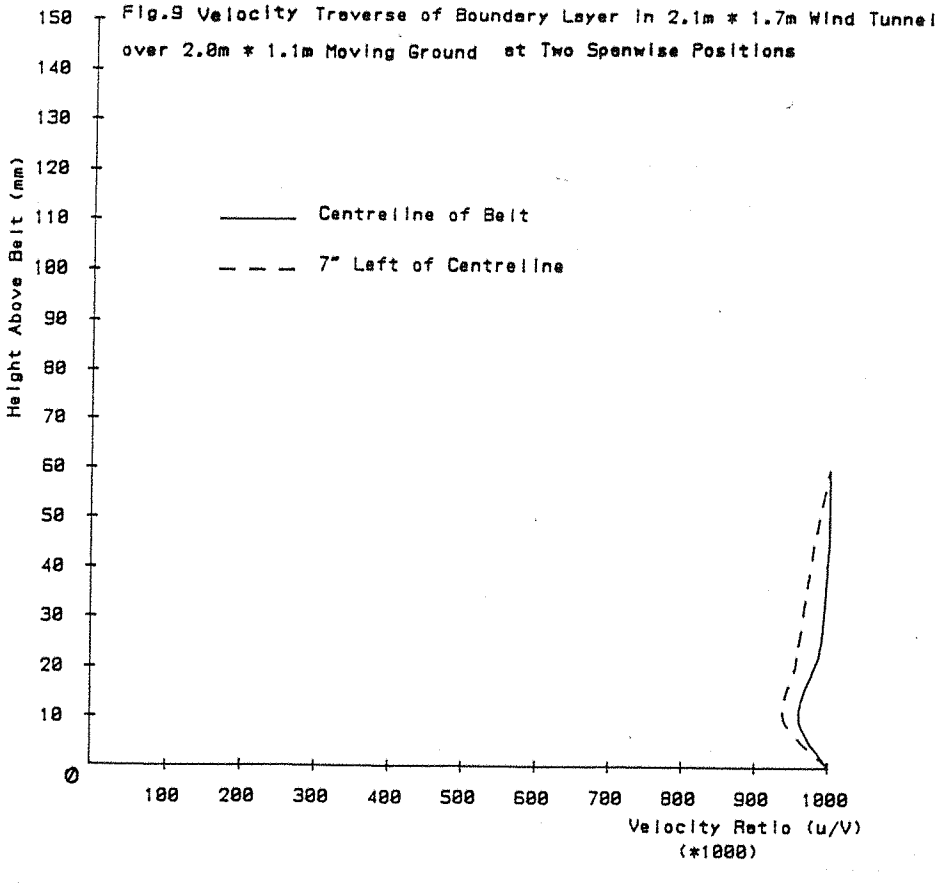
Fig.9 Velocity Traverse of Boundary Layer in 2.1m * 1.7m Wind Tunnel over 2.0m * 1.1m Moving Ground at Two Spanwise Positions
Centreline of Belt
7" Left of Centreline
Height Above Belt (mm)
Velocity Ratio (u/V) (*1000)
150
140
130
120
110
100
90
80
70
60
50
40
30
20
10
0
100
200
300
400
500
600
700
800
900
1000

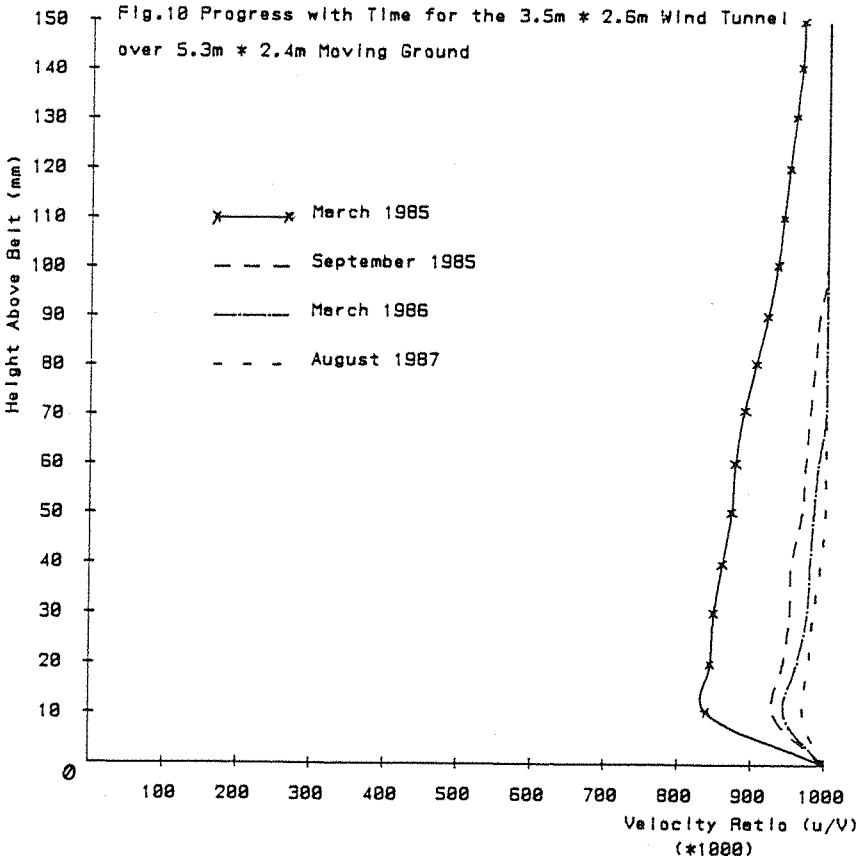
Fig.10 Progress with Time for the 3.5m * 2.6m Wind Tunnel
over 5.3m * 2.4m Moving Ground
March 1985
September 1985
March 1986
August 1987
Height Above Belt (mm)
150
140
130
120
110
100
90
80
70
60
50
40
30
20
10
0
100
200
300
400
500
600
700
800
900
1000
Velocity Ratio (u/V)
(*1000)

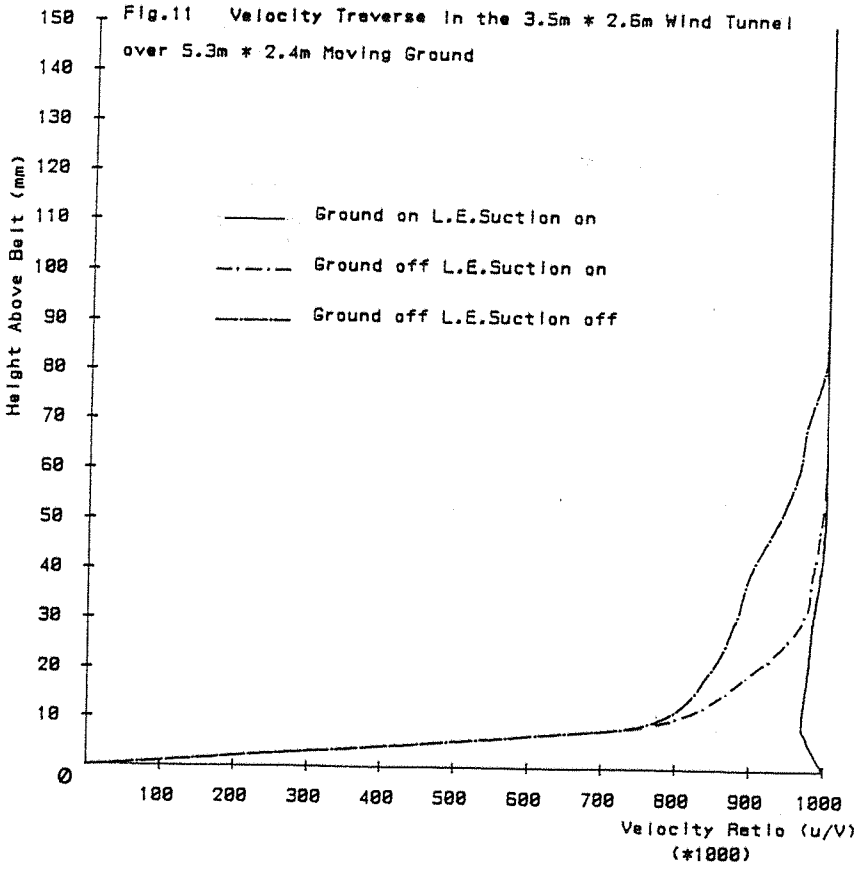
Fig.11 Velocity Traverse in the 3.5m * 2.6m Wind Tunnel
over 5.3m * 2.4m Moving Ground
Ground on L.E.Suction on
Ground off L.E.Suction on
Ground off L.E.Suction off
Height Above Belt (mm)
150
140
130
120
110
100
90
80
70
60
50
40
30
20
10
0
100
200
300
400
500
600
700
800
900
1000
Velocity Ratio (u/V)
(*1000)

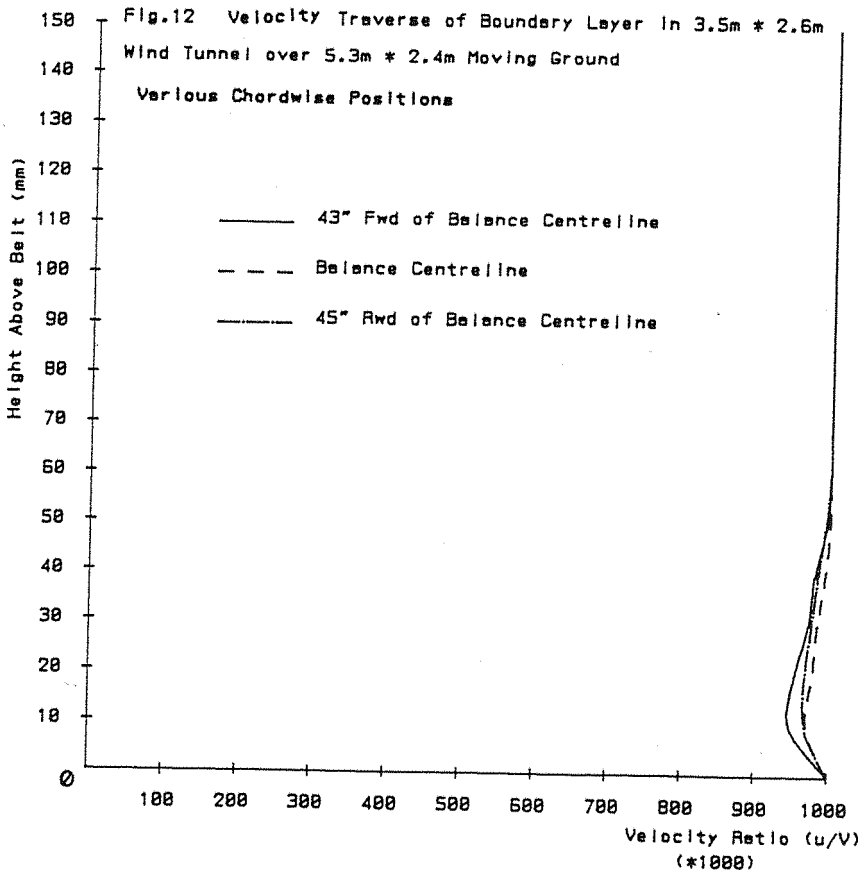
Fig.12 Velocity Traverse of Boundary Layer in 3.5m * 2.6m
Wind Tunnel over 5.3m * 2.4m Moving Ground
Various Chordwise Positions
43" Fwd of Balance Centreline
Balance Centreline
45" Rwd of Balance Centreline
Height Above Belt (mm)
150
140
130
120
110
100
90
80
70
60
50
40
30
20
10
0
100
200
300
400
500
600
700
800
900
1000
Velocity Ratio (u/V)
(*1000)

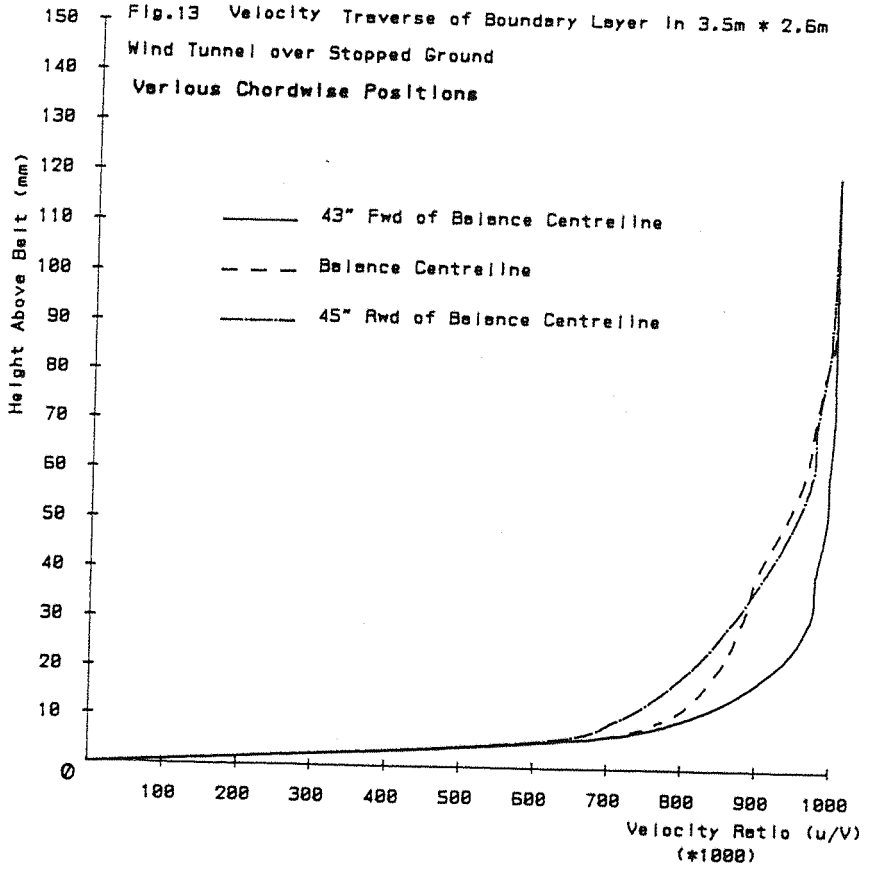
Fig.13 Velocity Traverse of Boundary Layer in 3.5m * 2.6m
Wind Tunnel over Stopped Ground
Various Chordwise Positions
43" Fwd of Balance Centreline
Balance Centreline
45" Rwd of Balance Centreline
Height Above Belt (mm)
150
140
130
120
110
100
90
80
70
60
50
40
30
20
10
0
100
200
300
400
500
600
700
800
900
1000
Velocity Ratio (u/V)
(*1000)

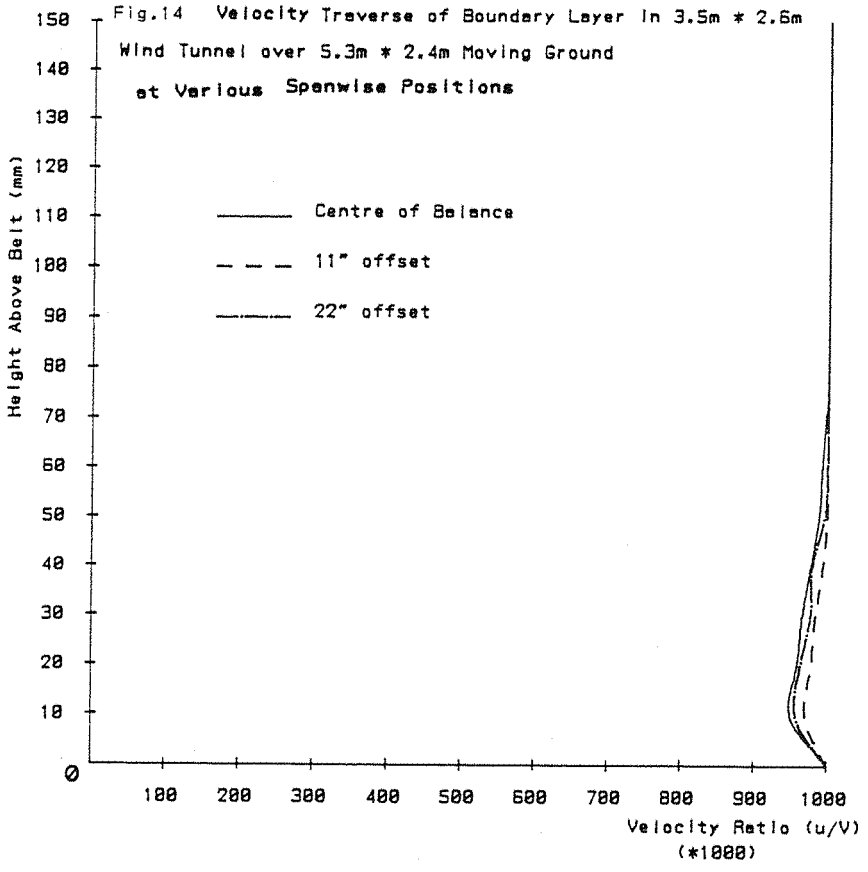
Fig.14 Velocity Traverse of Boundary Layer In 3.5m * 2.6m
Wind Tunnel over 5.3m * 2.4m Moving Ground
at Various Spanwise Positions
Centre of Balance
11" offset
22" offset
Height Above Belt (mm)
150
140
130
120
110
100
90
80
70
60
50
40
30
20
10
0
100
200
300
400
500
600
700
800
900
1000
Velocity Ratio (u/V)
(*1000)

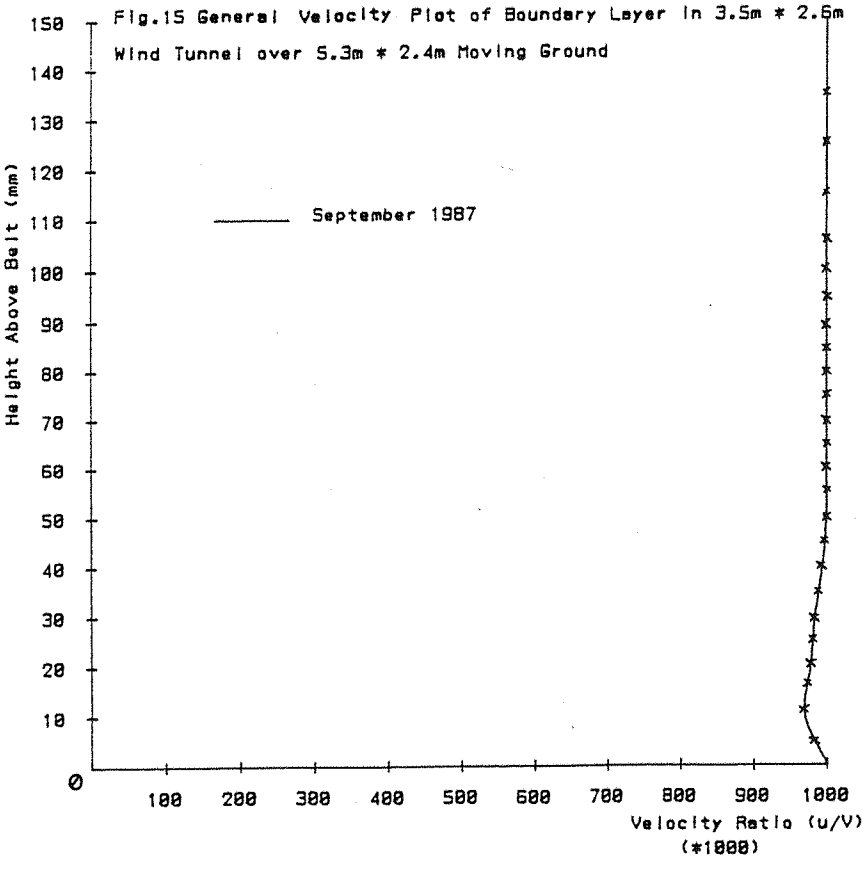
Fig.15 General Velocity Plot of Boundary Layer In 3.5m * 2.6m
Wind Tunnel over 5.3m * 2.4m Moving Ground
September 1987
Height Above Belt (mm)
150
140
130
120
110
100
90
80
70
60
50
40
30
20
10
0
100
200
300
400
500
600
700
800
900
1000
Velocity Ratio (u/V)
(*1000)

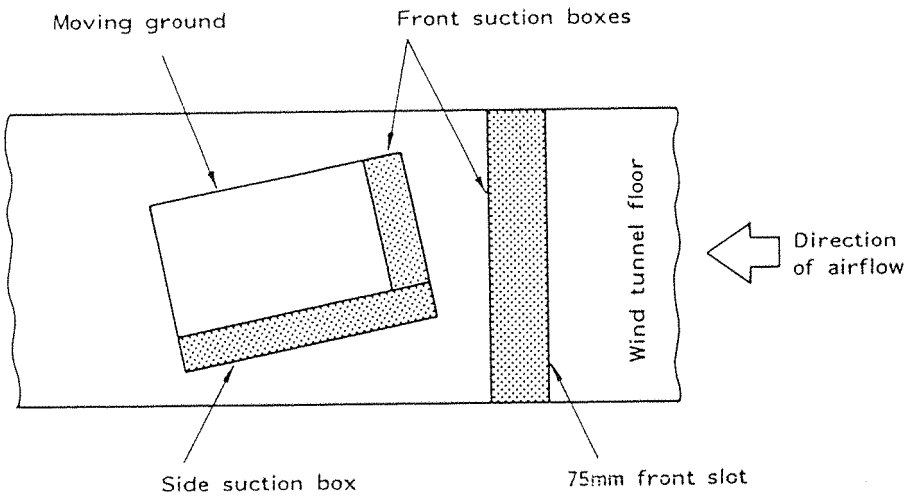

Fig.16 Schematic Plan View of Yawed 2.8m * 1.1m Moving Ground in the 3.5m * 2.6m Wind Tunnel

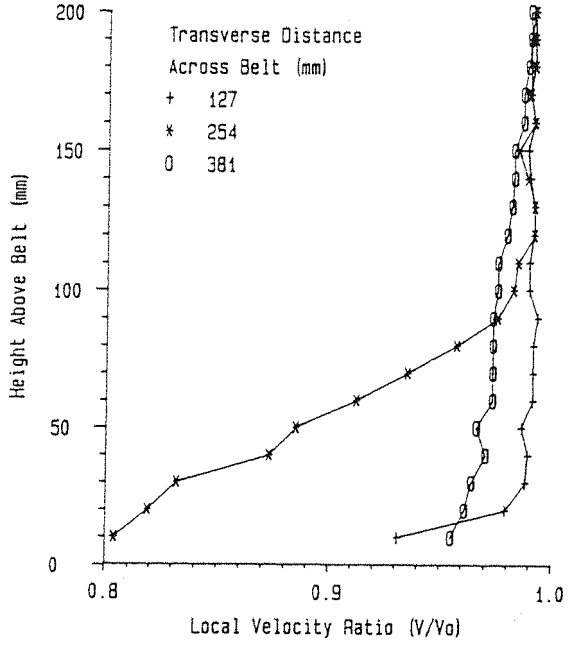

Fig.17 Boundary Layer Plot over Yawed 2.0m*1.1m Ground in 3.5m*2.6m Wind Tunnel (0 deg.Yaw)

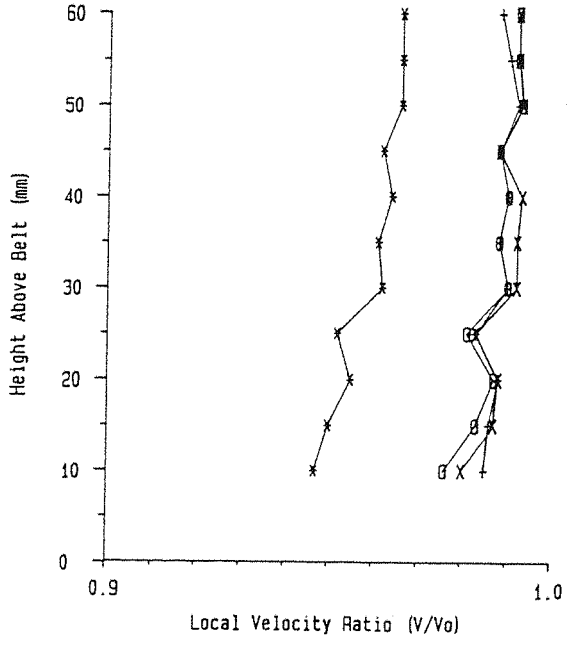

Fig.18 Boundary Layer Plot over Yawed 2.0m*1.1m Ground in 3.5m*2.6m Wind Tunnel (15 deg.Yaw)

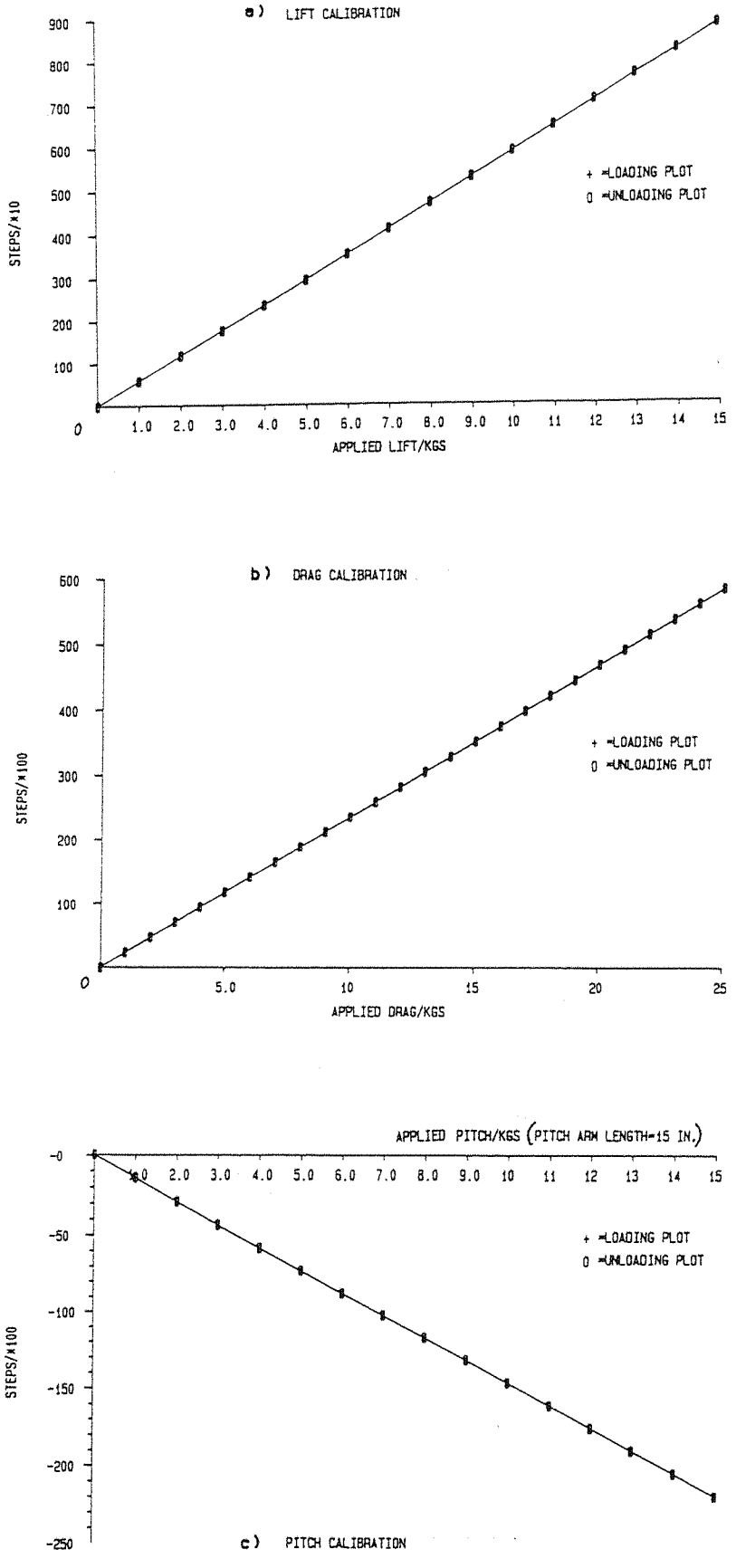

Fig.19 2.1m * 1.7m Tunnel Overhead Weighbeam Balance Calibrations

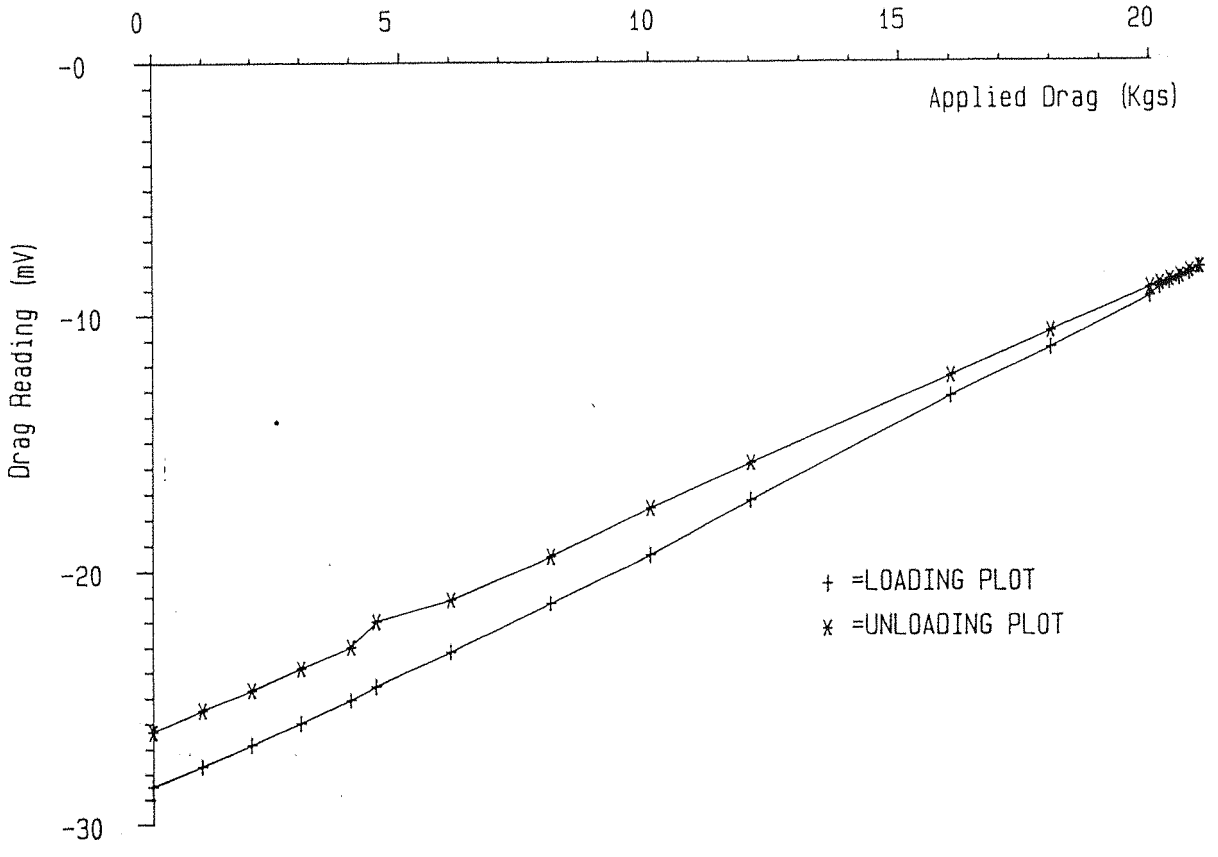

Fig.20 Typical 3.5m*2.6m Overhead Load Cell Balance Calibration

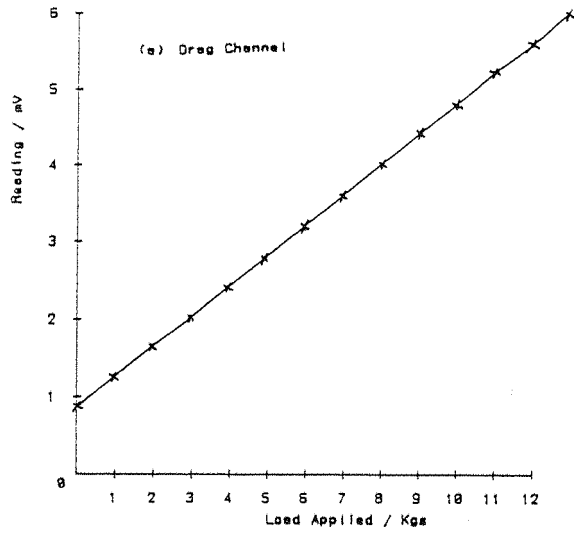

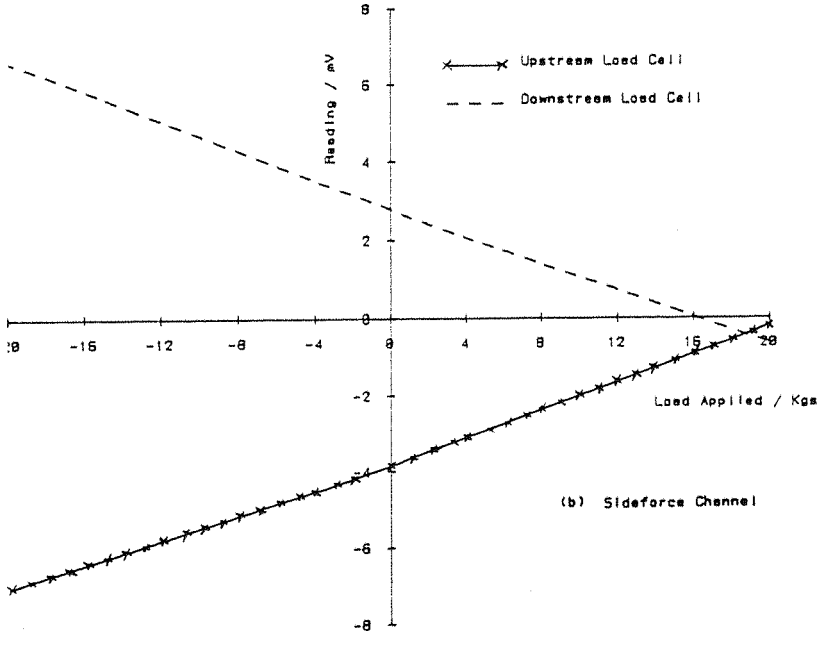

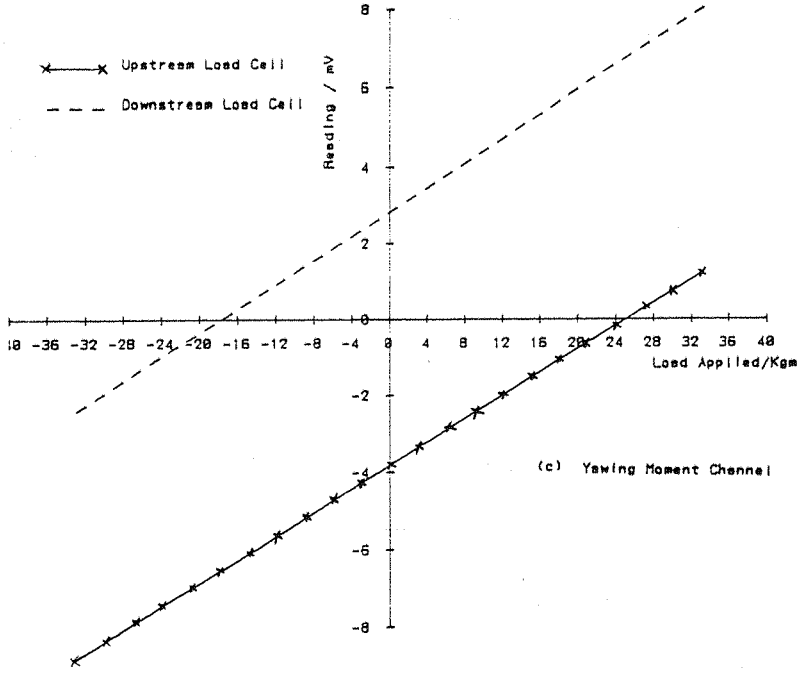

Fig.21 Load Cell Balance Calibrations

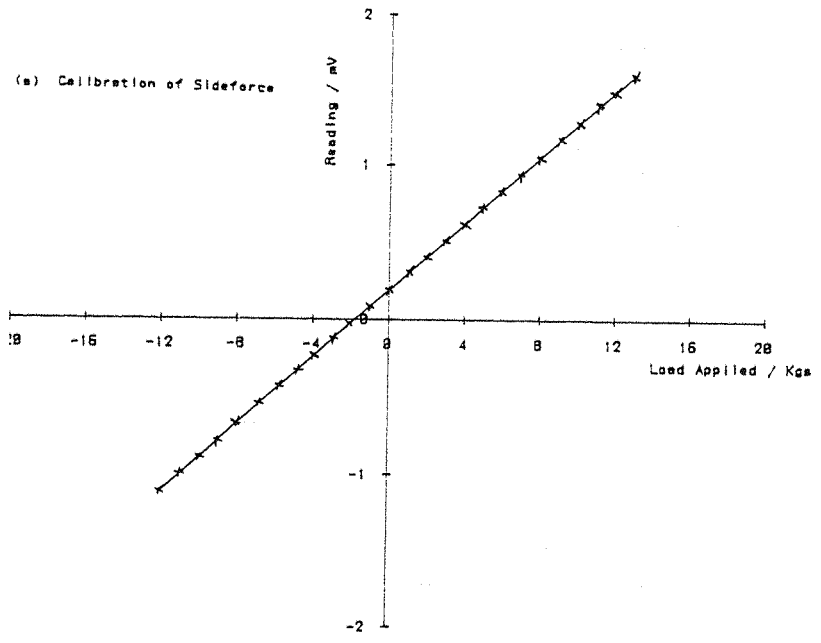

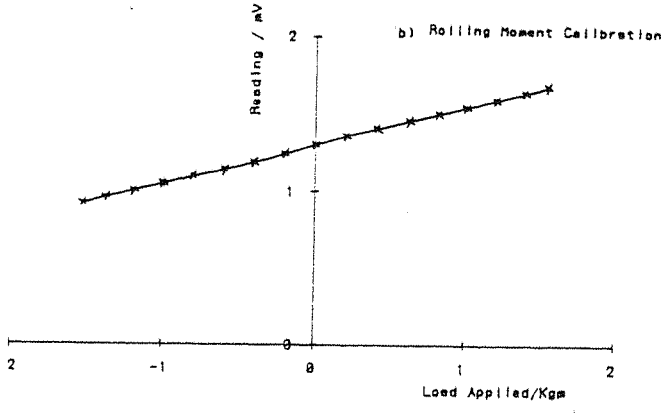

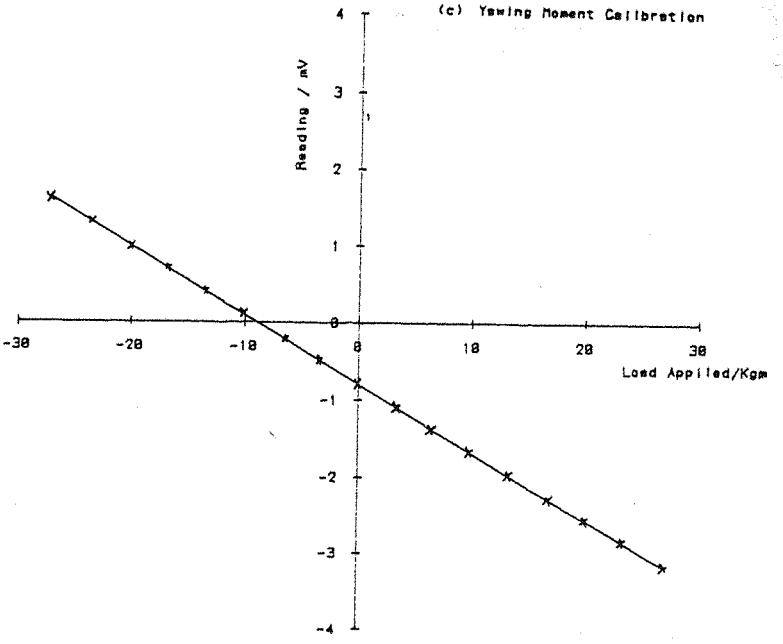

Fig.22 Strain Gauge Dynamometer Calibrations

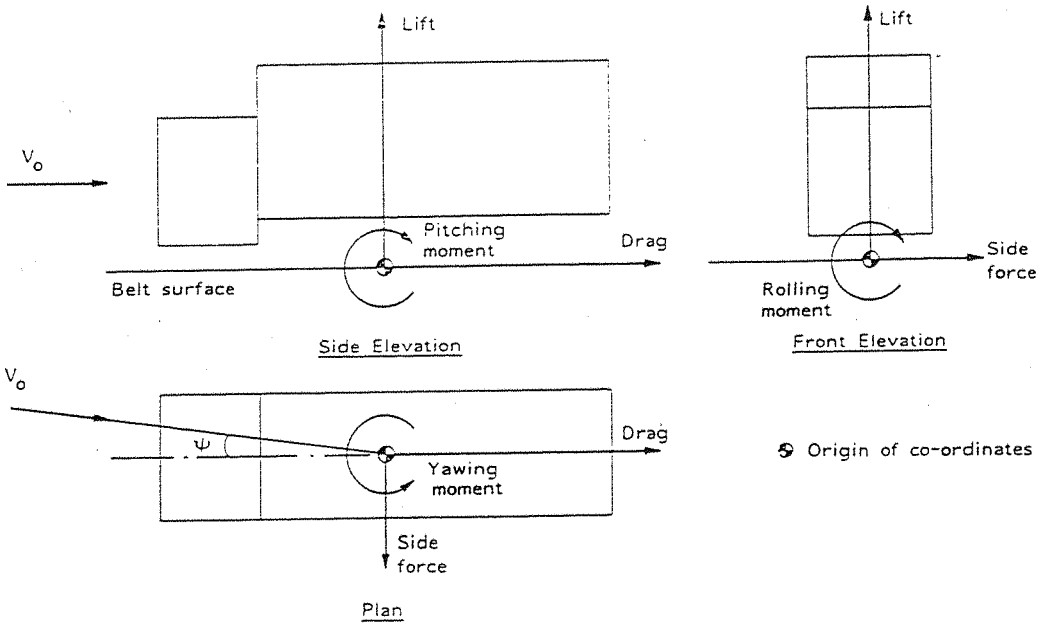

Fig.23 BODY AXIS CO-ORDINATE SYSTEM

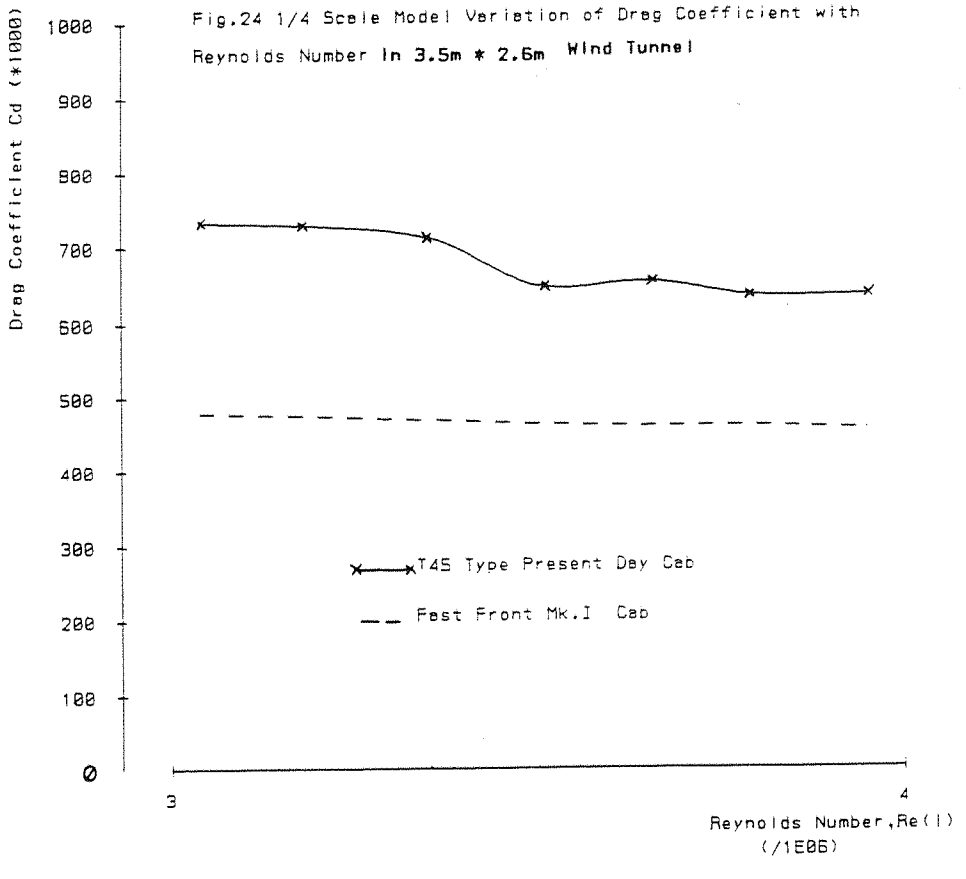

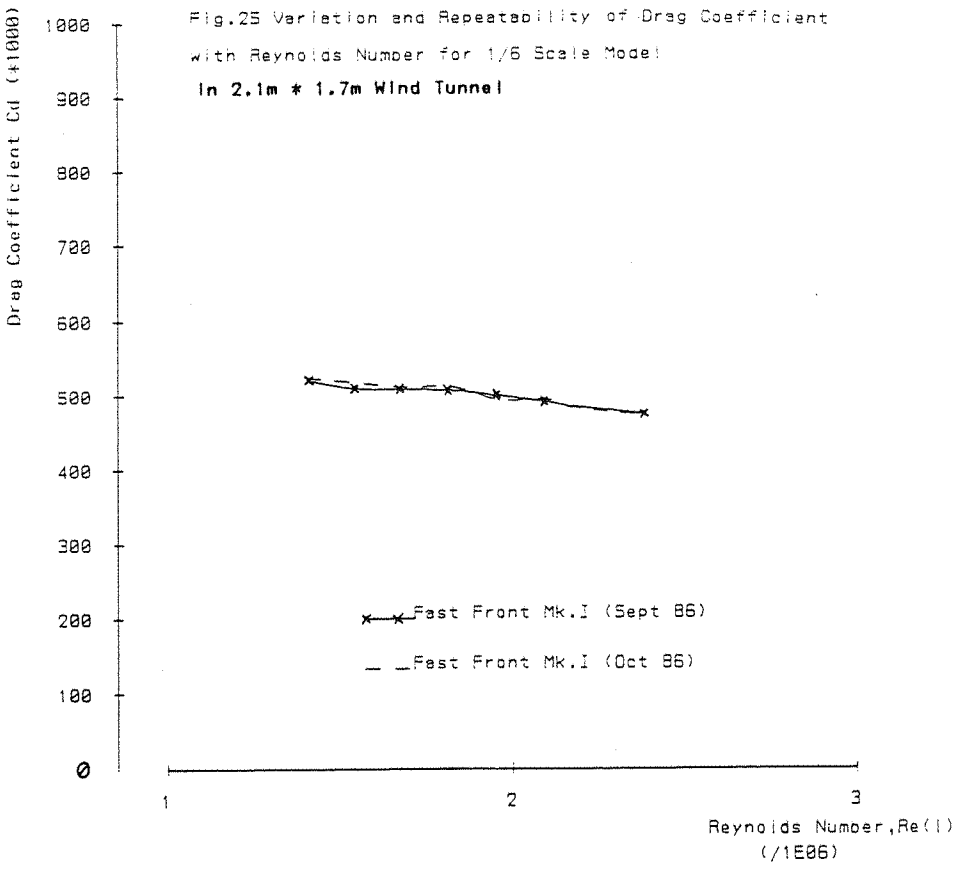

Fig.25 Variation and Repeatability of Drag Coefficient with Reynolds Number for 1/6 Scale Model In 2.1m * 1.7m Wind Tunnel

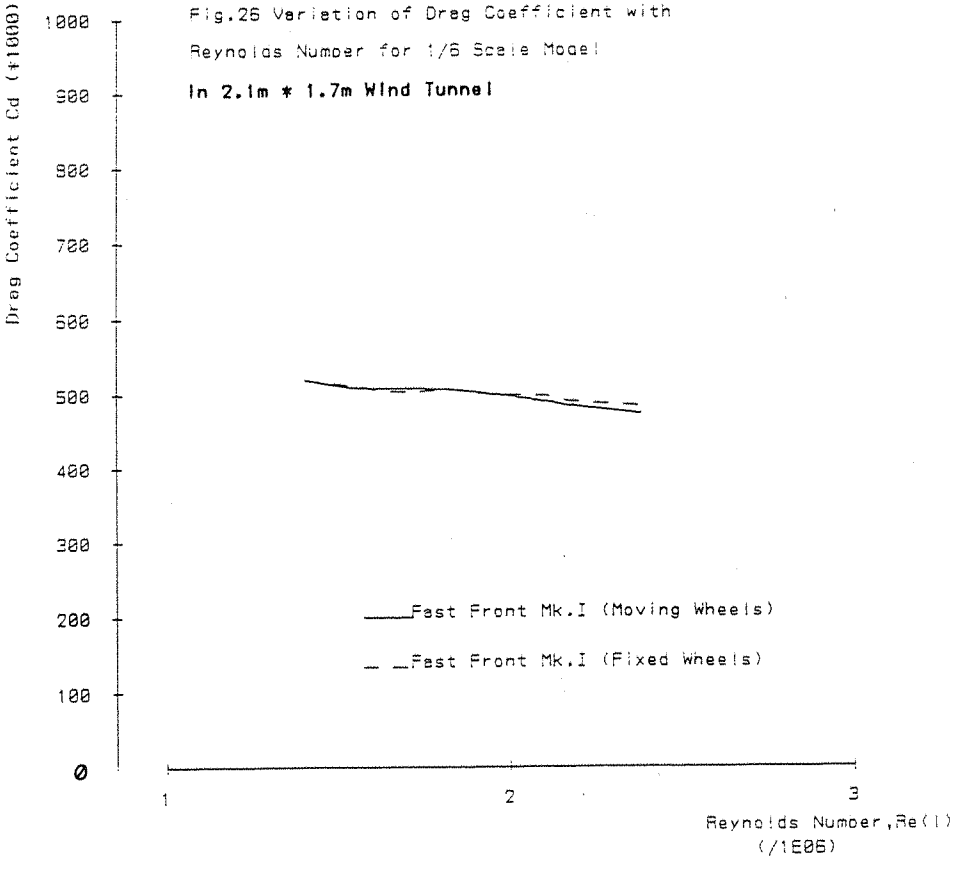

Fig.26 Variation of Drag Coefficient with Reynolds Number for 1/6 Scale Model In 2.1m * 1.7m Wind Tunnel

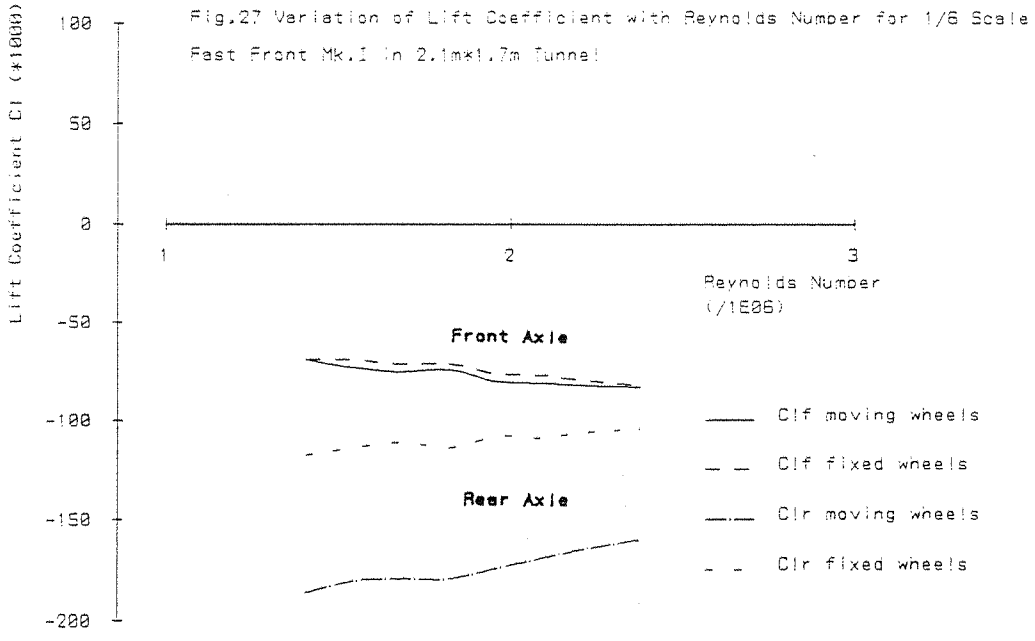
Fig.27 Variation of Lift Coefficient with Reynolds Number for 1/6 Scale Fast Front Mk.I in 2.1mx1.7m Tunnel
Lift Coefficient Cl (*1000)
100
50
0
-50
-100
-150
-200
1
2
3
Reynolds Number (/1E06)
Front Axle
Rear Axle
Clf moving wheels
Clf fixed wheels
Clr moving wheels
Clr fixed wheels

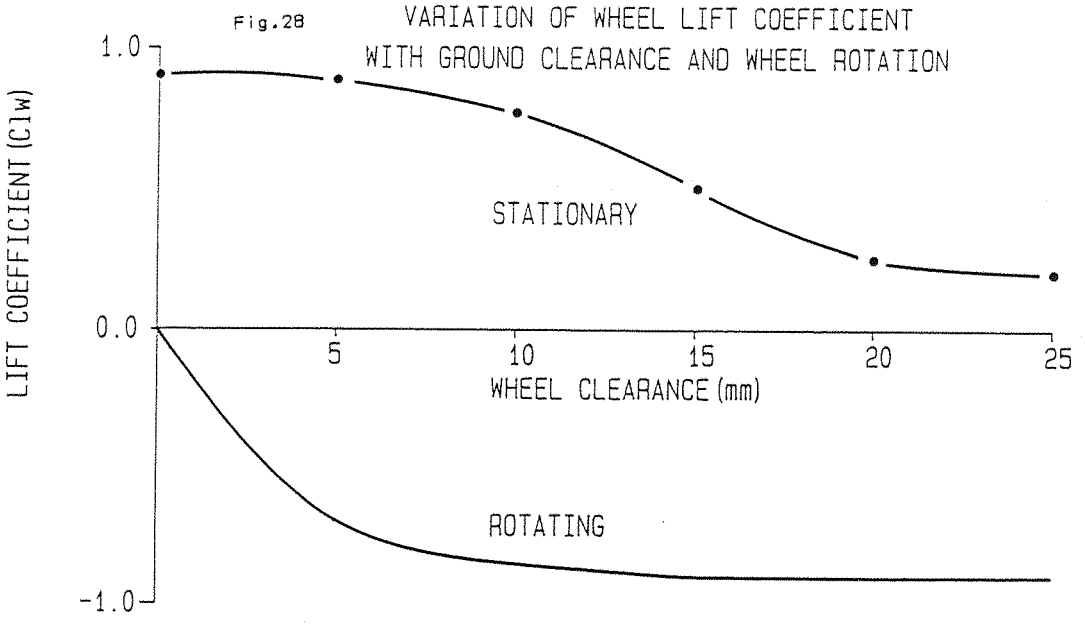
Fig.28
VARIATION OF WHEEL LIFT COEFFICIENT
WITH GROUND CLEARANCE AND WHEEL ROTATION
LIFT COEFFICIENT (Clw)
1.0
0.0
-1.0
STATIONARY
ROTATING
5
10
15
20
25
WHEEL CLEARANCE (mm)

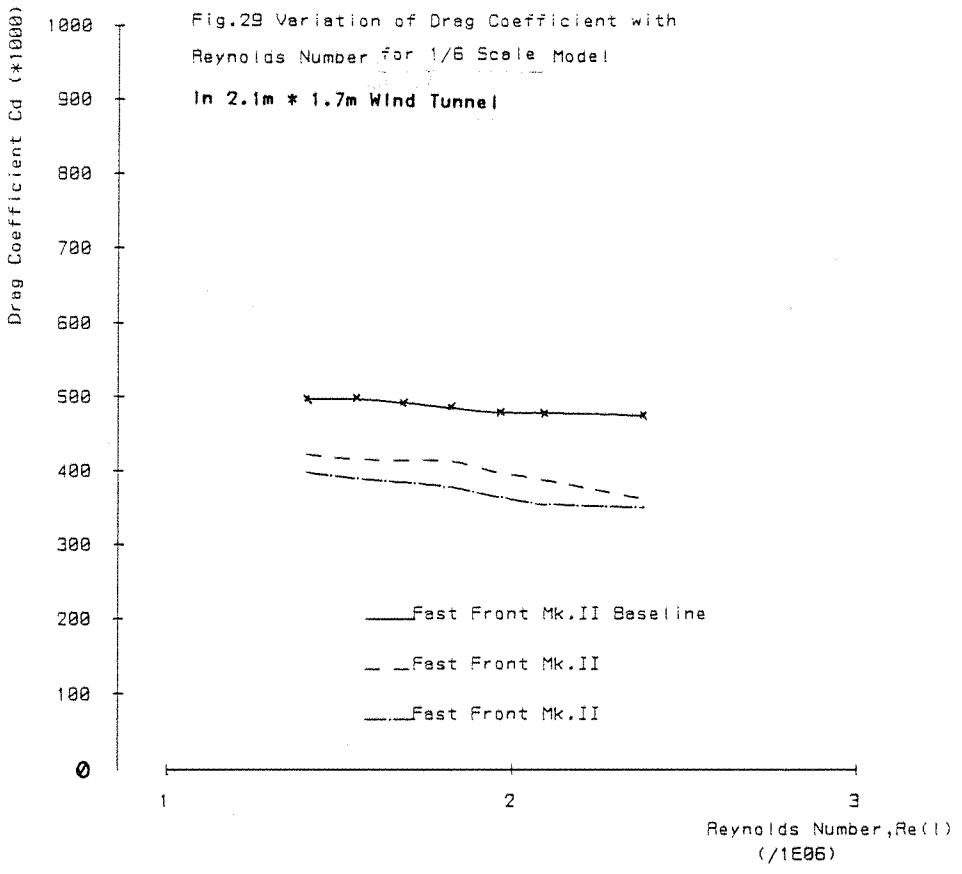

Fig.29 Variation of Drag Coefficient with Reynolds Number for 1/6 Scale Model in 2.1m * 1.7m Wind Tunnel

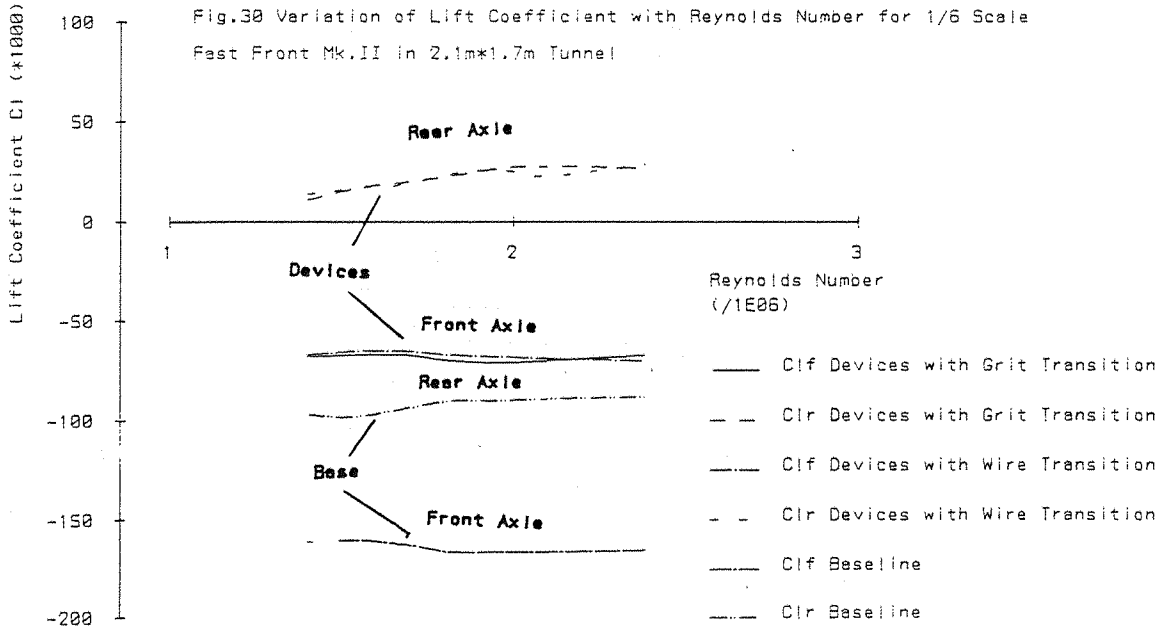

Fig.30 Variation of Lift Coefficient with Reynolds Number for 1/6 Scale Fast Front Mk.II in 2.1m*1.7m Tunnel

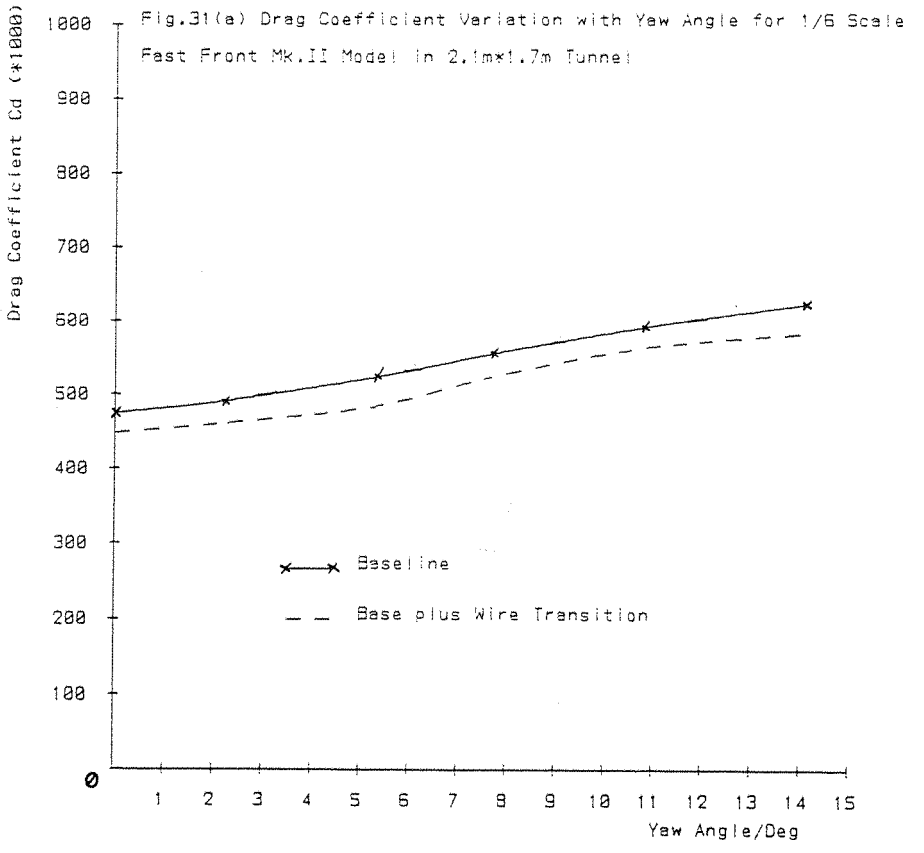
Fig.31(a) Drag Coefficient Variation with Yaw Angle for 1/6 Scale
Fast Front Mk.II Model in 2.1m*1.7m Tunnel
Drag Coefficient Cd (*1000)
1000
900
800
700
600
500
400
300
200
100
0
1 2 3 4 5 6 7 8 9 10 11 12 13 14 15
Yaw Angle/Deg
Baseline
Base plus Wire Transition

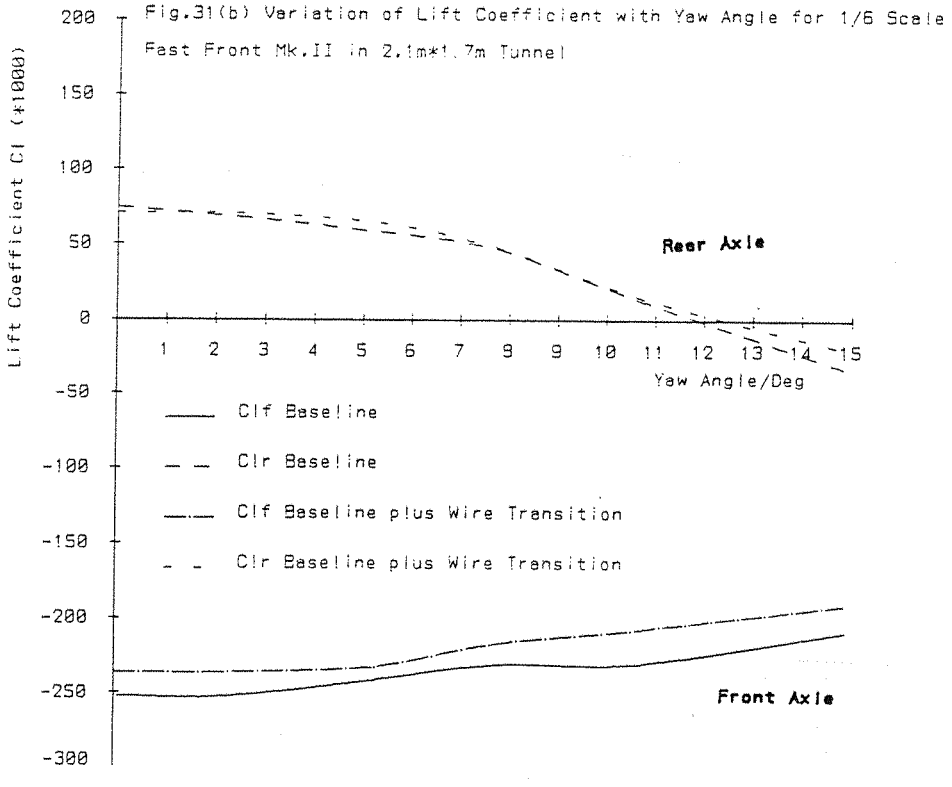
Fig.31(b) Variation of Lift Coefficient with Yaw Angle for 1/6 Scale
Fast Front Mk.II in 2.1m*1.7m Tunnel
Lift Coefficient Cl (*1000)
200
150
100
50
0
-50
-100
-150
-200
-250
-300
1 2 3 4 5 6 7 8 9 10 11 12 13 14 15
Yaw Angle/Deg
Rear Axle
Front Axle
Clf Baseline
Clr Baseline
Clf Baseline plus Wire Transition
Clr Baseline plus Wire Transition

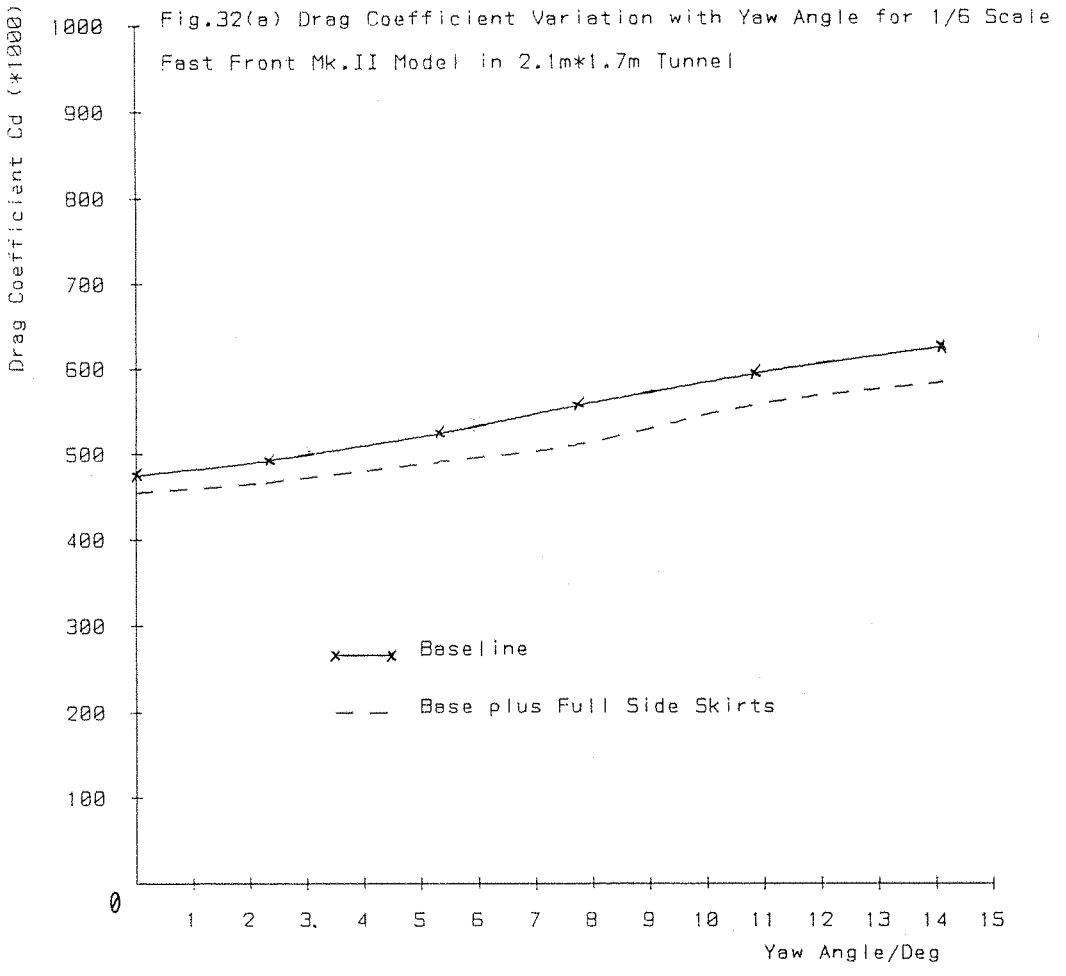
Fig.32(a) Drag Coefficient Variation with Yaw Angle for 1/6 Scale
Fast Front Mk.II Model in 2.1m*1.7m Tunnel
Drag Coefficient Cd (*1000)
1000
900
800
700
600
500
400
300
200
100
0
1 2 3 4 5 6 7 8 9 10 11 12 13 14 15
Yaw Angle/Deg
Baseline
Base plus Full Side Skirts

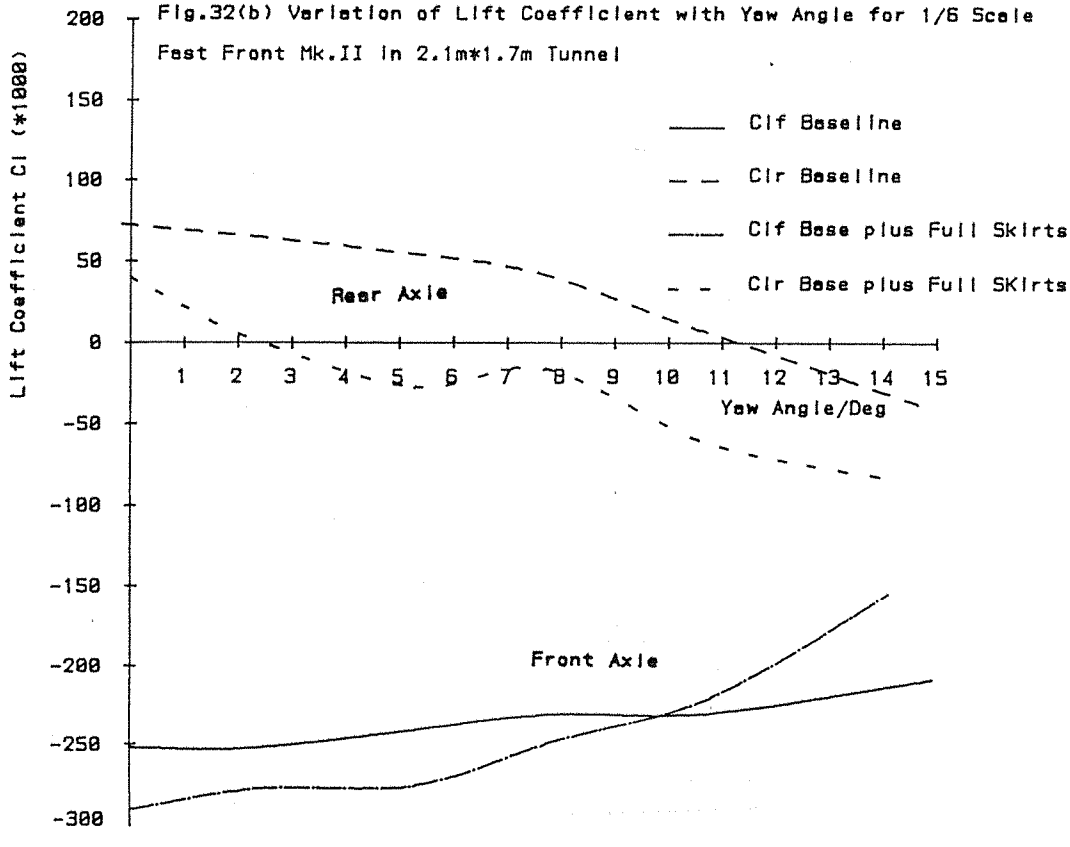
Fig.32(b) Variation of Lift Coefficient with Yaw Angle for 1/6 Scale
Fast Front Mk.II in 2.1m*1.7m Tunnel
Lift Coefficient Cl (*1000)
200
150
100
50
0
-50
-100
-150
-200
-250
-300
1 2 3 4 5 6 7 8 9 10 11 12 13 14 15
Yaw Angle/Deg
Clf Baseline
Clr Baseline
Clf Base plus Full Skirts
Clr Base plus Full SKirts
Rear Axle
Front Axle

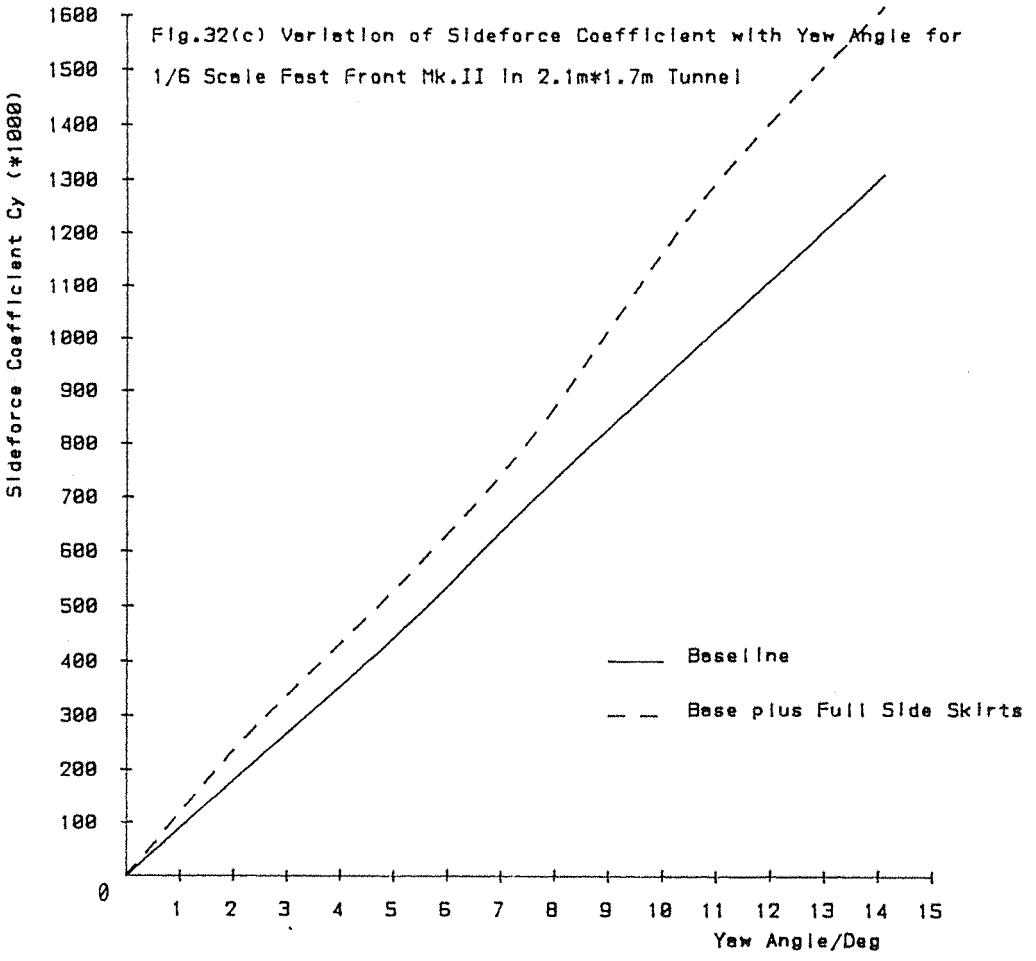
Fig.32(c) Variation of Sideforce Coefficient with Yaw Angle for 1/6 Scale Fast Front Mk.II in 2.1m*1.7m Tunnel
Sideforce Coefficient Cy (*1000)
1600
1500
1400
1300
1200
1100
1000
900
800
700
600
500
400
300
200
100
0
1 2 3 4 5 6 7 8 9 10 11 12 13 14 15
Yaw Angle/Deg
Baseline
Base plus Full Side Skirts

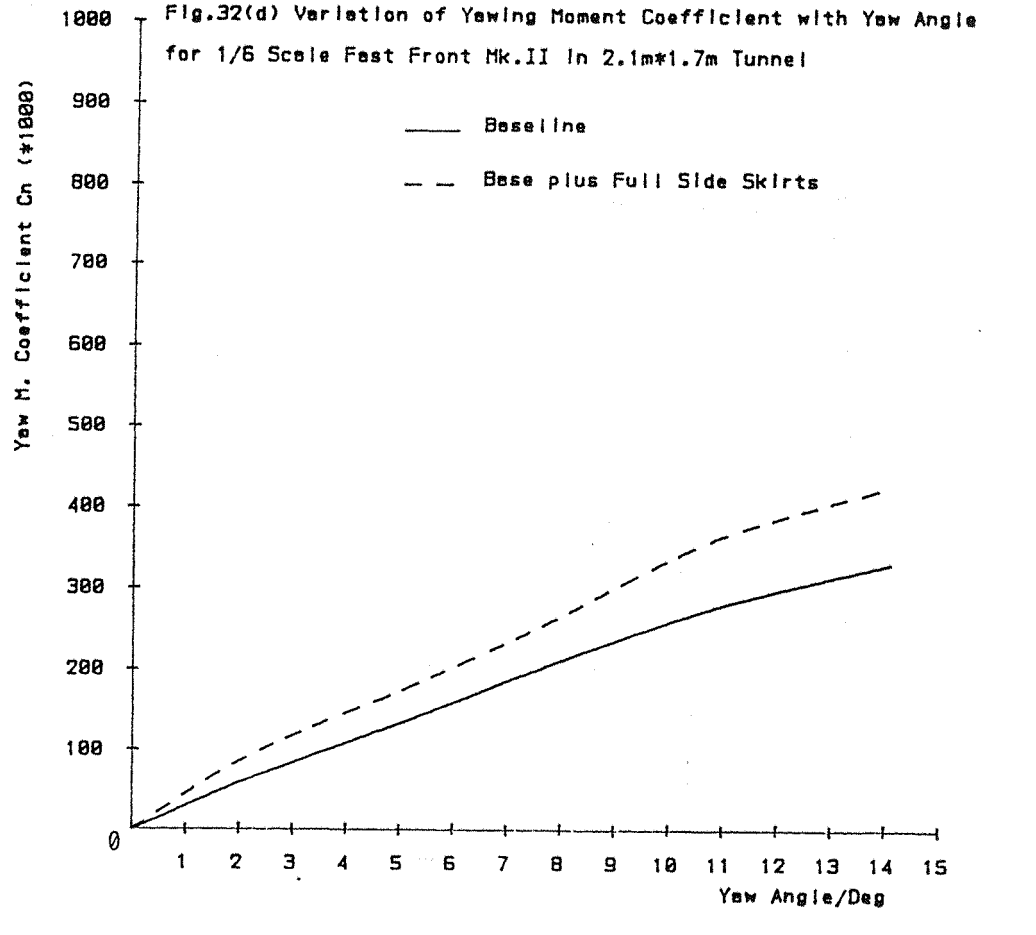
Fig.32(d) Variation of Yawing Moment Coefficient with Yaw Angle for 1/6 Scale Fast Front Mk.II in 2.1m*1.7m Tunnel
Yaw M. Coefficient Cn (*1000)
1000
900
800
700
600
500
400
300
200
100
0
1 2 3 4 5 6 7 8 9 10 11 12 13 14 15
Yaw Angle/Deg
Baseline
Base plus Full Side Skirts

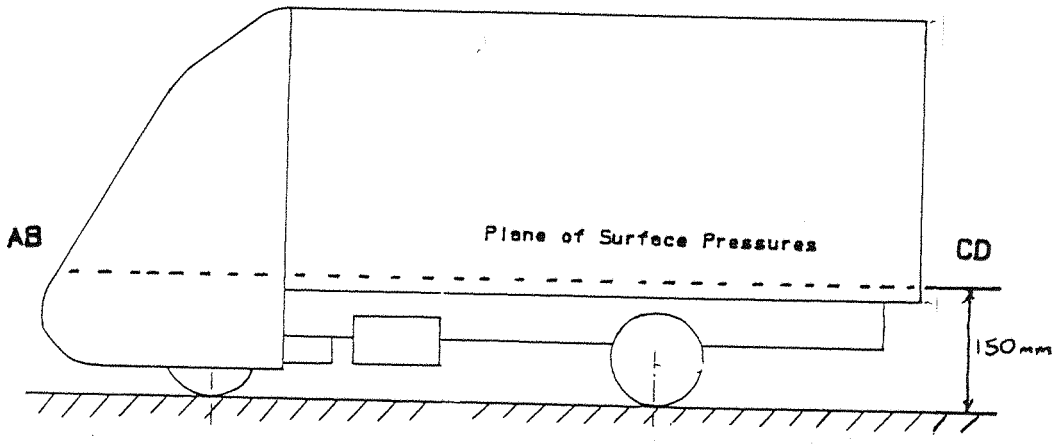

a) Side View

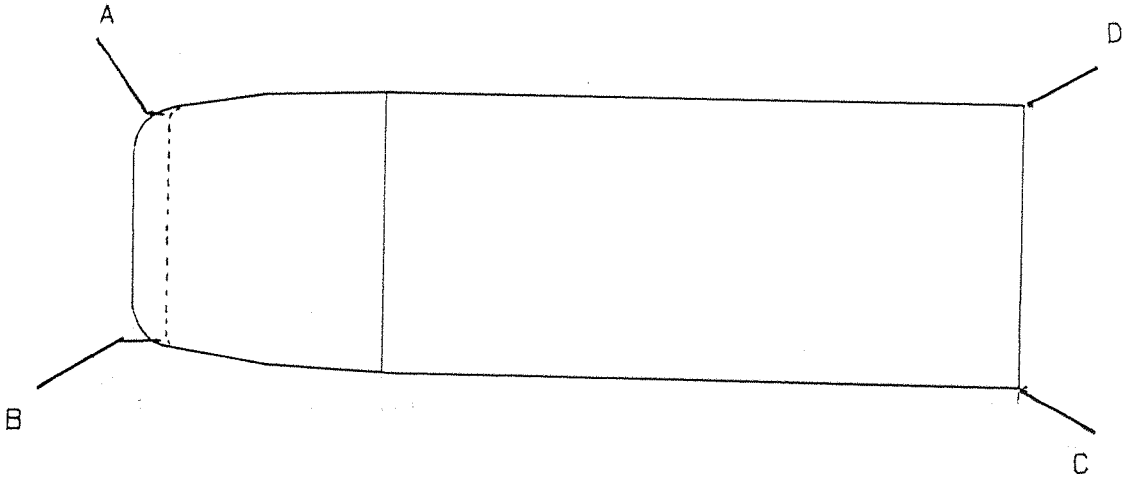

b) Plan View Showing Marks (Cp's Plotted Anti-clockwise)

Fig.33 Location of Surface Pressure Tappings

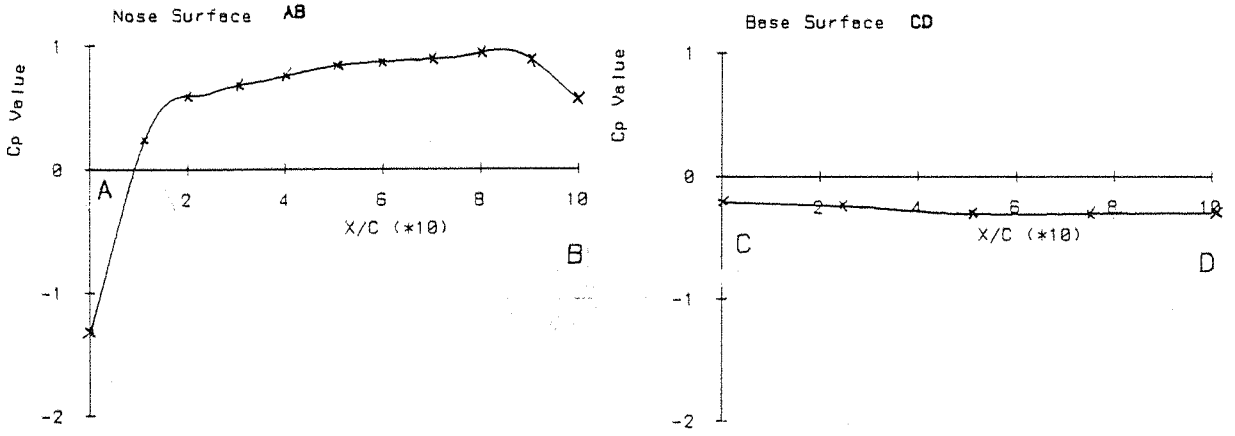

X/C= Non-dimension Position Along Row of Tappings

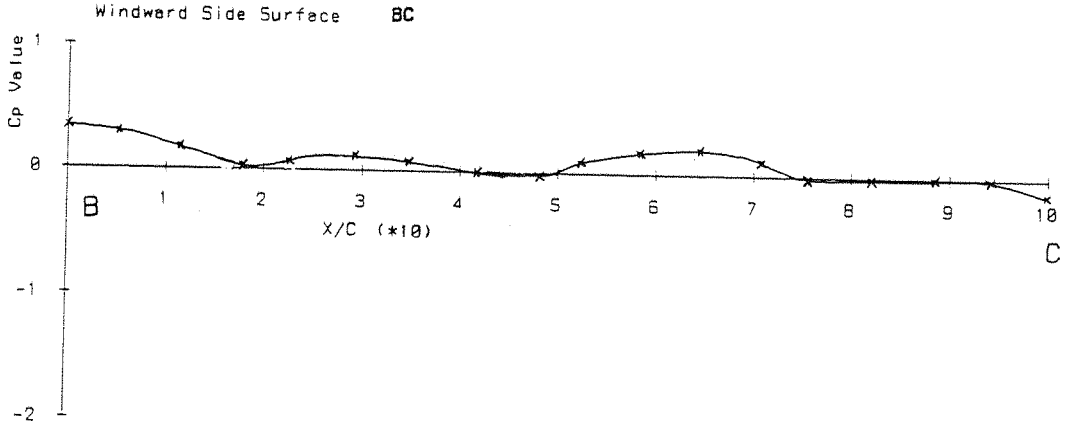

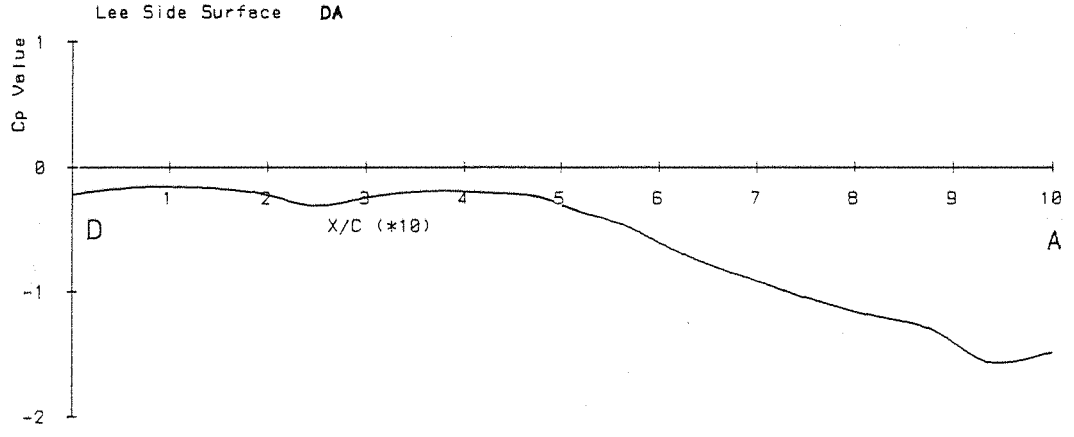

Fig.33(c)

Surface Pressure Coefficients for 1/6 Scale Fast Front Mk.I

Baseline at 15 Degrees Yaw

In 2.1m * 1.7m Wind Tunnel

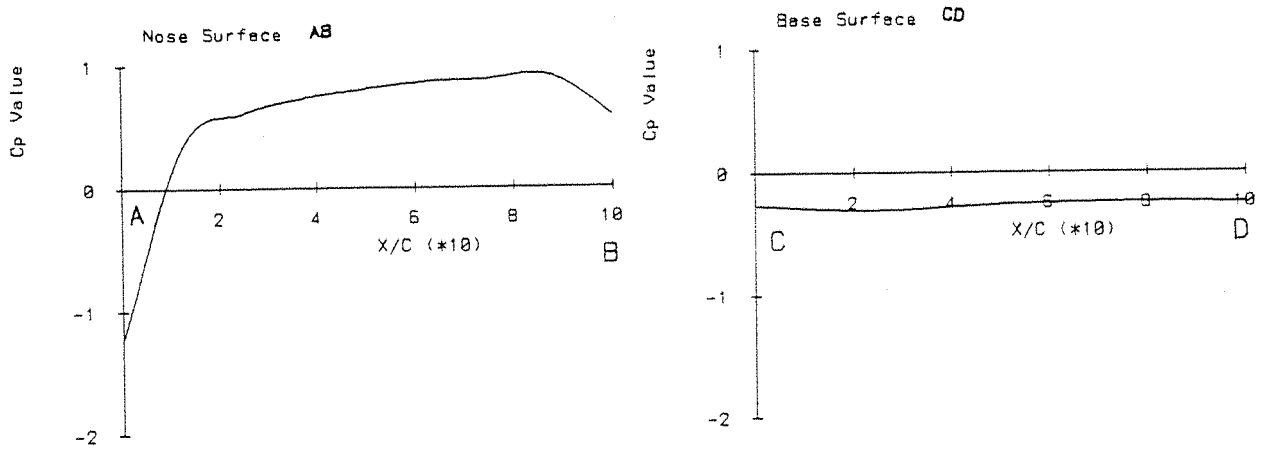

X/C= Non-dimension Position Along Row of Tappings

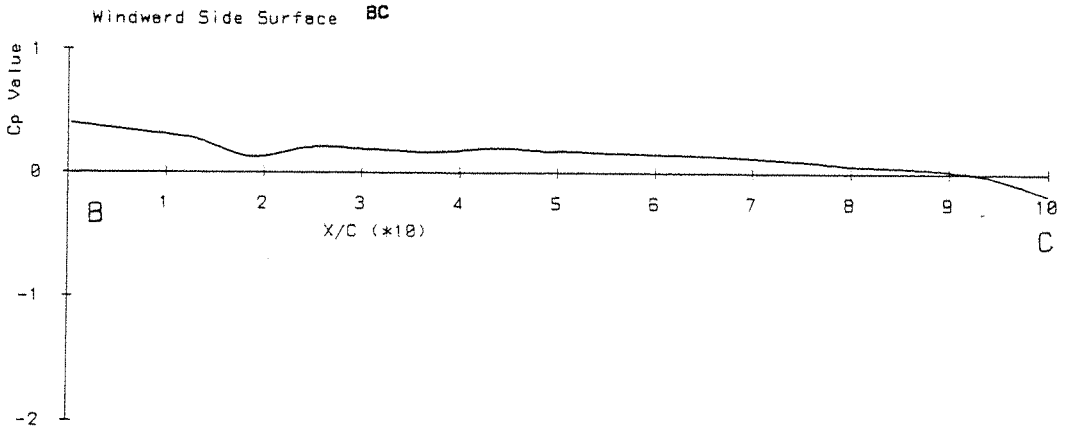

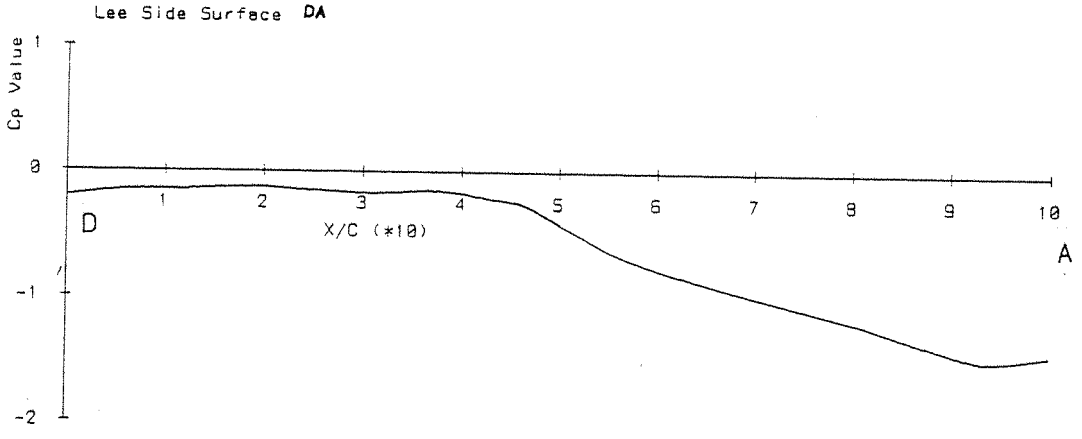

Fig.33(d)

Surface Pressure Coefficients for 1/6 Scale Fast Front Mk.I

Base plus Full Side Skirts at 15 Degrees Yaw

In 2.1m * 1.7m Wind Tunnel

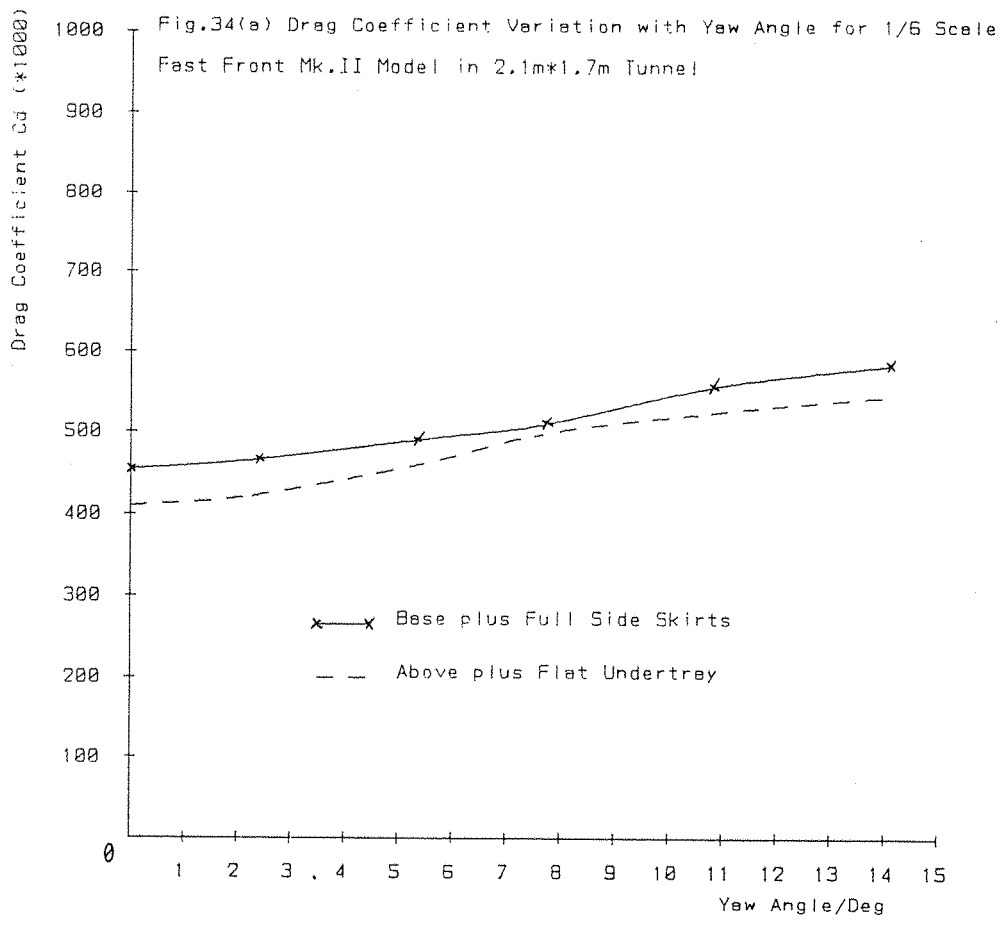
Fig.34(a) Drag Coefficient Variation with Yaw Angle for 1/6 Scale
Fast Front Mk.II Model in 2.1m*1.7m Tunnel
Drag Coefficient Cd (*1000)
1000
900
800
700
600
500
400
300
200
100
0
1 2 3 4 5 6 7 8 9 10 11 12 13 14 15
Yaw Angle/Deg
Base plus Full Side Skirts
Above plus Flat Undertray

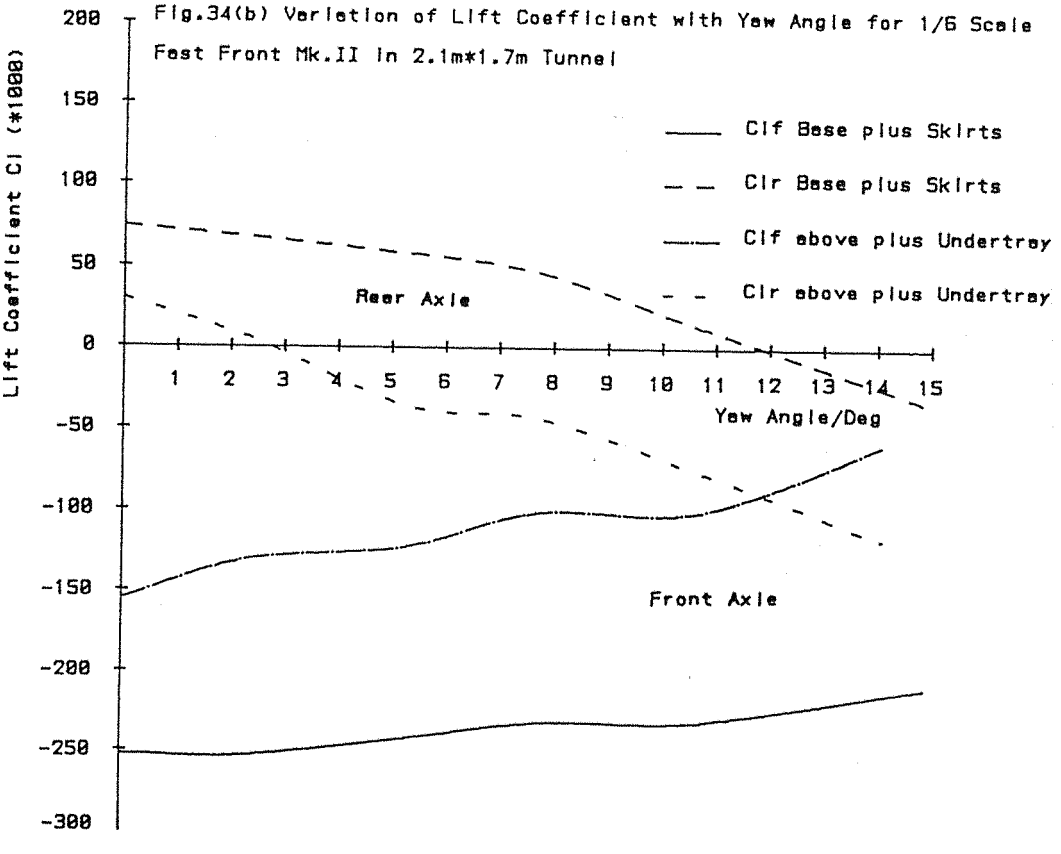
Fig.34(b) Variation of Lift Coefficient with Yaw Angle for 1/6 Scale
Fast Front Mk.II in 2.1m*1.7m Tunnel
Lift Coefficient Cl (*1000)
200
150
100
50
0
-50
-100
-150
-200
-250
-300
1 2 3 4 5 6 7 8 9 10 11 12 13 14 15
Yaw Angle/Deg
Clf Base plus Skirts
Clr Base plus Skirts
Clf above plus Undertray
Clr above plus Undertray
Rear Axle
Front Axle

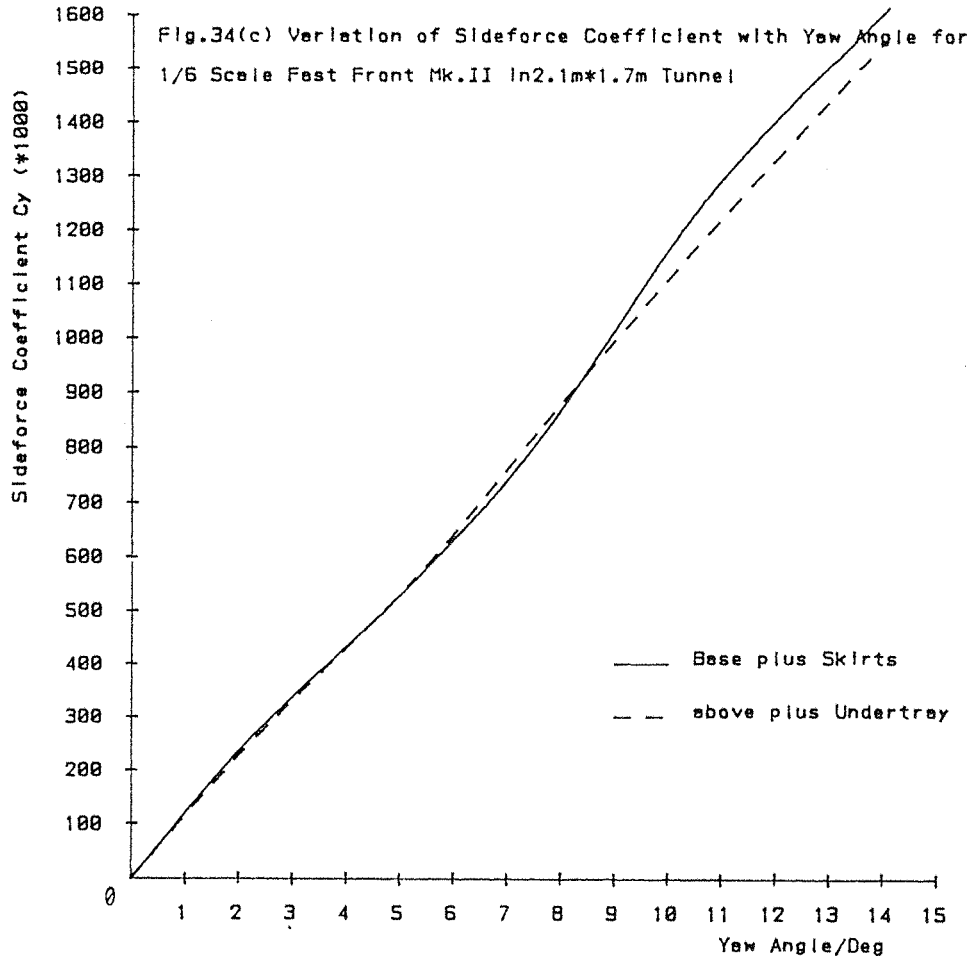
Fig.34(c) Variation of Sideforce Coefficient with Yaw Angle for 1/6 Scale Fast Front Mk.II In2.1m*1.7m Tunnel
Sideforce Coefficient Cy (*1000)
1600
1500
1400
1300
1200
1100
1000
900
800
700
600
500
400
300
200
100
0
1 2 3 4 5 6 7 8 9 10 11 12 13 14 15
Yaw Angle/Deg
Base plus Skirts
above plus Undertray

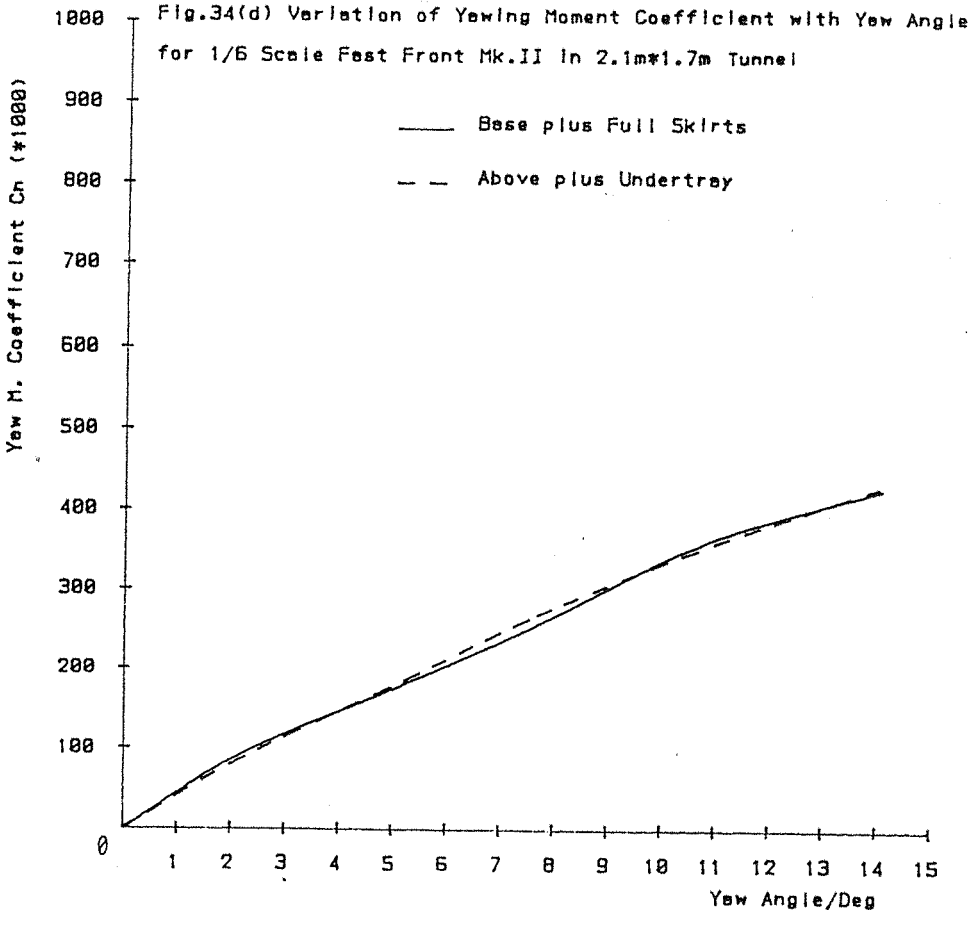
Fig.34(d) Variation of Yawing Moment Coefficient with Yaw Angle for 1/6 Scale Fast Front Mk.II In 2.1m*1.7m Tunnel
Yaw M. Coefficient Cn (*1000)
1000
900
800
700
600
500
400
300
200
100
0
1 2 3 4 5 6 7 8 9 10 11 12 13 14 15
Yaw Angle/Deg
Base plus Full Skirts
Above plus Undertray

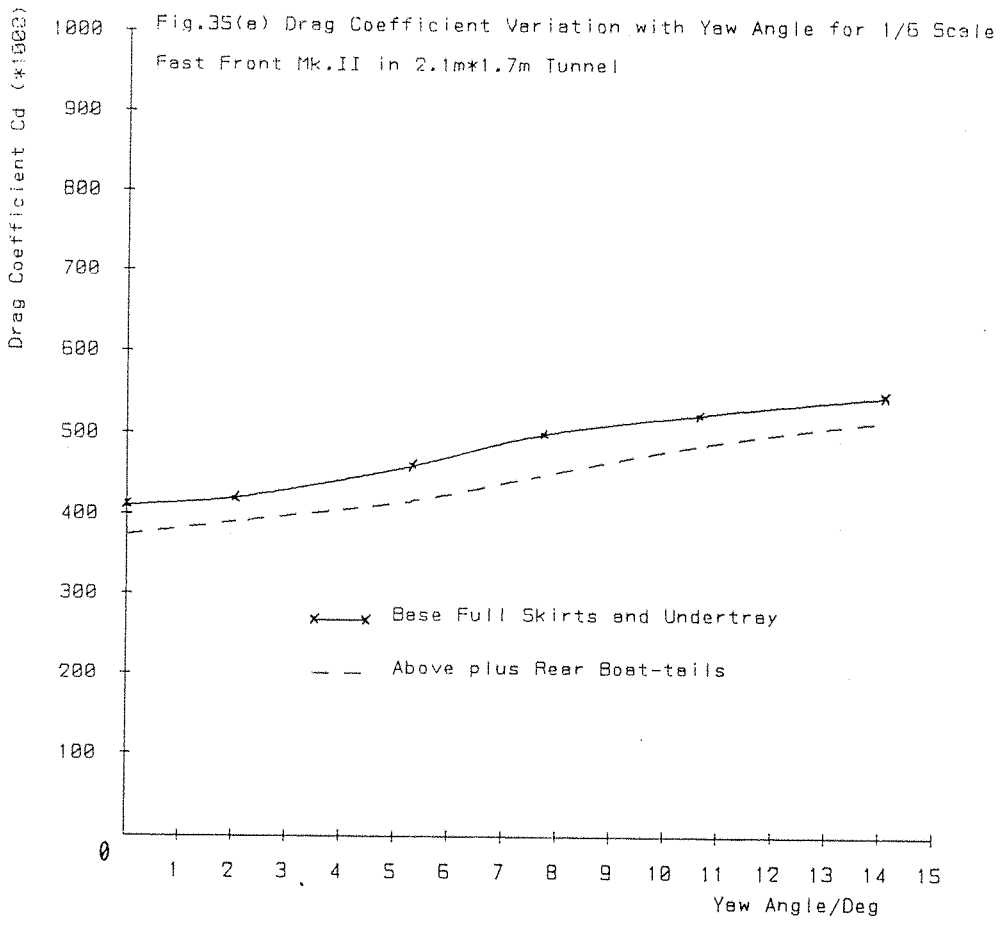
Fig.35(a) Drag Coefficient Variation with Yaw Angle for 1/6 Scale
Fast Front Mk.II in 2.1m*1.7m Tunnel
Drag Coefficient Cd (*1000)
1000
900
800
700
600
500
400
300
200
100
0
1 2 3 4 5 6 7 8 9 10 11 12 13 14 15
Yaw Angle/Deg
Base Full Skirts and Undertray
Above plus Rear Boat-tails

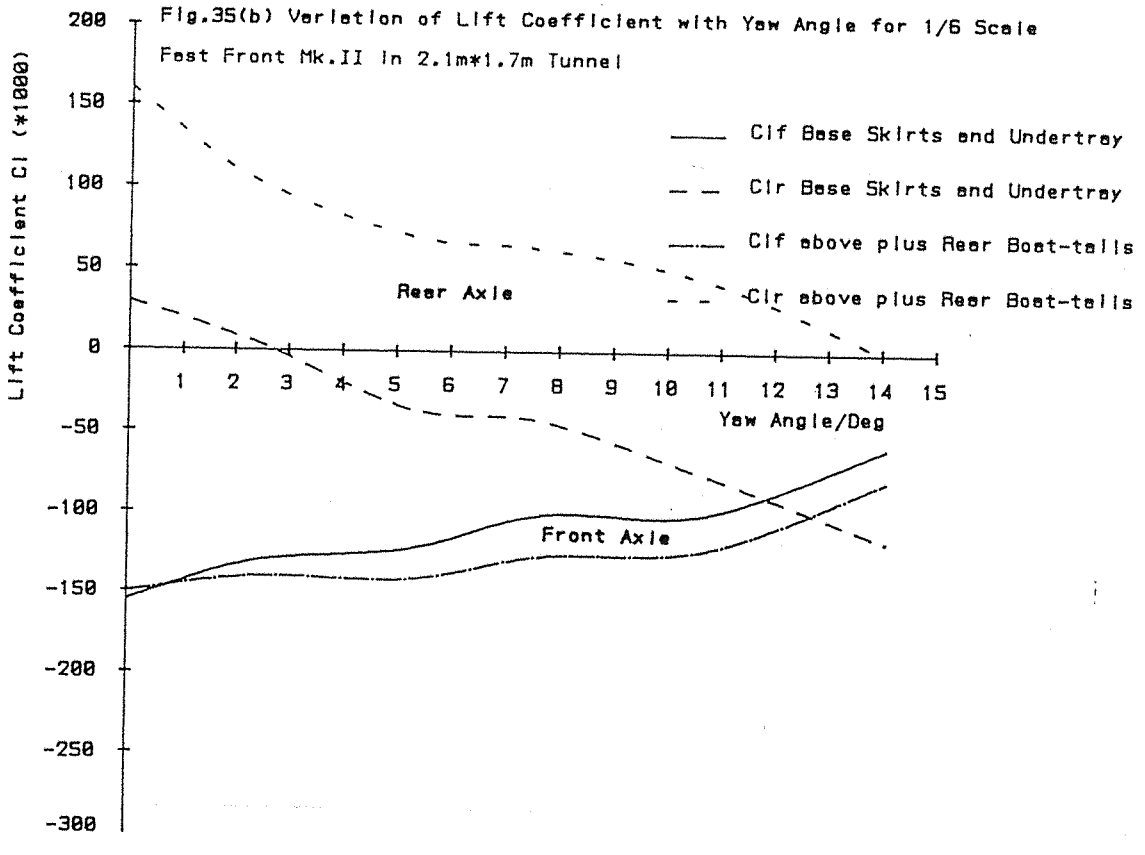
Fig.35(b) Variation of Lift Coefficient with Yaw Angle for 1/6 Scale
Fast Front Mk.II in 2.1m*1.7m Tunnel
Lift Coefficient Cl (*1000)
200
150
100
50
0
-50
-100
-150
-200
-250
-300
1 2 3 4 5 6 7 8 9 10 11 12 13 14 15
Yaw Angle/Deg
Clf Base Skirts and Undertray
Clr Base Skirts and Undertray
Clf above plus Rear Boat-tails
Clr above plus Rear Boat-tails
Rear Axle
Front Axle

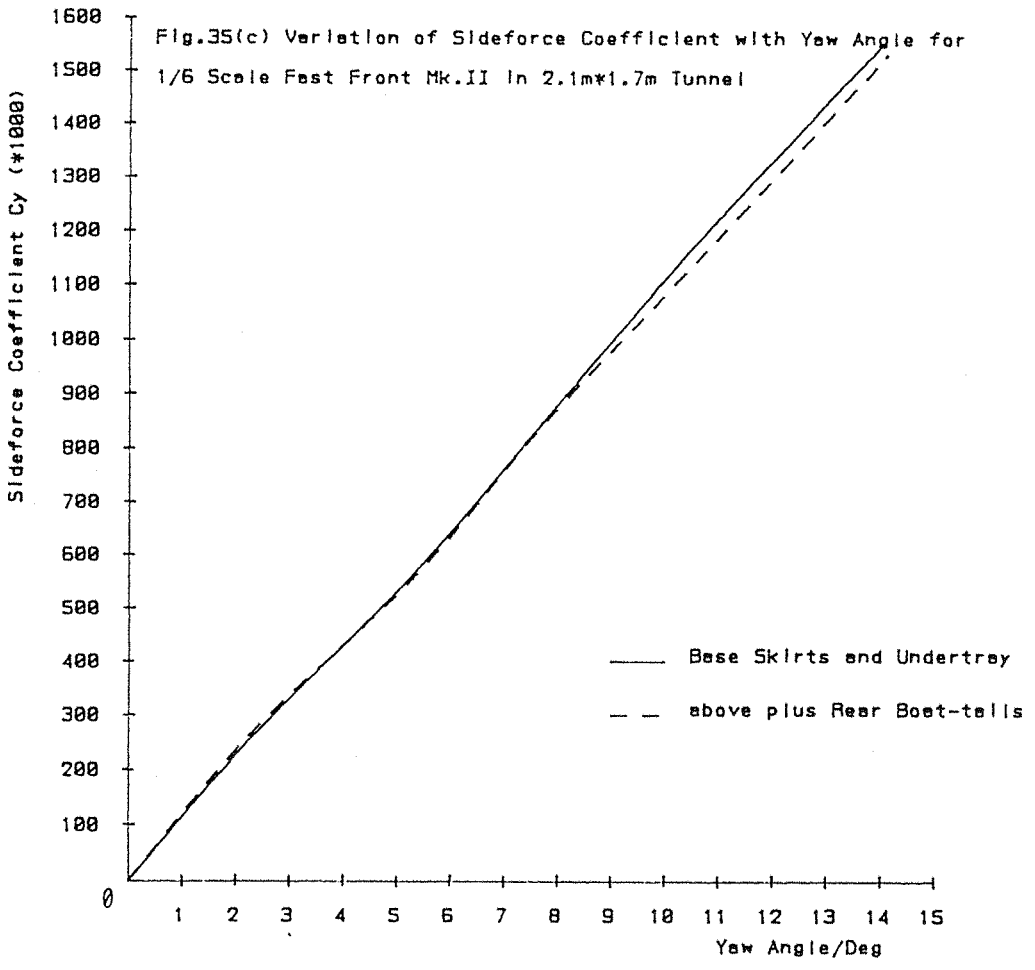
Fig.35(c) Variation of Sideforce Coefficient with Yaw Angle for 1/6 Scale Fast Front Mk.II in 2.1m*1.7m Tunnel
Sideforce Coefficient Cy (*1000)
1600
1500
1400
1300
1200
1100
1000
900
800
700
600
500
400
300
200
100
0
1 2 3 4 5 6 7 8 9 10 11 12 13 14 15
Yaw Angle/Deg
Base Skirts and Undertray
above plus Rear Boat-tails

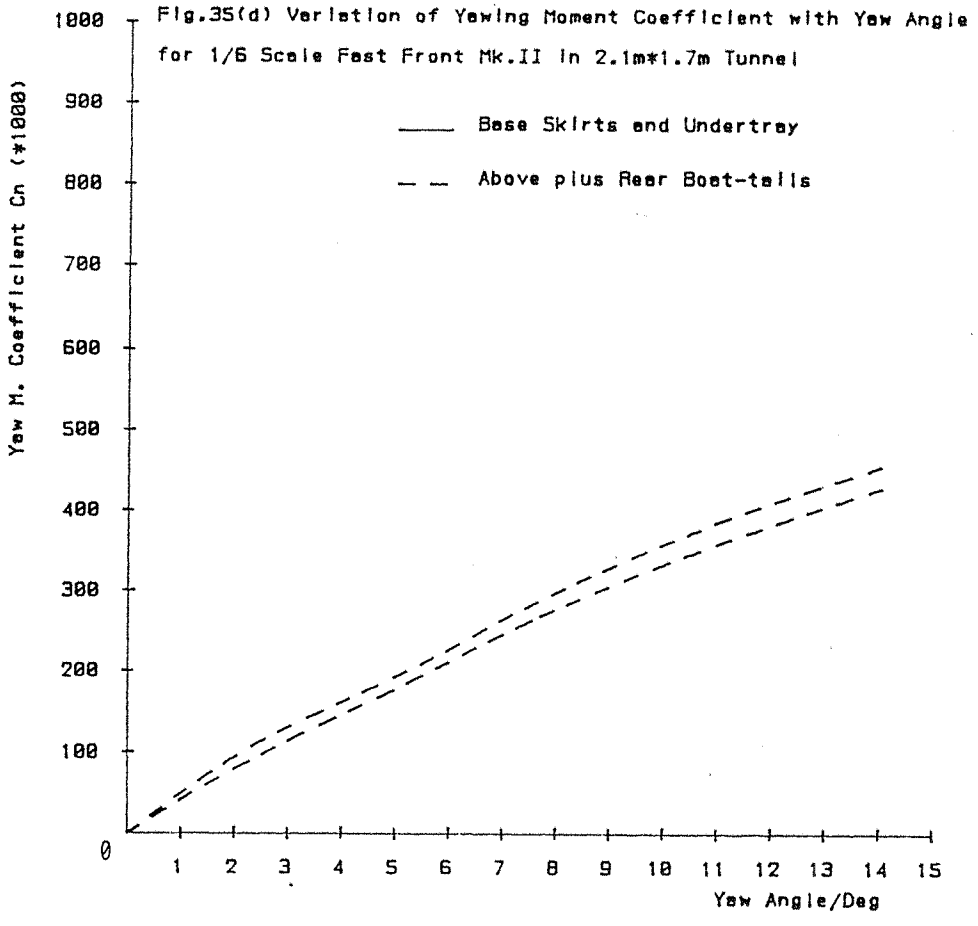
Fig.35(d) Variation of Yawing Moment Coefficient with Yaw Angle for 1/6 Scale Fast Front Mk.II in 2.1m*1.7m Tunnel
Yaw M. Coefficient Cn (*1000)
1000
900
800
700
600
500
400
300
200
100
0
1 2 3 4 5 6 7 8 9 10 11 12 13 14 15
Yaw Angle/Deg
Base Skirts and Undertray
Above plus Rear Boat-tails

Fig.36 Variation of Drag Coefficient with Reynolds Number for 1/4 Scale Model **In the 3.5m * 2.6m Wind Tunnel**

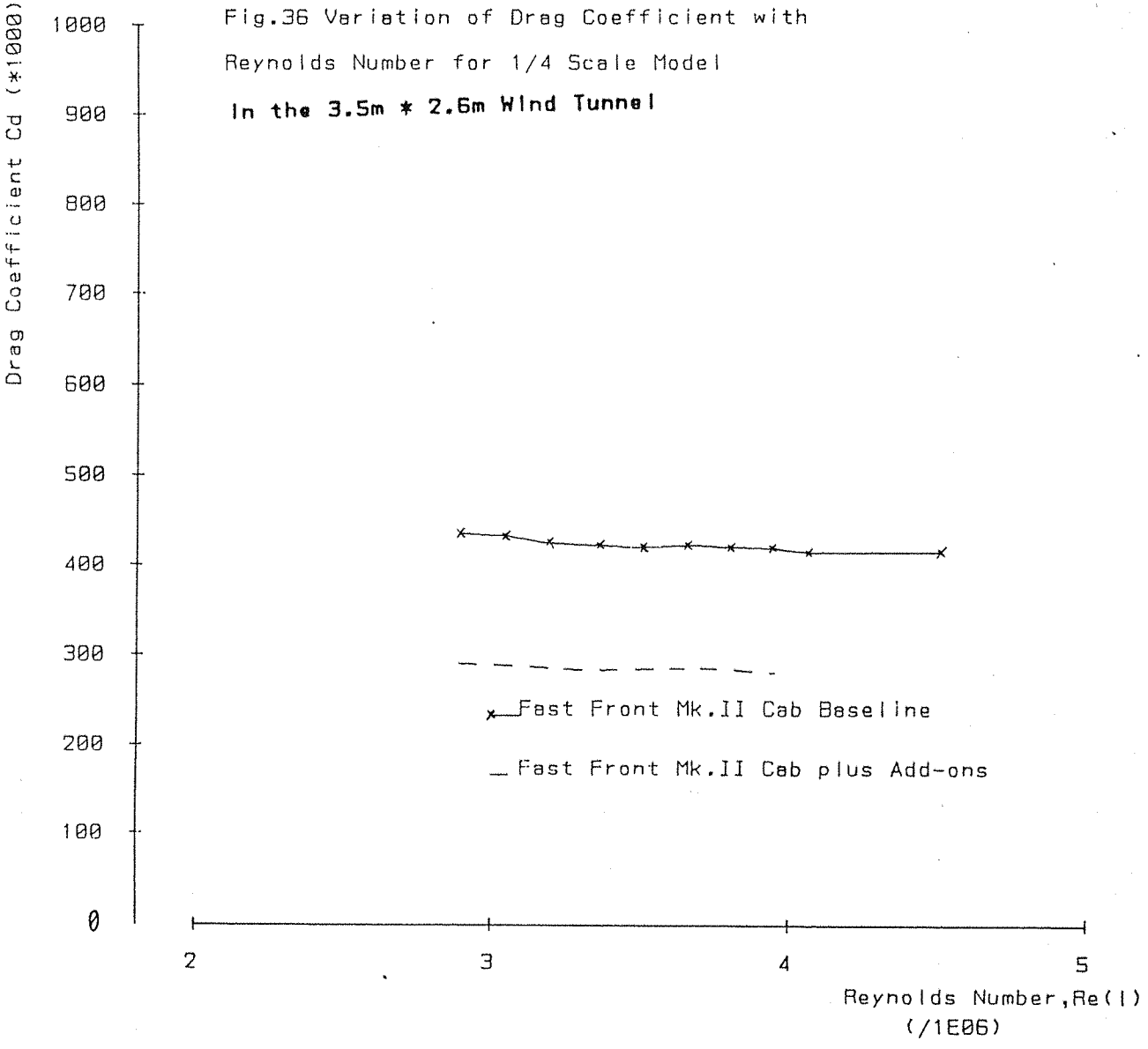

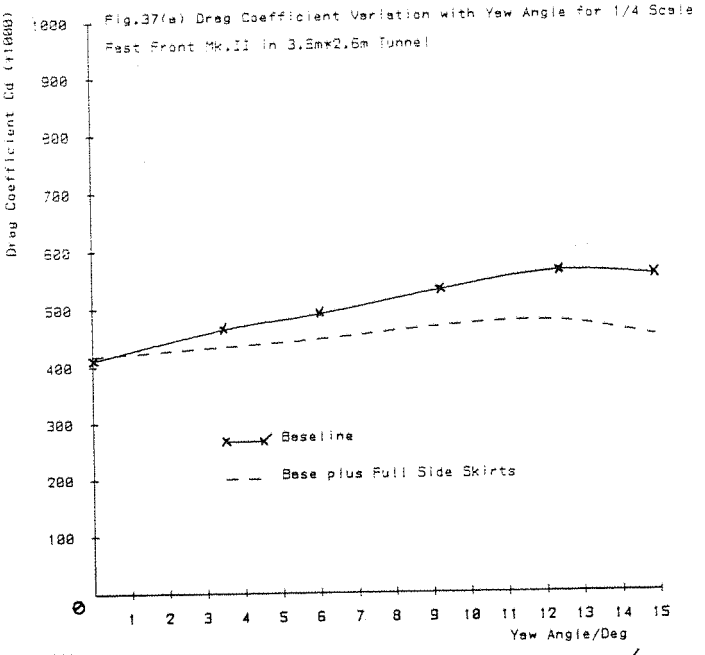
Fig.37(a) Drag Coefficient Variation with Yaw Angle for 1/4 Scale Fast Front Mk.II in 3.5m*2.6m Tunnel
Drag Coefficient Cd (*1000)
1000
900
800
700
600
500
400
300
200
100
0
1 2 3 4 5 6 7 8 9 10 11 12 13 14 15
Yaw Angle/Deg
Baseline
Base plus Full Side Skirts

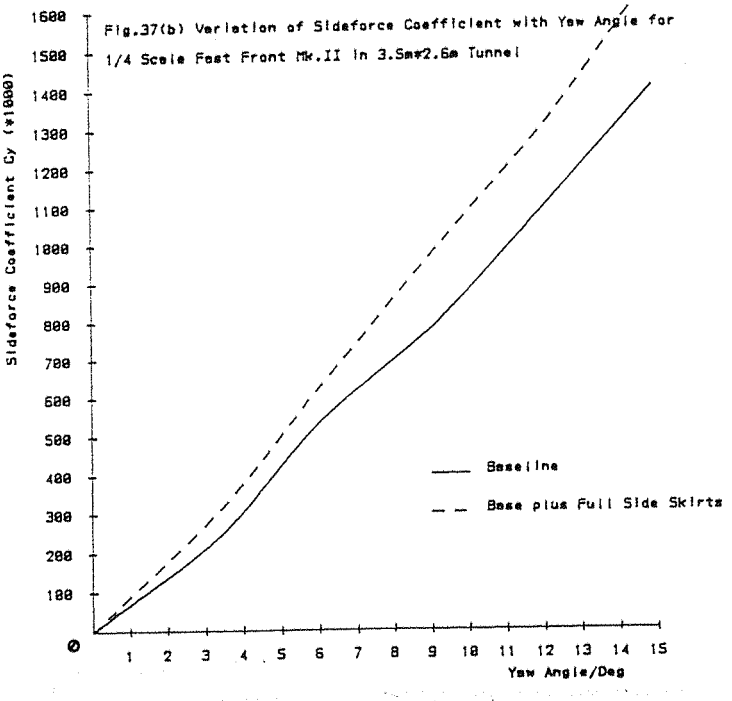
Fig.37(b) Variation of Sideforce Coefficient with Yaw Angle for 1/4 Scale Fast Front Mk.II in 3.5m*2.6m Tunnel
Sideforce Coefficient Cy (*1000)
1600
1500
1400
1300
1200
1100
1000
900
800
700
600
500
400
300
200
100
0
1 2 3 4 5 6 7 8 9 10 11 12 13 14 15
Yaw Angle/Deg
Baseline
Base plus Full Side Skirts

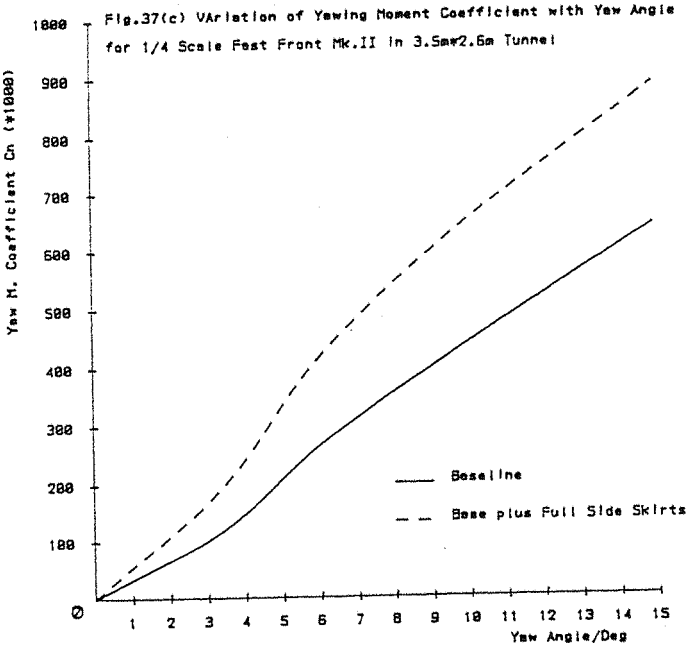
Fig.37(c) VAriation of Yawing Moment Coefficient with Yaw Angle for 1/4 Scale Fast Front Mk.II in 3.5m*2.6m Tunnel
Yaw M. Coefficient Cn (*1000)
1000
900
800
700
600
500
400
300
200
100
0
1 2 3 4 5 6 7 8 9 10 11 12 13 14 15
Yaw Angle/Deg
Baseline
Base plus Full Side Skirts

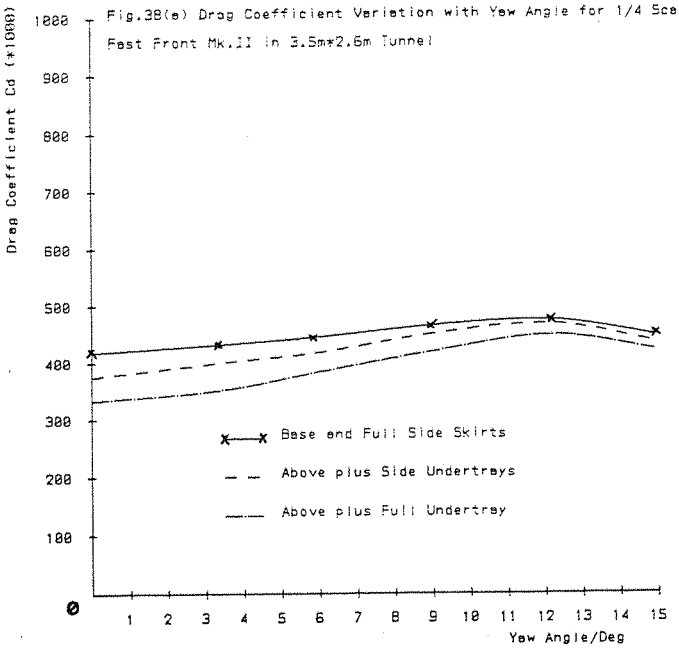
Fig.38(a) Drag Coefficient Variation with Yaw Angle for 1/4 Scale
Fast Front Mk.II in 3.5m*2.6m Tunnel
Drag Coefficient Cd (*1000)
1000
900
800
700
600
500
400
300
200
100
0
1 2 3 4 5 6 7 8 9 10 11 12 13 14 15
Yaw Angle/Deg
Base and Full Side Skirts
Above plus Side Undertrays
Above plus Full Undertray

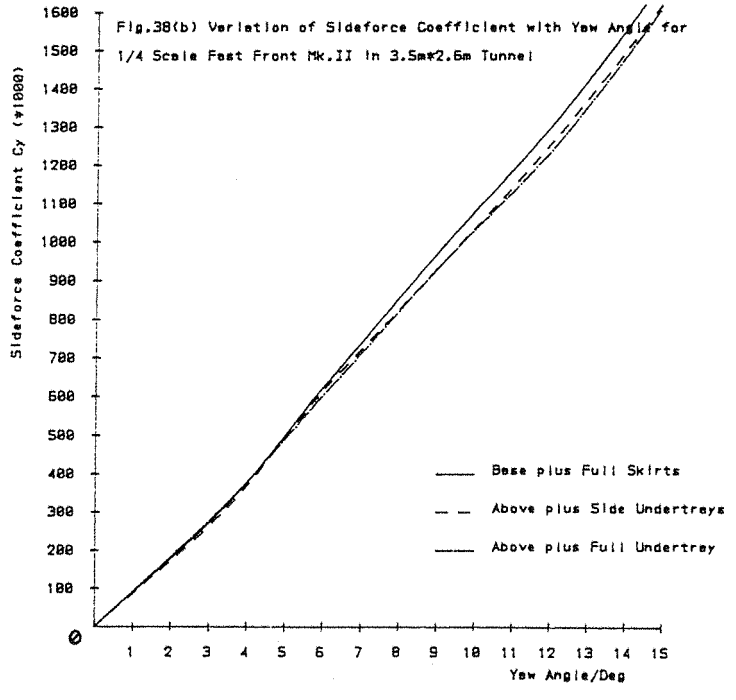
Fig.38(b) Variation of Sideforce Coefficient with Yaw Angle for
1/4 Scale Fast Front Mk.II in 3.5m*2.6m Tunnel
Sideforce Coefficient Cy (*1000)
1600
1500
1400
1300
1200
1100
1000
900
800
700
600
500
400
300
200
100
0
1 2 3 4 5 6 7 8 9 10 11 12 13 14 15
Yaw Angle/Deg
Base plus Full Skirts
Above plus Side Undertrays
Above plus Full Undertray

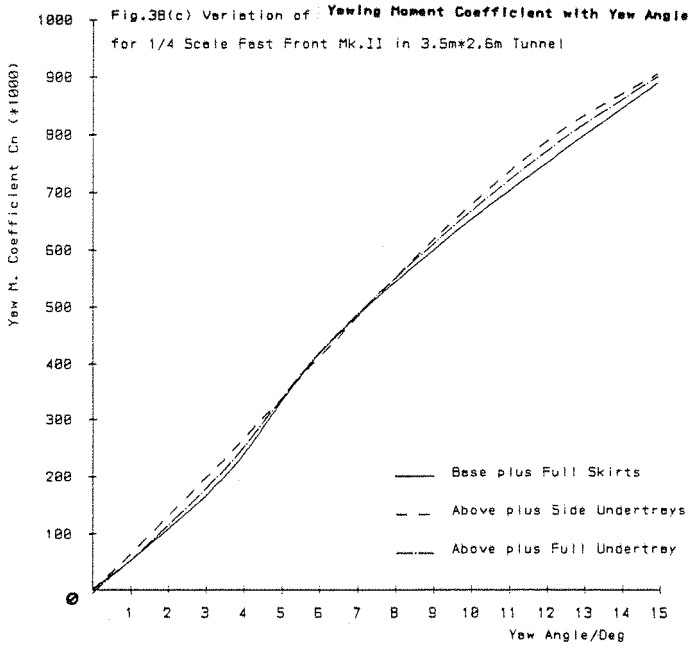
Fig.38(c) Variation of Yawing Moment Coefficient with Yaw Angle
for 1/4 Scale Fast Front Mk.II in 3.5m*2.6m Tunnel
Yaw M. Coefficient Cn (*1000)
1000
900
800
700
600
500
400
300
200
100
0
1 2 3 4 5 6 7 8 9 10 11 12 13 14 15
Yaw Angle/Deg
Base plus Full Skirts
Above plus Side Undertrays
Above plus Full Undertray

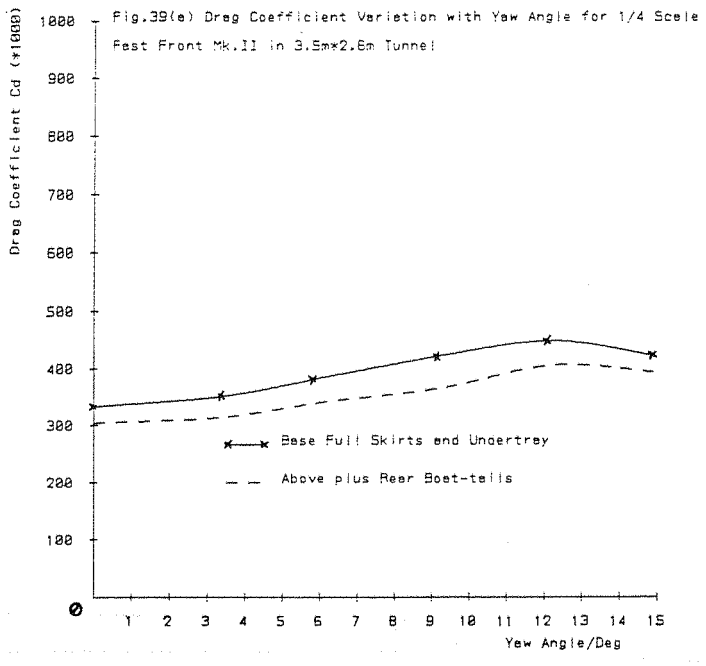
Fig.39(a) Drag Coefficient Variation with Yaw Angle for 1/4 Scale Fast Front Mk.II in 3.5m*2.6m Tunnel
Drag Coefficient Cd (*1000)
1000
900
800
700
600
500
400
300
200
100
0
1 2 3 4 5 6 7 8 9 10 11 12 13 14 15
Yaw Angle/Deg
Base Full Skirts and Undertray
Above plus Rear Boat-tails

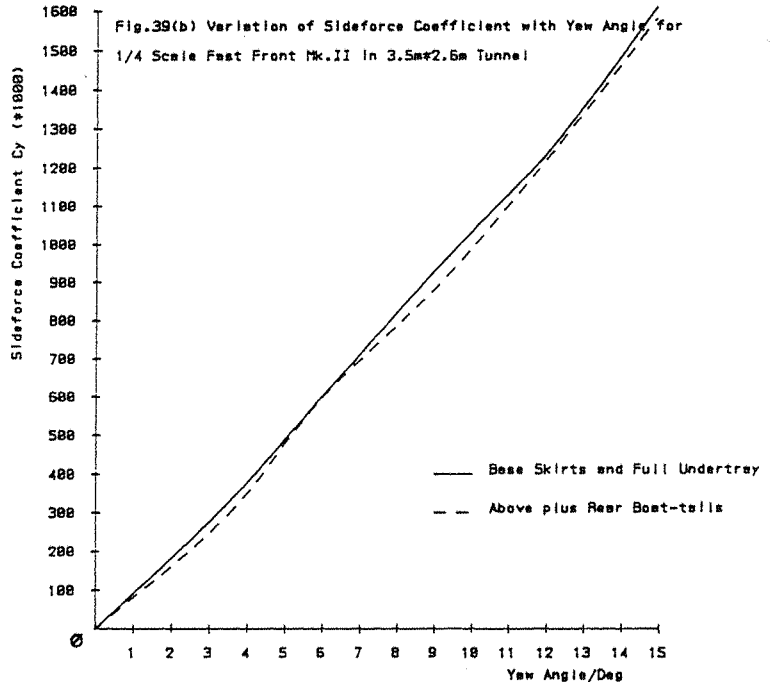
Fig.39(b) Variation of Sideforce Coefficient with Yaw Angle for 1/4 Scale Fast Front Mk.II in 3.5m*2.6m Tunnel
Sideforce Coefficient Cy (*1000)
1600
1500
1400
1300
1200
1100
1000
900
800
700
600
500
400
300
200
100
0
1 2 3 4 5 6 7 8 9 10 11 12 13 14 15
Yaw Angle/Deg
Base Skirts and Full Undertray
Above plus Rear Boat-tails

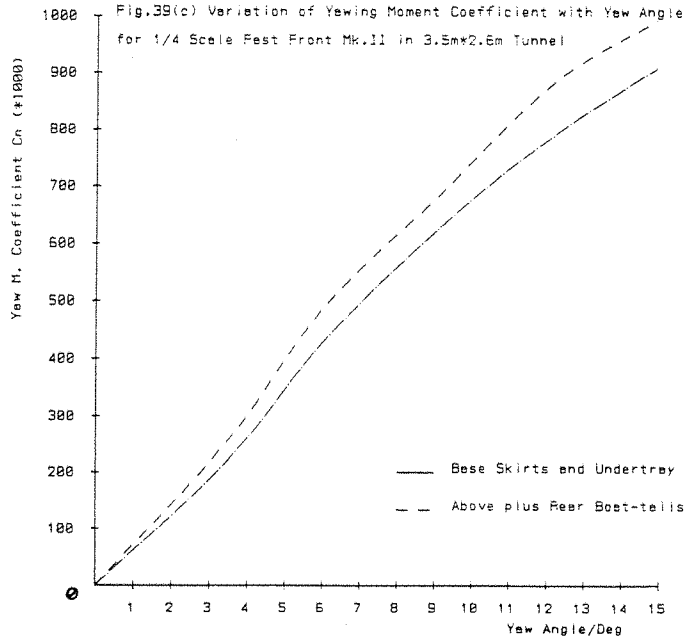
Fig.39(c) Variation of Yawing Moment Coefficient with Yaw Angle for 1/4 Scale Fast Front Mk.II in 3.5m*2.6m Tunnel
Yaw M. Coefficient Cn (*1000)
1000
900
800
700
600
500
400
300
200
100
0
1 2 3 4 5 6 7 8 9 10 11 12 13 14 15
Yaw Angle/Deg
Base Skirts and Undertray
Above plus Rear Boat-tails

Fig.40(a) Comparison of the Drag Coefficient Variation with Reynolds Number for 1/6 Scale Model in 2.1m*1.7m and 3.5m*2.6m Tunnels

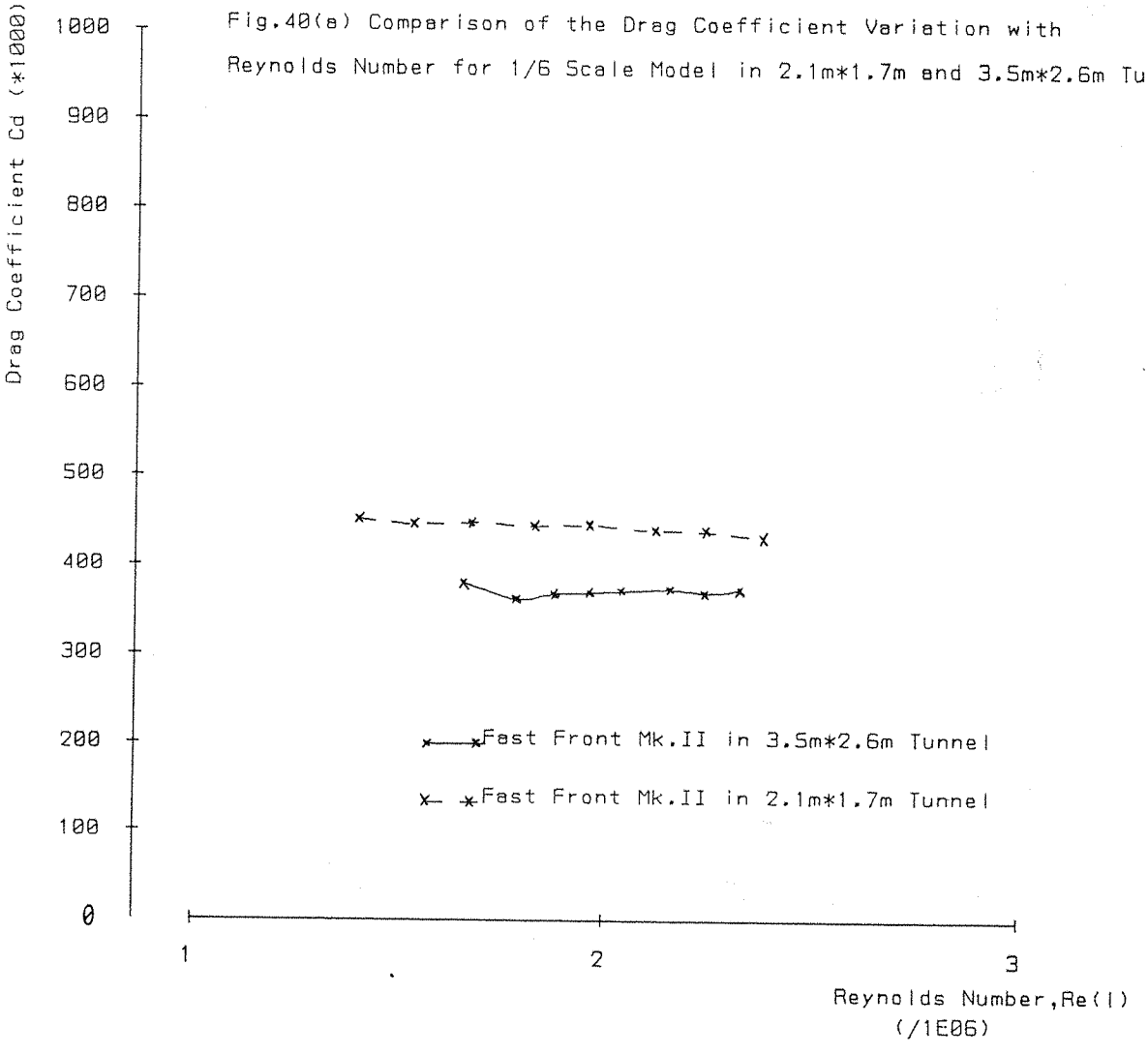

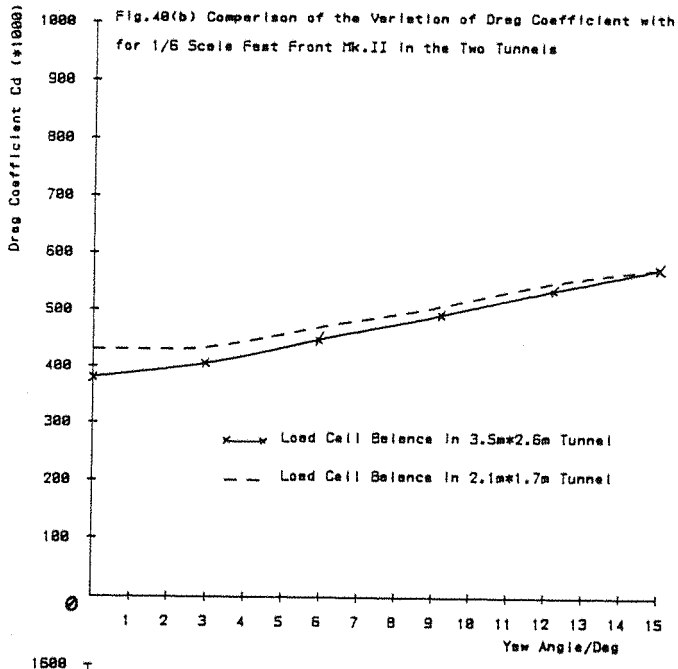
Fig.40(b) Comparison of the Variation of Drag Coefficient with Yaw Angle for 1/6 Scale Fast Front Mk.II in the Two Tunnels
Drag Coefficient Cd (*1000)
1000
900
800
700
600
500
400
300
200
100
0
1 2 3 4 5 6 7 8 9 10 11 12 13 14 15
Yaw Angle/Deg
Load Cell Balance in 3.5m*2.6m Tunnel
Load Cell Balance in 2.1m*1.7m Tunnel

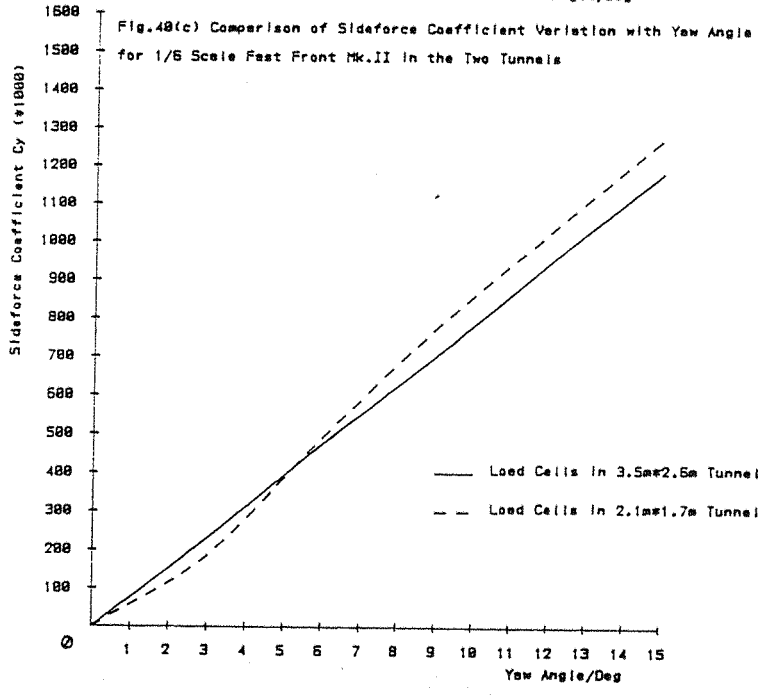
Fig.40(c) Comparison of Sideforce Coefficient Variation with Yaw Angle for 1/6 Scale Fast Front Mk.II in the Two Tunnels
Sideforce Coefficient Cy (*1000)
1600
1500
1400
1300
1200
1100
1000
900
800
700
600
500
400
300
200
100
0
1 2 3 4 5 6 7 8 9 10 11 12 13 14 15
Yaw Angle/Deg
Load Cells in 3.5m*2.6m Tunnel
Load Cells in 2.1m*1.7m Tunnel

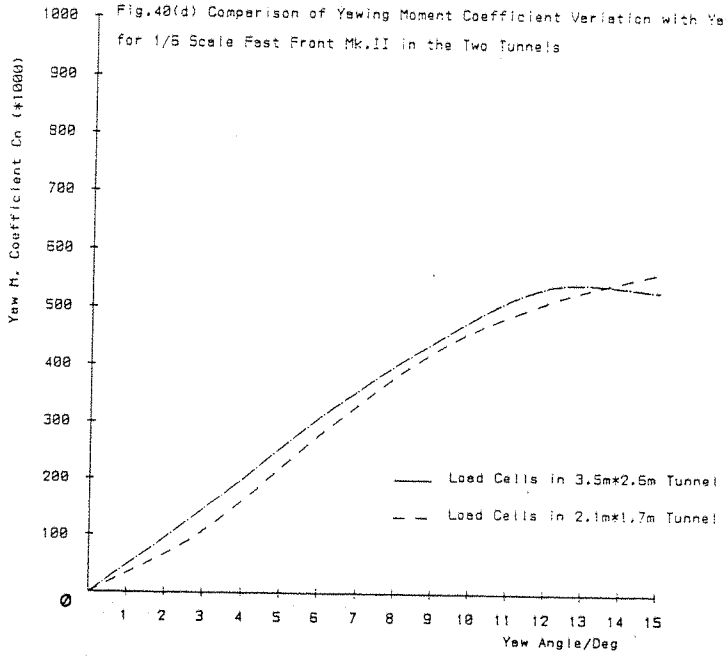
Fig.40(d) Comparison of Yawing Moment Coefficient Variation with Yaw Angle for 1/6 Scale Fast Front Mk.II in the Two Tunnels
Yaw M. Coefficient Cn (*1000)
1000
900
800
700
600
500
400
300
200
100
0
1 2 3 4 5 6 7 8 9 10 11 12 13 14 15
Yaw Angle/Deg
Load Cells in 3.5m*2.6m Tunnel
Load Cells in 2.1m*1.7m Tunnel

Fig.41(a) Comparison of Drag Coefficient Variation with Reynolds Number for Various Model Scales and Test Techniques

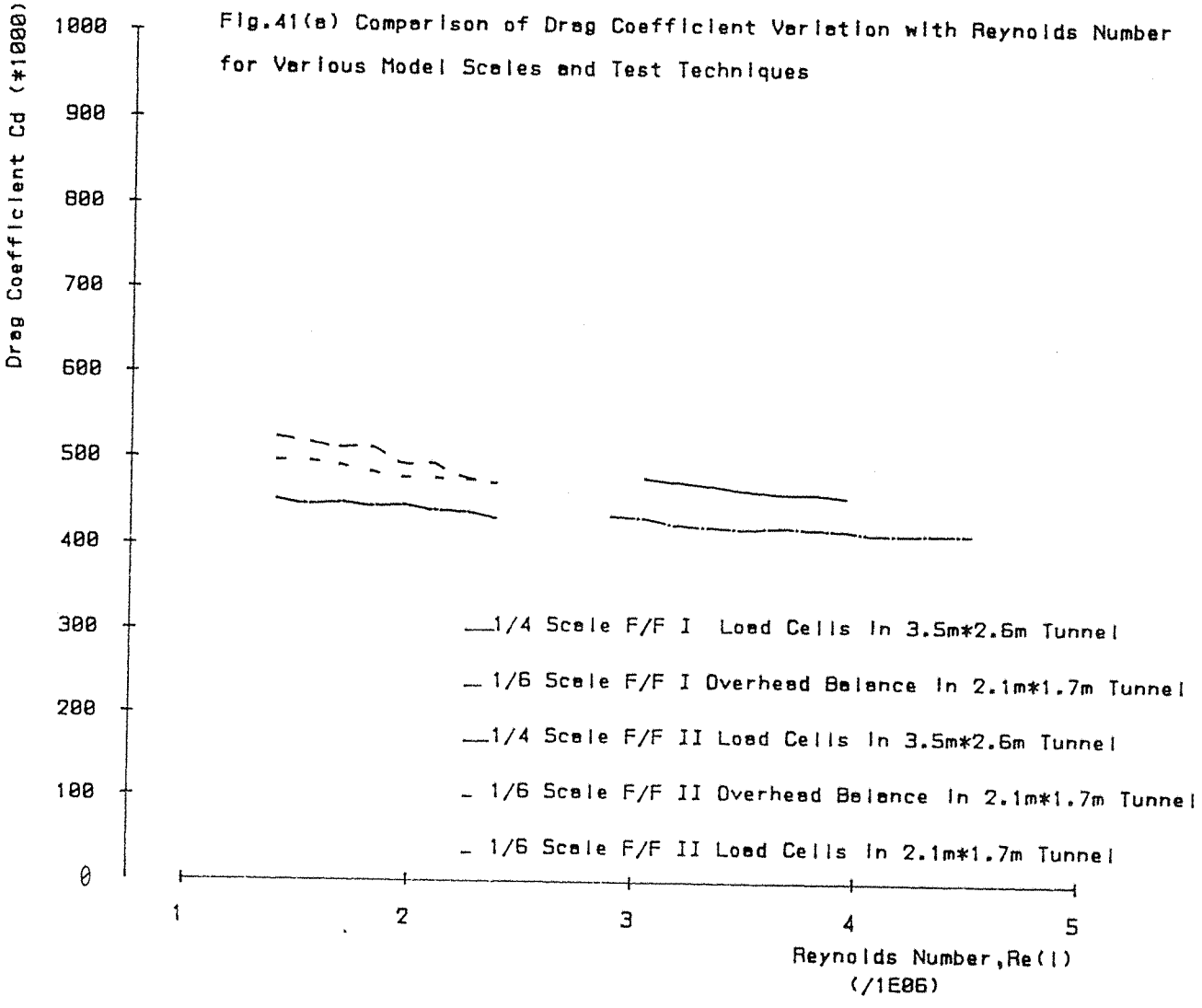

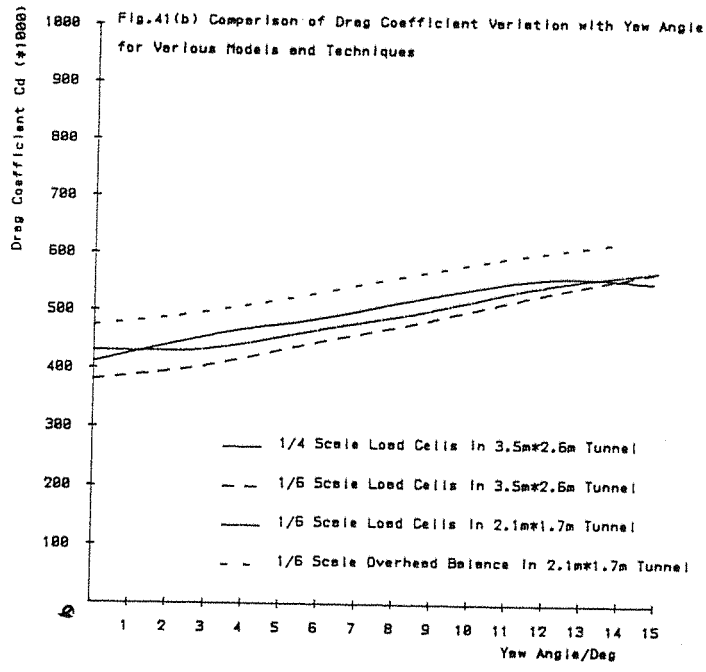
Fig.41(b) Comparison of Drag Coefficient Variation with Yaw Angle for Various Models and Techniques
Drag Coefficient Cd (*1000)
1000
900
800
700
600
500
400
300
200
100
0
1 2 3 4 5 6 7 8 9 10 11 12 13 14 15
Yaw Angle/Deg
1/4 Scale Load Cells in 3.5m*2.6m Tunnel
1/6 Scale Load Cells in 3.5m*2.6m Tunnel
1/6 Scale Load Cells in 2.1m*1.7m Tunnel
1/6 Scale Overhead Balance in 2.1m*1.7m Tunnel

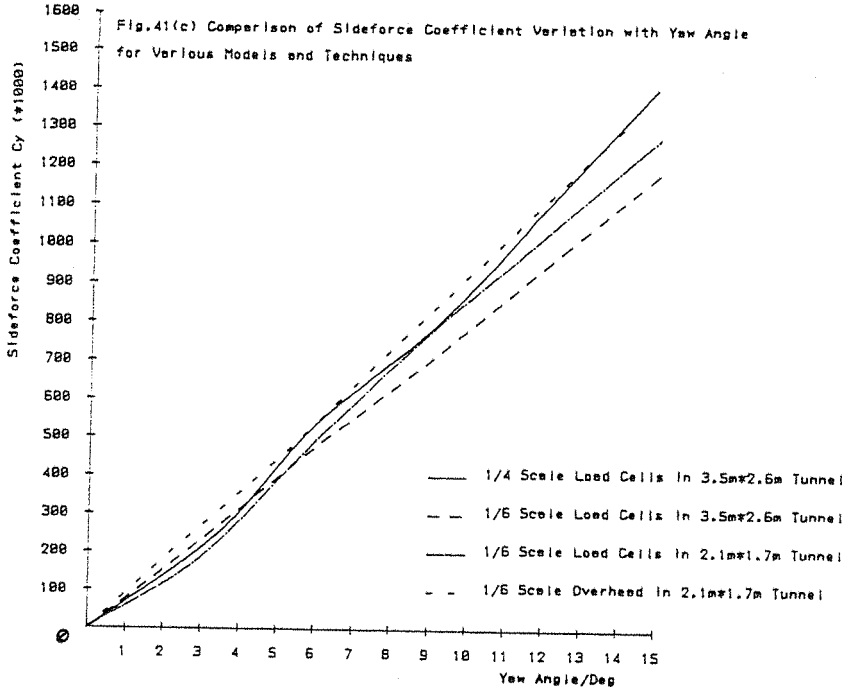
Fig.41(c) Comparison of Sideforce Coefficient Variation with Yaw Angle for Various Models and Techniques
Sideforce Coefficient Cy (*1000)
1600
1500
1400
1300
1200
1100
1000
900
800
700
600
500
400
300
200
100
0
1 2 3 4 5 6 7 8 9 10 11 12 13 14 15
Yaw Angle/Deg
1/4 Scale Load Cells in 3.5m*2.6m Tunnel
1/6 Scale Load Cells in 3.5m*2.6m Tunnel
1/6 Scale Load Cells in 2.1m*1.7m Tunnel
1/6 Scale Overhead in 2.1m*1.7m Tunnel

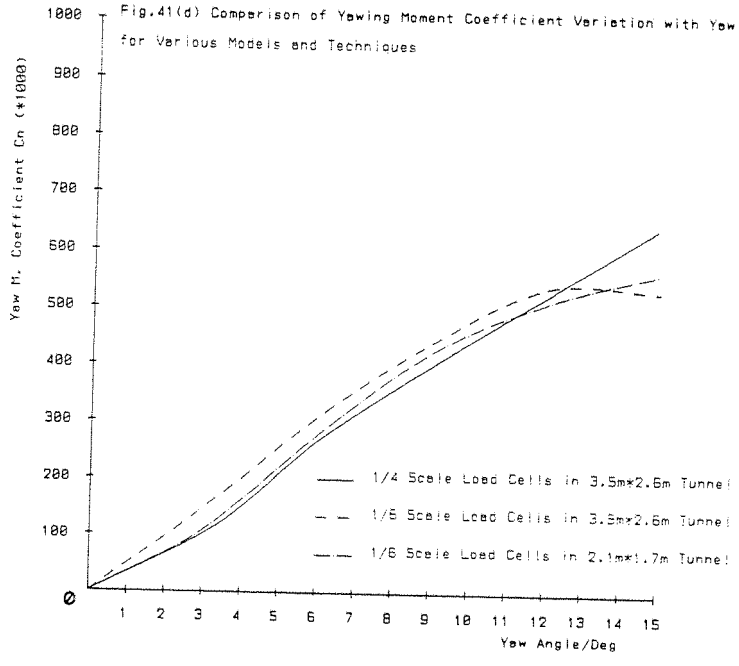
Fig.41(d) Comparison of Yawing Moment Coefficient Variation with Yaw Angle for Various Models and Techniques
Yaw M. Coefficient Cn (*1000)
1000
900
800
700
600
500
400
300
200
100
0
1 2 3 4 5 6 7 8 9 10 11 12 13 14 15
Yaw Angle/Deg
1/4 Scale Load Cells in 3.5m*2.6m Tunnel
1/6 Scale Load Cells in 3.5m*2.6m Tunnel
1/6 Scale Load Cells in 2.1m*1.7m Tunnel

Fig.42(a) Contour Plot for 1/6 Scale Fast Front Mk.II

Baseline 0 Degrees Yaw Rotating Wheels

2.1m * 1.7m Wind Tunnel 185mm Rearwards of Model Base

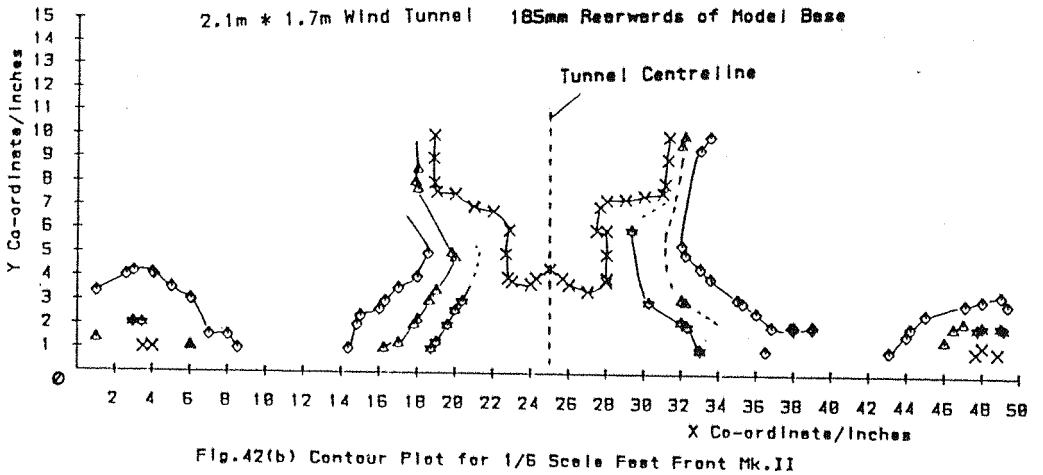

Fig.42(b) Contour Plot for 1/6 Scale Fast Front Mk.II

Base plus Full Side Skirts 0 Degrees Yaw Rotating Wheels

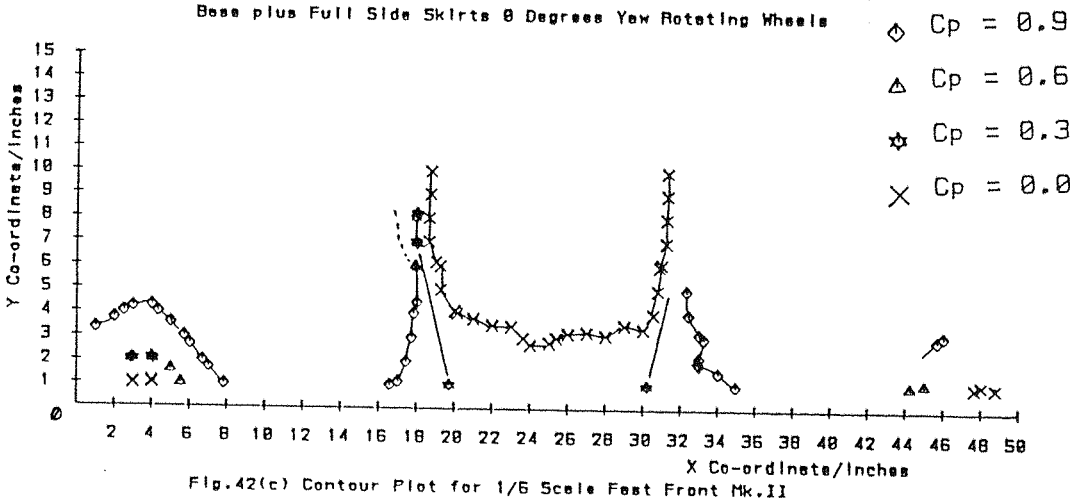

Fig.42(c) Contour Plot for 1/6 Scale Fast Front Mk.II

Base Skirts plus Underbody 0 Degrees Yaw Rotating Wheels

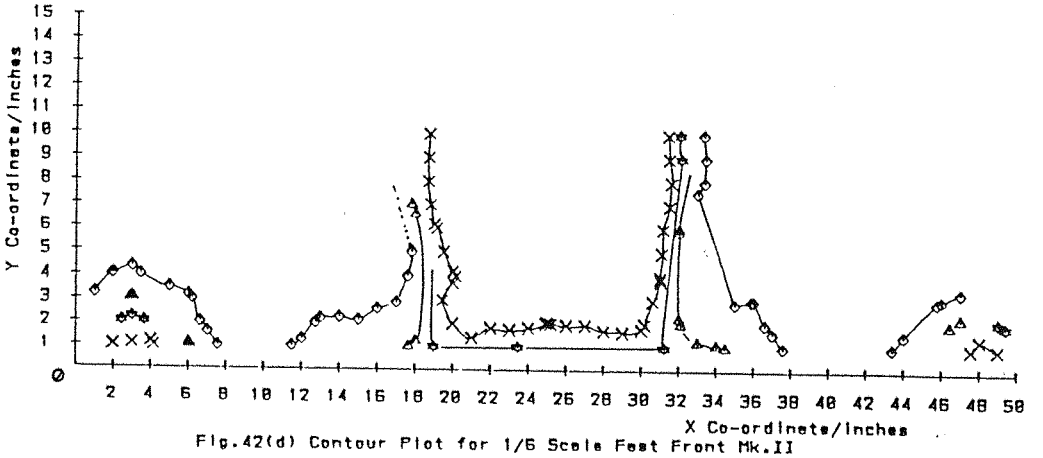

Fig.42(d) Contour Plot for 1/6 Scale Fast Front Mk.II

Skirts Undertray and Rear Boat-tails 0 Degrees Yaw Rotating Wheels

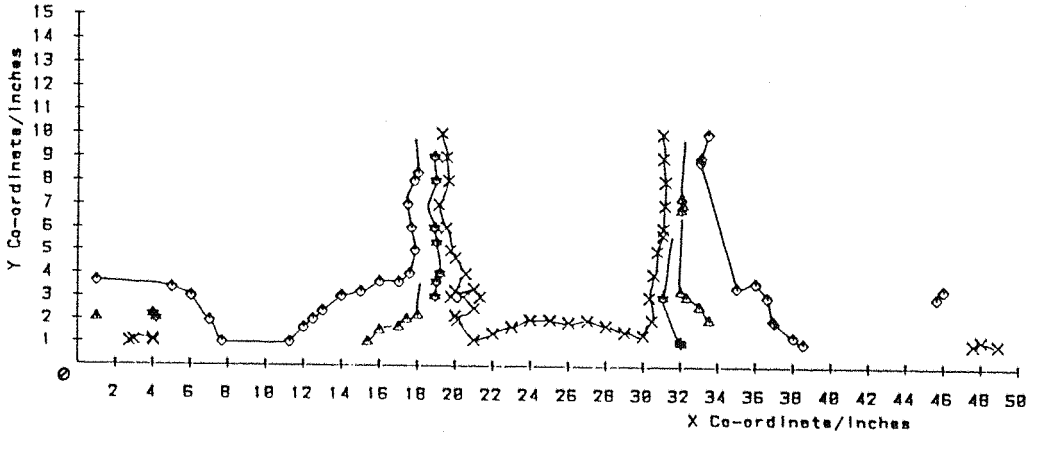

Fig.43(a) Contour Plot for 1/6 Scale Fast Front Mk.II

Baseline 0 Degrees Yaw Rotating Wheels

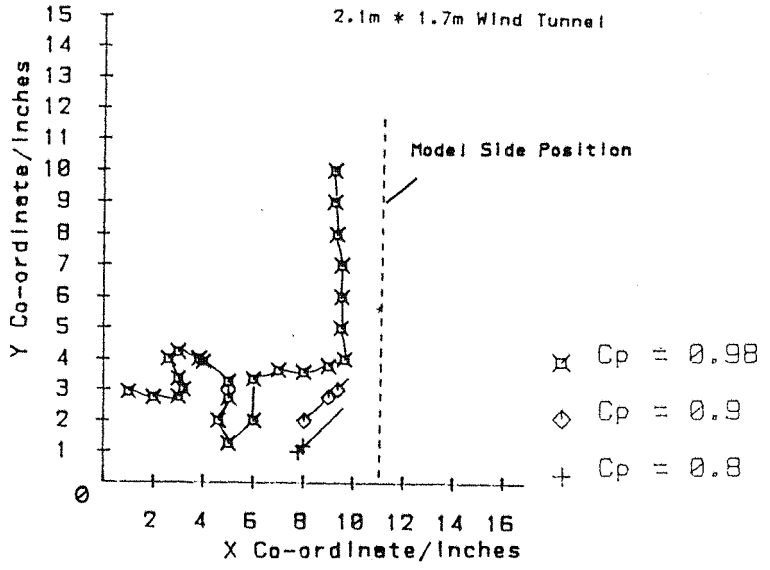

Fig.43(b) Contour Plot for 1/6 Scale Fast Front Mk.II

Base plus Skirts 0 Degrees Yaw Rotating Wheels

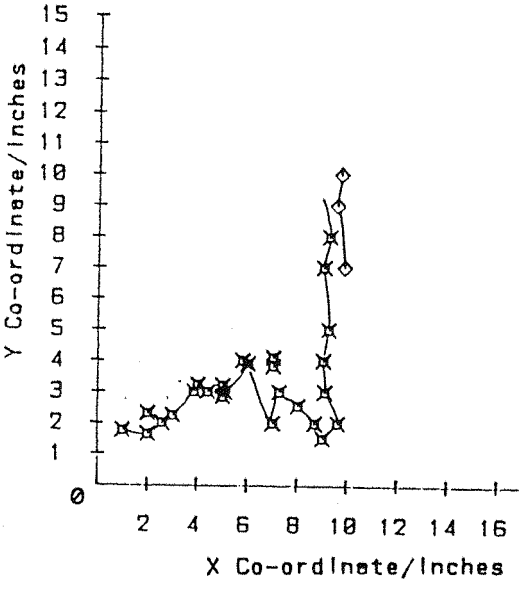

Fig.43(c) Contour Plot for 1/6 Scale Fast Front Mk.II

Skirts and Undertray 0 Degrees Yaw Rotating Wheels

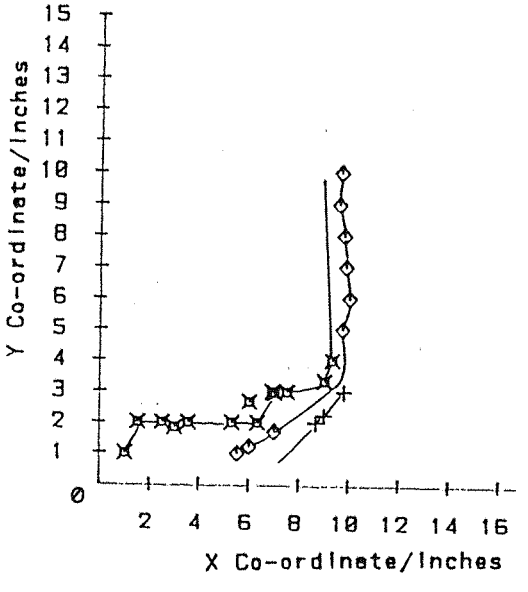

Fig.44(a) Contour Plot for 1/6 Scale Fast Front Mk.II

Baseline 0 Degrees Yaw

In 2.1m * 1.7m Wind Tunnel

1000mm Rearwards of Model Base

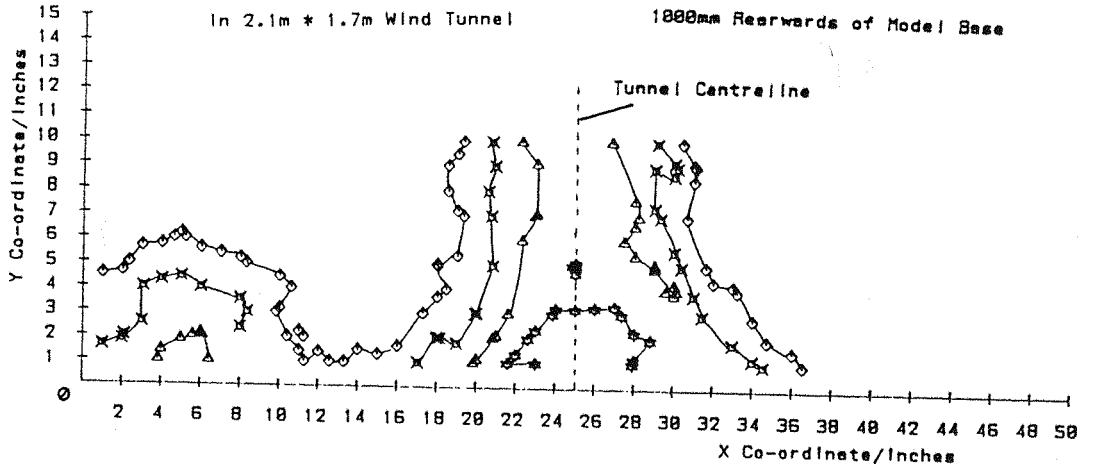

Fig.44(b) Contour Plot for 1/6 Scale Fast Front Mk.II

Base plus Skirts 0 Degrees Yaw Rotating Wheels

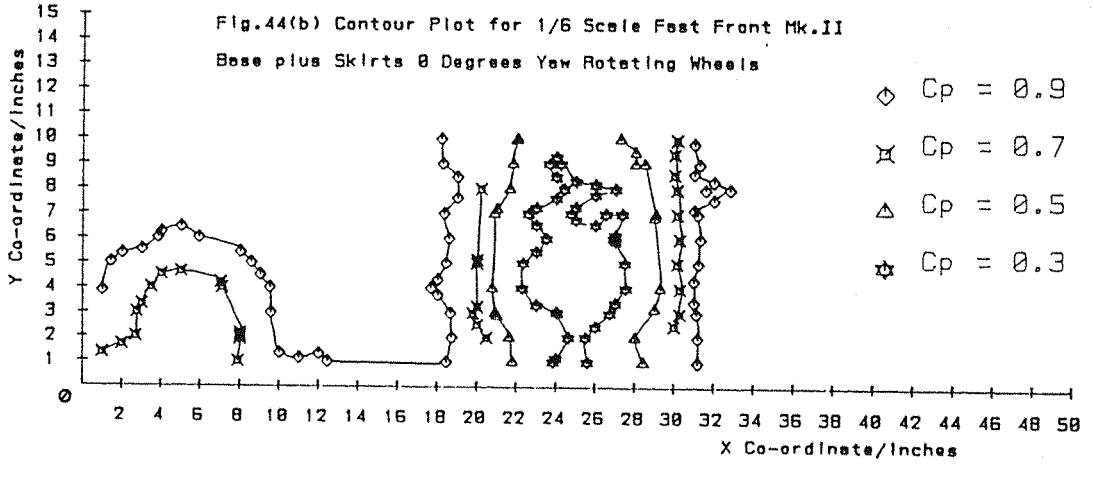

Fig.44(c) Contour Plot for 1/6 Scale Fast Front Mk.II

Skirts and Undertray 0 Degrees Yaw Rotating Wheels

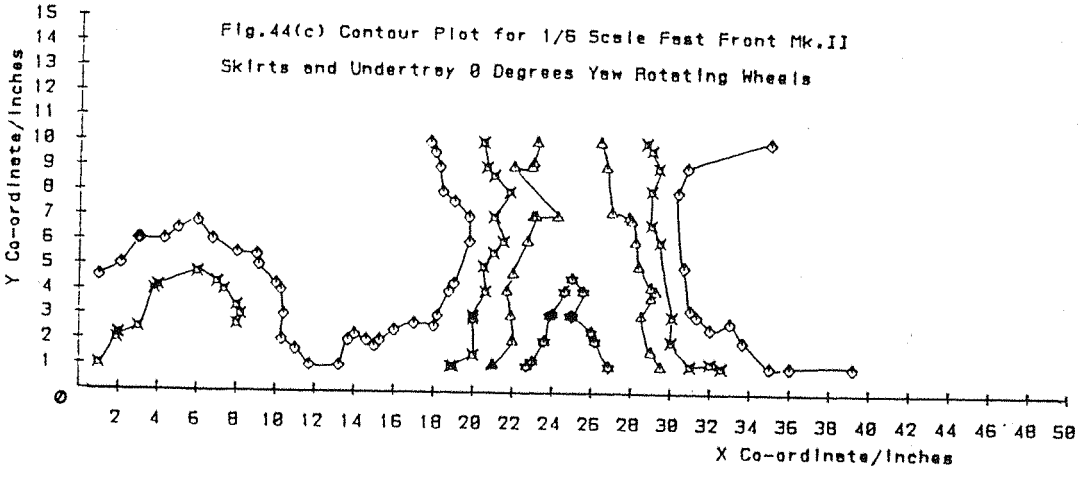

Fig.44(d) Contour Plot for 1/6 Scale Fast Front Mk.II

Skirts Undertray and Rear Boat-tails 0 Degrees Yaw Rotating Wheels

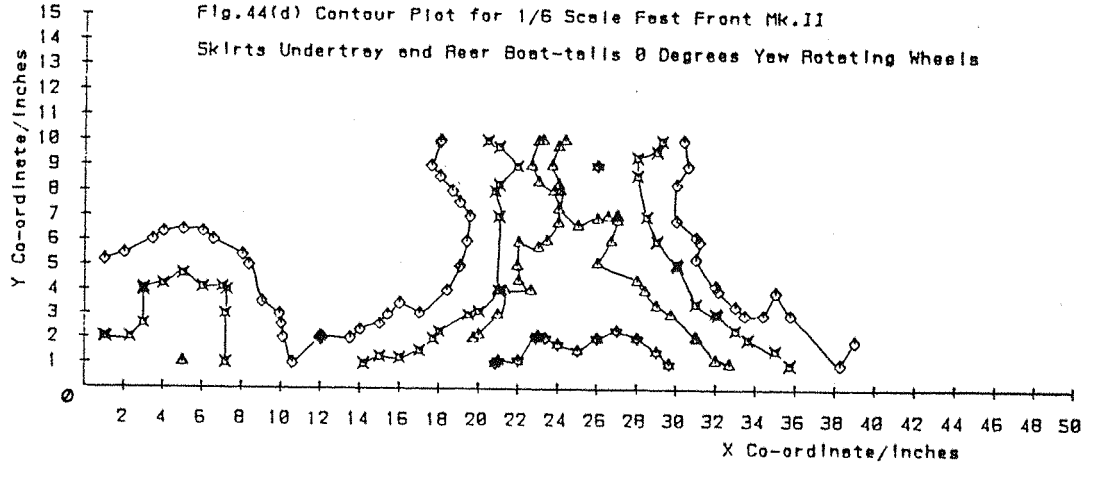

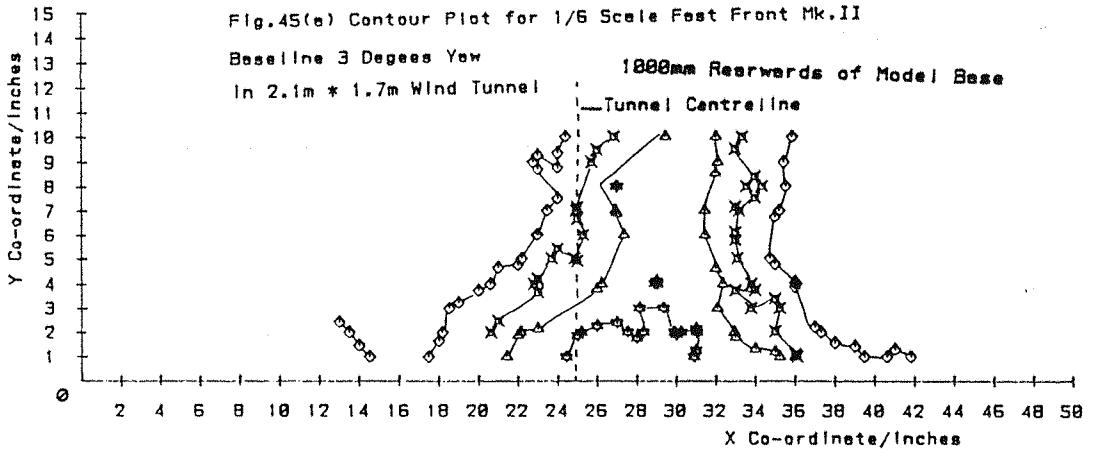
Fig.45(a) Contour Plot for 1/6 Scale Fast Front Mk.II
Baseline 3 Degees Yaw
In 2.1m * 1.7m Wind Tunnel
1000mm Rearwards of Model Base
Tunnel Centreline
Y Co-ordinate/Inches
X Co-ordinate/Inches

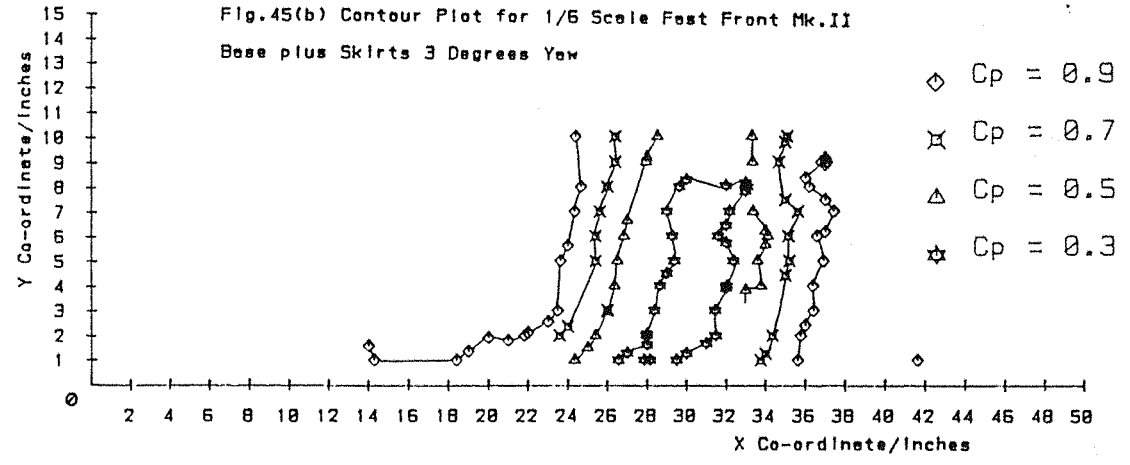
Fig.45(b) Contour Plot for 1/6 Scale Fast Front Mk.II
Base plus Skirts 3 Degrees Yaw
Cp = 0.9
Cp = 0.7
Cp = 0.5
Cp = 0.3
Y Co-ordinate/Inches
X Co-ordinate/Inches

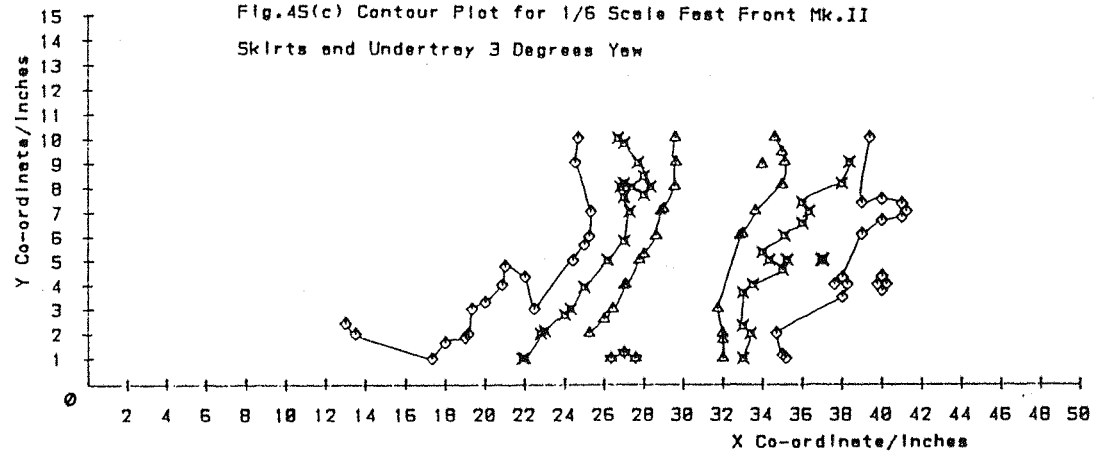
Fig.45(c) Contour Plot for 1/6 Scale Fast Front Mk.II
Skirts and Undertray 3 Degrees Yaw
Y Co-ordinate/Inches
X Co-ordinate/Inches

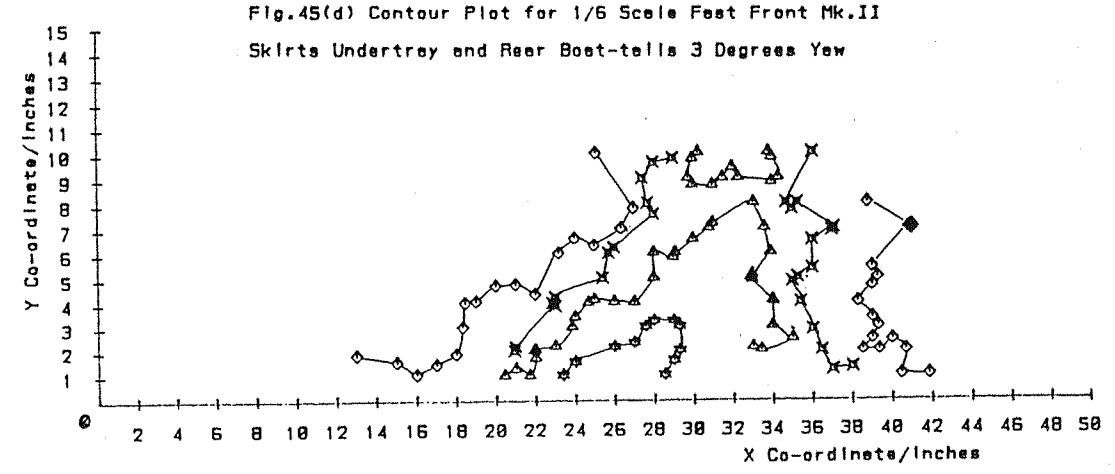
Fig.45(d) Contour Plot for 1/6 Scale Fast Front Mk.II
Skirts Undertray and Rear Boat-tails 3 Degrees Yaw
Y Co-ordinate/Inches
X Co-ordinate/Inches

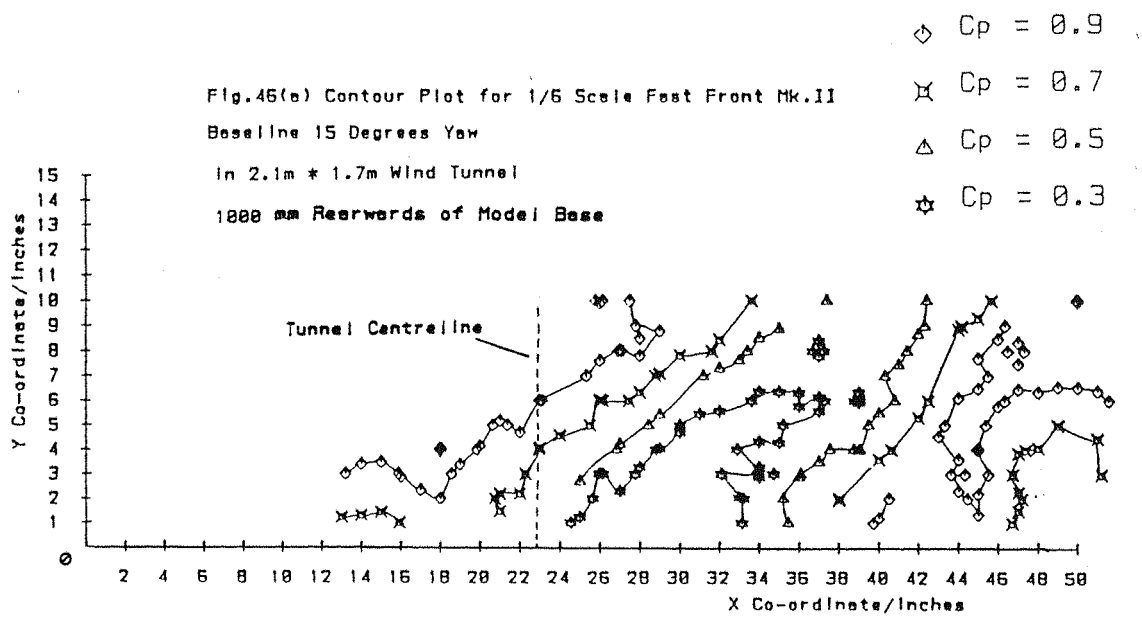

Fig.46(a) Contour Plot for 1/6 Scale Fast Front Mk.II
Baseline 15 Degrees Yaw
in 2.1m * 1.7m Wind Tunnel
1000 mm Rearwards of Model Base

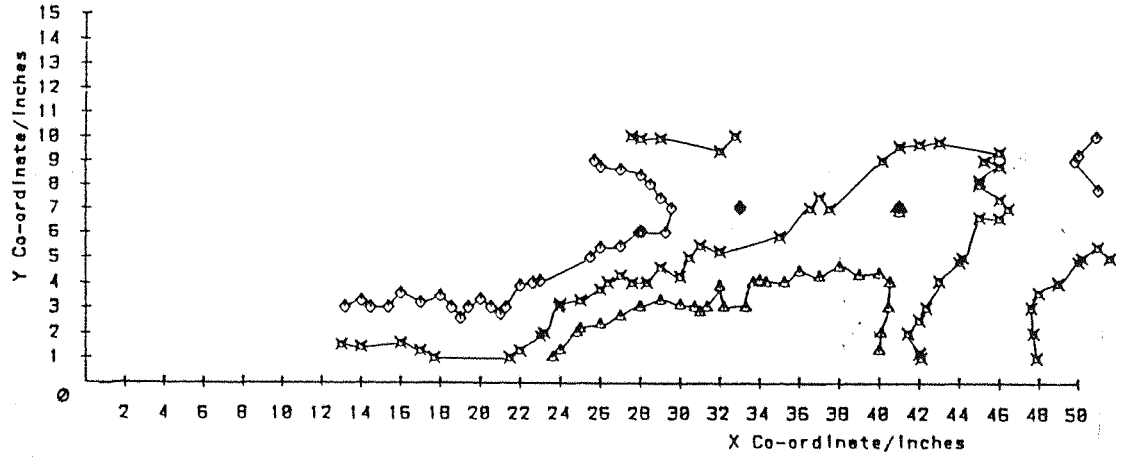

Fig.46(b) Contour Plot for 1/6 Scale Fast Front Mk.II
Skirts Undertray and Rear Boat-tails 15 Degrees Yaw

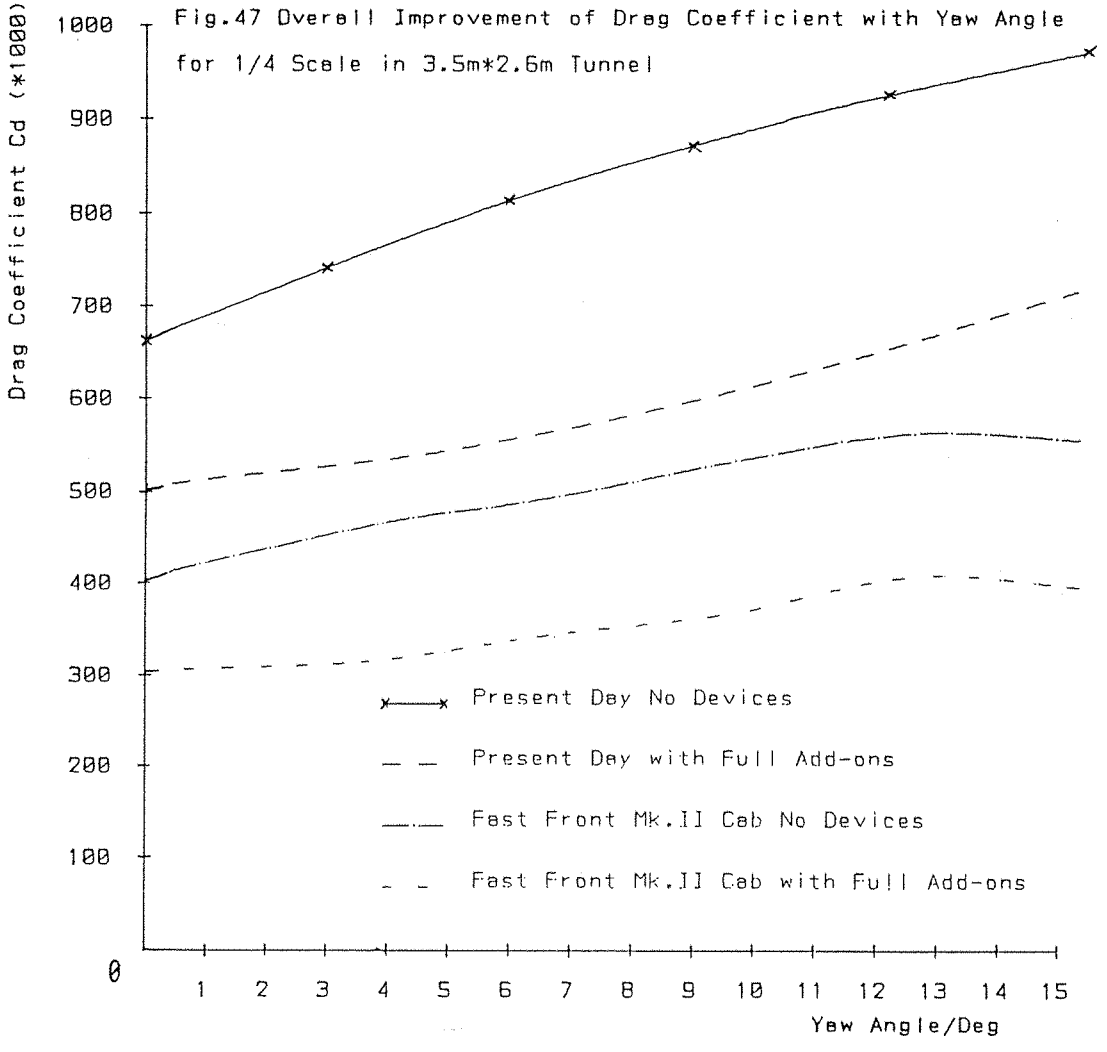
Fig.47 Overall Improvement of Drag Coefficient with Yaw Angle
for 1/4 Scale in 3.5m*2.6m Tunnel
Drag Coefficient Cd (*1000)
1000
900
800
700
600
500
400
300
200
100
0
1
2
3
4
5
6
7
8
9
10
11
12
13
14
15
Yaw Angle/Deg
Present Day No Devices
Present Day with Full Add-ons
Fast Front Mk.II Cab No Devices
Fast Front Mk.II Cab with Full Add-ons

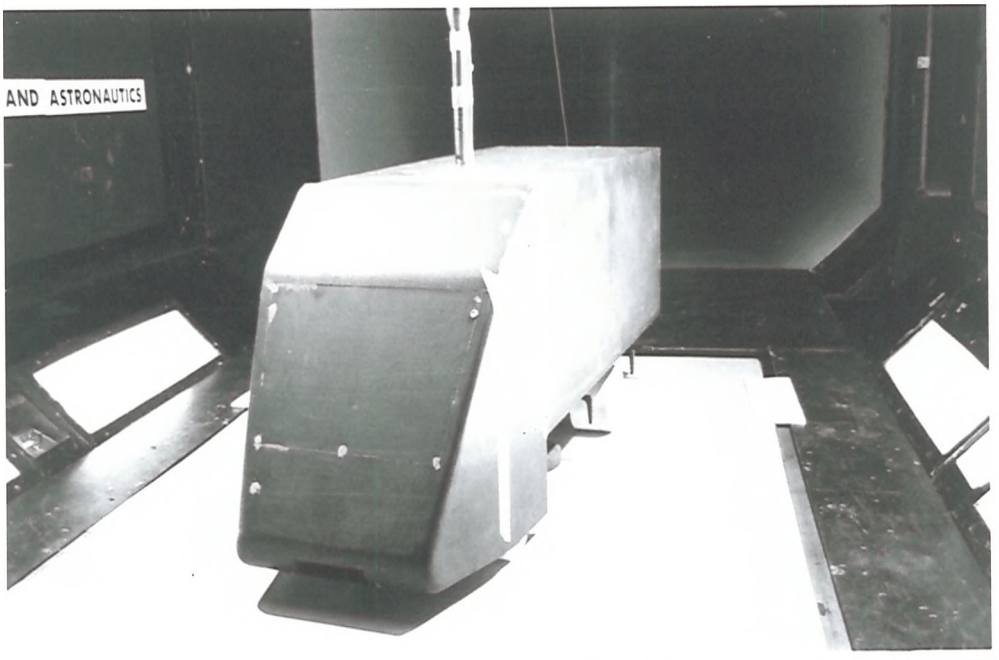

Plate 1(a) 1/6 Scale Fast Front Mk.I

in 2.1m*1.7m Tunnel

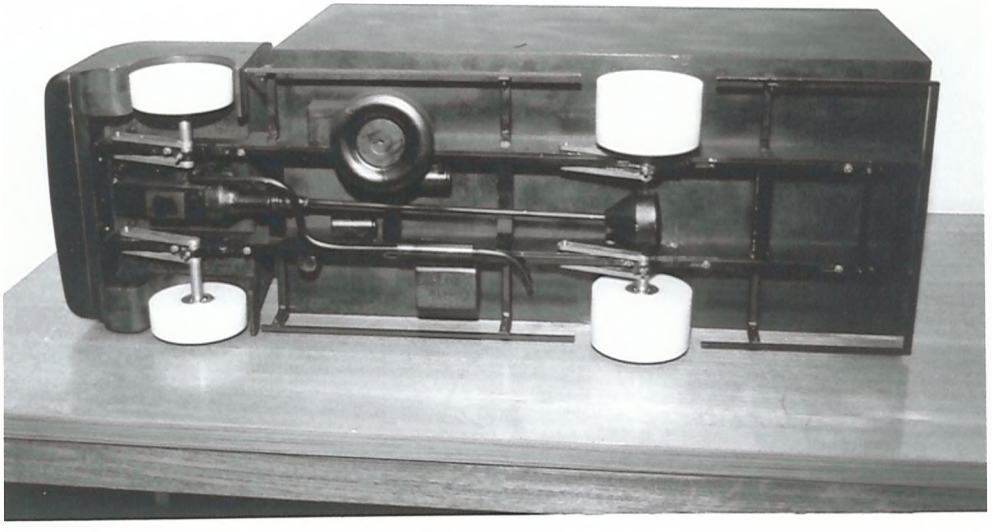

Plate 1(b) 1/6 Scale Model Underbody Detail

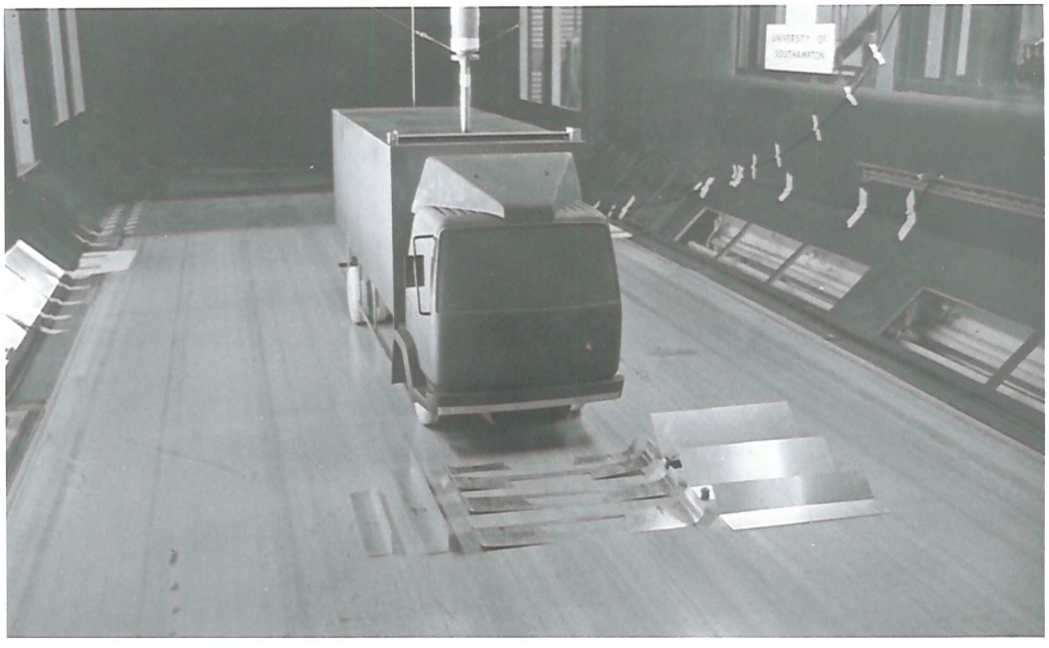

Plate 2(a) 1/4 Scale T45 Type Cab

with Various Deflectors and Spoilers

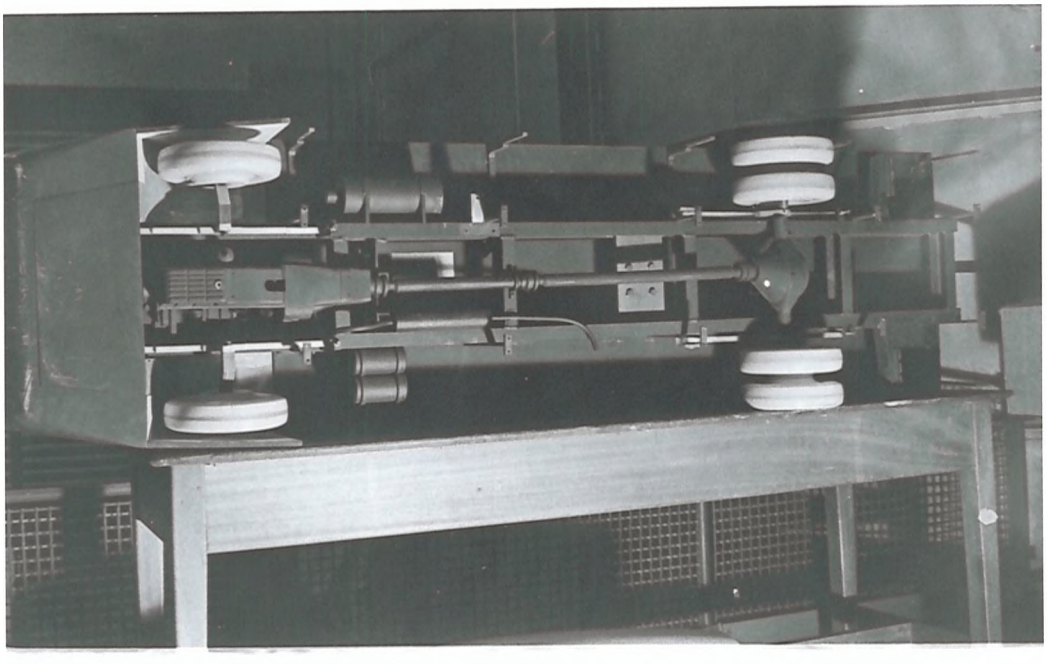

Plate 2(b) 1/4 Scale Fast Front Mk.II

Underbody Detail

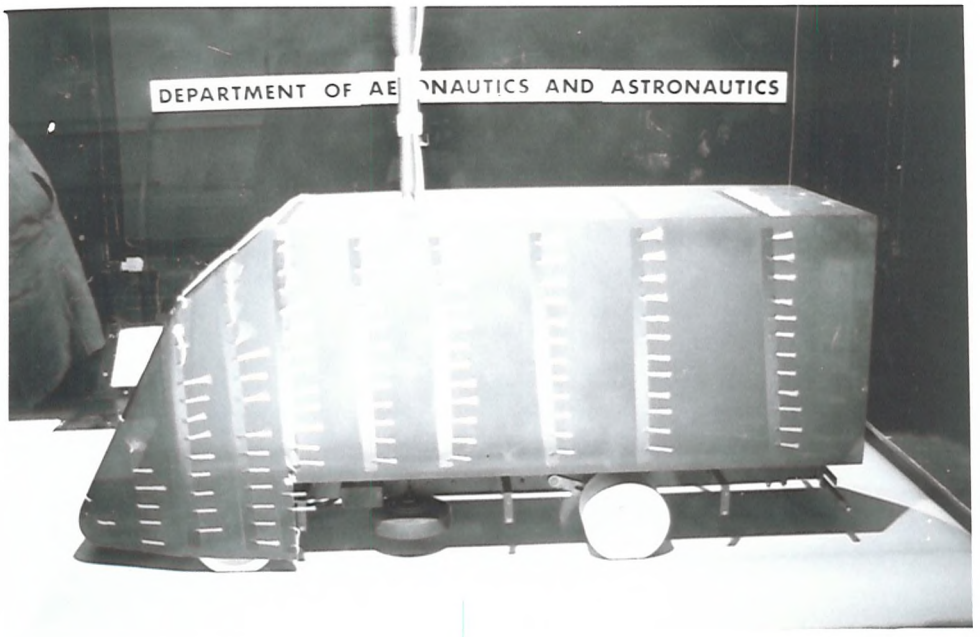

Plate 3(a) 1/6 Scale Fast Front Mk.I in 2.1m*1.7m Tunnel

Baseline 0 Degrees Yaw 24.86 m/s

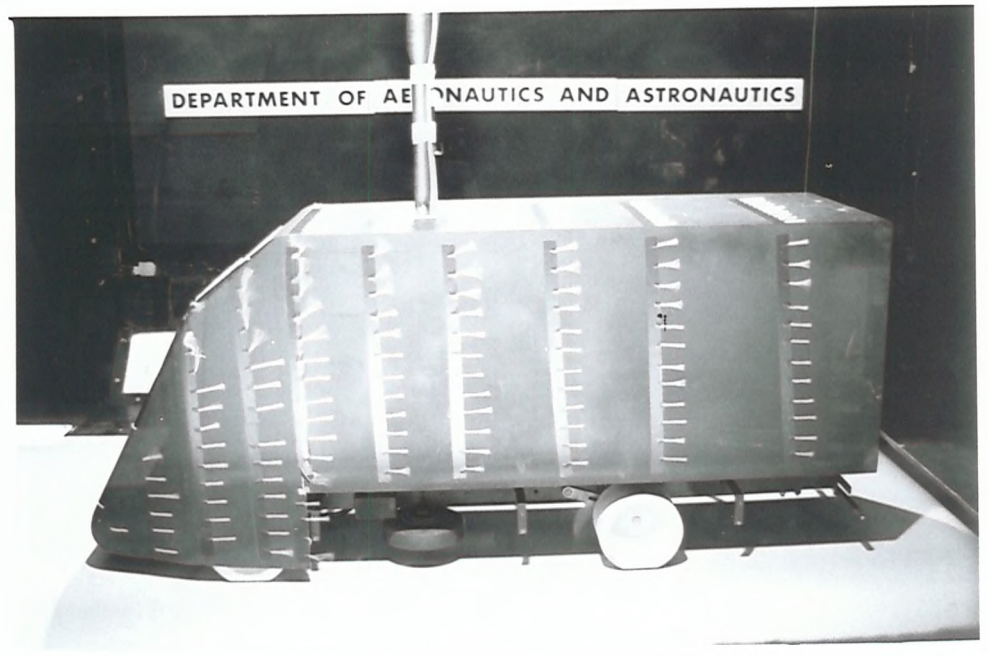

Plate 3(b) 1/6 Scale Fast Front Mk.I in 2.1m*1.7m Tunnel

Baseline 0 Degrees Yaw 30 m/s

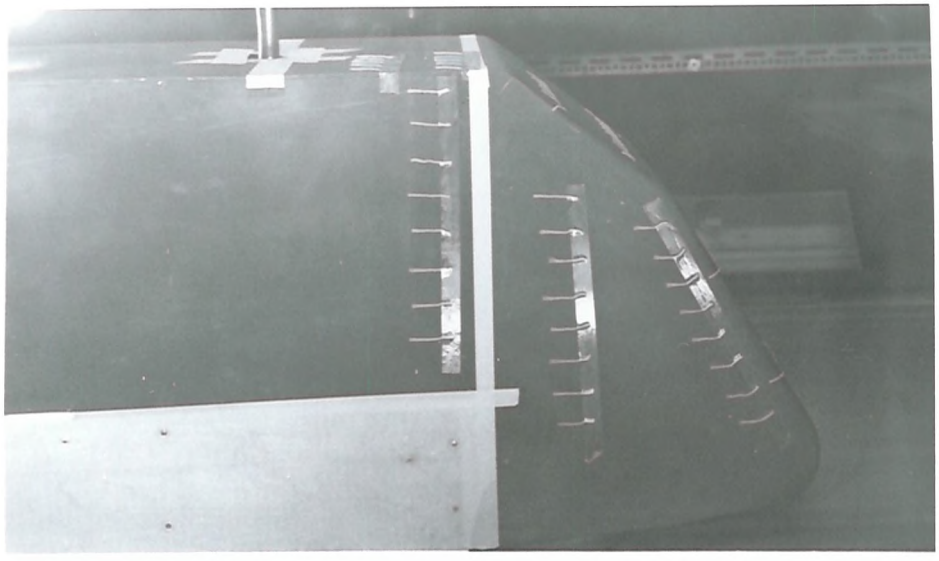

Plate 4 1/4 Scale Fast Front Mk.I in 3.5m*2.6m Tunnel

Base plus Skirts 0 Degrees Yaw 28.55 m/s

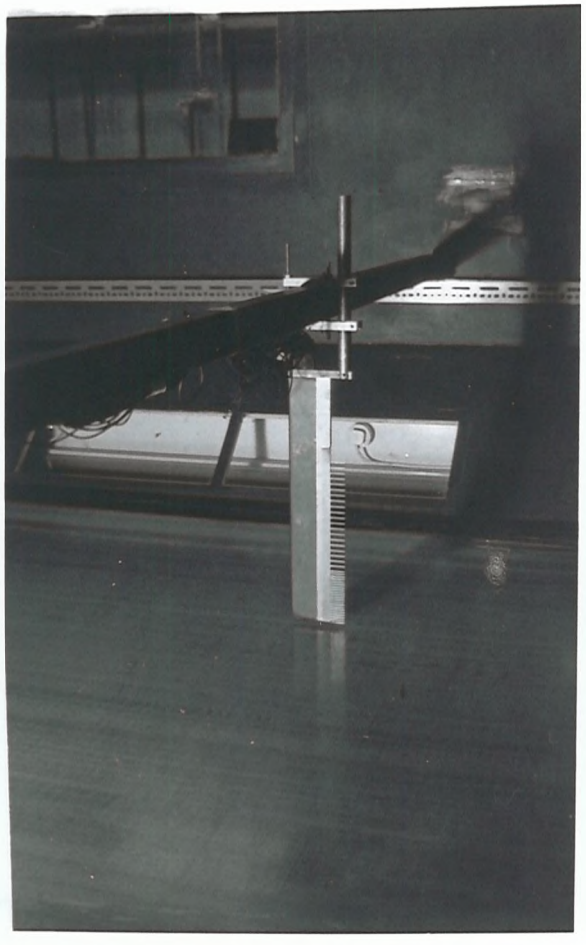

Plate 5 Boundary Layer Rake in 3.5m*2.6m Tunnel

over 5.3m*2.4m Moving Ground

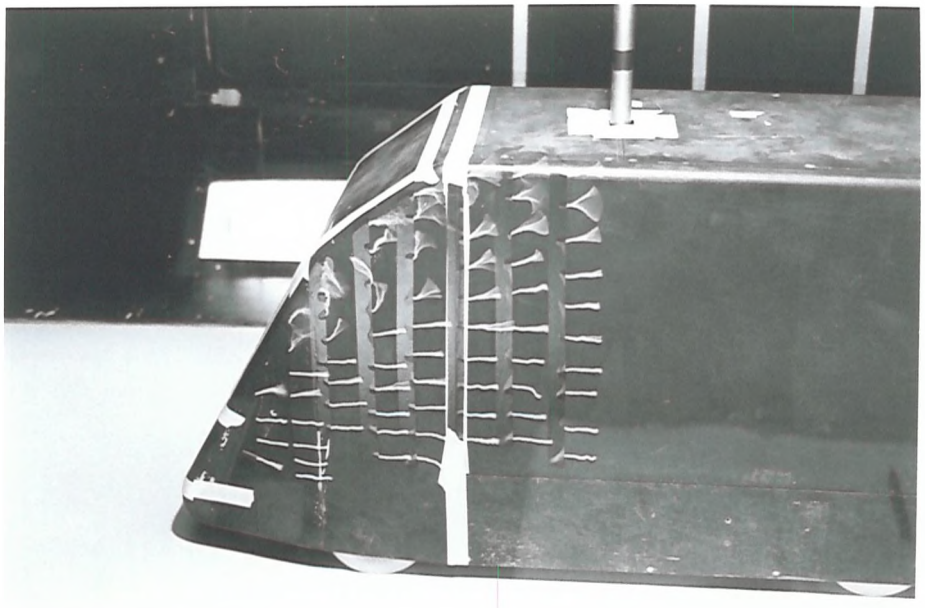

Plate 6(a) 1/6 Scale Fast Front Mk.II in 2.1m*1.7m Tunnel

Cab Flow 0 Degrees Yaw 24.86 m/s

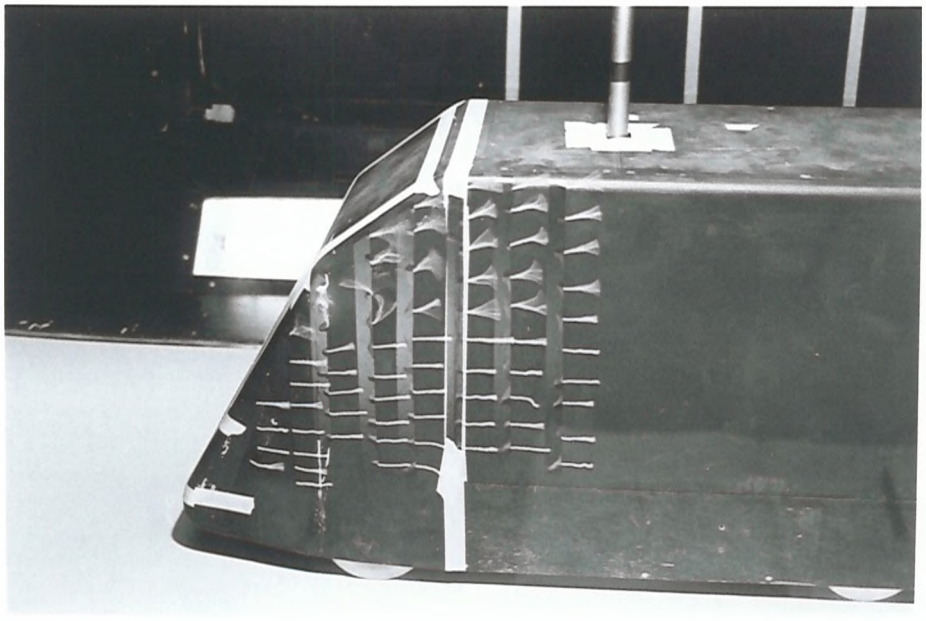

Plate 6(b) 1/6 Scale Fast Front Mk.II in 2.1m*1.7m Tunnel

Cab Flow 0 Degrees Yaw 30 m/s

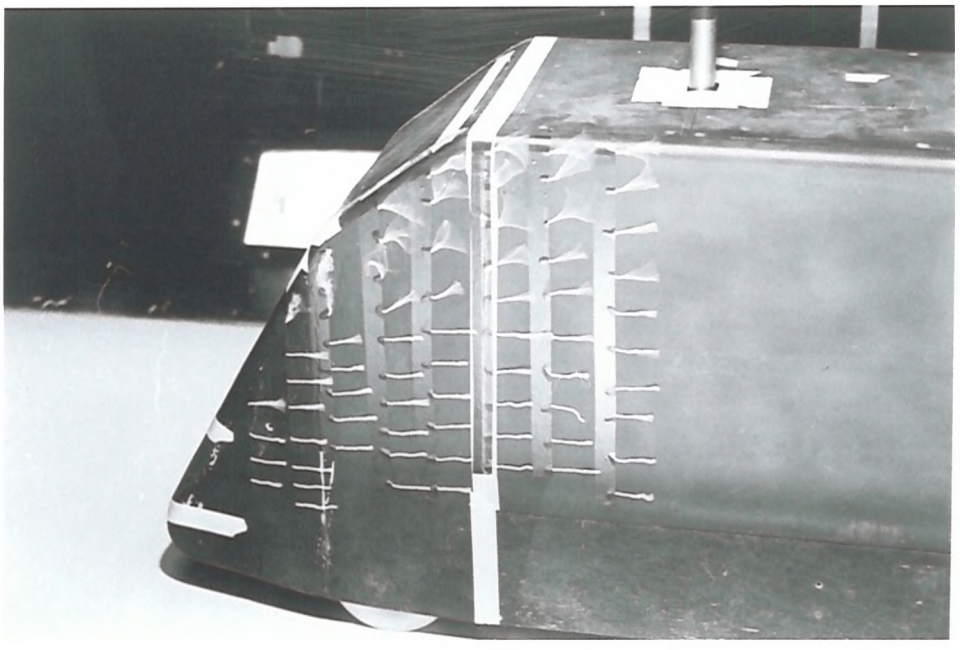

Plate 7(a) 1/6 Scale Fast Front Mk.II in 2.1m*1.7m Tunnel

Cab Flow with Grit Transition 0 Degrees Yaw 24.86 m/s

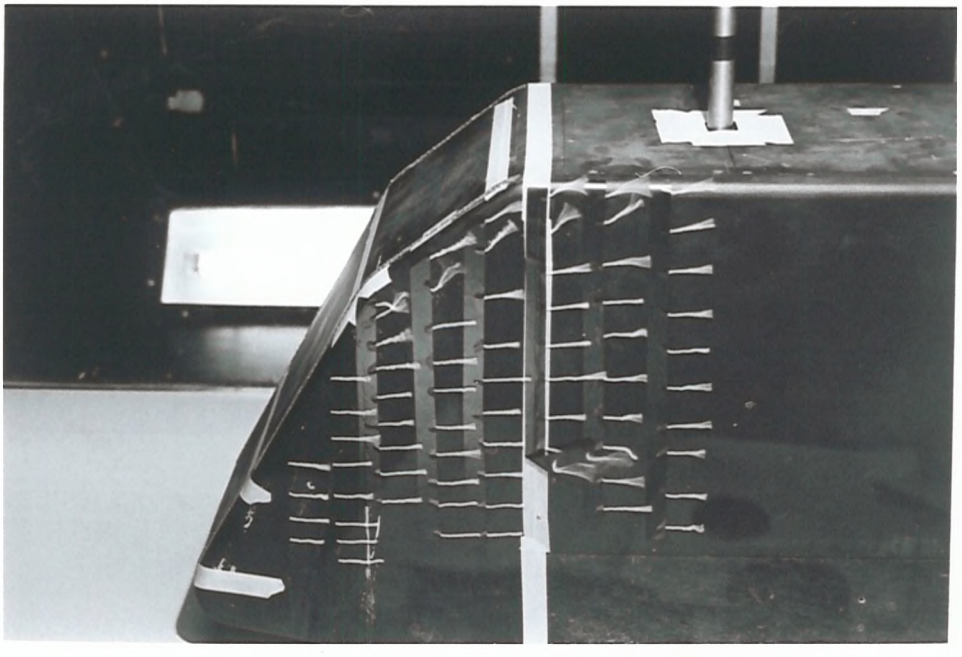

Plate 7(b) 1/6 Scale Fast Front Mk.II in 2.1m*1.7m Tunnel

Cab Flow with Grit Transition 0 Degrees Yaw 30 m/s

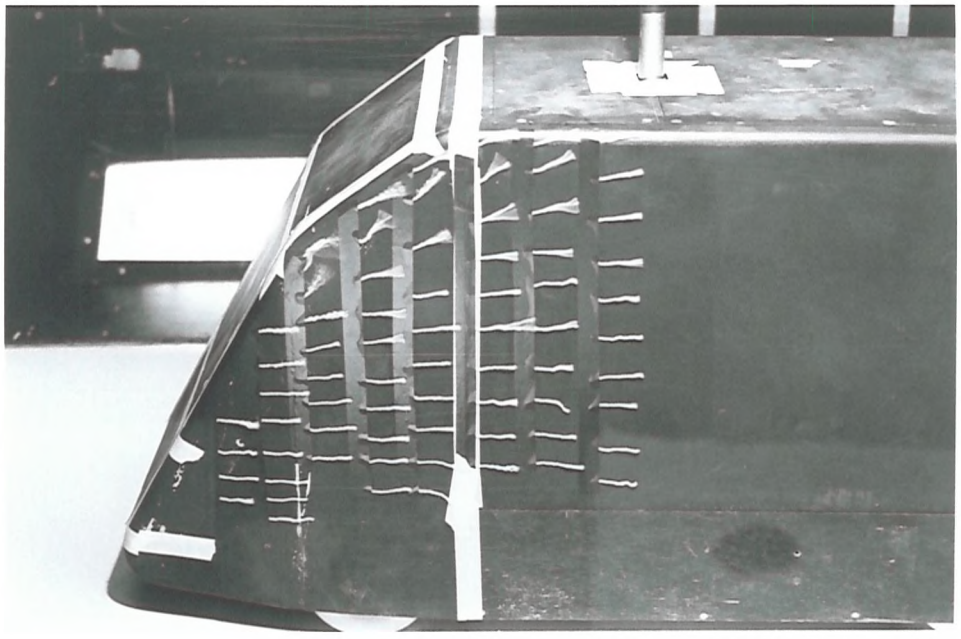

Plate 8(a) 1/6 Scale Fast Front Mk.II in 2.1m*1.7m Tunnel

Cab Flow with Wire Transition 0 Degrees Yaw 24.86 m/s

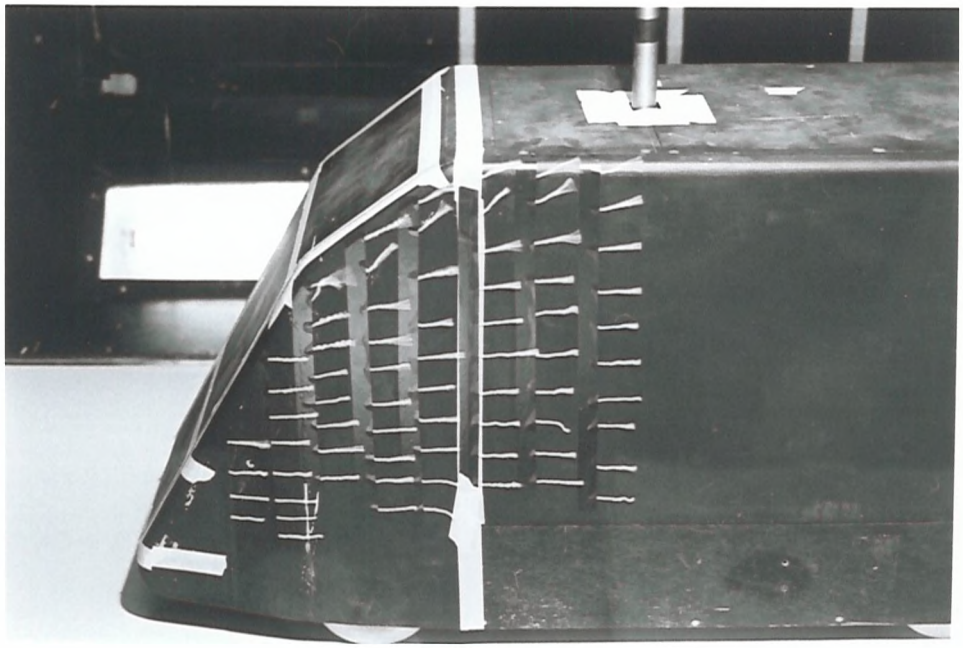

Plate 8(b) 1/6 Scale Fast Front Mk.II in 2.1m*1.7m Tunnel

Cab Flow with Wire Transition 0 Degrees Yaw 30 m/s

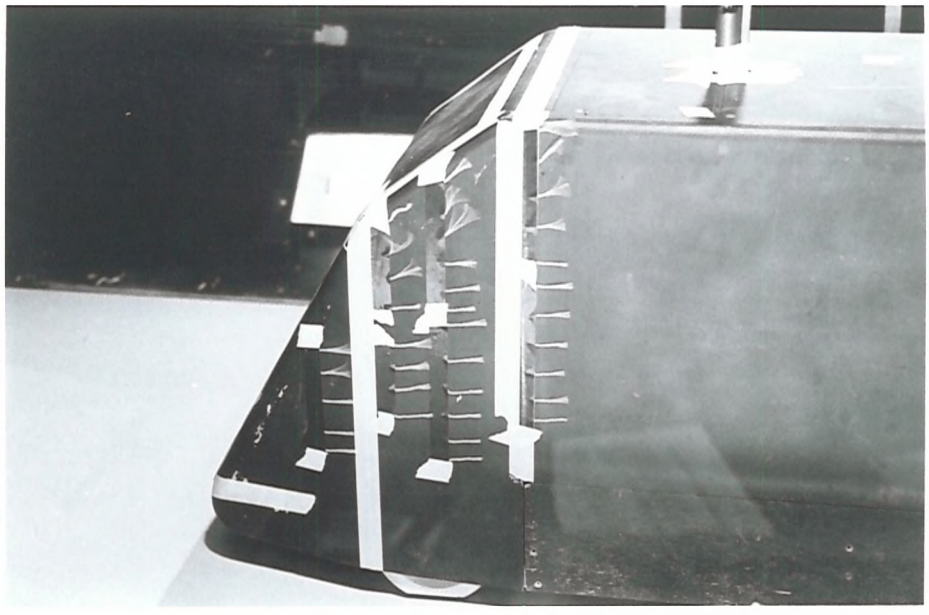

Plate 9 1/6 Scale Fast Front Mk.II in 2.1m*1.7m Tunnel

Lee-side Cab Flow with Wire Transition 3 Degrees Yaw 24.86 m/s

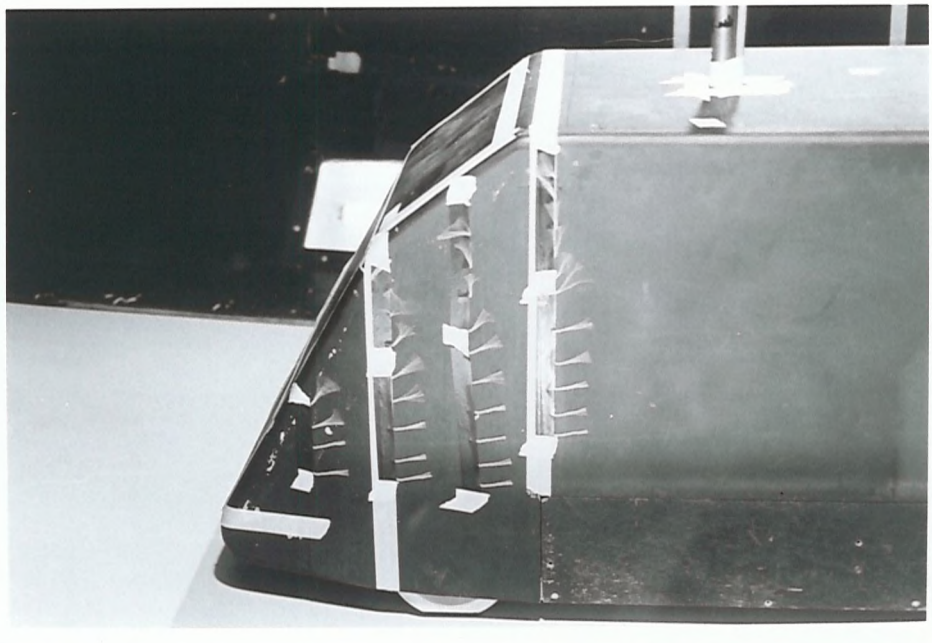

Plate 10 1/6 Scale Fast Front Mk.II in 2.1m*1.7m Tunnel

Lee-side Cab Flow with Wire Transition 9 Degrees Yaw 24.86 m/s

Plate 11 1/6 Scale Fast Front Mk.I in 2.1m*1.7m Tunnel

Lee-side Cab Flow without Transition 9 Degrees Yaw 24.86 m/s

Plate 12(a) 1/4 Scale Fast Front Mk.II in 3.5m*2.6m Tunnel

Baseline at 0 Degrees Yaw

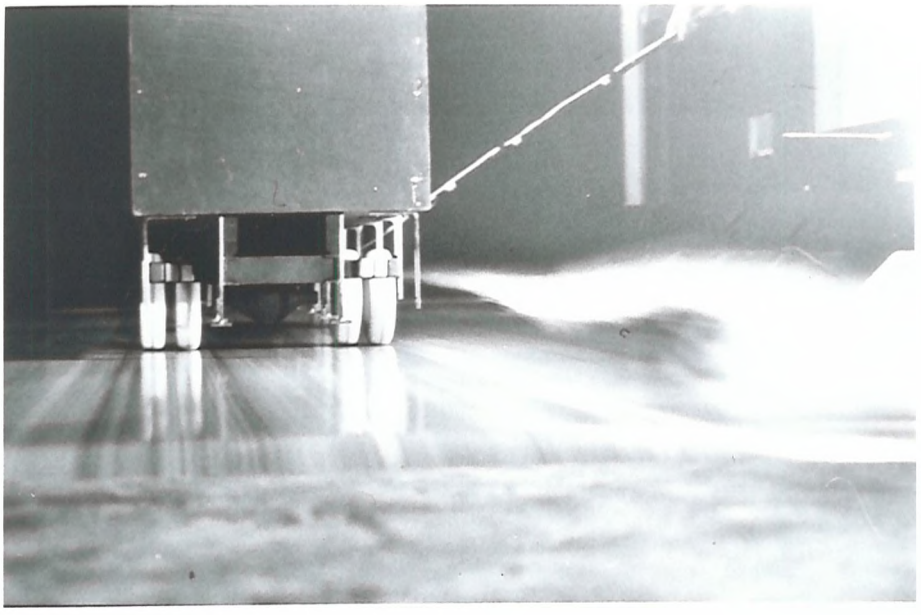

Plate 12(b) 1/4 Scale Fast Front Mk.II in 3.5m*2.6m Tunnel

Baseline at 0 Degrees Yaw

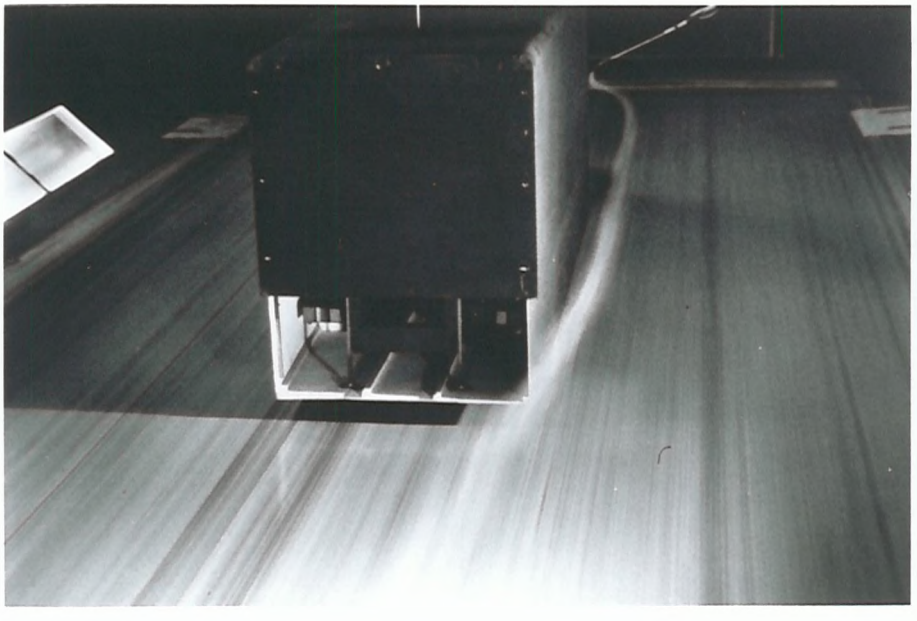

Plate 13(a) 1/4 Scale Fast Front Mk.II in 3.5m*2.6m Tunnel

Base plus Full Side Skirts 0 Degrees Yaw

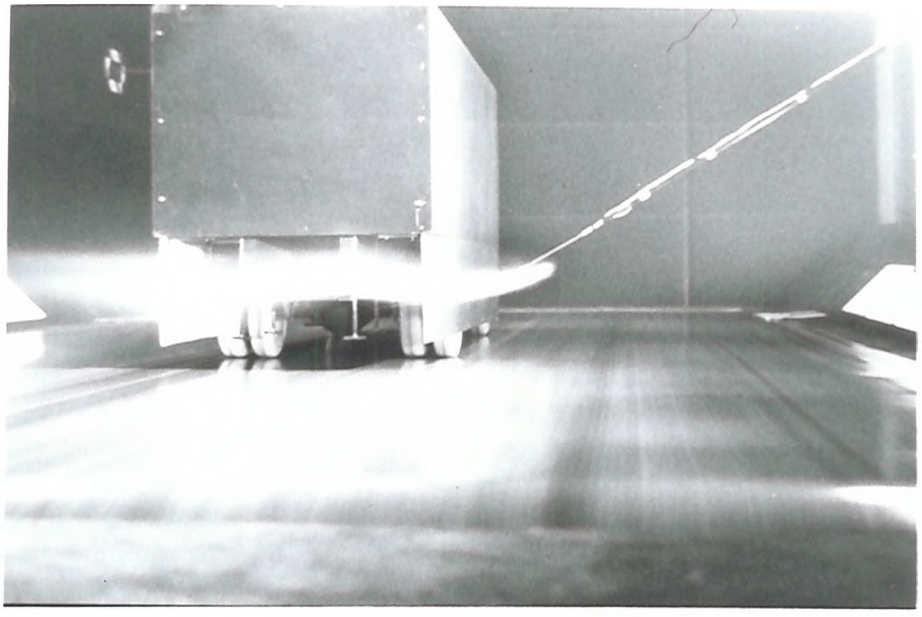

Plate 13(b) 1/4 Scale Fast Front Mk.II in 3.5m*2.6m Tunnel

Base plus Full Side Skirts 0 Degrees Yaw

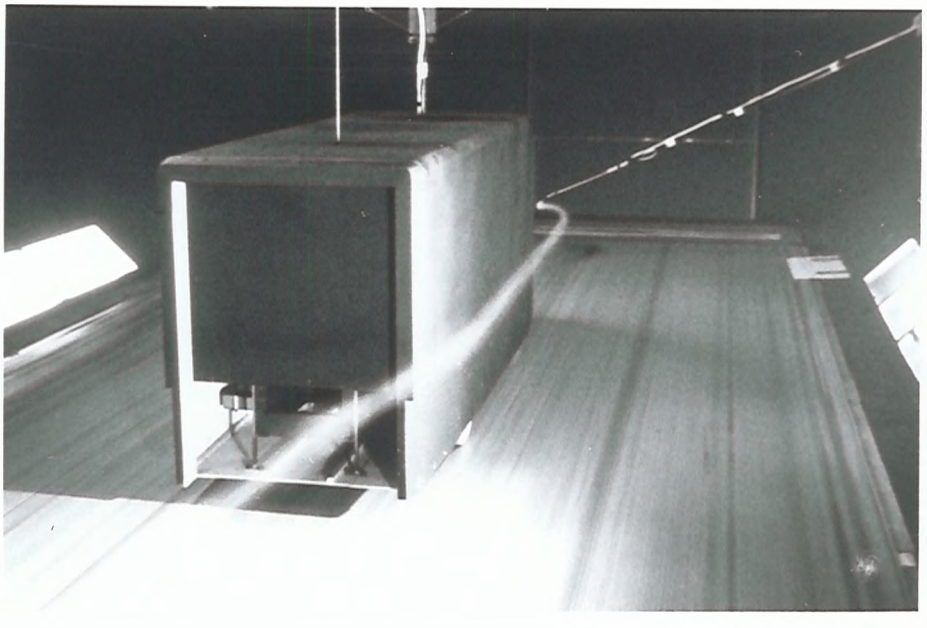

Plate 14(a) 1/4 Scale Fast Front Mk.II in 3.5m*2.6m Tunnel

Base Full Skirts plus Rear Boat-tails 0 Degrees Yaw

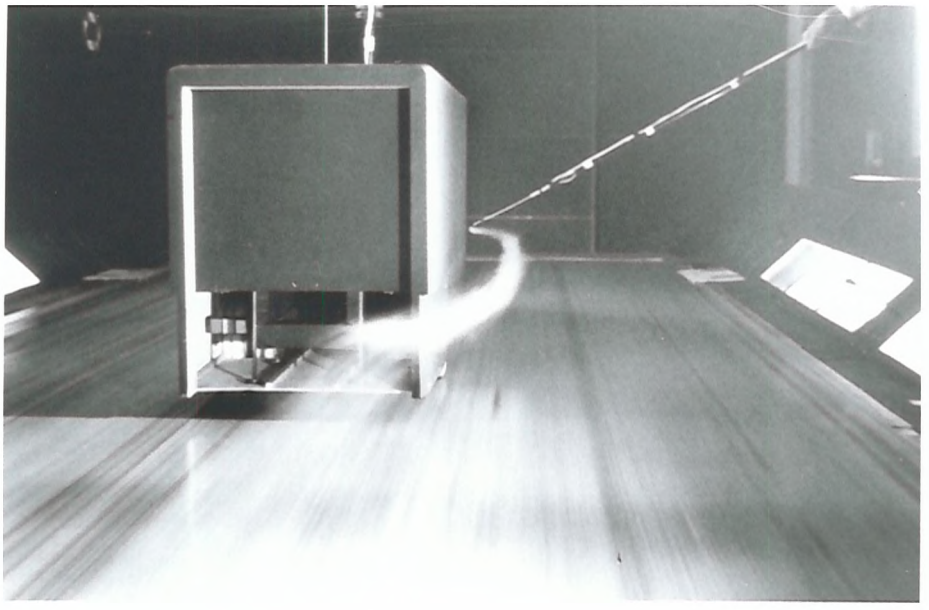

Plate 14(b) 1/4 Scale Fast Front Mk.II in 3.5m*2.6m Tunnel

Base Full Skirts plus Rear Boat-tails 0 Degrees Yaw

Plate 15(a) 1/4 Scale Fast Front Mk.II in 3.5m*2.6m Tunnel

Baseline 6 Degrees Yaw

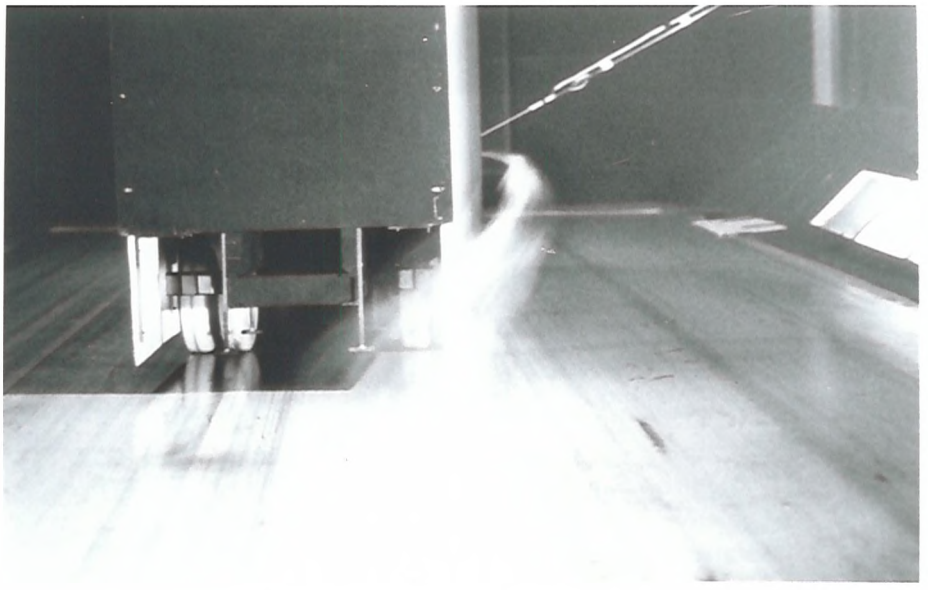

Plate 15(b) 1/4 Scale Fast Front Mk.II in 3.5m*2.6m Tunnel

Base plus Full Side Skirts 6 Degrees Yaw

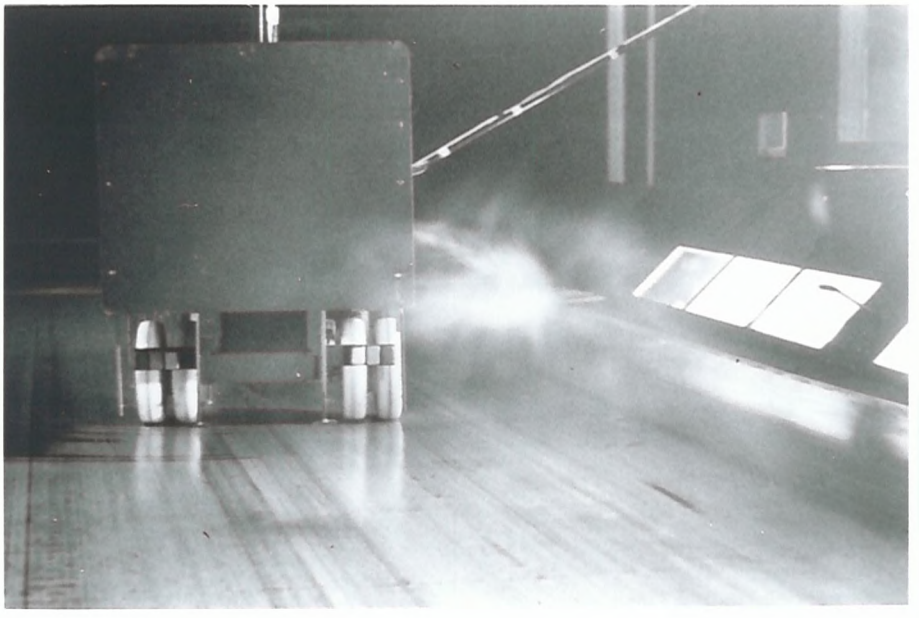

Plate 16(a) 1/4 Scale Fast Front Mk.II in 3.5m*2.6m Tunnel

Baseline 12 Degrees Yaw

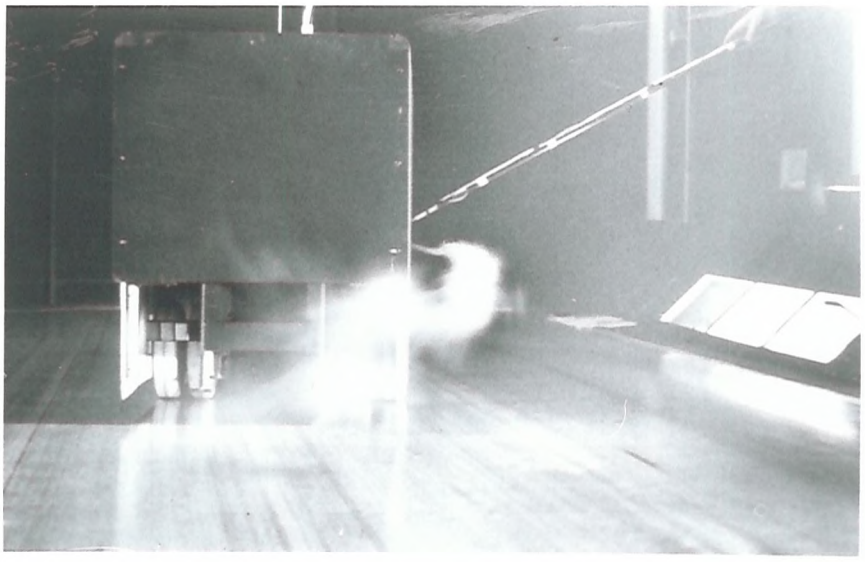

Plate 16(b) 1/4 Scale Fast Front Mk.II in 3.5m*2.6m Tunnel

Base plus Full Side Skirts 12 Degrees Yaw

Plate 17 Total Pressure Rake for Wake Studies

in 2.1m*1.7m Tunnel with Author